

2012-01-01

Metal Catalyzed Activation Of E-H Bonds, E = Si, Ge, Sn

Renzo Nelson Arias Ugarte

University of Texas at El Paso, rnarias@miners.utep.edu

Follow this and additional works at: https://digitalcommons.utep.edu/open_etd



Part of the [Inorganic Chemistry Commons](#)

Recommended Citation

Arias Ugarte, Renzo Nelson, "Metal Catalyzed Activation Of E-H Bonds, E = Si, Ge, Sn" (2012). *Open Access Theses & Dissertations*. 2233.

https://digitalcommons.utep.edu/open_etd/2233

This is brought to you for free and open access by DigitalCommons@UTEP. It has been accepted for inclusion in Open Access Theses & Dissertations by an authorized administrator of DigitalCommons@UTEP. For more information, please contact lweber@utep.edu.

METAL CATALYZED ACTIVATION OF E-H BONDS,

E = Si, Ge, Sn

RENZO NELSON ARIAS UGARTE

Department Of Chemistry

APPROVED:

Keith H. Pannell, Ph.D., Chair

Hemant K. Sharma, Ph.D.

Jose Nunez, Ph.D.

Katja Michael, Ph.D.

Charles S. Weinert, Ph.D.

Benjamin C. Flores, Ph.D.
Acting Dean of the Graduate School

Copyright ©

by

Renzo N. Arias Ugarte

2011

Dedication

Quero agradecer antes que nada a Dios por haberme llevado por el camino correcto, sin sus bendiciones en mi vida esto no hubiera podido ser posible. Doy gracias a mis padres Facunda Ugarte Martinez y Juan Lucio Arias Castillo por haberme inculcado tantos valores en mi vida. A ellos les debo ser quien soy, pero especialmente a mi madre que con tanto sacrificio nos ha forzado a acabar nuestras carreras y este es el reflejo de su esfuerzo y dedicación. A mis hermanas, Marilu, Cristina y Teresa por creer en mi, y por su incondicional apoyo en cada etapa de mi vida y de mi carrera profesional. A mis hermanos Steve, Gustavo y Jack por que de ellos he aprendido tantas cosas en la vida, virtudes que jamas se van a borrar de mi memoria, sus virtudes me han servido mucho para enfrentar con gallardia y coraje los problemas. A Jenny por haber creido en mi, aunque las cosas no hayan salido como uno esperara, siempre me apoyo con sus palabras y con su incondicional amor. A mi nueva familia que se ha intregado a mi vida, que Dios nos bendiga y proteja siempre, Alina el nuevo amor en mi vida, Itzia, Hayley y Kenny. Deseando que las nuevas generaciones que vienen detrás de mi pueda escalar aun mas en la vida que el destino nos tiene guardada.

METAL CATALYZED ACTIVATION OF E-H BONDS,

E = Si, Ge, Sn

by

RENZO NELSON ARIAS UGARTE, Ch.E.

DISSERTATION

Presented to the Faculty of the Graduate School of

The University of Texas at El Paso

in Partial Fulfillment

of the Requirement

for the Degree of

DOCTOR OF PHILOSOPHY

Department of Chemistry

The University of Texas at El Paso

December 2011

Acknowledgements

I would like to thank Dr. Keith Pannell for the opportunity to work with him and learn from him, I would not be able to be in the USA pursuing a career without his support, letting me explore my potential and for teaching me how to do research. Deepest thanks go to everyone who has passed through the Pannell lab during my stay; special thanks to Dr. Hemant Sharma, for showing me how to do science, for pushing me to be better and for sharing his knowledge. To Dr. Ramesh Kapoor, Dr. Paula Apodaca, Dr Teresita Munguia and Dr Mukesch Kumar for being part of my professional-development.

The research was supported by the Robert Welsh Foundation, Houston, TX and SCORE-NIH.

Table of contents

Acknowledgements.....	v
Table of contents.....	vi
List of schemes	xii
List of figures.....	xiii
List of tables	xvii
Dehydrogenative dimerization of $t\text{Bu}_2\text{SnH}_2$, catalyzed by iron and molybdenum complexes	1
Abstract	1
Statement of problem	2
Justification of importance	3
Research objectives	3
1.1 Introduction	4
1.1.1 Applications of organotin (OTs)	4
1.1.2 Polystannanes.....	5
1.1.3 Polystannane properties	8
1.1.4 Transition metal carbonyl complexes	10
1.1.5 Transition metal alkyl complexes	11
1.1.6 Oxidative addition and reductive elimination.....	15
1.2 Experimental	17

1.2.1	Synthesis of $(\eta^5\text{-C}_5\text{H}_5)\text{Fe}(\text{CO})_2\text{Sn}^t\text{Bu}_2\text{Cl}$	18
1.2.2	Synthesis of $(\eta^5\text{-C}_5\text{H}_5)\text{Fe}(\text{CO})_2\text{Sn}^t\text{Bu}_2\text{H}$	18
1.2.3	Synthesis of $(\eta^5\text{-C}_5\text{H}_5)\text{Fe}(\text{CO})(\text{PPh}_3)\text{Sn}^t\text{Bu}_2\text{Cl}$	19
1.2.4	Synthesis of $(\eta^5\text{-C}_5\text{H}_5)\text{Fe}(\text{CO})(\text{PPh}_3)\text{Sn}^t\text{Bu}_2\text{H}$	19
1.2.5	Synthesis of $(\eta^5\text{-C}_5\text{H}_5)\text{Mo}(\text{CO})_3\text{Sn}^t\text{Bu}_2\text{Cl}$	20
1.2.6	Synthesis of $(\eta^5\text{-C}_5\text{H}_5)\text{Mo}(\text{CO})_3\text{Sn}^t\text{Bu}_2\text{H}$	21
1.2.7	Synthesis of $\text{H}^t\text{Bu}_2\text{Sn-Sn}^t\text{Bu}_2\text{H}$	21
1.3	Results and discussion.....	22
1.3.1	Photochemical and thermal transformation of $^t\text{Bu}_2\text{SnH}_2$ into $\text{H}^t\text{Bu}_2\text{Sn-Sn}^t\text{Bu}_2\text{H}$	22
1.3.2	Proposed mechanism for stannane dimerization.....	26
1.3.3	Structural analysis of $(\eta^5\text{-C}_5\text{H}_5)\text{M}(\text{CO})_n(\text{L})^t\text{Bu}_2\text{SnH}$ complex, ($\text{M} = \text{Fe}$, $n = 1$; Mo , $n = 2$)	30
1.3.4	Observations related to $(\eta^5\text{-C}_5\text{H}_5)\text{M}(\text{CO})_n\text{H}$ transients suggested in the proposed mechanism, ($\text{M} = \text{Fe}$, $n = 2$; Mo , $n = 3$).....	31
1.3.5	Attempts to isolate the intermediate $(\eta^5\text{-C}_5\text{H}_5)\text{M}(\text{CO})_n\text{H}(^t\text{BuSnH})_2$, ($\text{M} = \text{Fe}$, $n =$ 1 ; Mo , $n = 2$)	33
1.3.6	Extension to tin systems with less bulky groups.	34
1.4	Conclusions	35
1.5	References	36

Methyl transfer from Fe (and Mo) to Sn: Formation of $\eta^5\text{-C}_5\text{H}_5\text{M}(\text{CO})_n\text{Sn}^t\text{Bu}_2\text{Me}$ (M = Fe, n = 2; M = Mo, n = 3) complexes from the photochemical irradiation of $\eta^5\text{-C}_5\text{H}_5\text{M}(\text{CO})_n\text{Me}$ and $^t\text{Bu}_2\text{SnH}_2$ in the molar ratio 2:1	47
Abstract	47
Statement of problem	48
Justification of importance	48
Research objectives	49
1.6 Introduction	49
1.6.1 Synthesis of carbon-tin bonds	49
1.6.2 Reaction of organometallic reagents with tin halides:	49
1.6.3 Reaction of stannylmetallic compounds with organic electrophiles.....	51
1.6.4 Reaction of tin or tin (II) compound with alkyl halides.....	51
1.6.5 Hydrostannation of alkenes and alkynes.....	52
1.7 Experimental	54
1.7.1 Synthesis of $(\eta^5\text{-C}_5\text{H}_5)\text{Fe}(\text{CO})_2\text{Sn}^t\text{Bu}_2\text{Cl}$	55
1.7.2 Synthesis of $(\eta^5\text{-C}_5\text{H}_5)\text{Fe}(\text{CO})_2\text{Sn}^t\text{Bu}_2\text{H}$	55
1.7.3 Synthesis of $(\eta^5\text{-C}_5\text{H}_5)\text{Fe}(\text{CO})_2\text{Sn}^t\text{Bu}_2\text{Me}$	56
1.7.4 Synthesis of $(\eta^5\text{-C}_5\text{H}_5)\text{Fe}(\text{CO})_2\text{Sn}^t\text{Bu}_2(\eta^5\text{-C}_5\text{H}_5)\text{Mo}(\text{CO})_3$	56
1.7.5 Synthesis of $[\{(\eta^5\text{-C}_5\text{H}_5)\text{Fe}(\text{CO})\}_2(\mu\text{-Sn}^t\text{Bu}_2)(\mu\text{-CO})]$ (5)	57
1.7.6 Synthesis of $(\eta^5\text{-C}_5\text{H}_5)\text{Mo}(\text{CO})_3\text{Sn}^t\text{Bu}_2\text{Cl}$:	58
1.7.7 Synthesis of $(\eta^5\text{-C}_5\text{H}_5)\text{Mo}(\text{CO})_3\text{Sn}^t\text{Bu}_2\text{Me}$	58
1.7.8 Synthesis of $(\eta^5\text{-C}_5\text{H}_5)\text{Mo}(\text{CO})_3\text{Sn}^t\text{Bu}_2\text{H}$	59

1.7.9	Photochemical reaction of $(\eta^5\text{-C}_5\text{H}_5)\text{Mo}(\text{CO})_3\text{Me}$, 2a with $^t\text{Bu}_2\text{SnH}_2$	59
1.8	Results and discussion.....	60
1.8.1	Synthesis of $(\eta^5\text{-C}_5\text{H}_5)\text{Mo}(\text{CO})_3^t\text{Bu}_2\text{Sn-Me}$ using $(\eta^5\text{-C}_5\text{H}_5)\text{Mo}(\text{CO})_3\text{Me}$ with $^t\text{Bu}_2\text{SnH}_2$ in benzene 3:1 Ratio	60
1.8.2	Crystal structure characterization of $(\eta^5\text{-C}_5\text{H}_5)\text{M}(\text{CO})_n\text{Sn}^t\text{Bu}_2\text{Cl}$, (M = Fe, n = 2; Mo, n = 3)	64
1.8.3	Proposed mechanism for the methyl transfer from metal to tin center.....	65
1.8.4	Observations related to the formation of $^t\text{Bu}_2(\text{H})\text{Sn-Me}$	70
1.9	Conclusions	71
1.10	References	73
Metal-catalyzed reduction of HCONR_2, R = Me (DMF); Et (DEF), by silanes to produce R_2NMe and disiloxanes: A mechanism unraveled		77
Abstract		77
Statement of the problem		79
Justification of importance		79
Research objectives		80
2.1	Introduction	81
2.1.1	Hydrosilylation	81
2.1.2	Silicon hydrogen bond activation by transition metals.....	83
2.1.3	Hydrosilylation of carbonyl derivatives by transition metals	86
2.1.4	Use of Si-H bonds for M-Si bond formation	90
2.1.5	Synthesis of siloxanes	92

2.2 Experimental	93
2.2.1 Isolation of siloxymethylamines $R_3SiOCH_2NMe_2$ from the catalytic cycle:.....	93
2.2.2 Isolation of siloxyethylamine, $PhMe_2SiOCH_2NEt_2$ using DEF from the catalytic cycle:.....	94
2.2.3 The reaction of $PhMe_2SiOCH_2NMe_2$ with $PhMe_2SiH$ using $Mo(CO)_6$ as a catalyst:	95
2.2.4 Synthesis of symmetrical disiloxanes: Reaction of siloxymethylamines $R_3SiOCH_2NR'_2$ and R_3SiH in the presence of either $Mo(CO)_6$, $(\eta^5-C_5H_5)Mn(CO)_3$ or $(\eta^5-C_5H_5)Mo(CO)_3Me$ as a catalyst	95
2.2.5 Synthesis of digermoxanes using $Mo(CO)_6$ as a catalyst	96
2.2.6 Synthesis of digermoxanes using $(\eta^5-C_5H_5)Mo(CO)_2(PPh_3)Me$, 2b, as a catalyst:	96
2.2.7 Synthesis of unsymmetrical disiloxanes, and mixed siloxy-germanes, siloxy-stannanes using $(\eta^5-C_5H_5)Mo(CO)_3Me$ as a catalyst.....	97
2.2.8 Reactions of $Me_3SiOCH_2NMe_2$ with R_3ECl to form unsymmetrical disiloxanes, and mixed siloxy-germanes, siloxy-stannanes:.....	97
2.2.9 The reaction of $Me_3SiOCH_2NMe_2$ with $PhMe_2SiH$ and $Mo(CO)_5THF$ complex:	100
2.2.10 Reaction of $Mo(CO)_6$ with Et_3SiH and DMF:	100
2.2.11 Synthesis of unsymmetrical disiloxanes using excess DMF without a catalyst:	100
2.2.12 Synthesis of $PhMe_2SiOSiPhMe_2$ from a catalytic cycle using $M(CO)_6$, ($M = Cr, W$) catalysts.....	101

2.2.13	Synthesis of R_3ESER_3 , $E = Si, Ge, Sn$ with $Mo(CO)_6$ as catalyst:	102
2.2.14	Synthesis of $R_3SiSSiR_3$ with $Mo(CO)_5(S=CHNMe_2)$ as catalyst	104
2.2.15	Synthesis of $R_3SiSSiR_3$ with $Mo(CO)_5NMe_3$ as catalyst.....	104
2.2.16	Synthesis of $Mo(CO)_5(S=CHNMe_2)$ with $Mo(CO)_5NMe_3$ and thioformamide	104
2.2.17	Synthesis of $R_3SiSSiR_3$ with $Mo(CO)_5(S=CHNMe_2)$ and $PhMe_2SiH$	104
2.3	Results and discussion.....	105
2.3.1	Reduction of amides by R_3EH in the presence of iron and molybdenum complexes	105
2.3.2	Isolation of the intermediates $R_3SiOCH_2NMe_2$ in the presence of $M(CO)_6$, $M =$ Mo, Cr, W	120
2.3.3	Final proposed mechanism	125
2.3.4	Extension to the catalytic reduction of thioformamide.....	130
2.4	Conclusions	135
2.5	References	136
	Appendices.....	144
	Curriculum vita.....	204

List of schemes

Scheme 1.1 :	The proposed mechanism for dimerization of ${}^t\text{Bu}_2\text{SnH}_2$	1
Scheme1.2:	Chemical vapor deposition of multiwalled carbon nanotubes using $(\eta^5\text{-C}_5\text{H}_5)\text{Fe}(\text{CO})_2\text{Me}$	13
Scheme 1.3:	DNA cleavage by $(\eta^5\text{-C}_5\text{H}_5)\text{M}(\text{CO})_n\text{R}$ complexes ($\text{M} = \text{Fe, W, Mo, Cr; R} = \text{Me, Ph}$).....	14
Scheme 1.4:	Catalytic hydrogenation of propylene.....	16
Scheme 1.5:	Sigma bond metathesis mechanism	16
Scheme 1.6:	Proposed mechanism to explain the results on Sn-CH_3 bond formation. $\text{M} = \text{Fe, n} = 1$, (1a) $\text{M} = \text{Mo, n} = 2$, $\text{L} = \text{CO}$ (2a)	47
Scheme 1.7:	Hydrostannation of alkenes and alkynes.....	53
Scheme 1.8:	Proposed mechanism for the formation of $(\eta^5\text{-C}_5\text{H}_5)\text{M}(\text{CO})_n\text{Sn}^t\text{Bu}_2\text{H}$	66
Scheme 1.9:	Proposed mechanism for the formation of bridging compounds of the type M-Sn-M bond.....	68
Scheme-1.10:	Photochemical activation of Fe-E bond in the presence of $(\eta^5\text{-C}_5\text{H}_5)\text{Fe}(\text{CO})_2\text{Me}$, $\text{E} = \text{Si, Ge, Sn}$	70
Scheme 1.11:	Proposed mechanism for the M-E activation, $\text{E} = \text{Si, Ge, Sn}$	71
Scheme 2.1:	Proposed mechanism for the reduction of amides to amines in the presence of $\text{M}(\text{CO})_6$ as catalyst, $\text{M} = \text{Mo, Cr, and W}$	78
Scheme 2.2:	Initial proposed mechanism for siloxane formation	113
Scheme 2.3:	Proposed catalytic cycle for the formation of Me_3N and $\text{R}_3\text{SiSSiR}_3$ from the reaction between R_3EH and thioformamide.	134

List of figures

Figure 1.1:	Tin production worldwide	4
Figure 1.2:	Potential dehydrocoupling oligostannanes for polymerizations	7
Figure 1.3:	Depolymerization of $\text{H}(\text{Sn}^n\text{Bu}_2)_n\text{H}$ ($M_n = 7800$) upon irradiation (380 nm).....	8
Figure 1.4:	Thermochromic behavior of polystannanes under different temperatures.....	9
Figure 1.5:	Thermochromic materials applications	9
Figure 1.6:	Tin oxide and metallic tin formation in different environments - SnO_2 (O_2), -- Sn (N_2).	10
Figure 1.7:	Metal surface interaction on dihydroxylated or hydrosilated γ alumina.....	13
Figure 1.8:	Oxidative addition concept.....	15
Figure 1.9:	Covalent and ionic electron-counting systems	23
Figure-1.10:	Catalytic synthesis of $\text{H}^t\text{Bu}_2\text{Sn-Sn}^t\text{Bu}_2\text{H}$ using $(\eta^5\text{-C}_5\text{H}_5)\text{Mo}(\text{CO})_3\text{Me}$ as catalyst in C_6D_6	24
Figure 1.11:	Catalytic synthesis of $^t\text{Bu}_2\text{HSn-Sn}^t\text{Bu}_2\text{H}$ using $(\eta^5\text{-C}_5\text{H}_5)\text{Mo}(\text{CO})_2(\text{Ph}_3\text{P})\text{Me}$ as catalyst in benzene.....	26
Figure 1.12:	Photochemical irradiation of $^t\text{Bu}_2\text{SnH}_2$ with $(\eta^5\text{-C}_5\text{H}_5)\text{Mo}(\text{CO})_3\text{Me}$ 3:1 ratio	27
Figure 1.13:	Catalytic synthesis of $\text{H}^t\text{Bu}_2\text{Sn-Sn}^t\text{Bu}_2\text{H}$ using $(\eta^5\text{-C}_5\text{H}_5)\text{Mo}(\text{CO})_3^t\text{Bu}_2\text{SnH}$ as catalyst in C_6D_6	29
Figure1.14:	Crystal structure of $(\eta^5\text{-C}_5\text{H}_5)\text{Fe}(\text{CO})(\text{Ph}_3\text{P})^t\text{Bu}_2\text{SnH}$ (1b) and $(\eta^5\text{-C}_5\text{H}_5)\text{Mo}(\text{CO})_3^t\text{Bu}_2\text{SnH}$ (2b).....	31
Figure 1.15:	Catalytic synthesis of $\text{H}^t\text{Bu}_2\text{Sn-Sn}^t\text{Bu}_2\text{H}(\Delta)$ using $\text{Mn}(\text{CO})_5\text{Me}$ as catalyst in C_6D_6	35
Figure 1.16:	Photochemical irradiation of $^t\text{Bu}_2\text{SnH}_2$ with $(\eta^5\text{-C}_5\text{H}_5)\text{Mo}(\text{CO})_3\text{Me}$ 3:1 ratio	61
Figure 1.17:	^{119}Sn NMR spectroscopy showing the disappearance of $^t\text{Bu}_2\text{SnH}_2(*)$ into $(\eta^5\text{-C}_5\text{H}_5)\text{Mo}(\text{CO})_3\text{Sn}^t\text{Bu}_2\text{Me}(\diamond)$ under photochemical conditions.	62

Figure 1.18: ^{119}Sn NMR spectroscopy showing the disappearance of $^t\text{Bu}_2\text{SnH}_2(*)$ into $(\eta^5\text{-C}_5\text{H}_5)\text{Fe}(\text{CO})_2\text{Sn}^t\text{Bu}_2\text{Me}(\diamond)$ under photochemical conditions.....	63
Figure 1.19: Molecular structure of $(\eta^5\text{-C}_5\text{H}_5)\text{Mo}(\text{CO})_3\text{Sn}^t\text{Bu}_2\text{Cl}$	65
Figure 1.20: Molecular structure of (stannylene)(carbonyl) bridged diiron complex (5).....	69
Figure 1.21: ^{119}Sn NMR spectroscopy showing the isomerization of (stannylene)(carbonyl) bridged diiron complex (5) into (cis) 5a and (trans) 5b	69
Figure 2.1: Hydrosilylation of alkenes	83
Figure 2.2: Chalk- Harrod mechanism	84
Figure 2.3: Mechanism for the Si-H bond activation	84
Figure 2.4: Si-H bond activation by oxidative addition and three center two electron bonding	85
Figure 2.5: Sigma bond and π backbonding for the Si-H activation	86
Figure 2.6: Mechanism of the Rh-catalyzed hydrosilylation of ketones.....	87
Figure 2.7: Iridium catalyzed hydrosilylation of ketones.....	88
Figure 2.8: Molybdenum catalyzed hydrosilylation of aldehydes	89
Figure 2.9: Formation of metal-silicon bonds using SiH compounds.....	90
Figure 2.10: Important symmetrical siloxanes	92
Figure 2.11: ^{29}Si NMR spectroscopic monitoring showing the disappearance of Ph_2MeSiH in the presence a 5 mol% 2a catalyst in DMF- C_6D_6 , photochemically irradiated	106
Figure 2.12: ^{29}Si NMR spectroscopic monitoring showing the disappearance of Ph_2MeSiH in the presence a 5 mol% Mo-catalyst UV-light and thermally 70°C in DMF- C_6D_6	107
Figure 2.13: ^{13}C NMR spectroscopic monitoring showing the disappearance of $\text{Et}_3\text{GeH}(*)$ and the appearance of $\text{Et}_3\text{Ge-O-GeEt}_3(\diamond)$ in the presence of 2b at 70°C	108

Figure 2.14: ^{119}Sn NMR spectroscopy showing the disappearance of Bu_3SnH (*) and the formation of $\text{Bu}_3\text{SnOSnBu}_3$ (\diamond) in the presence of 2b catalyst.....	110
Figure 2.15: Proposed hydrosilylation product in the first step of the catalytic reduction of amide.....	114
Figure 2.16: Characterization by ^{29}Si and ^{13}C NMR spectroscopy of $\text{Me}_3\text{Si-O-CH}_2\text{NMe}_2$..	115
Figure 2.17: ^{119}Sn NMR spectroscopic monitoring the disappearance of Bu_3SnH (1) and $\text{Me}_3\text{SiOCH}_2\text{NMe}_2$ into $\text{Bu}_3\text{SnOSiMe}_3$ (2) in C_6D_6	117
Figure 2.18: ^{29}Si NMR spectroscopic monitoring the disappearance of Ph_3SiH (1) and $\text{Me}_3\text{SiOCH}_2\text{NMe}_2$ (2) into $\text{Ph}_3\text{SiOSiMe}_3$ (3) in the presence a 5 mol % Mo-catalyst in C_6D_6	118
Figure 2.19: ^{13}C NMR spectroscopic monitoring the disappearance of Et_3GeH (1) and $\text{Me}_3\text{SiOCH}_2\text{NMe}_2$ (2) into $\text{Et}_3\text{GeOSiMe}_3$ (3) in the presence a 5 mol % Mo-catalyst in C_6D_6	119
Figure 2.20: ^{13}C NMR spectroscopic monitoring the disappearance of Bu_3SnH (1) and $\text{Me}_3\text{SiOCH}_2\text{NMe}_2$ (2) into $\text{Bu}_3\text{SnOSiMe}_3$ (3) in the presence a 5 mol % Mo-catalyst in C_6D_6	119
Figure 2.21: Left, ^{29}Si NMR showing the disappearance of PhMe_2SiH (-17.3 ppm) and transient formation of 4a (5.4 ppm) en route to $(\text{PhMe}_2\text{Si})_2\text{O}$ (0.6ppm): Right, ^{13}C spectra illustrating formation of $\text{PhMe}_2\text{SiOCH}_2\text{NMe}_2$ (4a). in the presence of $\text{Mo}(\text{CO})_6$	122
Figure 2.22: ^{13}C NMR spectroscopy showing the disappearance of $\text{Et}_3\text{SiOCH}_2\text{NMe}_2$ (Δ) and Et_3SiH (*) into $(\text{Et}_3\text{Si})_2\text{O}$ (\diamond) with concomitant formation of Me_3N at 90°C in the presence excess DMF.....	124
Figure 2.23: Proposed activation of the Si-H bond by DMF coordination.	125
Figure 2.24: Metal carbonyl dissociation and metal coordination or Si-H activation.....	126

Figure 2.25: Metal coordination and Si-H activation (ii,iii).....	126
Figure 2.26: Molybdenum carbonyl tri-substituted complex	127
Figure 2.27: Reductive elimination of intermediate $R_3SiOCH_2NMe_2$ (iii,iv).....	127
Figure 2.28: NMR monitoring of the reaction between $PhMe_2SiH$ and $HC(=S)NMe_2$ catalyzed by $Mo(CO)_6$ showing the formation of $Mo(CO)_5(S=CHNMe_2)$ and disappearance of $PhMe_2SiH$ to form $PhMe_2SiSSiMe_2Ph$ and Me_3N : (A) ^{29}Si spectra; (B) ^{13}C	131
Figure 2.29: NMR monitoring of the reaction between $Mo(CO)_5NMe_3$ and $HC(=S)NMe_2$ (\diamond) showing the complete disappearance of $Mo(CO)_5NMe_3$ to form $Mo(CO)_5(S=CHNMe_2)$ and Me_3N at room temperature : ^{13}C Spectra.....	132
Figure 2.30: ^{13}C Spectra NMR monitoring of the reaction between $Mo(CO)_5(S=CHNMe_2)$ and $PhMe_2SiH$ (*) showing the complete disappearance of $Mo(CO)_5(S=CHNMe_2)$ to form $PhMe_2SiSSiPhMe_2$ (\diamond) and Me_3N at $120^\circ C$...	133

List of tables

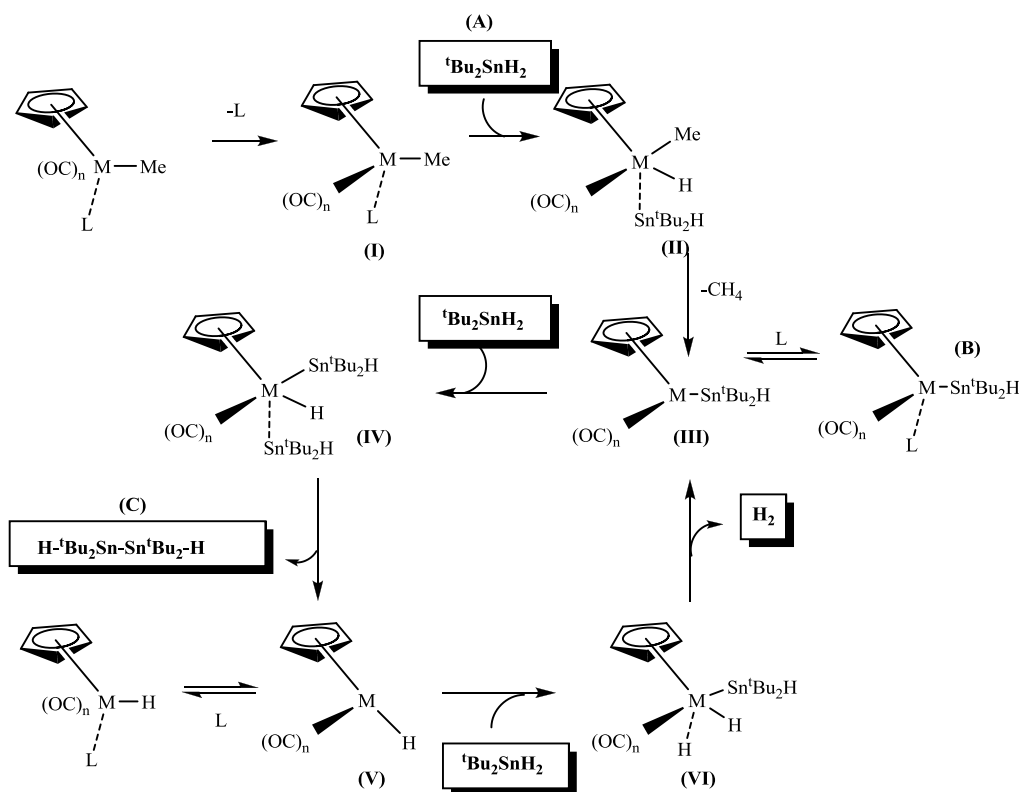
Table 1.1:	Molecular weight data for dehydropolymerization of ${}^n\text{Bu}_2\text{SnH}_2$, as function of catalyst (reactions were run with neat monomer and 2-4mol% catalyst)8
Table 1.2:	Some examples of metal alkyl intermediates in catalytic reactions 12
Table 1.3:	${}^{13}\text{C}$ NMR spectroscopy of iron and molybdenum complexes23
Table 1.4:	Photochemical and thermal transformation of ${}^t\text{Bu}_2\text{SnH}_2$ to $\text{H}^t\text{Bu}_2\text{SnSn}^t\text{Bu}_2\text{H}$ using the iron and molybdenum complexes.....25
Table 1.5:	M-Sn and Sn-H bond length for $(\eta^5\text{-C}_5\text{H}_5)\text{Fe}(\text{CO})(\text{Ph}_3\text{P})^t\text{Bu}_2\text{SnH}$ and $(\eta^5\text{-C}_5\text{H}_5)\text{Mo}(\text{CO})_3^t\text{Bu}_2\text{SnH}$30
Table 1.6 :	Bond dissociation energy (BDE) and bond dissociation free energies(BDEg) for M-H bonds in group 8 and group 6.33
Table 1.7:	${}^{119}\text{Sn}$ spectroscopy for $(\eta^5\text{-C}_5\text{H}_5)\text{Fe}(\text{CO})(\text{H})(\text{Bu}_3\text{Sn})_2$ and $(\eta^5\text{-C}_5\text{H}_5)\text{Fe}(\text{CO})(\text{H})(^t\text{Bu}_2\text{SnH})_2$34
Table 1. 8:	Important synthetic methodologies to form Sn-C bonds54
Table 1.9:	${}^{119}\text{Sn}$ NMR spectroscopy from the photochemical reaction 3:1 between ${}^t\text{Bu}_2\text{SnH}_2$ and $(\eta^5\text{-C}_5\text{H}_5)\text{Mo}(\text{CO})_3\text{Me}$61
Table 2.1:	Enthalpies of reaction of metal carbonyls with triethylsilane (ΔH).....85
Table 2.2:	Synthesis of $\text{R}_3\text{SiOSiR}_3$ in the presence of $\text{R}_3\text{SiOCH}_2\text{NR}'_2$ and R_3SiH using $(\eta^5\text{-C}_5\text{H}_5)\text{Mn}(\text{CO})_3$, $(\eta^5\text{-C}_5\text{H}_5)\text{Mo}(\text{CO})_3$, $\text{Mo}(\text{CO})_6$ as catalyst.96
Table 2.3:	Synthesis of $\text{R}_3\text{SiOSiR}_3$: Reaction of $\text{R}_3\text{SiOCH}_2\text{NR}'_2$ and R_3SiH using excess of DMF/DEF without a catalyst..... 101
Table 2.4:	Catalytic reduction of DMF with $\text{R}_3\text{E-H}$, ($\text{E} = \text{Si, Ge, Sn}$) in the presence of 5 mol% Mo Catalyst 2a or 2b* in C_6D_6 107
Table 2.5:	Synthesis of disiloxanes, digermoxanes and distannoxanes using Fe, Mo catalysts with excess 2 -8 fold of DMF. 109

Table 2.6:	Photochemical reaction of $\text{Me}_3\text{SiOCH}_2\text{NMe}_2$ with $\text{R}_3\text{E-H}$, ($\text{E} = \text{Si, Ge, Sn}$) in the presence of 5 mol% Mo (2a) catalyst in C_6D_6	116
Table 2.7:	Thermal reaction of $\text{Me}_3\text{SiOCH}_2\text{NMe}_2$ with R_3ECl , ($\text{E} = \text{Si, Ge, Sn}$) in C_6D_6	120
Table 2.8:	Synthesis of disiloxanes, and digermoxanes using $\text{M}(\text{CO})_6$, $\text{M} = \text{Mo}$ (3a), Cr(4), W(5) catalysts with excess 2 -8 fold of DMF.	121
Table 2.9:	Synthesis of $\text{R}_3\text{SiOCH}_2\text{NMe}_2$ using 3a.....	123
Table 2.10:	Catalytic reduction of DMF with $\text{R}_3\text{E-H}$, ($\text{E} = \text{Si, Ge}$) in the presence of 5 mol% Mo Catalyst* in C_6D_6	129
Table 2.11:	Synthesis of disila-, digerma-, and distanna-thianes.....	130

Dehydrogenative dimerization of ${}^t\text{Bu}_2\text{SnH}_2$, catalyzed by iron and molybdenum complexes

Abstract

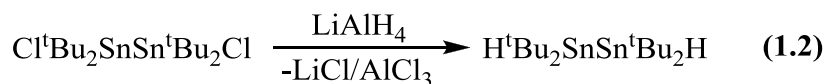
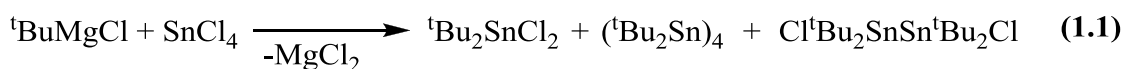
A new catalytic system involving iron and molybdenum complexes of the type: $(\eta^5\text{-C}_5\text{H}_5)\text{M}(\text{CO})_n\text{Me}$, and $(\eta^5\text{-C}_5\text{H}_5)\text{M}(\text{CO})_{n-1}(\text{PPh}_3)\text{Me}$, $\text{M} = \text{Fe}$, $n = 2$ (**1**); $\text{M} = \text{Mo}$, $n = 3$ (**2**), were used to catalyze the dehydrogenative dimerization of di-*t*-butyltin dihydride to 1,2-dihydro-1,1,2,2-tetra-*t*-butyl-distannane, ${}^t\text{Bu}_2\text{HSn-SnH}{}^t\text{Bu}_2$ both photochemically and thermally. The thermal catalytic process is much more efficient than the photochemical process and the Mo catalysts are relatively more active than the corresponding Fe catalysts. A mechanism involving oxidative addition and reductive elimination steps has been suggested involving the intermediacy of $(\eta^5\text{-C}_5\text{H}_5)\text{M}(\text{CO})_n\text{Sn}{}^t\text{Bu}_2\text{H}$. This complex was observed during the reaction and was independently synthesized and completely characterized by single crystal X-ray structural analysis and ${}^{13}\text{C}$, ${}^{119}\text{Sn}$ and ${}^1\text{H}$ NMR spectroscopy. It was also shown to be catalytically active for dehydrogenative dimerization, Scheme 1.1.



Scheme 1.1 : The proposed mechanism for dimerization of ${}^t\text{Bu}_2\text{SnH}_2$ using catalysts 1 and 2

Statement of problem

The general area of this investigation involves the formation of Sn-Sn bonds, specifically distannanes.¹ A large number of hexaorgano substituted distannanes are known² since they are widely used in different types of organic reaction, such as cross coupling agents,³ radical sources,⁴ and industrial catalysis.⁵ However, only a limited number of functional distannane compounds of the type $\text{XR}_2\text{Sn-SnR}_2\text{X}$, $\text{X} = \text{halogen, alkali metal or hydrogen}$, are described in the literature. Many of these compounds are only known as minor products from various reactions and only a small number could be isolated as pure substances $\text{XSnR}_2\text{-Sn(X)R}_2$ ($\text{X} = \text{Cl, Br, I}$),⁶ and $\text{HSnR}_2\text{-Sn(H)R}_2$,⁷ ($\text{R} = \text{t-butyl}$). A recent report by Uhlig *et al.* described the synthesis of 1,2-dihydro-tetra-*t*-butyldistannane in a two step process with a yield of 2.5%, eq. 1.1,1.2.⁸



Thus, the question posed relates to the possibility of obtaining better yields *via* use of new chemistry, specifically using transition metal complexes as catalysts to promote the coupling of secondary tin hydrides R_2SnH_2 . This suggestion stems from previous research that reported coupling of tertiary stannanes, R_3SnH , to produce $\text{R}_3\text{Sn-SnR}_3$.

Justification of importance

Polysilanes are well-studied due to their interesting electronic, optical and chemical properties,⁹ and this has stimulated interest in the heavier element congeners, such as Ge and Sn.¹⁰ Polymeric materials containing Sn-Sn bonds,^{4,5} might be expected to give greater σ -delocalization, lower band gaps, and more metallic character due to more diffuse bonding orbitals.¹⁰ Furthermore, such properties could be used for applications in charge-transport, photoresists in microlithography, nonlinear optical materials, semiconductors in doping, and electronic devices.¹¹ However, the synthetic methodologies reported until now make use extensively of transition metals and the yields and size distributions depend enormously on the type of catalyst and the conditions performed.^{11a} Secondary tin hydrides, R_2SnH_2 , have been used successfully to promote the dehydrogenative coupling into polystannanes, $(R_2Sn)_n$, but unfortunately mixtures of products containing small oligomers, cyclooligomers and polymers of low molecular weight are obtained.¹¹

It has been suggested that distannanes and other small oligomers, $(H-(R_2Sn-R_2Sn)_n-H)$ could be better monomers for dehydrocoupling allowing the formation of higher molecular weight polymers.^{11a} However, until the Uhlig report there were no well-defined synthetic methodologies for the synthesis of 1,2-dihydrodistannanes.⁸ Given the overall 2.5% yield the need for alternative approaches is self-evident.

Research objectives

- ❖ To develop a catalytic process for the high yield synthesis of functional distannanes, $XSnR_2SnR_2X$, preferably using transition metal catalysis.
- ❖ To determine a plausible mechanism for the newly discovered chemistry.

1.1 Introduction

1.1.1 Applications of organotins (OTs)

Tin has been known as a metal since time immemorial and the discovery, in about 3500 BC, that it formed a strong, hard alloy with copper, started the Bronze Age, which lasted until 1200BC. The abundance of tin in the Earth's crust is about 2 ppm, significantly less than zinc (94 ppm), copper (63 ppm), or lead (12 ppm) and the most important ore is cassiterite, SnO_2 .¹²

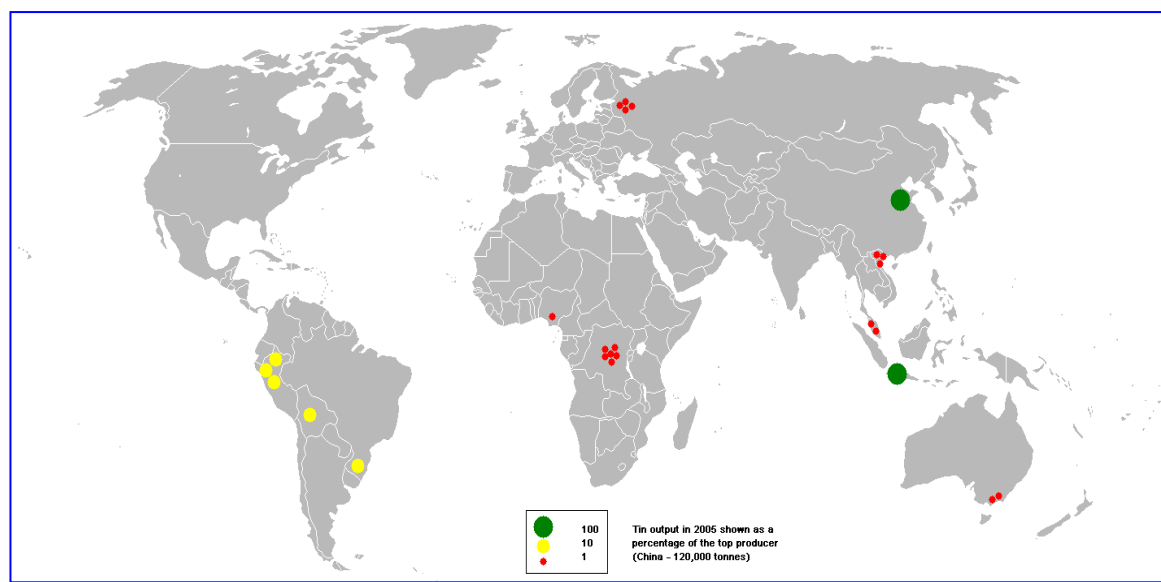


Figure 1.1 Tin production worldwide¹²

About 75% of the world's production comes from China and South East Asia, and about 18% from South America, Fig. 1.1, but the annual Figures are sensitive to political, social and economic factors.¹³ Organotins (OTs) are a class of chemicals that contain at least one tin-carbon bond and the important classes can be generalized as $\text{R}_n\text{SnX}_{4-n}$, R = organic group, X = H, halogen, alkoxy, carboxylato, etc.

The most common uses of OTs involve the following:

PVC stabilizers: Organotins have been used to capture the chlorinated compounds, produced in the synthesis of PVC.^{14,15}

Catalytic agents: Catalytic reactions have been used for silicone vulcanization,^{18,19} and polyurethanes formation.¹⁶ Dibutyltin dioctanoate, dibutyltin dilaurate, stannous octanoate, and recently the use of stannoxanes are particularly effective for both systems.^{17,20} Other catalytic applications involve the use of Bu_2SnO , BuSnO_2H and $\text{Bu}_2\text{Sn}(\text{Ac})_2$ in the transesterification process.²¹

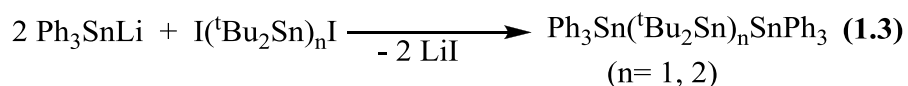
Biocidal compounds: Organotins containing at least one good leaving group, e.g. halogen, carboxylato, etc., have found a wide range of uses in agriculture, wood preservatives and antifouling paints. The chain length (n) of the R group is a crucial feature in determining biocidal activity. The most toxic organotin compounds towards mammals are those with n -alkyl chains containing 1-2 carbons, whereas $n = 3, 4$ are useful antibacterial species. For $n = 6, 7, 8$ the biocidal activity drops off rapidly, presumably due to the very hydrophobic nature of the resulting materials that make transport through membranes difficult.²²⁻²⁵ Aryl groups have been used for antifungal applications, e.g. Ar_3SnCl .²⁶

1.1.2 Polystannanes

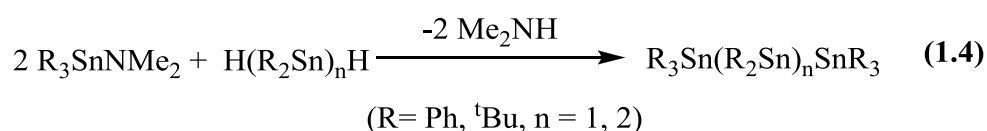
It is well known that group 14 elements have the ability to form polymeric chains.¹² The chemistry of polysilanes is well known and has been explored in detail, because of their important applications related to their use as sensors, coating materials, etc.^{9,27} However, as one goes down in the group the tendency to catenate decreases from carbon to lead.¹² Special interest has been focused on the formation of polystannanes due to the fact that it is believed that they will present interesting electronic properties associated with lower band gaps due to the presence of more diffuse bonding orbitals.¹⁰ In general the most interesting techniques

reported until now for the formation of oligostannanes and polystannanes can be summarized as:

- Salt-elimination reactions to build up to six tin atom chains, eq. 1.3. These reactions are not clean and mixture of products are produced because of Sn-Sn bond cleavage by the lithium reagents.²⁸



- Amine elimination reactions between tin amines and organotin hydrides, eq. 1.4.^{29a}

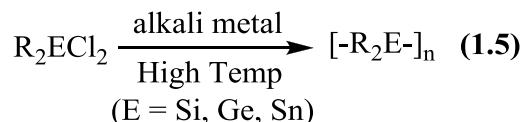


- The use of protecting groups to facilitate the formation of longer tin chains using the β -alkoxy group has been reported.^{29b} This process requires many steps and the purification process is time-consuming, even though there have been attempts to improve the process to up to 15 tin atoms in the chain.³⁰

Electrochemical reduction of diorganotin dihalides has been used for the formation of moderate molecular weight polystannanes.^{31,32} However, the method is high cost because the electrodes have to be replaced every time.

- Wurtz coupling reactions are known to make Si-Si bonds, however, it is highly sensitive to the substituents on the substrate, solvents, concentrations, alkali metals, reaction periods, and temperature.³³ Consequently it is often difficult to optimize and reproduce the conditions for the synthesis of high molecular weight polymers. Polysilanes and polygermanes have been synthesized by high temperature reductive coupling of the R_2ECl_2 , E = Si, Ge with alkali metals in hydrocarbon or ethereal solvents and this has been applied for

polystannanes, eq. 1.5.³³ However, due to the relative weakness of the Sn-Sn bond,³⁴ the relatively harsh conditions generally produce low molecular weight polystannanes or cyclic oligomers, in relatively poor yield.³⁵



Dehydropolymerization is another important concept that uses transition metals, e.g. Ti, Zr, Hf, Cr, Mo, W, Rh, Pt, and heterobimetallic Fe-Pd complexes,³⁶⁻⁵³ for the formation of polystannanes, eq. 1.6. Even though the process has been improved, the necessity to get more selectivity, and a more generalized methodology to obtain polymers of high molecular weight with narrowed polydispersities and mild conditions persist.



An important observation in this chemistry, reported by Tilley and Imori, using (η^5 -C₅H₅)₂Zr(H)Me as catalyst under the conditions described in Table. 1.1, was the detection of monomers by GPC, indicating that in this polymerization distannanes and small oligomers Fig. 1.2, are much more reactive than monomer toward dehydrocoupling.³⁷ This observation suggests that distannanes of the type HR₂SnSnR₂H could be useful starting materials for polymerization.

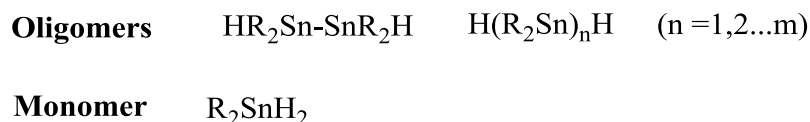


Figure 1.2 Potential dehydrocoupling oligostannanes for polymerizations

Table 1.1 Molecular weight data for dehydropolymerization of ${}^n\text{Bu}_2\text{SnH}_2$, as function of catalyst (reactions were run with neat monomer and 2-4mol% catalyst)

Catalyst	React. Time	% Cyclic	Cyclic + Linears		Linear Fraction	
			Mn	Mw	Mn	Mw
$[(\eta^5\text{-C}_5\text{H}_5)_2\text{Zr(H)Me}]$	0.5 h	7(58) ^a	2900	13200	5400	13400
	3.5 h	43(18) ^a	2300	11100	6600	17100
	6 h	45(27) ^a	1100	7600	6100	14300
	18 h	57(17) ^a	1000	5700	8700	18800
	2 d	98	900	1000		

^a The number in parentheses represents the approximate percentage of material remaining as monomer.
Taken from Reference ³⁷

1.1.3 Polystannane properties

The properties associated with polystannanes are of technological interest. For example in Fig. 1.3, irradiation of a polystannane into the region of 380 nm causes a “photobleaching” effect and effectively a depolymerization that can expose an underlying surface. Such properties can be used, in addition to photoresists, for applications in charge transport, microlithography, nonlinear optical materials, semiconductors and electronic devices.¹¹

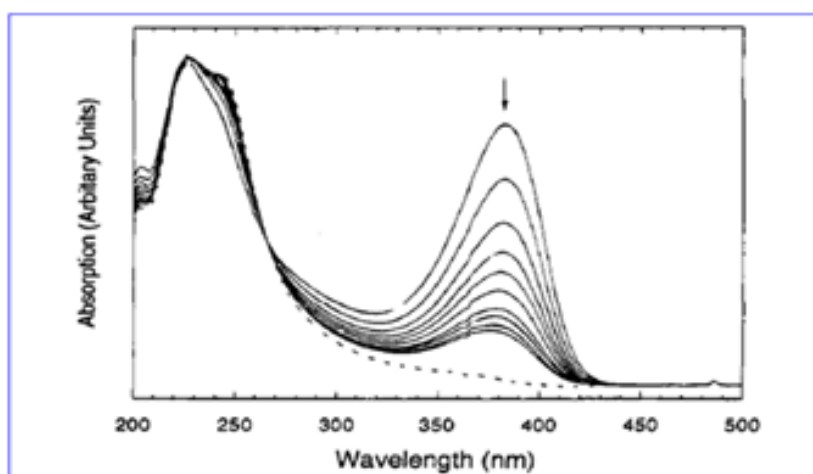


Figure 1.3 Depolymerization of $\text{H}(\text{SnnBu}_2)_n\text{H}$ ($\text{Mn}=7800$) upon irradiation (380 nm)

Taken from Reference ¹¹

Polystannanes also exhibit interesting thermochromic effects where the low energy band in the UV/VIS changes with temperature, Fig. 1.4.

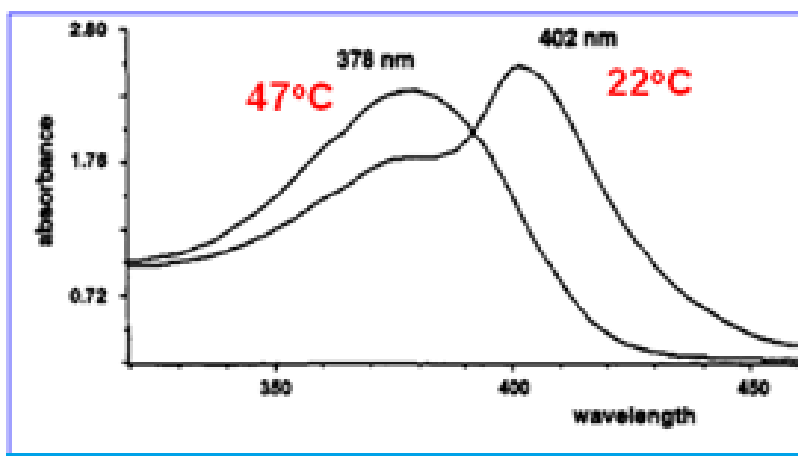


Figure 1.4 Thermochromic behavior of polystannanes under different temperatures. Taken from reference ¹¹

In this particular example the changes in absorption as a function of temperature are reversible.^{10b,10e} Thermochromism has several entertaining applications as noted in Fig. 1.5.



Figure 1.5 Thermochromic materials applications

A further notable use of polystannanes is their ability to be transformed to thin films of SnO_2 in the presence of O_2 under relatively mild conditions. This is illustrated in Fig. 1.6, where the film obtained depends upon the atmosphere used for the degradation.^{11a}

polymer	atmosphere	onset temp for dec (°C)	% ceramic yield at 400 °C
H(Sn ⁿ Bu ₂) _n H	N ₂	255	18
	air	239	53
	O ₂	196	66
H(Sn ⁿ Hex ₂) _n H	N ₂	265	24
	air	220	50
H(Sn ⁿ Oct ₂) _n H	N ₂	271	34
	air	245	44

Figure 1. 6 Tin oxide and metallic tin formation in different environments -SnO₂ (O₂), --Sn (N₂). Taken from reference ^{11a}

Tin films containing either SnO₂ or Sn are potential candidates to produce semiconductor materials. For example, the conductivity of tin films associated with the dehydropolymerization of H(SnⁿOct₂)_nH and H(SnⁿBu₂)_nH with a value of 0.30 Scm⁻¹ and 0.10 Scm⁻¹ respectively, are comparable with polysilanes with a value of 1 Scm⁻¹. ^{9,11a}

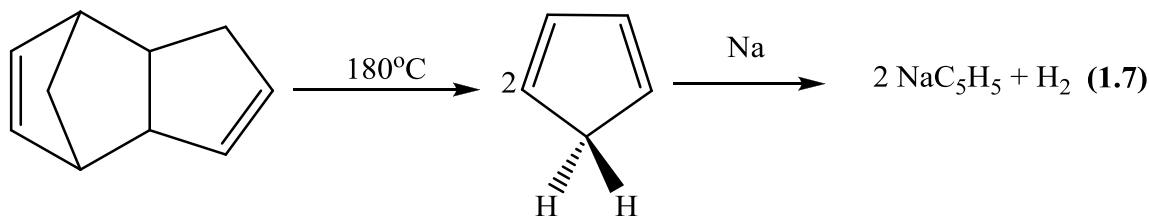
1.1.4 Transition metal carbonyl complexes

Transition metal carbonyls are among the best known classes of organometallic compounds. They are common starting materials in the synthesis of other low valent metal complexes. Not only can the carbonyl ligand be substituted for a large number of other ligands (Lewis bases, olefins, arenes),⁵⁴ but the remaining CO stabilizes the molecule against oxidation or thermal degradation.^{54b}

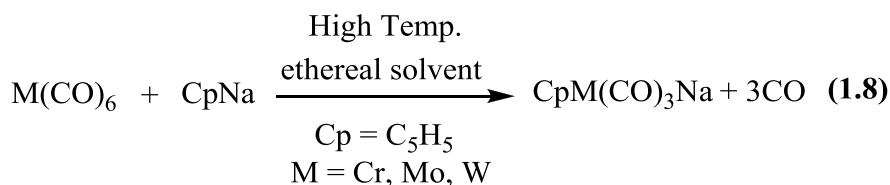
Cyclopentadienyl complexes

The cyclopentadienyl ligand, Cp = (η⁵-C₅H₅), is the most important of the polyenyls because they are firmly bound and general inertness to nucleophilic or electrophilic reagents. This makes it reliable spectator ligand for a series of complexes (η⁵-C₅H₅)ML_n (n = 2-4; L = CO, PPh₃, alkyl radical etc.). Whether we want chemistry to occur at the ML_n group/ (η⁵-C₅H₅)ML_n are often referred to as “two-, three-, or four legged piano stools,” with the (η⁵-C₅H₅) regarded as the seat, and the other ligands as a legs.⁵⁵

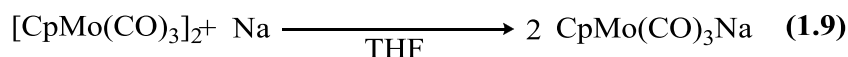
Dicyclopentadiene must first be “cracked” to give monomeric C_5H_6 ,⁵⁶ eq. 1.7. Cyclopentadiene is a weak acid ($P_{ka} = 15$) and can be deprotonated by strong bases or alkali metals. Cyclopentadienylsodium ($Na(\eta^5-C_5H_5)$) is the most common reagent for the introduction of cyclopentadienyl ligands.⁵⁷



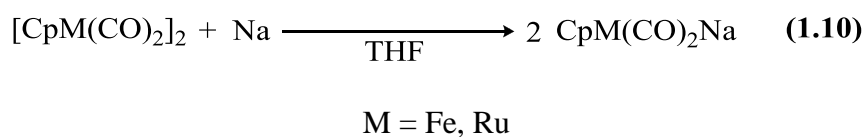
The cyclopentadienyl salt has been used to prepare metal carbonyl complexes, in which 3 carbonyls are displaced, as for example,^{54a,58} eq. 1.8. $\text{Cp} = (\eta^5-C_5H_5)$ $\text{CpM}(\text{CO})_3\text{Na}^+$



The preparation of $(\eta^5-C_5H_5)\text{Mo}(\text{CO})_3\text{Na}^+$ has an advantage from the reaction of $[(\eta^5-C_5H_5)\text{Mo}(\text{CO})_3]_2$ and sodium/amalgam, eq. 1.9.^{54a,59} in that the $\text{Mo}(\text{CO})_6$ is more readily available and less expensive than $[(\eta^5-C_5H_5)\text{Mo}(\text{CO})_3]_2$.



Other examples involve the use of Fe or Ru complexes,^{54a,59} eq. 1.10.



1.1.5 Transition metal alkyl complexes

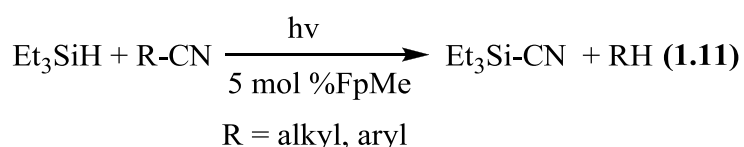
Transition metal alkyl complexes have attracted considerable attention because they are catalytic precursors or key intermediates in many homogeneous and heterogeneous catalytic reactions, Table. 1.2.^{60,61}

Table 1.2 Some examples of metal alkyl intermediates in catalytic reactions

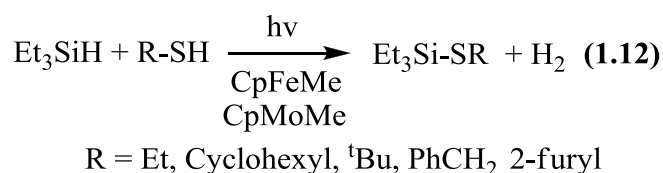
Metal-alkyl species	Catalytic reaction
Ti-R	Alkene polymerization
Zr-R	Alkene polymerization
W-R	Alkene metathesis
Fe-R	Fischer-Tropsch process
Ru-R	Fischer-Tropsch process
Co-R	Hydroformylation and Fischer-Tropsch
Rh-R	Alkane activation
Rh-R	Hydroformylation and acetic acid synthesis
Pd-R	Co-polymerisation of CO and C ₂ H ₄
Pt-R	Alkene hydrogenation

Those metal complexes could be used as potential model compounds to study the reactivity and catalytic activity in these important catalytic cycles, by NMR and IR spectroscopies.⁶¹ More recently, interest has been focused on the use of inexpensive transition metal complexes containing iron, such as $(\eta^5\text{-C}_5\text{H}_5)\text{Fe}(\text{CO})(\text{L})\text{Me}$, ($\text{L} = \text{CO}$, Ph_3 , etc) and related molybdenum systems such as $(\eta^5\text{-C}_5\text{H}_5)\text{Mo}(\text{CO})_2(\text{L})\text{Me}$; $\text{L} = \text{CO}$, Ph_3P , Etc).⁶¹ A variety of catalytic and interesting reactions have been reported in the literature including:

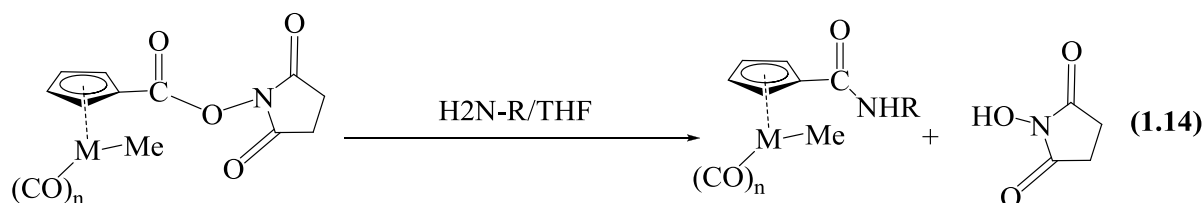
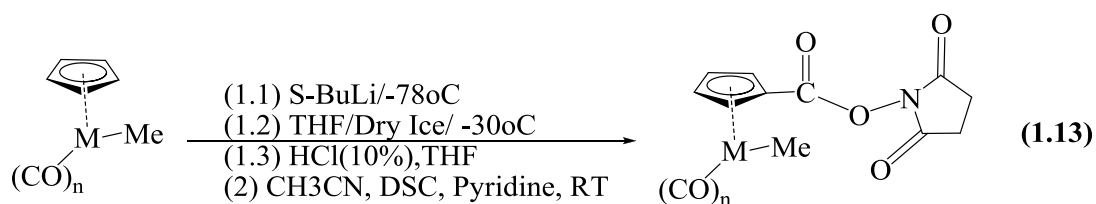
- C-C bond cleavage of RCN.⁶²



- Si-S coupling reactions using, $\text{Cp} = (\eta^5\text{-C}_5\text{H}_5)$, $(\eta^5\text{-C}_5\text{H}_5)\text{Fe}(\text{CO})_2\text{Me}$, and $(\eta^5\text{-C}_5\text{H}_5)\text{Mo}(\text{CO})_3\text{Me}$, as catalyst.⁶³



- Precursor materials for aminoacids labeling using $(\eta^5\text{-C}_5\text{H}_5)\text{M}(\text{CO})_n\text{LMe}$ $\text{M} = \text{Fe}$, $n = 2$, Mo , $n = 3$, eq. 1.13, 1.14.⁶⁴



- Model compounds for studies of potential surface transformations.⁶⁵ Fig. 1.7.

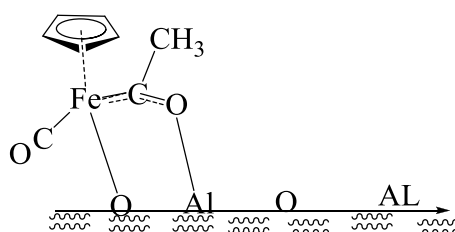
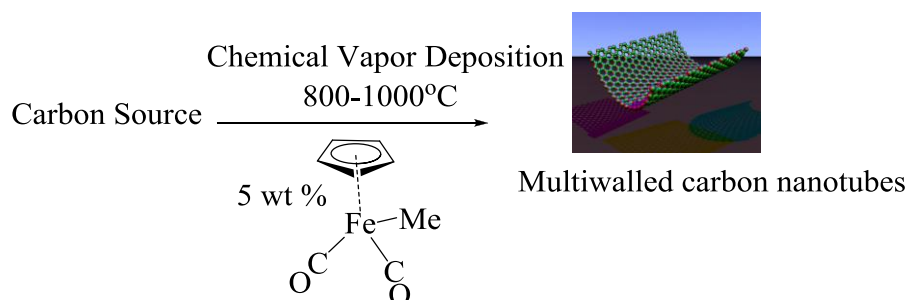


Figure 1.7 Metal surface interaction on dihydroxylated or hydrosilated γ alumina

$(\eta^5\text{-C}_5\text{H}_5)\text{Fe}(\text{CO})_2\text{Me}$ was used because of the multiplicity of metal surface transformations, including surface induced migratory insertion. Fig. 1.7. shows a surface induced migratory CO insertion to yield a carbene-like acyl complex as the major pathway.

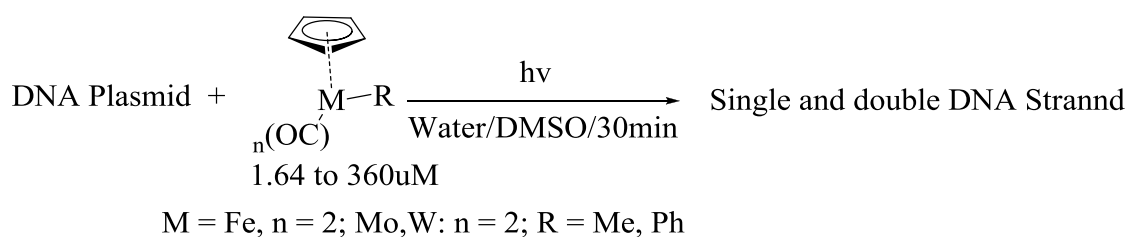
- Catalytic materials for CVD (chemical vapor deposition) multiwalled carbon nanotubes, Scheme. 1.2.⁶⁶



Scheme 1.2 Chemical vapor deposition of multiwalled carbon nanotubes using $(\eta^5\text{-C}_5\text{H}_5)\text{Fe}(\text{CO})_2\text{Me}$

- Photoinduced DNA cleavage $(\eta^5\text{-C}_5\text{H}_5)\text{MR}$ $\text{R} = \text{Me, Ph}$ $\text{M} = \text{Cr, Mo, W, Fe}$.⁶⁷ Scheme.

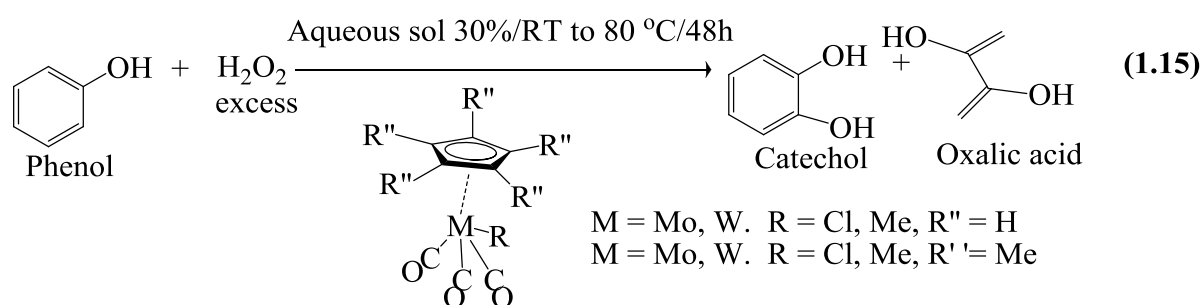
1.3.



Scheme 1.3 DNA cleavage by $(\eta^5\text{-C}_5\text{H}_5)\text{M}(\text{CO})_n\text{R}$ complexes ($\text{M} = \text{Fe, W, Mo, Cr}; \text{R} = \text{Me, Ph}$)

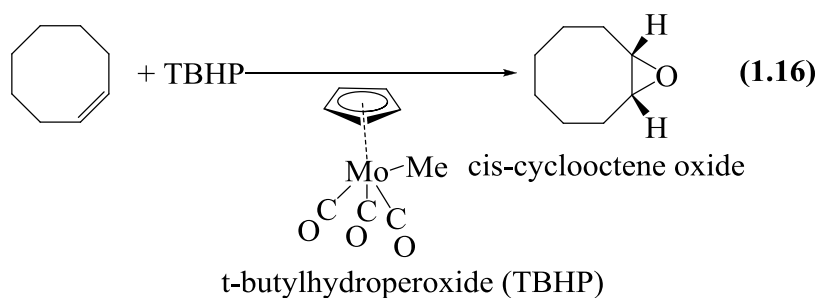
Whereas Fe and W complexes work efficiently, specially the phenyl derivatives, Mo and Cr do not produce any cleavage. It is believed that *carbon-centered radicals* are implicated as the active species leading to DNA strand scission.

- Photodegradation of phenols using H_2O_2 and $(\eta^5\text{-C}_5\text{H}_5)\text{M}(\text{CO})_3\text{R}$, $(\eta^5\text{-C}_5\text{Me}_5)\text{M}(\text{CO})_3\text{R}$; $\text{M} = \text{Mo, W}$ ($\text{R} = \text{Cl, Me}$). and $\text{Mo}(\text{CO})_6$.⁶⁸ eq. 1.15.



$(\eta^5\text{-C}_5\text{H}_5)\text{Mo}(\text{CO})_3\text{R}$ $\text{R} = \text{Cl, Me}$, were the most active catalyst using H_2O as solvent at 55°C and only trace of p-benzoquinone were detected.

- $(\eta^5\text{-C}_5\text{H}_5)\text{Mo}(\text{CO})_3\text{Me}$ is a catalyst precursor for epoxidation of olefins, eq. 1.16.⁶⁹



1.1.6 Oxidative addition and reductive elimination

As the name implies, oxidative addition is the addition of a substrate molecule to a transition metal complex whereby the metal center is oxidized. In the generic mononuclear examples below, Fig. 1.8, the metal goes from the x to the $x+2$ oxidation states and is therefore limited to the middle and late transition metals.⁷⁰

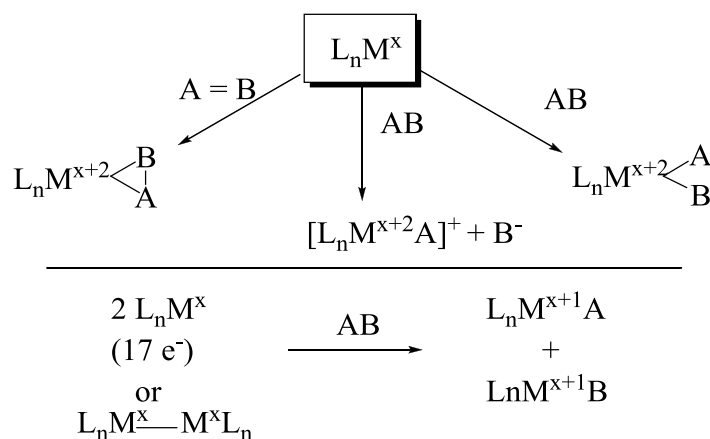
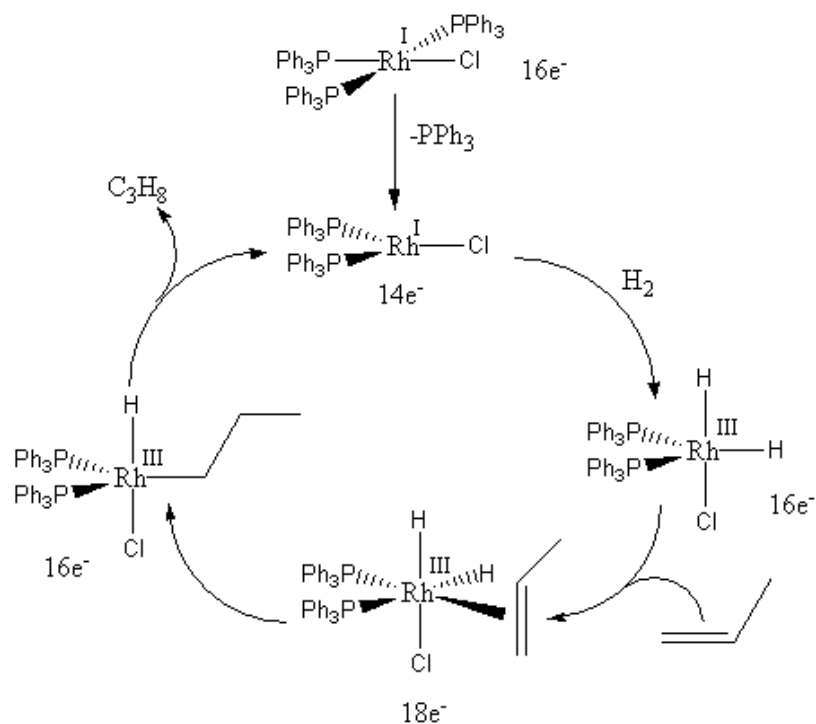


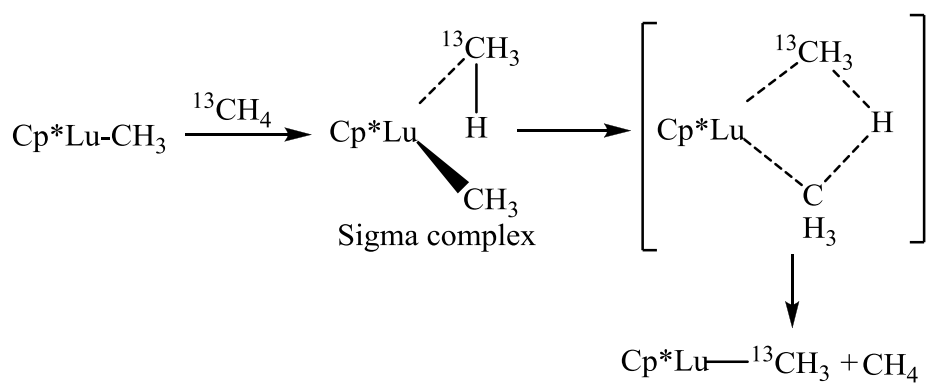
Figure 1.8 Oxidative addition concept

Oxidative addition and the reverse process, reductive elimination, are fundamental reaction steps in many homogenous catalysis,⁷¹ and have been extensively investigated both experimentally and theoretically.^{72,73} Using Wilkinson's catalyst,⁷⁶ a variety of industrially important catalytic cycles, for example (The Monsanto process⁷⁴, alkene hydrogenation⁷⁵ have been reported, Scheme. 1.4.



Scheme 1.4 Catalytic hydrogenation of propylene⁷⁵

Oxidative addition reactions cannot occur on metal centers that are already in their highest oxidation state, so a sigma bond metathesis reaction is a likely alternative, Scheme 1.5.⁷⁷



Scheme 1.5 Sigma bond metathesis mechanism

This kind of concerted process is believed to occur through a four-centered transition state, that maintains the central atom in the normal oxidation state.⁷⁸

At this point I have mentioned the most important concepts that are related the use of transition metals and the main properties associated with their reactivity. Such reactivity could be influenced by a variety of factors, including their position in the periodic table, electronic conFiguration, and metal ligand interactions. The metal carbonyl complexes I have chosen for this project are of the type: $(\eta^5\text{-C}_5\text{H}_5)\text{M}(\text{CO})_n(\text{L})\text{Me}$, (**1a**), $\text{M} = \text{Fe}$, $n = 1$, $\text{L} = \text{CO}$; (**1b**), $\text{M} = \text{Fe}$, $n = 1$, $\text{L} = (\text{Ph}_3)\text{P}$; (**2a**), $\text{M} = \text{Mo}$, $n = 2$, $\text{L} = \text{CO}$; (**2b**), $\text{M} = \text{Mo}$, $n = 2$, $\text{L} = (\text{Ph}_3)\text{P}$.

1.2 Experimental

All manipulations were performed using standard Schlenk techniques under argon atmosphere. Tetrahydrofuran (THF) was dried and distilled from sodium-benzophenone. Diethyl ether, benzene, toluene and hexanes were dried and distilled over sodium wire. The following reagents were purchased from Aldrich and used as received: *t*-dibutyltin dichloride, dibutyltin dichloride and lithium aluminum hydride. The iron and molybdenum dimers $[(\eta^5\text{-C}_5\text{H}_5)\text{Fe}(\text{CO})_2]_2$, $[(\eta^5\text{-C}_5\text{H}_5)\text{Mo}(\text{CO})_3]_2$ were purchased from Strem Chemicals. NMR spectra were recorded on Bruker 300 MHz spectrometer using CDCl_3 or C_6D_6 as solvent; infrared spectra were recorded on an ATI Mattson Infinity Series FTIR; elemental analyses were performed by Galbraith Laboratories. Tin dihydrides, $^t\text{Bu}_2\text{SnH}_2$ and Bu_2SnH_2 ⁷⁹ were synthesized by the reduction of corresponding tin dichlorides with lithium aluminum hydride in ether. The iron and molybdenum complexes $(\eta^5\text{-C}_5\text{H}_5)\text{M}(\text{CO})_n\text{-CH}_3$ ^{80a,b} and $(\eta^5\text{-C}_5\text{H}_5)\text{M}(\text{CO})_{n-1}(\text{PPh}_3)\text{-CH}_3$ ^{80c,d} ($\text{M} = \text{Fe}$, $n = 2$; $\text{M} = \text{Mo}$, $n = 3$) were synthesized by the reported method.

1.2.1 Synthesis of $(\eta^5\text{-C}_5\text{H}_5)\text{Fe}(\text{CO})_2\text{Sn}^t\text{Bu}_2\text{Cl}$: To 80 mL of a hexanes solution of $(\eta^5\text{-C}_5\text{H}_5)\text{Mo}(\text{CO})_3\text{Na}^+$ (prepared from 2.0 g (5.65 mmol) of $[(\eta^5\text{-C}_5\text{H}_5)\text{Fe}(\text{CO})_2]_2$) in a 250 mL Schlenk flask, was added slowly *via* a syringe 3.44 g (11.3 mmol) of *t*-butylindichloride in 20 mL of hexane at room temperature. The heterogeneous solution was stirred at room temperature for 2 d. The solution was filtered over Celite and the remaining residue was extracted with 20 mL of benzene and filtered over Celite again. The two filtrates were combined and the solvents were removed under vacuum. The yellow residue was recrystallized from 1:1 hexane benzene mixture. Yield: 4.65 g (92 %). ^1H NMR (300 MHz) (C_6D_6): δ 1.39 (s, 18H, ^tBu , $^3J^{119}_{\text{Sn}-^1\text{H}}=78$ Hz; $^3J^{117}_{\text{Sn}-^1\text{H}}=72$ Hz), 4.16 (s, 5 H, $(\eta^5\text{-C}_5\text{H}_5)$). ^{13}C NMR (75.4 MHz) (C_6D_6): δ 30.80 (^tBu), 40.57 $\text{C}(\text{CH}_3)_3$, 81.87 ($(\eta^5\text{-C}_5\text{H}_5)$), 214.04 (CO). ^{119}Sn NMR (111.93 MHz) (C_6D_6): δ 384.4. IR (ν CO, cm^{-1}) (Hexane): 2012.8, 1999.3, 1969.4, 1953.1. Anal. Calcd. for $\text{C}_{15}\text{H}_{23}\text{ClFeO}_2\text{Sn}$: C, 40.45; H, 5.21. Found: C, 40.92; H, 5.20.

1.2.2 Synthesis of $(\eta^5\text{-C}_5\text{H}_5)\text{Fe}(\text{CO})_2\text{Sn}^t\text{Bu}_2\text{H}$: A flame dried three-necked 100 mL round-bottom flask equipped with reflux condenser and a dropping funnel was charged with 0.0064 g (0.016 mmol) of LiAlH_4 in 15 mL of dry ether. The temperature was maintained at -15°C and at this temperature was added slowly *via* a dropping funnel 20 mL solution of 0.15 g (0.33 mmol) of $(\eta^5\text{-C}_5\text{H}_5)\text{Fe}(\text{CO})_2\text{Sn}^t\text{Bu}_2\text{Cl}$ in ether. The mixture was stirred for 30 minutes maintaining the temperature of the bath between -15 to -10°C . After 30 mints the mixture was filtered through Celite. The ether was removed under vacuum and the residue was extracted with 20 mL of hexane and again filtered through Celite. The hexanes were removed under vacuum and the yellow residue was recrystallized from hexanes. Yield: 0.11g (81 %). ^1H NMR (300 MHz) (C_6D_6): δ 1.37 (s, 18 H, ^tBu , $^3J^{119}_{\text{Sn}-^1\text{H}}=66$ Hz;), 4.19 (s, 5 H, $(\eta^5\text{-C}_5\text{H}_5)$), 5.28 (1.H, Sn-H, $^1J^{119}_{\text{Sn}-^1\text{H}}=1212$ Hz; $^1J^{117}_{\text{Sn}-^1\text{H}}=1158$ Hz). ^{13}C NMR (75.4 MHz) (C_6D_6): δ 33.11 (^tBu), 31.70 $\text{C}(\text{CH}_3)_3$, 80.74 ($(\eta^5\text{-C}_5\text{H}_5)$), 215.59 (CO). ^{119}Sn NMR (111.93

MHz) (C_6D_6): δ 155.5. IR (ν CO, cm^{-1}) (Hexane): 1995.5, 1947.7, 1748(w, Sn-H). Anal. Calcd. for $C_{15}H_{24}FeO_2Sn$: C, 43.84; H, 5.89. Found: C, 43.45; H, 5.96.

1.2.3 Synthesis of $(\eta^5-C_5H_5)Fe(CO)(PPh_3)Sn^tBu_2Cl$: To a solution of $(\eta^5-C_5H_5)Fe(CO)_2Sn^tBu_2Cl$ (1.00 g) (2.2 mmol) in 40 mL of THF, in a quartz tube, was added 0.59 g (2.2 mmol) of Ph_3P and solution was degassed twice. The solution was irradiated by Hanovia 450-W medium pressure mercury lamp at a distance of 4 cm. The progress of the photochemical reaction monitored by ^{119}Sn NMR and ^{31}P NMR spectroscopy indicated that after 10 h the ^{119}Sn resonance of the starting material $(\eta^5-C_5H_5)Fe(CO)_2Sn^tBu_2Cl$ at 384.4 ppm had been replaced by a doublet at 366 ppm and new resonance appeared in the ^{31}P NMR at 74.25 ppm and solution became dark red. The red solution was concentrated to 10 mL and 30 mL hexane was added and stirred for 30 mins. Red compound precipitated and washed with cold hexane twice; hexanes decanted and the red compound was dried under vacuum. It was finally recrystallized from 1:1 mixture of hexanes/benzene. Yield 1.1 g (73 %). 1H NMR (300 MHz) (C_6D_6): δ 1.40 (s, 9 H, tBu), 1.45 (s, 9 H, tBu), 4.36 (s, 5 H, $(\eta^5-C_5H_5)$), 6.97, 7.48 (m, 15 H, Ph). ^{13}C NMR (75.4 MHz) (C_6D_6): δ 31.95 (tBu), 32.16 (tBu), 40.74 d, $J_{P-C} = 6$ Hz, $C(CH_3)_3$, 40.78 d, $J_{P-C} = 5$ Hz, $C(CH_3)_3$, 81.49 ($(\eta^5-C_5H_5)$), 128.31, 129.95(d) $J_{P-C} = 2.3$ Hz, 133.74(d) $J_{P-C} = 9.8$ Hz, 137.58(d) $J_{P-C} = 42.2$ Hz, (Ph); 221.17 (d, $^2J_{P-C} = 32$ Hz) (CO). ^{119}Sn NMR (111.93 MHz) (C_6D_6): δ 363.4 (d, $^2J_{^{119}Sn-^{31}P} = 290$ Hz), ^{31}P NMR (121.49 MHz) (C_6D_6): 74.3. IR (ν CO, cm^{-1}) (Hexane): 1925.9 Anal. Calcd. for $C_{32}H_{38}ClFeOPSn$: C, 56.55; H, 5.64. Found: C, 55.83; H, 5.70.

1.2.4 Synthesis of $(\eta^5-C_5H_5)Fe(CO)(PPh_3)Sn^tBu_2H$: A flame dried three-necked 100 mL round-bottom flask equipped with reflux condenser and a dropping funnel was charged with 0.045 g (1.18 mmol) of $LiAlH_4$ in 20 mL ether. The temperature was maintained at 0 °C and at this temperature was added slowly *via* a dropping funnel 20 mL solution of 0.82 g (1.8

mmol) of $(\eta^5\text{-C}_5\text{H}_5)\text{Fe}(\text{CO})(\text{PPh}_3)\text{Sn}^t\text{Bu}_2\text{Cl}$ in THF. The mixture was stirred for 30 minutes maintaining the temperature about 0°C . After 30 min the mixture was filtered through Celite. The solvents were removed under vacuum and the residue was extracted with 10 mL of benzene and again filtered through Celite. The benzene was removed under vacuum and the red residue was recrystallized from hexanes/benzene mixtures. Yield: 0.42 g (36 %). ^1H NMR (300 MHz) (C_6D_6): δ 1.29 (s, 9 H, ^tBu), 1.53 (s, 9 H, ^tBu), 4.34 (s, 5 H, $(\eta^5\text{-C}_5\text{H}_5)$), 4.79 (d, $^2J_{\text{Sn-P}} = 6$ Hz), 6.98, 7.55 (m, 15 H, Ph). ^{13}C NMR (75.4 MHz) (C_6D_6): δ 30.60, $\text{C}(\text{CH}_3)_3$, 30.76 d., $\text{C}(\text{CH}_3)_3$, 34.10 (^tBu), 34.30 (^tBu), 79.62 ($(\eta^5\text{-C}_5\text{H}_5)$), 128.16, 129.55(d) $J_{\text{P-C}} = 2.3$ Hz, 133.63(d) $J_{\text{P-C}} = 9.6$ Hz, 138.04(d) $J_{\text{P-C}} = 41.5$ Hz, (Ph); 220.75 (d, $^2J_{\text{P-C}} = 32$ Hz) (CO). ^{119}Sn NMR (111.93 MHz) (C_6D_6): δ 150.3 (d, $^2J_{^{119}\text{Sn}-^{31}\text{P}} = 181$ Hz). ^{31}P NMR (121.49 MHz) (C_6D_6): 77.4. IR (Hexane, cm^{-1}) (ν CO), 1915.2; (ν Sn-H) 1717.4 (w br). Anal. Calcd. for $\text{C}_{32}\text{H}_{39}\text{FeOPSn}$: C, 59.57; H, 6.09. Found: C, 59.68; H, 6.14.

1.2.5 Synthesis of $(\eta^5\text{-C}_5\text{H}_5)\text{Mo}(\text{CO})_3\text{Sn}^t\text{Bu}_2\text{Cl}$: To 80 mL of THF solution of Mp^-Na^+ ($\text{Mp} = (\eta^5\text{-C}_5\text{H}_5)\text{Mo}(\text{CO})_3$) (prepared from 4.0 g (8.16 mmol) of $[(\eta^5\text{-C}_5\text{H}_5)\text{Mo}(\text{CO})_3]_2$) in a 250 mL Schlenk flask, was added slowly *via* a syringe 4.95 g (16.32 mmol) of *t*-butyltin dichloride in 20 mL of THF at room temperature. The reaction mixture was stirred at room temperature overnight. The solvent was removed under vacuum and 80 mL hexanes were added and the solution was filtered over Celite. The filtrate was collected and the solvent was removed under vacuum. The yellow solid residue was recrystallized from hexane at -5°C . Yield: 6.69 g (80 %). M.pt: 136°C . ^1H NMR (300 MHz) (C_6D_6): δ 1.43 (s, 18H, ^tBu , $^3J_{^{119}\text{Sn-H}} = 81$ Hz), 4.71 (s, 5 H, $(\eta^5\text{-C}_5\text{H}_5)$). ^{13}C NMR (75.4 MHz) (C_6D_6): δ 31.5 (^tBu), 42.6 $\text{C}(\text{CH}_3)_3$, 89.7 ($(\eta^5\text{-C}_5\text{H}_5)$), 226.0 (CO), 230.5 (CO). ^{119}Sn NMR (111.93 MHz) (C_6D_6): δ 328.6. IR (ν CO, cm^{-1}) (THF): 2003.4, 1935.7, 1905.7, Anal. Calcd. for $\text{C}_{16}\text{H}_{23}\text{ClMoO}_3\text{Sn}$: C, 37.42; H, 4.52. Found: C, 37.26; H, 4.53.

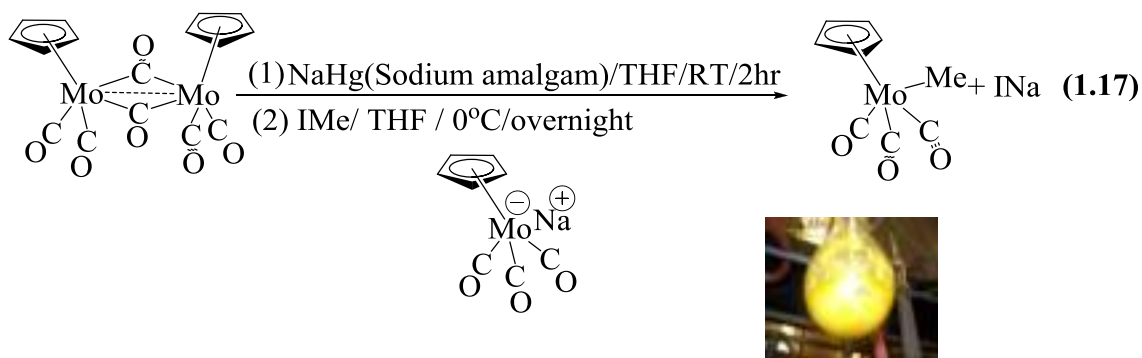
1.2.6 Synthesis of $(\eta^5\text{-C}_5\text{H}_5)\text{Mo(CO)}_3\text{Sn}^t\text{Bu}_2\text{H}$: A flame dried three-necked 100 mL round-bottom flask equipped with reflux condenser and a dropping funnel was charged with 0.038 g (0.99 mmol) of LiAlH_4 in 20 mL of dry ether. The temperature was maintained at -20°C and at this temperature was added slowly *via* a dropping funnel 20 mL solution of 0.5 g (0.97 mmol) of $\text{MpSn}^t\text{Bu}_2\text{Cl}$ in ether. The mixture was stirred for 1h maintaining the temperature of the bath between -20 to -10°C . After 1h the mixture was filtered through Celite. The ether was removed under vacuum and the residue was extracted with 20 mL of hexane and again filtered through nylon acrodisc filter. The hexanes were removed under vacuum and the red residue was recrystallized from diethyl ether at -10°C . Yield: 0.46g (92 %). M.pt: 84°C . ^1H NMR (300 MHz) (C_6D_6): δ 1.39 (s, 18 H, ^tBu , $^3J_{\text{Sn-H}} = 42$ Hz;), 4.66 (s, 5 H, $(\eta^5\text{-C}_5\text{H}_5)$), 5.51 (1.H, Sn-H, $^1J_{\text{Sn-H}}^{119} = 1298$ Hz; $^1J_{\text{Sn-H}}^{117} = 1240$ Hz). ^{13}C NMR (75.4 MHz) (C_6D_6): δ 33.4 (^tBu), 33.1 $\text{C}(\text{CH}_3)_3$, 88.8 ($(\eta^5\text{-C}_5\text{H}_5)$), 202.5 (CO), 234.0 (CO). ^{119}Sn NMR (111.93 MHz) (C_6D_6): δ 90.6 . IR (ν CO, cm^{-1}) (Hexane): 1991.7, 1895.9, 1750 (w, Sn-H). Anal. Calcd. for $\text{C}_{16}\text{H}_{24}\text{MoO}_3\text{Sn}$: C, 40.12; H, 5.05. Found: C, 39.55; H, 5.02.

1.2.7 Synthesis of $\text{H}^t\text{Bu}_2\text{Sn-Sn}^t\text{Bu}_2\text{H}$ using **1a,1b,2a,2b as catalyst:** In a typical experiment 0.2gr of $^t\text{Bu}_2\text{SnH}_2$ (0.9 mmol) and 5 mol% of catalyst in a C_6D_6 solution were photochemically irradiated with a medium-pressure mercury lamp or heated in an oil bath at 70°C in a sealed Pyrex NMR tube, which resulted in the progressive formation of $\text{H}^t\text{Bu}_2\text{Sn-Sn}^t\text{Bu}_2\text{H}$. The reaction was monitored by ^{119}Sn NMR Spectroscopy and stopped when all of the starting material $^t\text{Bu}_2\text{SnH}_2$ was consumed. Further purification was performed in a silica gel column through hexanes to give 70-90% yield of the product.

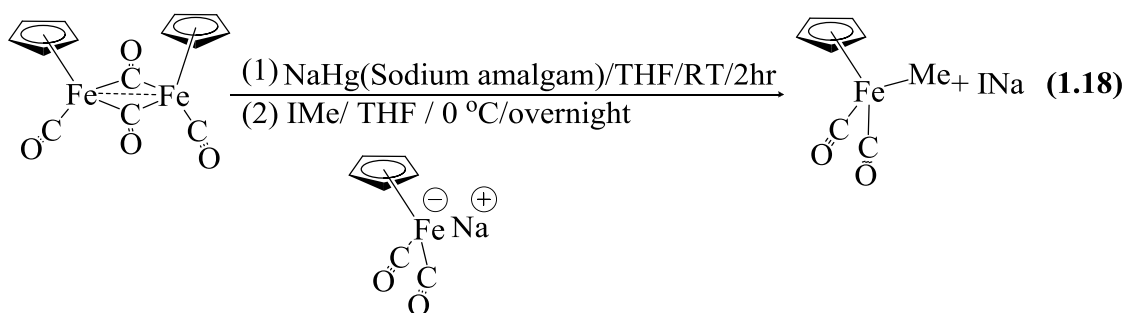
1.3 Results and discussion

1.3.1 Photochemical and thermal transformation of ${}^t\text{Bu}_2\text{SnH}_2$ into $\text{H}^t\text{Bu}_2\text{Sn-Sn}^t\text{Bu}_2\text{H}$

We have prepared those catalytic materials using the known salt-elimination reactions reported above.⁸⁰ eq. 1.17.



The product obtained is a yellow solid material (yield 85%) that has been properly characterized in the literature.⁶⁹ In a similar manner the iron analogues was prepared in very good yield from the reduction of $[(\eta^5\text{-C}_5\text{H}_5)\text{Fe}(\text{CO})_2]_2$, in very good yields (80%), as an orange solid, eq. 1.18.⁸⁰



By looking into their electronic configurations, we can see that those systems obey the 18 electron rule. In the following discussions description we will assume the metal in their neutral oxidation state M^0 , using the covalent method of counting.

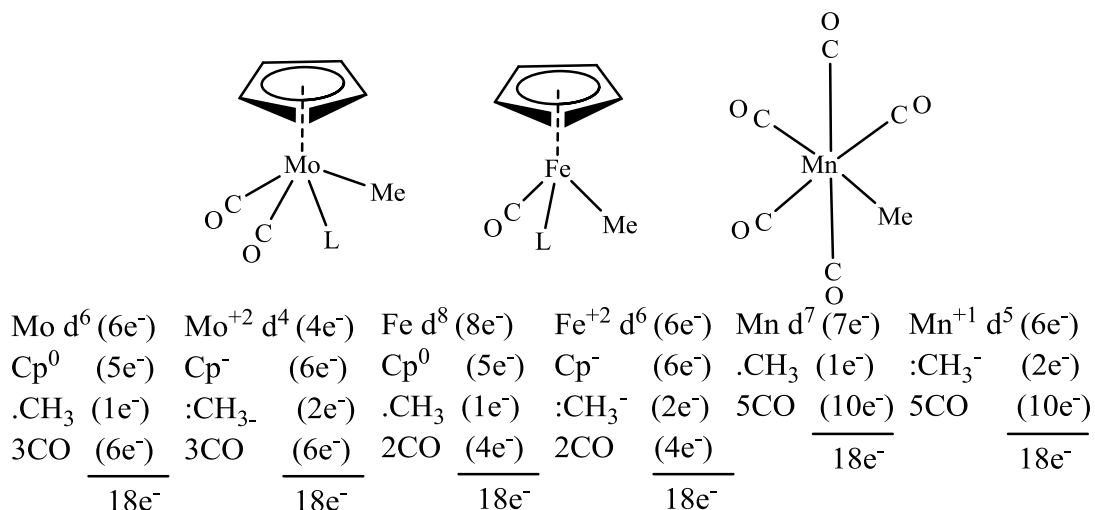


Figure 1.9 Covalent and ionic electron-counting systems

These 18e⁻ systems are diamagnetic and can be readily monitored by NMR spectroscopy, Table. 1.3. and readily exhibit CO bond dissociation under photochemical or thermal conditions.^{81,82}

Table 1.3 ¹³C NMR spectroscopy of iron and molybdenum complexes

¹³ C/C ₆ D ₆	(η ⁵ -C ₅ H ₅)	CO	Me
(η ⁵ -C ₅ H ₅)Fe(CO) ₂ Me	85	217	-23
(η ⁵ -C ₅ H ₅)Mo(CO) ₃ Me	92	227, 240	-22

Irradiation of a C₆D₆ solution of ^tBu₂SnH₂ (*) in the presence of 5 mol % of (η⁵-C₅H₅)Mo(CO)₃Me (**2a**) in a sealed Pyrex NMR tube with a medium-pressure mercury lamp resulted in the progressive formation of H^tBu₂SnSn^tBu₂H (Δ), eq. 1.19. The reaction was monitored by ¹¹⁹Sn NMR spectroscopy, Fig. 1.10., showing a clean transformation of ^tBu₂SnH₂ (*, ¹¹⁹Sn = -118.2 ppm) to H^tBu₂SnSn^tBu₂H (Δ, ¹¹⁹Sn = -83.4 ppm). At the end of the reaction there is still catalyst remaining in the solution based in the ¹³C NMR for the signal associated with the Cp = (η⁵-C₅H₅) of the catalyst at 92 ppm, illustrating the stability of the catalyst for further reactions.

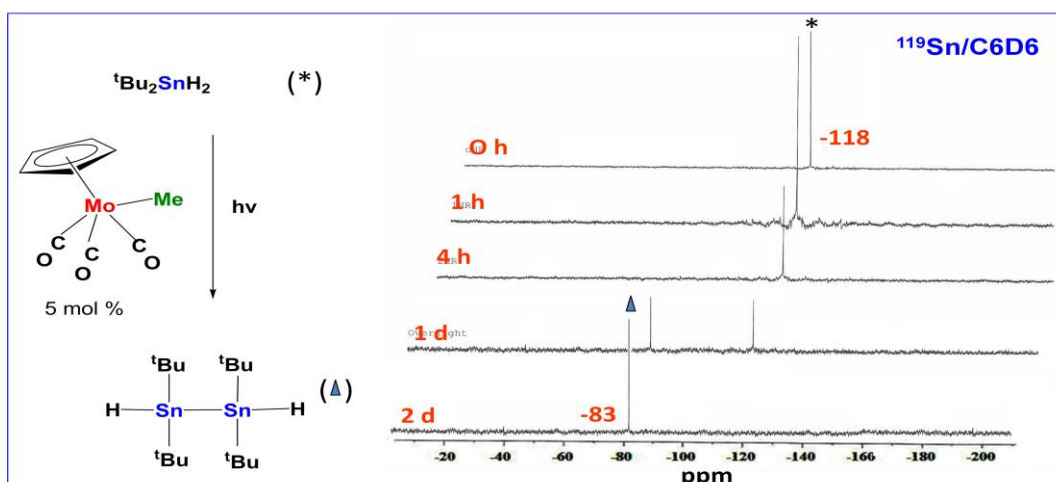
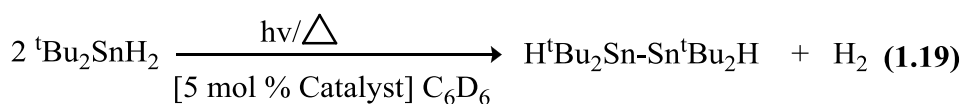
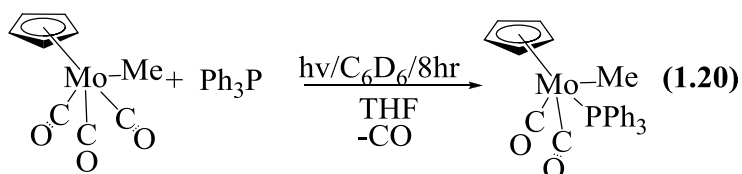


Figure 1.10 Catalytic synthesis of $\text{H}^t\text{Bu}_2\text{Sn-Sn}^t\text{Bu}_2\text{H}$ using $(\eta^5\text{-C}_5\text{H}_5)\text{Mo}(\text{CO})_3\text{Me}$ as catalyst in C_6D_6

In the case of the iron catalyst **1a**, after 30h of irradiation the process stops suggesting decomposition of the catalyst, a distinction to the chemistry using the molybdenum species **2a**.

We assume the key step in the catalytic process is the initial formation of a 16e-species via photochemical ligand dissociation. We expected that a similar process could occur thermally if the corresponding phosphine-substituted derivatives of **1a** and **2a** were used. Complex $(\eta^5\text{-C}_5\text{H}_5)\text{Mo}(\text{CO})_2(\text{Ph}_3\text{P})\text{Me}$ (**2b**), was readily synthesized by the carbonyl substitution of the $(\eta^5\text{-C}_5\text{H}_5)\text{Mo}(\text{CO})_3\text{Me}$ under photochemical conditions. eq. 1.20.⁸³



The solid material can be purified using column chromatography in toluene or hexanes in high yields, 70-80%, as can the iron analog, $(\eta^5\text{-C}_5\text{H}_5)\text{Fe}(\text{CO})(\text{Ph}_3\text{P})\text{Me}$ (**1b**) using the same synthetic approach.⁸³ Full synthetic details and spectroscopic data are reported in

the literature.⁸⁰

Treatment of a C₆D₆ solution of ^tBu₂SnH₂ in the presence of 5 mol % of **2b**, in a sealed pyrex NMR tube at 60-70°C, resulted in the 100% transformation of ^tBu₂SnH₂(*) to ^tBu₂SnSn^tBu₂H (Δ), as noted by monitoring the reaction by ¹¹⁹Sn NMR spectroscopy, Fig. 1.11. It was clear that catalytic complex (η⁵-C₅H₅)Mo(CO)₂(Ph₃P)Me (**2b**), present the same ability to thermally transform ^tBu₂SnH₂ to ^tBu₂SnSn^tBu₂H presumably via the same 16e⁻ species [(η⁵-C₅H₅)Mo(CO)₂Me]. No product decomposition was observed (the reaction solution remained clear as opposed to the photochemical reaction using catalyst **2a**). In addition the reaction times show a slight improvement compared to the photochemical process. As opposed to iron analogue (η⁵-C₅H₅)Fe(CO)₂Me (**1a**) using (η⁵-C₅H₅)Fe(CO)(Ph₃P)Me (**1b**), the reaction goes to completion, indicating the superiority of the phosphine derivative **1b**, over the carbonyl complex **1a**, as we can see in the Table. 1.4.

Table 1.4 Photochemical and thermal transformation of ^tBu₂SnH₂ to H^tBu₂SnSn^tBu₂H using the iron and molybdenum complexes

Catalyst 5 mol %	hv/Δ	Time Day	Yield% NMR ^a
1a	hv	4	(70)
1b	Δ	2	80(100)
2a	hv	2	90(100)
2b	Δ	1	90(100)

* **1a**: (η⁵-C₅H₅)Fe(CO)₂Me; **1b**: (η⁵-C₅H₅)Fe(CO)Ph₃PMe; **2a**: (η⁵-C₅H₅)Mo(CO)₃Me; **2b**: (η⁵-C₅H₅)Mo(CO)₂Ph₃PMe

^aYield based on the ¹H NMR.

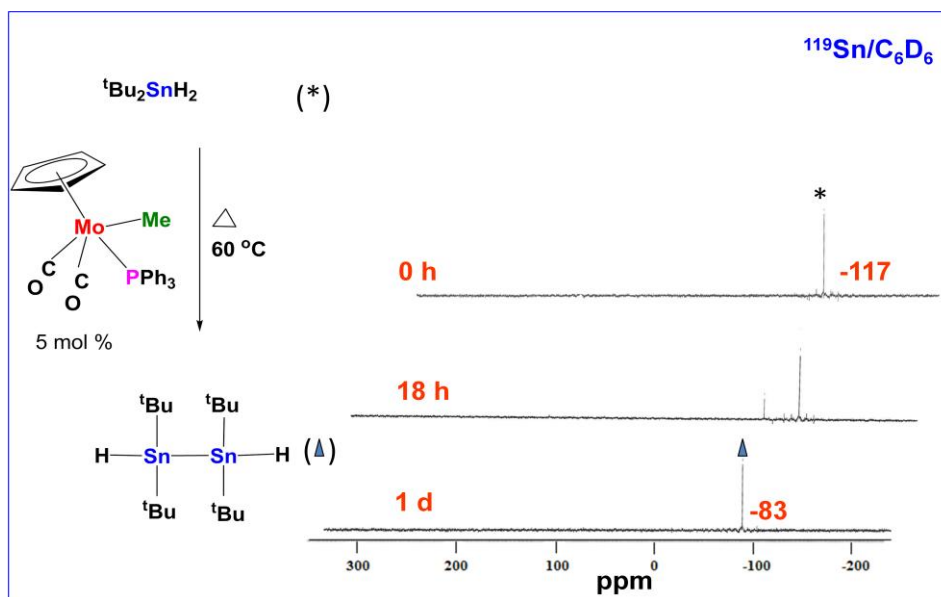
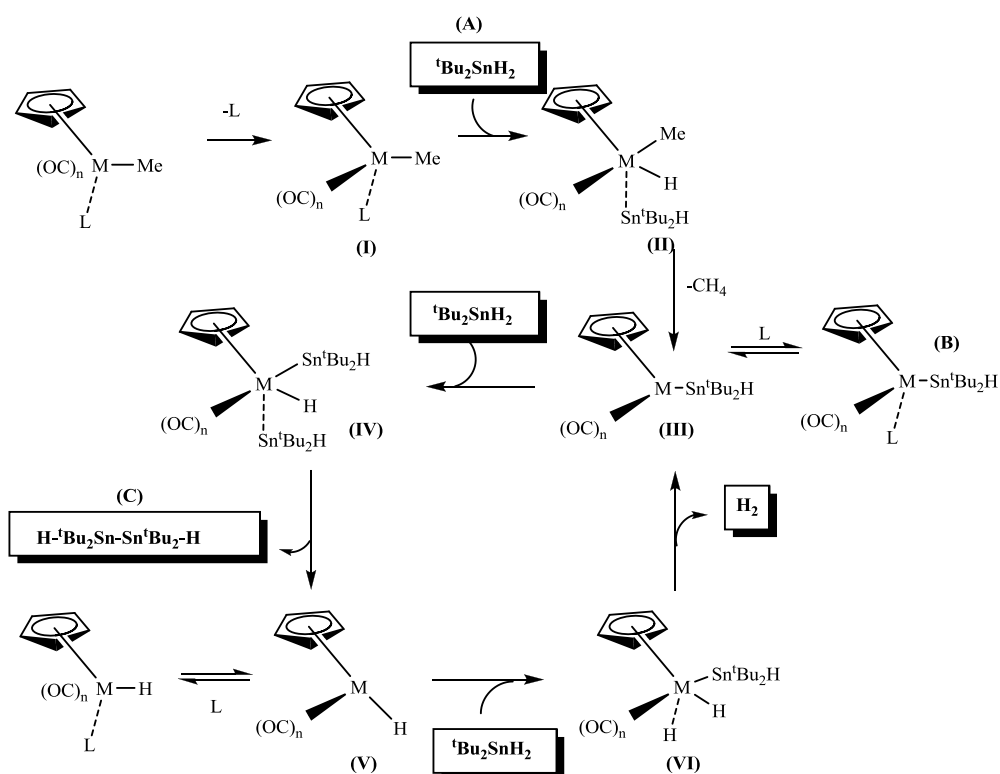


Figure 1.11 Catalytic synthesis of $\text{H}^t\text{Bu}_2\text{Sn-Sn}^t\text{Bu}_2\text{H}$ using $(\eta^5\text{-C}_5\text{H}_5)\text{Mo}(\text{CO})_2(\text{Ph}_3\text{P})\text{Me}$ as catalyst in benzene

1.3.2 Proposed mechanism for stannane dimerization

We suggest that the mechanism of the process follows that outlined in Scheme 1.1.



Scheme 1.1: Proposed mechanism for stannane dimerization, $n = 1$, $M = \text{Fe}$, $L = \text{CO}$ (**1a**), Ph_3P (**1b**); $n = 2$, $M = \text{Mo}$, $L = \text{CO}$ (**2a**), Ph_3P (**2b**)

Thus, a series of oxidative additions and reductive eliminations can account for the overall reaction culminating in reductive-elimination from a bis-stannyl metal complex. We observed no evidence for this intermediate. However, since the reactions occur in a sealed system where escape of the CO, the dissociated ligand, is not possible, the ability to observe the mono-stannyl metal transients should be possible if the reaction conditions can be suitably varied. In order to study our catalytic cycle, we decided to perform the stoichiometric reaction between **2a** and ${}^t\text{Bu}_2\text{SnH}_2$.

A 3:1 mixture of ${}^t\text{Bu}_2\text{SnH}_2$ and $(\eta^5\text{-C}_5\text{H}_5)\text{Mo}(\text{CO})_2\text{Me}$ in C_6D_6 was sealed in Pyrex NMR tube and irradiated for about 4 h times after which a series of signals were identified in the ${}^{119}\text{Sn}$ NMR Spectroscopy, after almost complete consumption of the ${}^t\text{Bu}_2\text{SnH}_2$ was observed, Fig.1.12.

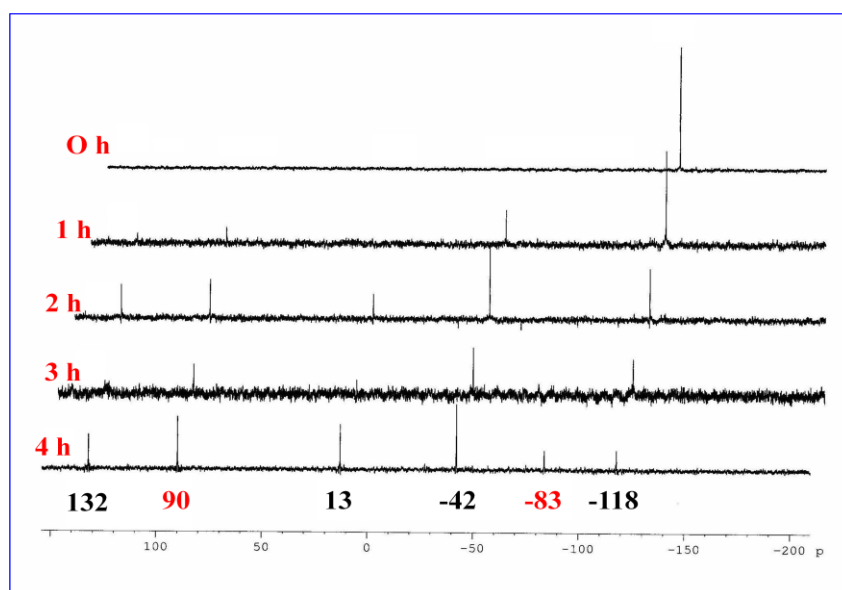
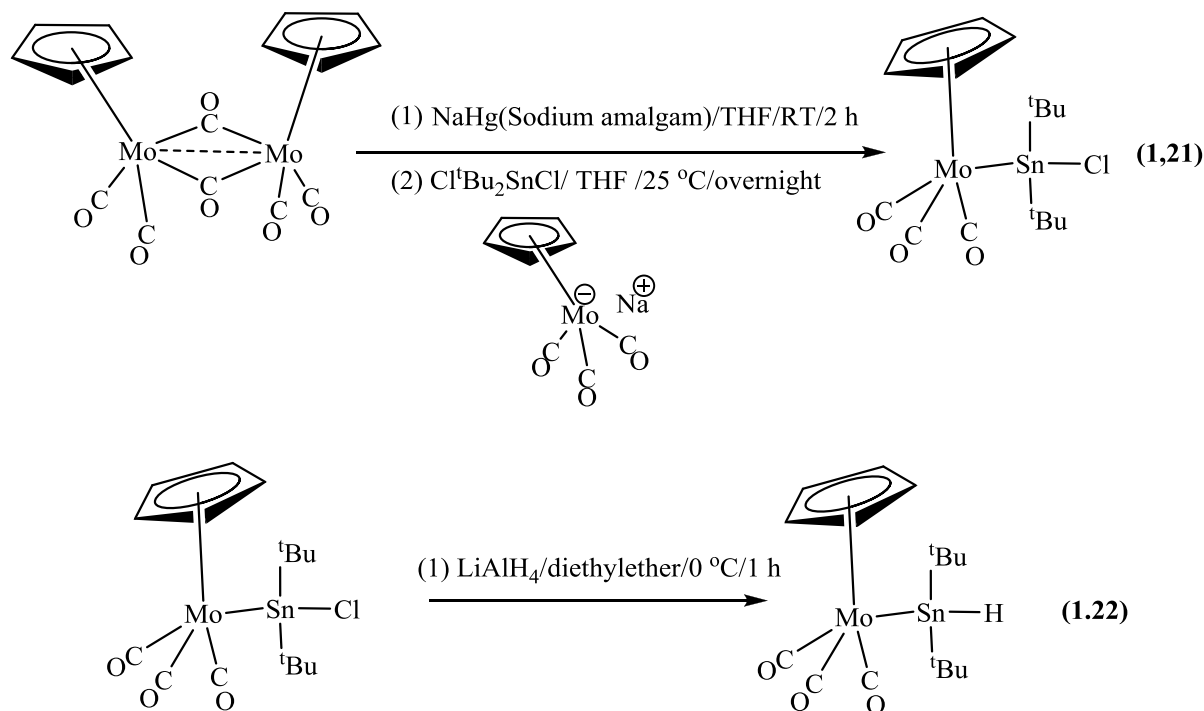


Figure 1.12 : Photochemical irradiation of ${}^t\text{Bu}_2\text{SnH}_2$ with $(\eta^5\text{-C}_5\text{H}_5)\text{Mo}(\text{CO})_3\text{Me}$ 3:1 ratio

After 4 hours of irradiation we could see new transient species via ${}^{119}\text{Sn}$ NMR spectroscopy including a signal at 90 ppm, which was characterized properly and determined to be $(\eta^5\text{-C}_5\text{H}_5)\text{Mo}(\text{CO})_3{}^t\text{Bu}_2\text{SnH}$ (**B**), Fig. 1.12.

We independently synthesized this material via the chemistry illustrated in eqs 1.21 and 1.22.



This independent synthesis and characterization proves the intermediacy of the mono-stannane complex in the catalytic cycle. Thus, it should also be a catalyst for the reaction since upon photochemistry, or thermal treatment, it could readily lose CO to form the 16e⁻ species **III** noted in the catalytic cycle above. A separate experiment using an independently synthesized sample of (η^5 -C₅H₅)Mo(CO)₃^tBu₂SnH (**B**) corroborated this prediction as can be noted in Figure 1.13. The efficient catalytic transformation of ^tBu₂SnH₂ (*) to H^tBu₂SnSn^tBu₂H (Δ), yielding only one single organotin product with insignificant loss of the catalyst, is clearly demonstrated.

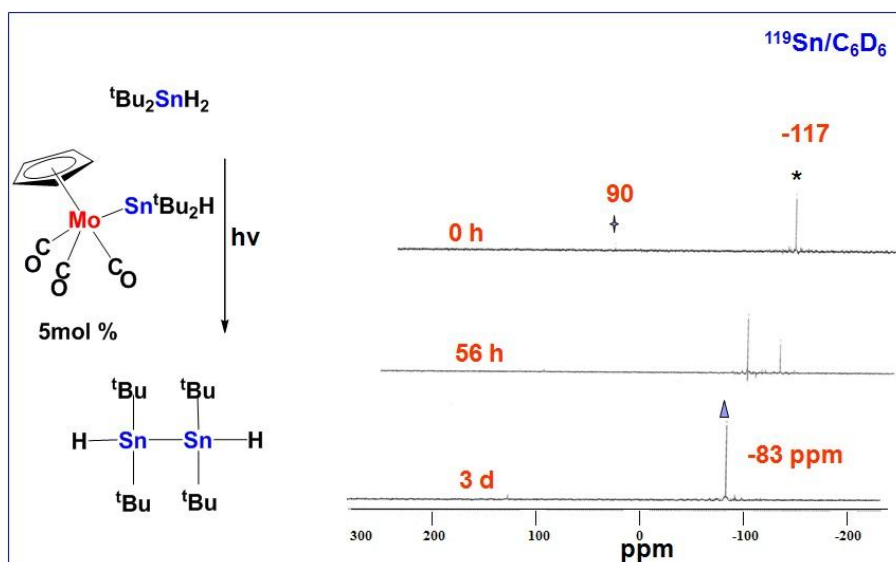


Figure 1.13 Catalytic synthesis of $\text{H}^t\text{Bu}_2\text{Sn-Sn}^t\text{Bu}_2\text{H}$ using $(\eta^5\text{-C}_5\text{H}_5)\text{Mo}(\text{CO})_3^t\text{Bu}_2\text{SnH}$ as catalyst in C_6D_6

The same results were observed using the iron analog $(\eta^5\text{-C}_5\text{H}_5)\text{Fe}(\text{CO})\text{Ph}_3^t\text{Bu}_2\text{SnH}$ as a catalyst to transform the $^t\text{Bu}_2\text{SnH}_2$ to $\text{H}^t\text{Bu}_2\text{SnSn}^t\text{Bu}_2\text{H}$ under thermal conditions.

Overall the mechanism suggested for the formation of distannane catalyzed by **1** and **2** seems in accord with all our experimental data. The first step should involve the photochemical or thermal ligand bond dissociation of the CO or Ph_3P to produce the unsaturated metal center $[(\eta^5\text{-C}_5\text{H}_5)\text{M}(\text{CO})_n\text{CH}_3]$ (**I**) 16e⁻,^{80b} Then the first oxidative addition of $^t\text{Bu}_2\text{SnH}_2$ (**A**) to the unsaturated metal complex $[(\eta^5\text{-C}_5\text{H}_5)\text{M}(\text{CO})_n\text{CH}_3]$, (**II**) followed by the reductive elimination of CH_4 to generate a new coordinatively unsaturated 16-electron species (**III**), $[(\eta^5\text{-C}_5\text{H}_5)\text{M}(\text{CO})_n(\text{Sn}^t\text{Bu}_2\text{H})]$. A second oxidative addition of $^t\text{Bu}_2\text{SnH}_2$ (**A**) to this intermediate leads to the formation of $[(\eta^5\text{-C}_5\text{H}_5)\text{M}(\text{CO})_n(\text{H})-(\text{Sn}^t\text{Bu}_2\text{H})_2]$ (**IV**), a type of reaction that is well established for reactions involving R_3SnH to form, for example, $[(\eta^5\text{-C}_5\text{H}_5)\text{Fe}(\text{CO})(\text{H})(\text{SnR}_3)_2]$.^{85,87-89} For $\text{M} = \text{Fe}$, the hydridobis(stannyl)metal complex then reacts with either CO or Ph_3P to reductively eliminate the distannane and form $[(\eta^5\text{-C}_5\text{H}_5)\text{M}(\text{CO})_n\text{H}]$, (**V**) or $[(\eta^5\text{-C}_5\text{H}_5)\text{M}(\text{CO})_n\text{Ph}_3\text{PH}]$, respectively, a reaction similar to the reported elimination of disilanes from $[(\eta^5\text{-C}_5\text{H}_5)\text{Fe}(\text{CO})(\text{H})(\text{SiR}_3)_2]$ complexes.⁸⁶ The metal complex $(\eta^5\text{-C}_5\text{H}_5)\text{M}(\text{CO})_n\text{H}$ could undergoes another oxidative addition of $^t\text{Bu}_2\text{SnH}_2$ (**VI**) and reductively

eliminate H₂ as the final step (**VII**) to regenerate the important transient (η^5 -C₅H₅)M(CO)_n^tBu₂SnH (**III**) to continue the cycle, (M = Fe, n = 2; M = Mo, n = 3).

It is clear from Figure 1.12, that the stoichiometric reaction between ^tBu₂SnH₂ and **2a** that there are many products in addition to (η^5 -C₅H₅)Mo(CO)₃^tBu₂SnH. The exact nature of these other materials, and the generality of their formation, will be discussed in Part 2 of this chapter.

1.3.3 Structural analysis of (η^5 -C₅H₅)M(CO)_n(L)^tBu₂SnH complex, (M = Fe, n = 1; Mo, n = 2)

We were able to obtain crystal structures for both **1b** and **2b** and these are illustrated in Figure 1.14. , The iron complex, (η^5 -C₅H₅)Fe(CO)(Ph₃P)^tBu₂SnH, adopts a normal three-legged piano stool geometry in which the hydrogen at Sn is oriented anti with respect to the (η^5 -C₅H₅) to minimize steric interactions of the ^tBu groups with Ph₃P, and the P-Fe-Sn angle becomes slightly wider to accommodate the Ph₃P group. The Fe-SnH and SnH bond length, outlined in Table. 1.5, are intermediate between those of related transition metal tin complexes.⁹⁰ The structure of Mo complex (η^5 -C₅H₅)Mo(CO)₃^tBu₂SnH illustrates the Sn is trans to the (η^5 -C₅H₅) ring, with the Sn-H distance being slightly longer, than in the Fe analog.

Table 1.5 M-Sn and Sn-H bond length for (η^5 -C₅H₅)Fe(CO)Ph₃P^tBu₂SnH and (η^5 -C₅H₅)Mo(CO)₃^tBu₂SnH

Bond	(η^5 -C ₅ H ₅)Fe(CO)Ph ₃ P ^t Bu ₂ SnH	(η^5 -C ₅ H ₅)Mo(CO) ₃ ^t Bu ₂ SnH
	Bond distance Å	
M-Sn	2.617	2.856
Sn-H	1.870	2.140

1b

2b

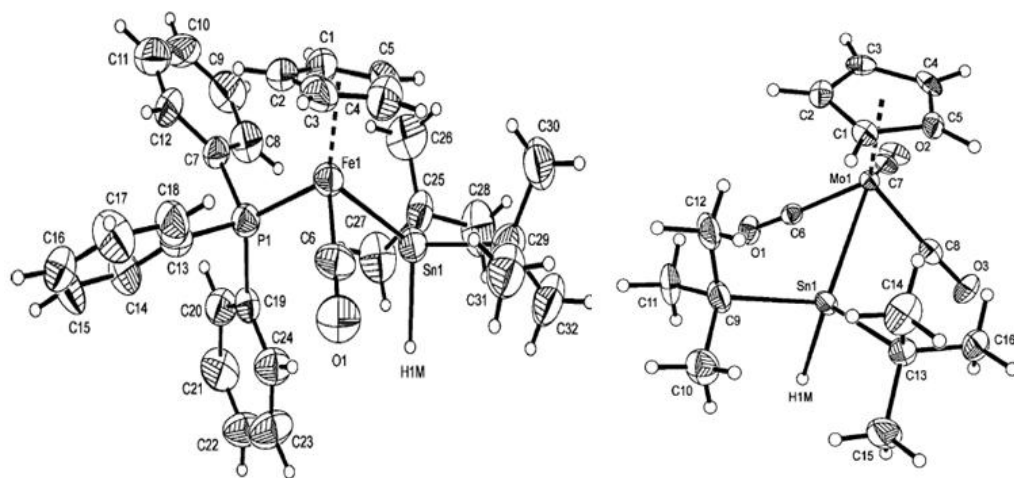


Figure 1.14 Crystal structure of $(\eta^5\text{-C}_5\text{H}_5)\text{Fe}(\text{CO})\text{Ph}_3\text{P}^t\text{Bu}_2\text{SnH}$ (1b) and $(\eta^5\text{-C}_5\text{H}_5)\text{Mo}(\text{CO})_3^t\text{Bu}_2\text{SnH}$ (2b)

The M-Sn bond distances for both metal complexes Fe and Mo could play important role in this chemistry, since we have seen better reactivity of the Mo catalyst system compared to iron and that could be associated with the energy required to promote the reductive elimination favorably in the Mo system since the bond are longer compared to iron, and can be easily activated.

1.3.4 Observations related to $(\eta^5\text{-C}_5\text{H}_5)\text{M}(\text{CO})_n\text{H}$ transients suggested in the proposed mechanism, (M = Fe, n = 2; Mo, n = 3)

Metal hydrides play an important role in transition metal chemistry, being involved in the mechanism of many catalytic (hydrogenation and hydroformylation of alkenes, etc) and stoichiometric processes (reduction, activation of C-H bonds, etc).^{84,91}

It was observed that the reaction catalyzed by the iron complex $(\eta^5\text{-C}_5\text{H}_5)\text{Fe}(\text{CO})_2\text{Me}$ (**1a**) did not go to completion photochemically but thermally using the $(\eta^5\text{-$

$\text{C}_5\text{H}_5\text{Fe}(\text{CO})(\text{Ph}_3\text{P})\text{Me}$ it went nicely to completion. We attribute that difference to two main factors:

The phosphine hydride complex $(\eta^5\text{-C}_5\text{H}_5)\text{Fe}(\text{CO})(\text{Ph}_3\text{P})\text{H}$ is stable enough to persist and can regenerate the catalytically active species or produce changes in the M-H reactivity, cf. $(\eta^5\text{-C}_5\text{H}_5)\text{Fe}(\text{CO})_2\text{H}$. The simple replacement of a CO by a phosphine increases the Pka by 7 units for $\text{H}[\text{Co}(\text{CO})_4]$ pka; 8.4 in acetonitrile and $\text{H}[\text{Co}(\text{CO})_3(\text{Ph}_3\text{P})]$ pka: 15.4. This control of the properties of a hydride through variation of the coordinating groups is useful in a catalyst. For example the hydroformylation of olefins have been promoted by adding Ph_3P to the catalyst enhancing not only the steric hindrance of the complex but also increasing the hydridic character of M-H).⁸⁴.

Alternatively $(\eta^5\text{-C}_5\text{H}_5)\text{Fe}(\text{CO})_2\text{H}$ being less kinetically stable than its phosphine analog could react more rapidly to form the dimeric metal complex $[(\eta^5\text{-C}_5\text{H}_5)\text{Fe}(\text{CO})_2]_2$.^{92,95} It has been suggested that metal hydride complexes with a bond dissociation energy (BDE) less than 56 kcal/mol are likely to lose H_2 at room temperature,⁹² eq. 1.23. Indeed, many hydrides (e.g. $(\eta^5\text{-C}_5\text{H}_5)\text{Cr}(\text{CO})_3\text{H}$ and $\text{HV}(\text{CO})_4(\text{dppm})$) that have stronger M-H bonds (61.5 and 57 kcal/mol, respectively)⁹³ are isolable at room temperature, unlike $(\eta^5\text{-C}_5\text{H}_5)\text{Fe}(\text{CO})_2\text{H}$, which evolves H_2 at room temperature in an open system despite its relatively strong M-H bond (68 kcal/mol in Table 1.6).^{92,93}



Table 1.6 : Bond dissociation energy (BDE) and bond dissociation free energies(BDEg) for M-H bonds in group 8 and group 6.

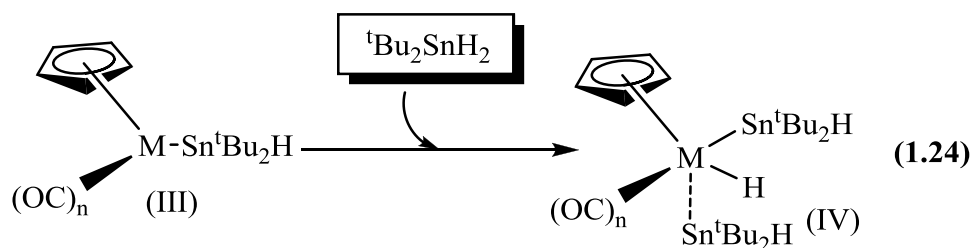
Compound	Pka	M-H(BDE)	M-H(BDEg)
$(\eta^5\text{-C}_5\text{H}_5)\text{Fe}(\text{CO})_2\text{H}$	27.1	68	63
$(\eta^5\text{-C}_5\text{H}_5)\text{Ru}(\text{CO})_2\text{H}$	28.3	77	72
$(\eta^5\text{-C}_5\text{H}_5)\text{Os}(\text{CO})_2\text{H}$	32.7	83	78
$(\eta^5\text{-C}_5\text{Me}_5)\text{Fe}(\text{CO})_2\text{H}$	29.7		
$(\eta^5\text{-C}_5\text{H}_5)\text{Cr}(\text{CO})_3\text{H}$	13.3	62	57
$(\eta^5\text{-C}_5\text{H}_5)\text{Mo}(\text{CO})_3\text{H}$	13.9	70	65
$(\eta^5\text{-C}_5\text{H}_5)\text{W}(\text{CO})_3\text{H}$	16.1	73	68
$(\eta^5\text{-C}_5\text{Me}_5)\text{Mo}(\text{CO})_3\text{H}$	17.1	69	64

BDEg: bond dissociation free energies
(substantial entropy change associated) ⁹⁴

It is important to note from eq. 1.23, that the M-M bond should be considered in determining the position of the equilibrium and the strong Fe-Fe bond could be responsible for the loss of catalytic activity and kill the active species $(\eta^5\text{-C}_5\text{H}_5)\text{M}(\text{CO})_n\text{H}$, Scheme. 1.1., Steps **III** to **VI**. The Mo analogues could exhibit the same behavior, but clearly do not.

1.3.5 Attempts to isolate the intermediate $(\eta^5\text{-C}_5\text{H}_5)\text{M}(\text{CO})_n\text{H}(\text{tBuSnH})_2$, (M = Fe, n = 1; Mo, n = 2)

The formation of bis-stannyl Fe step (IV) intermediates was an important step in the proposed mechanism, eq. 1.24; however, we have no evidence for the formation of this species.



An equimolar solution of $[(\eta^5\text{-C}_5\text{H}_5)\text{Fe}(\text{CO})_2(\text{tBu}_2\text{SnH})]$ and tBu_2SnH_2 in C_6D_6 in a sealed Pyrex NMR tube, was irradiated and examined spectroscopically. This reaction is complex; however, we could identify a transient tin species with a ^{119}Sn chemical shift of 126 ppm, in the similar range as the previously reported $(\eta^5\text{-C}_5\text{H}_5)\text{Fe}(\text{CO})\text{H}(\text{Bu}_3\text{Sn})_2$. Taking into

account the variation of chemical shift expected upon replacement of a Sn-butyl bond by a Sn-^tbutyl bond; however, this is the only evidence for such a species, Table. 1.7.

Table 1.7 ¹¹⁹Sn Spectroscopy for (η⁵-C₅H₅)Fe(CO)(H)(Bu₃Sn)₂ and (η⁵-C₅H₅)Fe(CO)(H)(^tBu₂SnH)₂

Metal Complex	¹¹⁹ Sn/C ₆ D ₆
(η ⁵ -C ₅ H ₅)Fe(CO)H(Bu ₃ Sn) ₂	136 ^{88C}
(η ⁵ -C ₅ H ₅)Fe(CO)H(^t Bu ₂ SnH) ₂	126 ^a
(η ⁵ -C ₅ H ₅)Fe(CO)H(^t Bu ₂ SnMe) ₂	166 ^b

^a[(η⁵-C₅H₅)Fe(CO)(H)-(Sn^tBu₂H)₂]: ¹H NMR: d = -12.85 (Fe-H), 1.38 (^tBu), 4.41 ((η⁵-C₅H₅)), 5.22 ppm (Sn-H); IR (hexane): ν̃(CO)=1928 cm⁻¹. IR: 1924 cm⁻¹ (CO), 1843br,w (Fe-H)

^b[(η⁵-C₅H₅)Fe(CO)H(^tBu₂SnMe)₂]: ¹H-NMR: -13.2(Fe-H); 0.24(Me); 1.27, 1.37 (^tBu); 4.54 ((η⁵-C₅H₅)) C-NMR: -7.3(Me); 32.4,32.7 (^tBu); 31.3,32.2 (C(CH₃)₃);76.6((η⁵-C₅H₅)) 221.1(CO)

Unfortunately a similar reaction with Mo complex **2a** did not yield informative data.

1.3.6 Extension to tin systems with less bulky groups.

A similar photochemical reaction of 6h duration using the isomeric stannane, ⁿBu₂SnH₂ resulted in a transformation to the corresponding distannane, (HⁿBuSn-SnⁿBu₂H)⁹⁶ ¹¹⁹Sn/C₆D₆; -208.2 and a complex mixture of cyclic and linear oligostannanes, H-(nBu₂Sn)_n-H (5% yield) with tin resonances at -202.5, -202.9, -208.1, -208.4, -209.9, and -220.5 ppm. Thus, this reaction is not productive for the formation of tetra-*n*-butyldistannane. It is clear that the catalytic reaction described in the previous pages is dominated by the nature of the groups on Sn. Likewise, the catalyst (η⁵-C₅H₅)Fe(CO)₂Me was consumed in this short period of time, at a rate much greater than with the *tert*-butyltin analogue, and this poses a problem for the utility of the process.

However, we extended the chemistry to the use of Mn(CO)₅Me as a catalytic species,⁹⁷ Fig. 1.15.

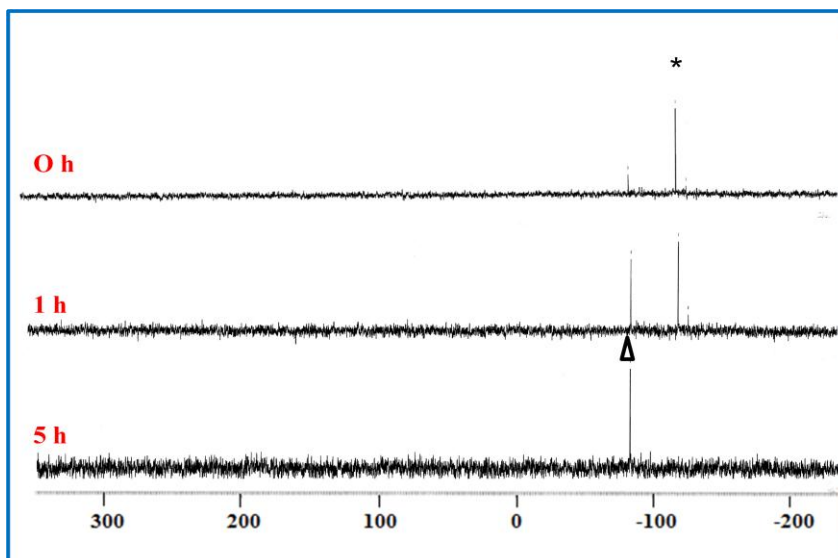


Figure 1.15 Catalytic synthesis of $\text{H}^t\text{Bu}_2\text{Sn-Sn}^t\text{Bu}_2\text{H}(\Delta)$ using $\text{Mn}(\text{CO})_5\text{Me}$ as catalyst in C_6D_6 .⁹⁷

In a sealed NMR tube was placed $^t\text{Bu}_2\text{SnH}_2$ and 5 mol% of $\text{Mn}(\text{CO})_5\text{Me}$.⁸⁰ The reaction was monitored by ^{119}Sn NMR spectroscopy. After 5 h of irradiation, $^t\text{Bu}_2\text{SnH}_2(*)$ had completely disappeared and the clean formation of $^t\text{Bu}_2\text{SnSn}^t\text{Bu}_2\text{H}(\Delta)$ could be noted. It is clear from this result the Mn catalyst is superior to both the Mo and Fe alkyl catalysts since the reaction is complete in a few hours compared to many hours.

1.4 Conclusions

1 For the first time, we report a new catalytic system involving molybdenum and iron complexes, for the dehydrogenative coupling of $^t\text{Bu}_2\text{SnH}_2$, both thermally and photochemically, to produce the functional distannane $\text{H}^t\text{Bu}_2\text{SnSn}^t\text{Bu}_2\text{H}$, in very good yields, 70-90%.

2 We have identified an intermediate in the above process $(\eta^5\text{-C}_5\text{H}_5)\text{M}(\text{CO})_n(\text{L})\text{Sn}^t\text{Bu}_2\text{H}$ and demonstrated, its utility as a catalyst.

3 The thermal catalytic process is much more efficient than the photochemical process for the Fe and Mo catalysts, and the Mo catalysts are superior to those of Fe.

1.5 References

- 1) Sawyer. A. K., in *Organotin Compounds*, Vol. 3, A. K. Sawyer (Ed.), Marcel Dekker, New York, **1971**.
- 2) Ingham, R. K.; Rosenberg. Sanders. D.; Gilman. H., *Chem. Rev.*, **1960**, 60 (5), 459-539; McFarlane. W., *J. Chem. Soc., A*, **1968**, 1630; Davies. A. G. *Organotin Chemistry*, Second (Ed.), Wiley-VCH Verlag GmbH and Co. KGaA, Germany, **2003**.
- 3) Davies, A. G. In *Comprehensive Organometallic Chemistry II*; Abel, E. W., Stone, F. G. A., Wilkinson, G., (Ed.), Pergamon Ltd; Oxford, **1995**; Vol. 2.; Harrison, P. G. *Chemistry of Tin*; Blackie: Glasgow, **1989**.; Pereyre, M.; Quintard, J. P.; Rahm, A. *Tin in Organic Synthesis*; Butterworth: London, **1987**.; Sato, T. In *Comprehensive Organometallic Chemistry II*; Abel, E. W., Stone, F. G. A., Wilkinson, G., Eds.; Pergamon: Oxford, **1995**; Vol. 11. Stille, J. K. *Angew. Chem., Int. Ed. Engl.* **1986**, 25, 508 and references therein. Farina, V.; Krishnamurthy, V.; Scott, W. J. In *Organic Reactions*; Wiley: New York, **1997**; Vol. 50, pp 1-652. Mitchell, T. N. In *Encyclopedia of Reagents for Organic Synthesis*; Paquette, L. A., Ed.; John Wiley & sons: New York, **1995**; Vol. 4.
- 4) (a) Keck, G. E.; Byers, J. H. *J. Org. Chem.*, **1985**, 50, 5442; (b) Keck, G. E.; Tafesh, A. M. *J. Org. Chem.*, **1989**, 54, 5845; (c) Storck, G.; Sher, P. *J. Am. Chem. Soc.* **1983**, 105, 6765; (d) Baldwin, J. E.; Kelly, D. R.; Ziegler, C. B., *J. Chem. Soc., Chem. Commun.*, **1984**, 133; (e) Snider, B. B.; Buckman, B. O. *J. Org. Chem.*, **1992**, 57, 4883; (f) Harendza, M.; Lessmann, K.; Neumann, W. P. *Synlett.*, **1993**, 283.
- 5) Davies, A. G.; Smith, P. G. *Adv. Inorg. Chem. Radiochem.*, **1980**, 23, 1 and references therein.; Cusack, P.; Smith, P. G. *Rev. Silicon, Germanium, Tin Lead Compd.* **1983**, 7,

- 1; Davies, A. G.; Smith, P. G. In *Comprehensive Organometallic Chemistry*; Wilkinson, G., Stone, F. G. A., Abel, E. W., Eds.; Pergamon: Oxford, **1982**; Vol. 2.; Evans, C. J. In *Chemistry of Tin*; Harrison, P. G., Ed.; Blackie:Glasgow, **1989**.(41) Wardell, J. L. In *Encyclopedia of Inorganic Chemistry*; King, R.B., Ed.; Wiley:, **1994**; Vol. 8.(42) Weis, R. W. In *Organometallic Compounds*; Springer:, **1973**; Vol. II, 2nd ed., First supplement. (43) Van der Weij, F. W. *Makromol. Chem.* **1980**, *181*, 2541. (44) Rusch, T. E.; Raden, D. S. *Plat. Compd.* **1980**, *3*, 61. (45). Evans, C. J.; Karpel, S. *Organotin Compounds in Modern Technology*; Elsevier: Amsterdam, **1985**.
- 6) (a) Mathiasch. B., *Inorg. Nucl. Chem. Lett.*, **1977**, *13*, 13; (b) Mathiasch. B., J. Organomet. Chem., **1977**, 141, 295. (c) Adams. S.; Drager. M.; Mathiasch, B.; Z. Anorg. Allg. Chem., **1986**, 532, 81. (d) Puff. H.; Breuer. B.; Gehrke-Brinkmann. G.; Kind. P.; Reuter. H.; Schuh. W.; Wald. W.; Weidenbruck. G., *J. Organomet. Chem.* **1989**, *363*, 265. (e) Masamune. S.; Sita. L.R., *J. Am. Chem. Soc.*, **1990**, *107*, 6390. (f) Al-Allaf. T.A.K.; Eaborn. C.; Hitchcock. P.B.; Lappert. M.F.; Pidcock. A., *J. Chem. Soc. Chem. Commun.*, **1985**, 548; (7) Adams. S.; Drager. M., *J. Organomet. Chem.* **1985**, 288, 295. (8) Puff. H.; Bach. C.; Schuh. W.; Zimmer. R., *J. Organomet. Chem.* **1986**, *312*, 313. (9) Devaud. M.; Engel. M.; Feasson. C., Lecat. J.-L., *J. Organomet. Chem.*, **1985**, *281*, 181; (10) Sawyer. A.K.; Brown. J.E.; Hanson. E.L.; *J. Organomet. Chem.*, **1965**, *3*, 464; (11) Neumann, W.P.; Pedain. J., *Tetrahedron Lett.*, **1964**, 2461. (12) Jousseau. B.; Chanson. E., *Synthesis.*, **1987**, 55; (13) Schror. U.; Neumann. W.P., *Angew. Chem.*, **1975**, *87*, 247; (14) Sawyer. A.K.; Kuivila. H.G., *J. Am. Chem. Soc.*, **1963**, *85*, 1010; (15) Mitchell. T.N., *J. Organomet. Chem.*, 1975, *92*, 311. (16) Jurkschat. K.; Tzschach. A.; Mugge. C.; Piret-Meunier. J.; Van Meersche. M.; Van Binst. G.; Wynants. C.; Gielen. M.; Willem. R., *Organometallics*, **1988**, *7*, 593.

- 7) (a) Kuivila. H.G., *Adv. Organomet. Chem.*, **1964**, 47; (b) Neumann. W.P.; Schwarz. A., *Angew. Chem.*, **1975**, 87, 844. (c) Maire. J.C.; Dufermont. J., *J. Organomet. Chem.*, **1967**, 10, 369.
- 8) Englich. U.; Hermann. U.; Prass. I.; Schollmeier. T.; Ruhlandt-Senge. K.; Uhlig. F., *J. Organomet. Chem.*, **2002**, 646, 271.
- 9) Miller. R. D.; Michl. J., *Chem. Rev.*, **1989**, 89 (6), 1359-1410.
- 10) (a) Lu. V.; Tilley. D.T., *Macromolecules.*, **1996**, 29, 5763-5764; (b) Braunstein. P.; Morise. X., *Chem. Rev.*, **2000**, 100 (10), 3541-3552; (c) Lu. V. Y.; Tilley. D.T., *Macromolecules.*, **2000**, 33 (7), 2403-2412; (d) Choffat. F. S.; Pascal Wolfer. K.; Schmid. D.; Mezzenga. R.; Smith. P.; Caseri. W., *Macromolecules.*, **2007**, 40 (22), 7878-7889; (e) Varma-Nair. M.; Cheng. J. Jin.; Wunderlich. Y. B., *Macromolecules.*, **1991**, 24, 5442.
- 11) (a) Imori. T.; Lu. V.; Hui C.; Tilley. D. T., *J. Am. Chem. Soc.*, **1995**, 117 (40), 9931-9940; (b) Skotheim. T. A.; *Hanbook of Conductive Polymers*, Marcel Dekker, New York, Vols. 1 & 2, **1986**; (c) Bredas. J. L.; Silbey. R., *Conjugated Polymers*, Kluwer Academic Publishers, Dordrecht Netherlands, **1991**; (d) Pitman. C.U.; Carraher. C.E.; Zeldin. M. J.; Sheats. E.; Culberston. B. M., in *Metal Containing Polymeric Materials.*, Plenum, New York, **1996**.
- 12) Davies, A. G.; Gielen. M.; Pannell. K. H., *In Tin Chemistry Fundamentals, Frontiers, and Applications.*, Eds.; John Wiley & Sons, Ltd. **2008**.
- 13) Web:"ITRI.Tin Use Survey 2007".
http://www.itri.co.uk/pooled/articles/BF_TECHART/view.asp?Q=BF_TECHART_297350. on 2008-11-21.
- 14) Piver. W. T., *National Institute of Environmental Health Sciences*, **1973**, 61-79.

- 15) Omae. I., *Applications of Organometallics Compounds*, Wiley, Chichester, **1998**;
Evans. C. J.; Karpel. S., *Organotin Compounds in Modern Technology*, Elsevier,
Amsterdam, **1985**.
- 16) Hostettler. F.; Cox. E.F., *Ind. Eng. Chem.*, **1960**, 52, 609.
- 17) Houghton. R.P.; Mulvaney. A.W., *J. Organomet. Chem.*, **1996**, 517, 107.
- 18) Brydson, J., *Plastics Materials.*, Butterworth, 9th Ed, **1999**.
- 19) Van der Weij. F.W., *Makromolekulare Chemie.*, **1980**, 181, 2541.
- 20) (a) Jousseume. B.; Gouron. V.; Pereyre. M.; Frances. J. M., *Appl. Organomet. Chem.*,
1991, 5, 135; (b) Jousseume. B.; Noiret. N.; Pereyre., M.; Saux. A., *Organometallics*,
1994, 13, 1034.
- 21) (a) Otera. J., *Chem. Rev.*, **1996**, 96, 1449; (b) Mascaretti, O. A.; Furlan. R.L.E.,
Aldrichimica Acta, **1997**, 30, 55.
- 22) Nath. M.; Pokharia, S.; Yadav. R., *Coord. Chem. Rev.*, **2001**, 215, 99-149.
- 23) Omae, I. *Appl. Organomet. Chem.*, **2003**, 17, 81-105.
- 24) Gielen. M., *Appl. Organomet. Chem.*, **2002**, 16, 481-494.
- 25) *Organotins in Agriculture. American Chemical Society.*, Washington, D. C., **1976**.
- 26) Hoch. M., *Applied Geochem.*, **2001**, 16, 719.
- 27) Miller. R. D.; Michl. Josef., *Chem. Rev.*, **1989**, 89 (6), 1359-1410.
- 28) Adams. S.; Drager. M., *Angew. Chem. Int. Ed. Engl.*, **1987**, 26, 1255.
- 29) (a) Sommers. R.; Schneider. B.; Neumann. W.P., *Justus Liebigs Ann. Chem.*, **1966**,
692, 12; (b) Sita. L. R., *Organometallics*, **1992**, 11, 1442.

- 30) Sita. L. R.; Terry. K.W.; Shibata. K., *J.Am.Chem.Soc.*, **1995**, 117,8049.
- 31) Okano. M.; Matsumoto. N.; Arakawa. M.; Tsuruta. T.; Hamano. H., *Chem. Commun.*, **1998**, 1799.
- 32) Okano. M.; Watanabe. K.; Totsuka. S., *Electrochemistry*, , **2003**, 71, 257.
- 33) West. R., *J. Organomet. Chem.*, **1986**, 300, 327; (b) Miller., R.D.; Michl. J., *Chem. Rev.*, **1989**, 89, 1359; (c) Trefonas. P.; West. R., *J. Polym. Sci., Polym. Chem, Ed.*, **1985**, 23, 2009; (d) Miller. R.D.; Sooriyakumaran. R., *J. Polym. Sci. Part A: Polymer Chem.*, **1987**, 25,111.
- 34) Gilbert. B.C.; Parsons. A.F., *J. Chem. Soc. Perkin Trans, II*, **2002**, 367.
- 35) Grugel. C.; Neumann. W. P.; Seifert. P., *Tetrahedron Lett.*, **1977**, 2205; Poller. R.C., *The chemistry of Organotin Compounds*, Academic Press, New York, Ch.9, 145, **1970**.
- 36) Zou. W.K.; Yang. N. L., *Polym. Prep., (Am. Chem. Soc. Div. Polym. Chem.)*., **1992**, 33,188.
- 37) Imori. T.; H. Lu. C.; Tilley. T.D., *J.Am. Chem. Soc.*, **1995**, 117, 9931.
- 38) Devylder. N.; Hill. M.; Molloy. K.C.; Price. G.J., *Chem, Commun.*, **1996**, 711.
- 39) Deacon. P.R.; Devylder. N.; Hill. M.S.; Mahon. M.F.; Molloy. K.C.; Price. G.J., *J. Organomet. Chem.*, **2003**, 687, 46.
- 40) Azemi. T.; Yokoyama. Y.; Mochida. K., *J. Organomet. Chem.*, **2005**, 690, 1588.
- 41) (a) Yokoyama. Y.; Hayakawa. M.; Azemi. T.; Mochida. K., *J. Chem. Soc. Chem. Commun.*, **1995**, 2275; (b) Mochida. K.; Hayakawa. M.; Tsuchikawa. T.; Yokoyama. Y.; Wakasa. M.; Hayashi. H., *Chem, Lett.*, **1998**, 91.
- 42) Elangovan. M.; Muthukumaran. A.; Kulandainathan. M., *Mater, Lett.*, **2006**, 60, 1099.
- 43) (a) Harrod. J. F.; Mu. Y.; Samuel. E., *Polyhedron.*, **1991**, 10, 1239; (b) Tilley. T.D.,

- Comm. Inorg. Chem.*, **1990**, 10,37; (c) Woo. H. G.; Walzer. J. F.; Tilley. T. D., *J. Am. Chem. Soc.*, 1992, 114, 7047; (d) Tilley. T. D., *Acc. Chem. Res.*, **1993**, 26, 22.
- 44) Aitken. C.; Harrod. J. F.; Malek. A.; Samuel. E., *J. organomet. Chem.*, **1988**, 349, 285.
- 45) (a) Imori. T.; Tilley. T. D., *J. Chem. Soc. Chem. Commun.*, **1993**, 1607; (b) Tilley. T. D.; Imori. T., *US Patent 5488091*, **1996**; *Chem. Abstr.*, **1996**, 124, P318158b,.
- 46) (a) Neale. N.R.; Tilley. T. D., *Tetrahedron*, **2004**, 60, 7247; (b) Neale. N.R.; Tilley. T.D., *J.Am.Chem.Soc.*, **2002**, 124, 3802.
- 47) (a) Lu. V.; Tilley. T. D., *Macromolecules*, **1996**, 29, 5763; (b) Lu. V.; Tilley. T. D., *Macromolecules*, **2000**, 33, 2403.
- 48) Kazusato. S.; Weinert. C. S.; Sita. L. R., *Organometallics*, **1998**, 17, 2241-2248.
- 49) King, R. B., *Transition-Metal Organometallic Chemistry: An Introduction*. Academic Press: New York, NY, **1969**.
- 50) Zeise, W. C., *Pogg. Annalen*. **1827**, 9, 632.
- 51) Mond, L.; Langer, C.; Quincke, F. *J. Chem. Soc.*, **1890**, 57, 749.
- 52) Kealy, T. J.; Pauson, P. L., *Nature*, **1951**, 168, 1039.
- 53) Miller, S. A.; Tebboth, J. A.; Tremaine.; J. F., *J. Chem. Soc., Abstracts.*, **1952**, 632-635.
- 54) (a) Bruce. Kin. R., *Acc. Chem. Res.*, **1970**, 3 (12), 417–427; (b) Elschenbroich. C., *Organometallics*, Third edition. Willey-VCH Verlag GmbH & Co.KGaA, Weinheim, **2006**.
- 55) (a) Kubacek. P.; Hoffmann. R.; Zdenek. H, *Organometallics*, **1982**, 1, 180-188; Crabtree. R. H., (b) *The organometallic chemistry of the transition metals*, Fourt edition, Wiler Interscience, **2005**, pag 140.

- 56) Benxian S. Z. C.; Zhong X. W. L.; Hao. L., *Energy & Fuels.*, **2009**, 23, 4077–4081.
- 57) Panda. T. K.; Gamer. M. T.; Roesky. P. W., *Organometallics*, **2003**, 22, 877-878.
- 58) Fischer. E.O.; Hafner. W.; Stahl. H.O., *Z. Anorg. Allg. Chem.*, **1955**, 282, 47; Wilkinson. G., *J. Am. Chem. Soc.*, **1954**, 76, 209; Hayter. R.G., *Inorg. Chem.*, **1963**, 2, 1031.
- 59) Abel. E.W.; Singh. A.; Wilkinson. G., *J.Chem. Soc.*, **1960**, 1321; Hayter. R.G., *Inorg. Chem.*, **1963**, 2, 1031.
- 60) (a) Gates. B. C., *Catalytic Chemistry* (Wiley, New York, **1992**); (b) Cotton. F. A.; Wilkinson. G., *Advanced Inorganic Chemistry* (Wiley, New York, **1988**).
- 61) Moss. J. R., *J. of Molecular Catalyst.*, **1996**, 107, ,169-174.
- 62) Nakazawa. H.; Kamata. K.; Masumi. I., *Chem. Comm.*, **2005**, 4004-4006.
- 63) Fukumoto. K.; Kasa. M.; Tsukuru. Oya.; Itazaki. M.; Nakazawa. H., *Organometallics, Communications*, **2011**.
- 64) Mouatassim. B.; Elamouri. H.; Vaissermann. J.; Jaouen. G., *Organometallic*, **1995**, 14, 3296-3302.
- 65) Toscano. P. J.; Marks. T. J., *Organometallics*, **1986**, 5, 400-4002.
- 66) Mohlala. M. S.; Coville. N. J., *Journal of Organometallic Chemistry.*, **2007**, 692, 2965–2970
- 67) Mohler. D. L.; Barnhardt. E. K.; Hurley. A. L., *J. Org. Chem.*, **2002**, 67, 4982-4984.
- 68) Wanga. Z.; Choon W. K.; Shenyu L.; Horab. A. T.S., Zhao. J., *Applied Catalysis A: General.*, **2011**, 393, 269–274.
- 69) Abrantes. M., *Journal of Molecular Catalysis A: Chemical.*, **2010**, 320, 19–26.

- 70) Crabtree, R. H., *The organometallic chemistry of the transition Metals.*, Fourt edition, Wiler Interscience, Chapter 6, **2005**.
- 71) (a) Collman, J. P.; Hegedus, L. S.; Norton, J. R.; Finke, R. G., *Principles and Applications of Organotransition Metal Chemistry*; University Science Books: Mill Valley, CA, **1987**; (b) Elschenbroich, Ch. A.; Salzer, A. *Organometallics: A Concise Introduction*; VCH: Weinheim, **1992**; (c) Grushin, V. V.; Alper, H., *Chem. Review.*, **1994**, 94, 1047. Amatore, C.; Jutand, A. *Acc. Chem. Res.*, **2000**, 33, 314. (d) Luh, T. Y.; Leung, M. k.; Wong, K. T., *Chem. Review.*, **2000**, 100, 3187.
- 72) (a) Luh, T. Y.; Leung, M. k.; Wong, K. T., *Chem. Review.*, **2000**, 100,3187; (b) Ritter, D.; Weisshaar, J. C., *J. Am. Chem. Soc.*, **1990**, 112, 6425; (c) Fayet, P.; Kaldor, A.; Cox, D. M. J., *Chem. Phys.*, **1990**, 92, 254; (e) Casado, A. L.; Espinet, P., *Organometallics*, **1998**, 17, 954; (f) Sturmer, R., *Angew. Chem.*, **1999**, 111, 3509; (g) Hinrichs, R. Z.; Schroden, J. J.; Davis, H. F., *J. Am. Chem. Soc.*, **2003**, 125, 860; (h) De Pater, B. C.; Zipp, E. J.; Fruhauf, H. W.; Ernsting, J. M.; Elsevier, C. J.; Vrieze, K., *Organometallics*, **2004**, 23, 269; (i) Espinet, P.; Echavarren, A., *Angew. Chem.*, **2004**, 116, 4808;
- 73) (a) Wang, G.; Chen, M.; Zhou, M., *Chem. Phys. Lett.*, **2005**, 412, 46; (b) Lersch, M.; Tilset, M., *Chem. Review.*, **2005**, 105, 2471; (c) Weisshaar, J. C., *Acc. Chem. Res.*, **1993**, 26, 213; (d) Carroll, J. J.; Haug, K. L.; Weisshaar, J. C.; Blomberg, M. R. A.; Siegbahn, P. E. M.; Svensson, M., *J. Phys. Chem.*, **1995**, 99, 13955; (e) Porembski, M.; Weisshaar, J. C., *J. Phys. Chem. A.*, **2000**, 104, 1524; (f) Haynes, A.; Maitlis, P. M.; Morris, G. E.; Sunley, G. J.; Adams, H.; Badger, P. W.; Bowers, C. M.; Cook, D. B.; Elliott, P. I. P.; Ghaffar, T.; Green, H.; Griffin, T. R.; Payne, M.; Pearson, J. M.; Taylor, M. J.; Vickers, P. W.; Watt, R. J., *J. Am. Chem. Soc.*, **2004**, 126, 2847; (h) Carroll, J. J.; Weisshaar, J. C., *J. Am. Chem. Soc.*, **1993**, 115, 800.

- 74) (a) Xiangai Y.; Siwei Bi.; Lingjun L.; Min S.; Jiayong W.; *Journal of Organometallic Chemistry.*, **2010**, 695, 1682-1687; (b) Fergusson, S. B.; Sanderson, L. J.; Shackleton, T. A.; Baird, M. C. *Znorg. Chim. Acta.*, **1984**, 83, L45; (c) Jones, J. H., *Platinum Metals Rev.* 2000, 44 (3), 94–105.
- 75) (a) Birch. A.; Williamson. D. H., *Organic Reactions.*, **1976**, 24,1ff (b) James. B.R., *Homogeneous Hydrogenation.*, John Wiley & Sons, New York, **1973**.
- 76) Osborn. J. A.; Jardine. F. H.; Young. J. F.; Wilkinson. G., *J. Chem. Soc. A*, **1966**, 1711-1732.
- 77) Jones. W. D., *Acc.Chem.Res.*, **2003**, 36, 140.
- 78) Labinger. J. A.; Bercaw. J.E., *Angew. Chem. Int. Ed.*, **1998**, 21, 120.
- 79) Kuivila. H. G., Sawyer. A. K., Armour. A. G., *J. Am. Chem. Soc.* **1961**, 26, 1426.
- 80) (a) Piper. T. S.; Wilkinson. G., *J. Inorg. Nucl. Chem.*, **1956**, 3, 104; (b) Marciniec, B. In *Applied Homogeneous Catalysis with Organometallic Compounds*; Cornils, B., Herrmann, W. A., Eds.; VCH: Weinheim, Germany, **1996**; 1, 487-506; (c) Folkes. C. R.; Rest. A. J., *J. Organomet.Chem.* **1977**, 136, 355. (d) Barnett. K. W.; Treichel. P. M., *Inorg. Chem.* **1967**, 6, 294.
- 81) (a) Lichtenberger, D. L.; Fenske, R. F., *J. Am. Chem. Soc.*, **1976**, 98(1), 50–63; Calabro, D. C.; Hubbard, J. L.; Blevins, C. H.; Campbell, A. C.; Lichtenberger, D. L., *J. Am. Chem. Soc.*, **1981**, 103 (23), 6839–6846; (b) Elschenbroich. C., *Organometallics*, Third edition. Willey-VCH Verlag GmbH & Co.KGaA, Weinheim, **2006**, pag 383.
- 82) Crabtree. R. H., *The organometallic chemistry of the transition metals.*, Fourt Edition, Wiler Interscience, **2005**, pag 116.

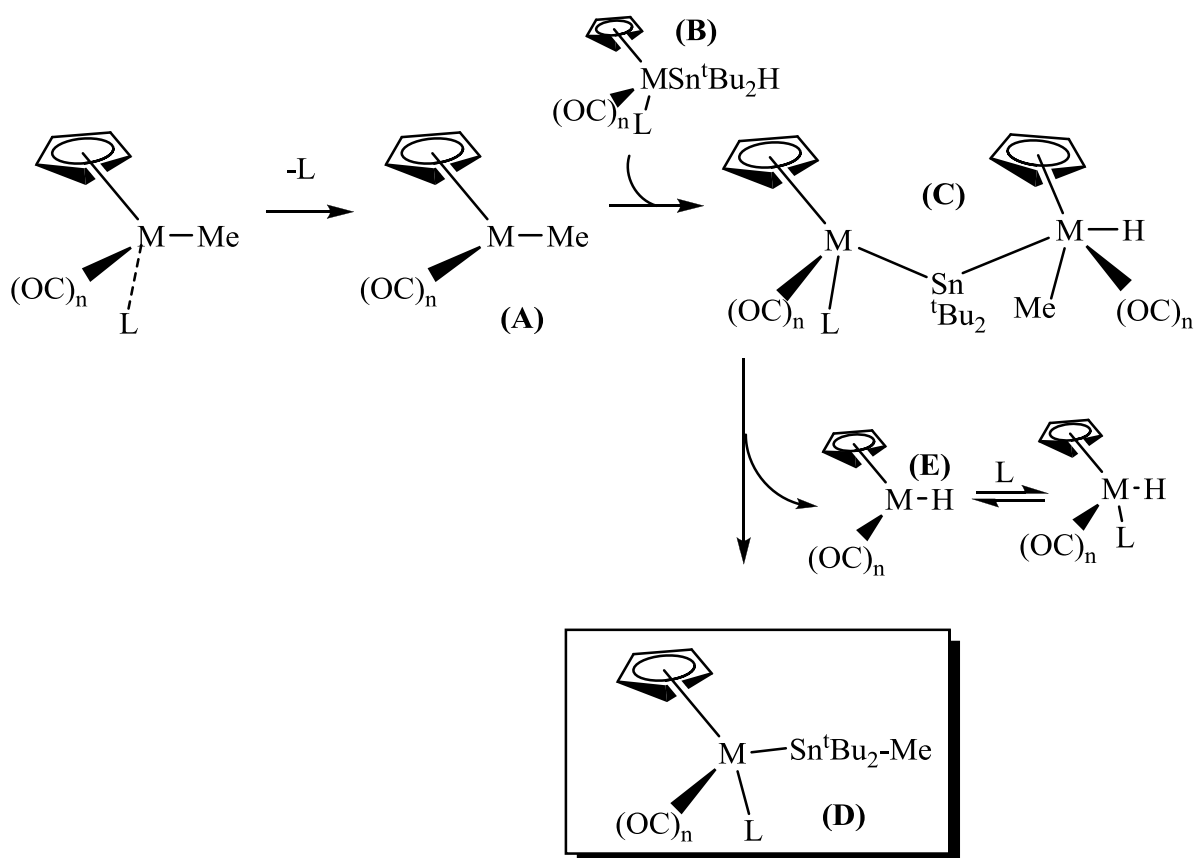
- 83) Sharma. H. K.; Arias-Ugarte. R.N.; Metta-Magana. A.; Pannell. K.H., *Angew. Chem. Int.* **2009**, *48*, 1-5.
- 84) Dagang. L.; Kou, Y.; Shufa. L.; Yingquan. Ma.; *Cuihua. Fenzi.*, **1997**, *11*(3), 180-184; b) Korneeva, G. A.; Bashkirov, A. N.; Kagan, Yu. B.; Shishkina, M. V.; Evezdkina, L. I. ; *Deposited Doc.*, (VINITI 1095-74), **1974**, 9.
- 85) Braunstein. P.; Morise. X., *Organometallics*, **1998**, *17*, 540
- 86) (a) Itazaki. M.; Ueda. K.; Nakazawa. H., *Angew. Chem.*, **2009**, *121*, 3363; (b) Itazaki. M.; Ueda. K.; Nakazawa. H., *Angew. Chem. Int. Ed.*, **2009**, *48*, 3313.
- 87) (a) Nakazawa, H.; Kamata. K.; Itazaki. M., *Chem Commun.*, **2005**, 4004; (b) Nakazawa. H.; Kamata. K.; Itazaki. M.; Ueda. K., *Chem. Asian J.*, **2007**, *2*, 882; (c) Fukumoto. K.; Oye. T.; Itazaki. M.; Nakazawa. H., *J. Am. Chem. Soc.*, **2009**, 131-38.
- 88) (a) Akita. M.; Oku. T.; Tanaka. M.; Moro-oka. Y., *Organometallics*, **1991**, *10*, 3080; (b) Zhang. S.; Brown. T., *Organometallic*, **1992**, *11*, 2122; (c) Sharma. H.K.; Pannell. K. H., *Organometallics*, **2001**, *20*, 7.
- 89) Kazlauskas. R.J.; Wrighton. M. S., *Organometallics* 1982, *1* , 602; b) Hooker. R. H.; Rest. A. J.; Whitwell. I., *J. Organomet. Chem.*, **1984**, 266, C27; (c) Mohamed. B.A.S.; Kikuchi. M.; Hashimoto. H.; Ueno. K.; Tobita. H.; Ogino. H., *Chem. Lett.*, **2004**, *33*, 112; (d) Adam. W.; Azzena. U.; Prechtel. F.; Hindahl. K.; Malisch. W., *Chem. Ber.*, **1992**, *125*, 1409.
- 90) (a) Schubert. U.; Gilbert. S.; Mock. S., *Chem. Ber.*, **1992**, *125*, 835; (b) G. Albertin.; A. S.; Bacchi. A.; Bortoluzzi. M.; Pelizzi. G.; Zanardo. G., *Organometallics*, **2006**, *25*, 4235; (c) Mohlen. M. M.; Rickard. C. E. F.; Roper. W. R.; Whittell. G.R.; Wright. L.J., *Inorg. Chim. Acta.*, **2007**, *360*, 1287; (d) Schubert. U.; Kunz. E.; Harkers. B.;

- Willnecker. J.; Meyer. J., *J.Am.Chem.Soc.*, **1989**, *111*, 2572; (e) Legzdins. P.; Shaw. M. J.; Batchelor. R.J.; Einstein. F.W.B., *Organometallics*, **1995**, *14*, 4721; (g) Albertin.V., Antoniutti. S.; Castro. J.; Garcia-Fontan. S.; Zanardo. G., *Organometallics*, **2007**, *26*, 2918.
- 91) (a) Dedieu. A., *Transition Metal Hydrides.*, VCH, New York, **1992**; (b) Francois. M.; Servin. A., *Molecular Chemistry of the Transtion Elements.*, Wiley & Sons Ltd, **1996**, Chapter 3.
- 92) Kiss, G.; Zhang, K.; Mukerjee, S. L.; Hoff, C. D.; Roper, G. C., *J. Am. Chem. Soc.* **1990**, *112*, 5657.
- 93) Choi, J.; Pulling, M. E.; Smith, D. M.; Norton, J. R., *J. Am. Chem.,Soc.*, **2008**, *130*, 4250.
- 94) Mader, E. A.; Larsen, A. S.; Mayer, J. M., *J. Am. Chem. Soc.*, **2004**, *126*, 8066.
- 95) Pugh, J. R.; Meyer, T. J., *J. Am. Chem. Soc.*, **1992**, *114*, 3784.
- 96) Neale. N. R.; Tilley. T.D., *J.Am.Chem.Soc.*, **2002**, *124*, 3802.
- 97) Nunez. A., Similar systems using $\text{Co}(\text{CO})_4\text{Ph}_3\text{PMe}$ have been also reported and the crystal structures associated with the $\text{Mn}(\text{CO})_5^t\text{Bu}_2\text{SnCl}$ and $\text{Co}(\text{CO})_4\text{Ph}_3\text{P}^t\text{Bu}_2\text{SnCl}$ have been isolated.

Methyl transfer from Fe (and Mo) to Sn: Formation of $(\eta^5\text{-C}_5\text{H}_5)\text{M}(\text{CO})_n\text{Sn}^t\text{Bu}_2\text{Me}$ ($\text{M} = \text{Fe}$, $n = 2$; $\text{M} = \text{Mo}$, $n = 3$) complexes from the photochemical irradiation of $(\eta^5\text{-C}_5\text{H}_5)\text{M}(\text{CO})_n\text{Me}$ and $^t\text{Bu}_2\text{SnH}_2$ in the molar ratio 2:1

Abstract

In the first part of this project we reported the use of $(\eta^5\text{-C}_5\text{H}_5)\text{M}(\text{CO})_n\text{Me}$, [$\text{M} = \text{Fe}$, $n = 2$ (**1a**) ; $\text{M} = \text{Mo}$, $n = 3$ (**2a**)], as catalysts for the dehydrocoupling dimerization of $^t\text{Bu}_2\text{SnH}_2$ to $\text{H}^t\text{Bu}_2\text{SnSn}^t\text{Bu}_2\text{H}$, eq. 1.19.⁸³ However, when we increase the concentration of the metal catalyst (**1a** or **2a**) to a stoichiometric ratio **2:1**, Fig. 1.12, photochemistry of such a mixture results in a different type of chemistry. The isolated product involves the formation of transition metal tin complexes of the type $(\eta^5\text{-C}_5\text{H}_5)\text{M}(\text{CO})_n\text{Sn}^t\text{Bu}_2\text{Me}$, ($\text{M} = \text{Fe}$, **3a** ; $\text{M} = \text{Mo}$, **4a**) involving the concomitant formation of an Sn-CH_3 and a Sn-M ($\text{M} = \text{Fe}$, Mo) bond, Scheme. 1.6.



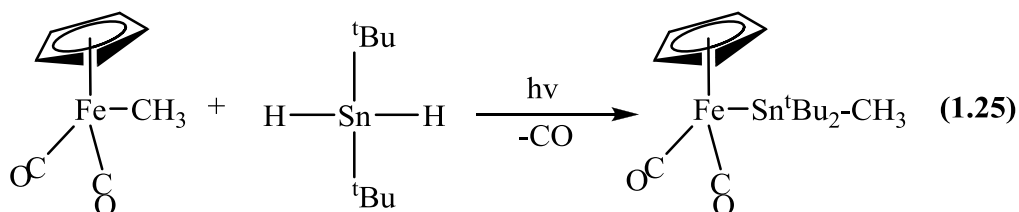
Scheme 1.6 Proposed mechanism to explain the results on Sn-CH_3 bond formation. $\text{M} = \text{Fe}$, $n = 1$, (**1a**) $\text{M} = \text{Mo}$, $n = 2$, $\text{L} = \text{CO}$ (**2a**)

Statement of problem

In part 1 of this chapter we noted that if the relative amounts of $(\eta^5\text{-C}_5\text{H}_5)\text{M}(\text{CO})_n\text{Me}$ and ${}^t\text{Bu}_2\text{SnH}_2$ were changed a much more complex chemistry occurred along with the formation of $\text{H}{}^t\text{Bu}_2\text{Sn-Sn}{}^t\text{Bu}_2\text{H}$, as noted by ${}^{119}\text{Sn}$ NMR monitoring, Figure. 1.12. The general area of this portion of my investigation is an extension of the chemistry associated with the formation of distannanes, Sn-Sn bonds.⁸³ In this particular case we want to understand how changing the relative amounts of $(\eta^5\text{-C}_5\text{H}_5)\text{M}(\text{CO})_n\text{Me}$ and ${}^t\text{Bu}_2\text{SnH}_2$, we can photochemically form $(\eta^5\text{-C}_5\text{H}_5)\text{M}(\text{CO})_n\text{Sn}{}^t\text{Bu}_2\text{Me}$?

Justification of importance

To our knowledge the concurrent formation of both a metal-tin and tin-carbon bond is extremely rare. In the present report the transition metal alkyl complex $(\eta^5\text{-C}_5\text{H}_5)\text{Fe}(\text{CO})_2\text{Me}$ was reacted with ${}^t\text{Bu}_2\text{SnH}_2$ to form the new product eq.1.25.



Thus our surprising result may lead to a new route for such chemistry, hence the need for a more detailed study into the new reaction. The finding of new synthetic methodologies that involve the formation of Sn-C bond is an important aspect to be considered, since Sn-C bonds are important precursor materials in organometallic chemistry, and most of the Sn-C derivatives require special considerations and conditions for their synthesis.⁹⁸⁻¹⁰⁵

Research objectives

- ❖ To determine the generality and mechanism of the methyl transfer from Fe (and Mo) to Sn during the photochemical irradiation of di-^tbutyltin dihydride, ^tBu₂SnH₂, with stoichiometric amounts of (η⁵-C₅H₅)M(CO)_nMe, [M = Fe, n = 2 (**1a**) ; M = Mo, n = 3 (**2a**)].

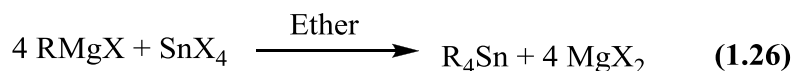
1.5 Introduction

1.5.1 Synthesis of carbon-tin bonds

The principal methods for forming a tin-carbon bond involve the reaction of organometallic reagents with tin halides and related compounds,¹⁰⁶⁻¹¹⁸ the reaction of stannylmetallic compounds with organic halides, the reaction of tin or tin(II) compounds with alkyl halides, the hydrostannation of alkenes or alkynes, and the reaction of acidic hydrocarbons with Sn-O and Sn-N bonded compounds. These methods will be briefly discussed.

1.5.2 Reaction of organometallic reagents with tin halides:

The nucleophilic alkylation of a tin compound with an organometallic reagent, e.g. a Grignard reagent, is the most common route to organotin compounds, eq. 1.26. Selective partial alkylation of the tin is usually difficult to achieve, and the reactions often go to completion to give R₄Sn.⁹⁸



M = Mg, Li, or Al; X: commonly a halide

Important examples reported in the literature include the formation of tetraethyltin, tetrapropyltin and tetrabutyltin obtained in 85-95% yields from the reactions of alkylmagnesium bromide and tin tetrachloride in refluxing ether.⁹⁸ On the industrial scale,

such reactions are performed in toluene containing minimum amount of ether which is needed to allow the Grignard reagent to be formed, (Schlenk equilibrium)⁹⁹⁻¹⁰⁰ eq. 1.27.



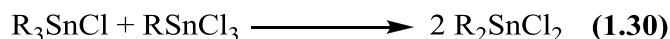
Any subsequent dealkylation, if required, can be achieved by the Kocheshkov reaction,¹⁰¹ eq. 1.28.



In the absence of a solvent, but sometimes in the presence of catalyst such as aluminium chloride, tetraorganostannanes and tin tetrahalides, or any organotin $\text{R}_n\text{SnX}_{4-n}$ and tin halide $\text{R}_m\text{SnX}_{4-m}$, undergo a redistribution of the alkyl and halogen groups.¹⁰² The reactivity follows the sequence $\text{R} = \text{phenyl} > \text{benzyl} > \text{vinyl} > \text{methyl} > \text{higher alkyl}$, and $\text{X} = \text{Cl} > \text{Br} > \text{I}$. For example $\text{R} = \text{alkyl}$ and $\text{X} = \text{halide}$, the first stage takes place rapidly at room temperature,¹⁰² eq. 1.29.



When $\text{R} > \text{Me}$, heating usually at 200°C is needed to induce the next step,¹⁰² eq. 1.30.



Wurtz coupling

There are a number of reports for the preparation of organotins in which a mixture of organic halide (RX) and tin halide is treated with metallic sodium,¹⁰³ eq. 1.31.



However, the formation of the R-Sn bond is accompanied by reduction of RX to form R-R.¹⁰⁴ Such problems can be reduced by working at high dilutions and with diorganotin halides rather than tetrahalides, or a using a two step reaction, eq. 1.32, 1.33.¹⁰⁵

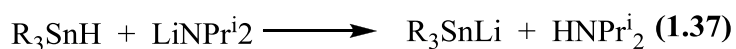
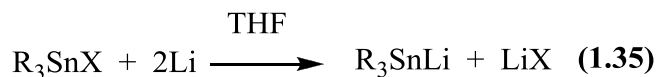


1.5.3 Reaction of stannylmetallic compounds with organic electrophiles

The reaction of a stannylmetallic compound (commonly a lithium salt) with an organic halide or other organic electrophile, is a versatile process.¹⁰⁶⁻¹¹⁰ eq. 1.34.

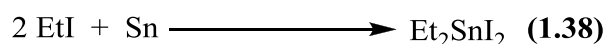


These stannylmetallic reagents can be easily prepared, e.g. from tin halides and lithium, eq. 1.35, from distannanes and an alkyl lithium, eq. 1.36, or tin hydrides and LDA,¹⁰⁶⁻¹⁰⁷ eq. 1.37.



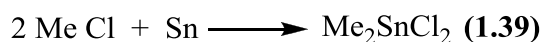
1.5.4 Reaction of tin or tin (II) compound with alkyl halides.

Frankland, in 1849, prepared the first organotin compound by heating ethyl iodide and metallic tin, eq. 1.38.¹¹¹



Despite the obvious attractions of this method (a “Direct Process”), particularly for industrial purposes, it is not widely used. However, a superior industrial process showed the

ability of metallic copper to catalyze the formation of Me_2SnX_2 $\text{X} = \text{Cl}, \text{Br}$, by passing the vapour of the halide through molten tin. Eq. 1.39.^{112,113}



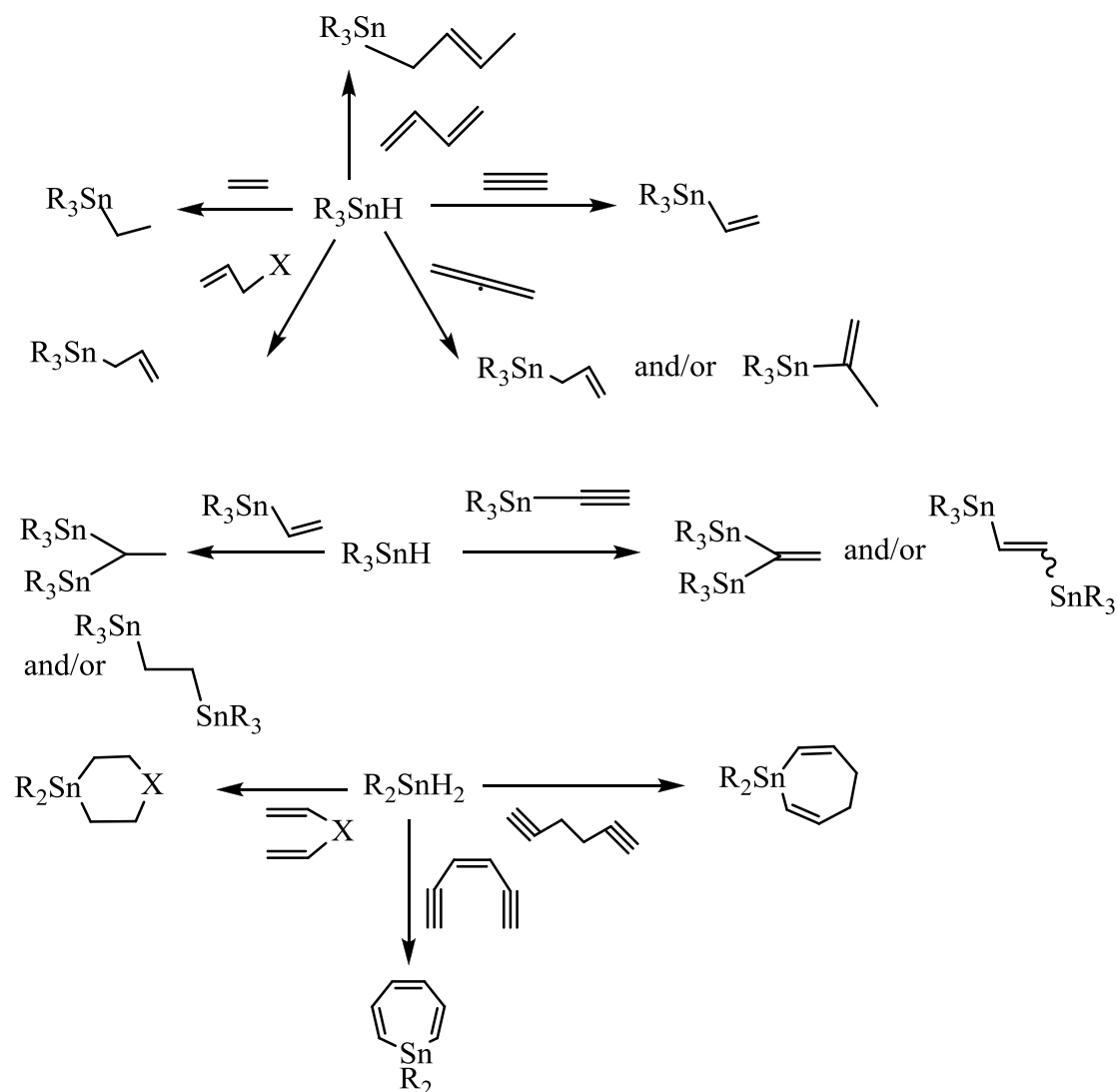
However the method does not work for butylchloride, butylbromide and bromobenzene. On the other hand an interesting industrial application has been reported for the extraction of tin from ores and slag, and 44% of tin can be recovered as the halides $\text{Me}_n\text{SnCl}_{4-n}$ ($n = 1-3$), and this is raised to 60-75% if copper is added.¹¹²

In general, the reactivity usually follows the sequence:

$\text{RI} > \text{RBr} > \text{RCl}$ and $\text{MeX} > \text{EtX} > \text{PrX} > \text{higher RX}$. The principal classes of catalyst are: (a) A metal or metal halide in the presence of ligand or polar solvent; (b) R_3M or $\text{R}_4\text{M}^+ \text{X}^-$, $\text{M} = \text{N}, \text{P}, \text{Sb}$; (c) KI and crown ether in polar solvent.¹¹³

1.5.5 Hydrostannation of alkenes and alkynes

This methodology provides a versatile way to prepare alkyl and vinyl-tin compounds. Variations on this general theme are illustrated in Scheme. 1.7.¹¹⁶



Scheme 1.7 Hydrostannation of alkenes and alkynes¹¹⁴

Several mechanisms are recognized for hydrostannations. Firstly, the tin hydride acting as a source of a tin centered radical, $(R_3Sn\cdot)^{115}$ eq. 1.40; the tin acting as either an electrophile (alkenes carry an electron strongly attracting group), eq. 1.41. $(R_3Sn^+)^{114}$ or acting as a nucleophile $(R_3Sn^-)^{115}$ eq. 1.42. In this latter case the tin always is introduced at the β -position.¹¹⁶

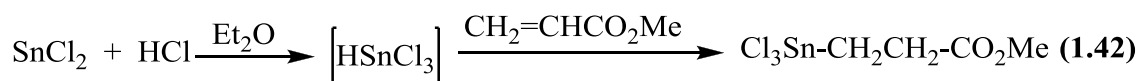
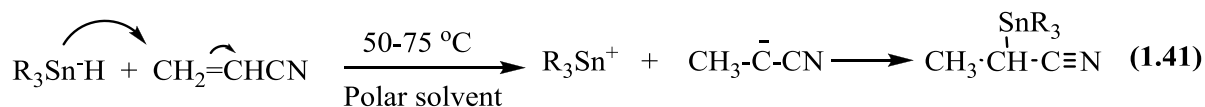
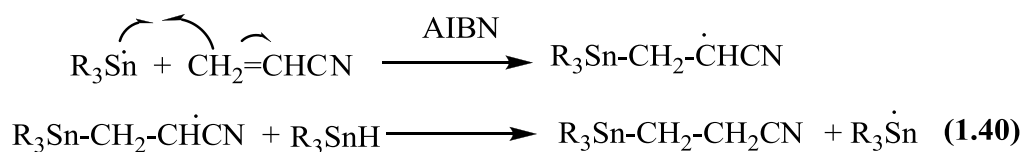


Table 1. 8 Important synthetic methodologies to form Sn-C bonds

Entry	Sn derivative	Carbon Source	Catalyst	Sn-C bond	Ref
1	R ₃ Sn-X	R-MgX	-	R ₃ Sn-R	98
2	R ₃ Sn-X	R-Na	-		103
3	R ₃ Sn-Li	R-X	-		106-110
		R=O	-		
4	Sn	R-X	Cu		111
5	R ₃ Sn-H	R=C,	AIBN		114
		$\text{R}\equiv\text{CR}'$			
6	R ₃ Sn-H	R=C,	Pd		118
		$\text{R}\equiv\text{CR}'$			
7	R ₃ Sn-H	R-Metal (Fe, Mo)	-	R ₃ Sn-R	
8	R ₃ Sn-H	R ₃ Sn-H	R-Metal (Fe, Mo)	R ₃ Sn-SnR ₃	83

1.6 Experimental

All manipulations were performed using standard Schlenk techniques under argon atmosphere. Tetrahydrofuran (THF) was dried and distilled from sodium-benzophenone. Diethyl ether, benzene, toluene and hexane were dried and distilled over sodium wire. The following reagents were purchased from Aldrich and used as received: t-dibutyltin dichloride and lithium aluminum hydride. The iron and molybdenum dimer $[(\eta^5\text{-C}_5\text{H}_5)\text{Fe}(\text{CO})_2]_2$ and $[(\eta^5\text{-C}_5\text{H}_5)\text{Mo}(\text{CO})_3]_2$ were purchased from Strem Chemicals. NMR spectra were

recorded on Bruker 300 MHz spectrometer using CDCl_3 or C_6D_6 as solvent; infrared spectra were recorded on an ATI Mattson Infinity Series FTIR; elemental analyses were performed by Galbraith Laboratories. Di-*t*-butyltinhydride, ${}^t\text{Bu}_2\text{SnH}_2$ ¹ was synthesized by the reduction of corresponding tin dichlorides with lithium aluminum hydride in ether. The iron complexes $(\eta^5\text{-C}_5\text{H}_5)\text{M}(\text{CO})_n\text{CH}_3$ and $(\eta^5\text{-C}_5\text{H}_5)\text{M}(\text{CO})_{n-1}(\text{PPh}_3)\text{CH}_3$ (M = Fe, n = 2; M = Mo, n = 3) were synthesized by the reported method.⁸⁰

1.6.1 Synthesis of $(\eta^5\text{-C}_5\text{H}_5)\text{Fe}(\text{CO})_2\text{Sn}{}^t\text{Bu}_2\text{Cl}$: To 80 mL of a hexanes solution of $(\eta^5\text{-C}_5\text{H}_5)\text{Fe}(\text{CO})_2\text{Na}^+$ (prepared from 2.0 g (5.65 mmol) of $[(\eta^5\text{-C}_5\text{H}_5)\text{Fe}(\text{CO})_2]_2$ in a 250 mL Schlenk flask, was added slowly via a syringe 3.44 g (11.3 mmol) of di-*t*-butyltin dichloride in 20 mL of hexane at room temperature. The heterogeneous solution was stirred at room temperature for 2 d. The solution was filtered over Celite and the remaining residue was extracted with 20 mL of benzene and filtered over Celite again. The two filtrates were combined and the solvents were removed under vacuum. The yellow residue was recrystallized from 1:1 hexane benzene mixture. Yield: 4.65 g (92 %). ¹H NMR (300 MHz) (C_6D_6): δ 1.39 (s, 18H, ${}^t\text{Bu}$, ${}^3\text{J}^{119\text{Sn-1H}}=78$ Hz; ${}^3\text{J}^{117\text{Sn-1H}}=72$ Hz), 4.16 (s, 5 H, $(\eta^5\text{-C}_5\text{H}_5)$). ¹³C NMR (75.4 MHz) (C_6D_6): δ 30.80 (${}^t\text{Bu}$), 40.57 C(CH₃)₃, 81.87 ($(\eta^5\text{-C}_5\text{H}_5)$), 214.04 (CO). ¹¹⁹Sn NMR (111.93 MHz) (C_6D_6): δ 384.4. IR (ν CO, cm^{-1}) (Hexane): 2012.8, 1999.3, 1969.4, 1953.1. Anal. Calcd. for $\text{C}_{15}\text{H}_{23}\text{ClFeO}_2\text{Sn}$: C, 40.45; H, 5.21. Found: C, 40.92; H, 5.20.

1.6.2 Synthesis of $(\eta^5\text{-C}_5\text{H}_5)\text{Fe}(\text{CO})_2\text{Sn}{}^t\text{Bu}_2\text{H}$: A flame dried three-necked 100 mL round-bottom flask equipped with reflux condenser and a dropping funnel was charged with 0.0064 g (0.016 mmol) of LiAlH_4 in 15 mL ether. The temperature was maintained at -15 °C and at this temperature was added slowly via a dropping funnel 20 mL solution of 0.15 g (0.33 mmol) of $(\eta^5\text{-C}_5\text{H}_5)\text{Fe}(\text{CO})_2\text{Sn}{}^t\text{Bu}_2\text{Cl}$ in ether. The mixture was stirred for 30 minutes

maintaining the temperature of the bath between -15 to -10 °C. After 30 min the mixture was filtered through Celite. The ether was removed under vacuum and the residue was extracted with 20 mL of hexane and again filtered through Celite. The hexanes were removed under vacuum and the yellow residue was recrystallized from hexanes. Yield: 0.11g (81 %). ¹H NMR (300 MHz) (C₆D₆): δ 1.37 (s, 18 H, ^tBu, ³J¹¹⁹Sn-¹H = 66 Hz;), 4.19 (s, 5 H, (η⁵-C₅H₅)), 5.28 (1H, Sn-H, ¹J¹¹⁹Sn-¹H = 1212 Hz; ¹J¹¹⁷Sn-¹H = 1158 Hz). ¹³C NMR (75.4 MHz) (C₆D₆): δ 33.11 (^tBu), 31.70 C(CH₃)₃, 80.74 ((η⁵-C₅H₅)), 215.59 (CO). ¹¹⁹Sn NMR (111.93 MHz) (C₆D₆): δ 155.5. IR (ν̄ CO, cm⁻¹) (Hexane): 1995.5, 1947.7, 1748(w, Sn-H). Anal. Calcd. for C₁₅H₂₄FeO₂Sn: C, 43.84; H, 5.89. Found: C, 43.45; H, 5.96.

1.6.3 Synthesis of (η⁵-C₅H₅)Fe(CO)₂Sn^tBu₂Me : A 5 mm Pyrex NMR tube was charged with a mixture of 0.38 g (1.98 mmol) of (η⁵-C₅H₅)Fe(CO)₂Me, 1a and 0.23 g (0.98 mmol) of ^tBu₂SnH₂ in 1.0 mL of degassed C₆D₆, and the tube was sealed under vacuum. The sealed NMR tube was irradiated with 450 W medium-pressure mercury lamp, and the reaction was monitored by ¹H, ¹³C, and ¹¹⁹Sn NMR spectroscopy. After 24h of irradiation, the photolysis was stopped and the solution was placed in 2.5 x 10 cm silica gel column, and yellow band was eluted with hexane. Upon removal of solvent in vacuum, 0.17 g (20 % yield) of (η⁵-C₅H₅)Fe(CO)₂Sn^tBu₂Me was obtained. ¹H NMR (300 MHz) (C₆D₆): δ 0.38 (s, 3H, Me, ²J¹¹⁹Sn-¹H = 34 Hz) 1.27 (s, 18 H, ^tBu, ³J¹¹⁹Sn-¹H = 63 Hz;), 4.24 (s, 5 H, (η⁵-C₅H₅)); ¹³C NMR (75.4 MHz) (C₆D₆): δ -9.01 (Me); 31.25 C(CH₃)₃, 32.22 (^tBu), 80.35 ((η⁵-C₅H₅)), 216.08 (CO); ¹¹⁹Sn NMR (111.93 MHz) (C₆D₆): δ 192.4. IR (ν̄ CO, cm⁻¹) (Hexane): 1990.1, 1942.4; Anal. Calcd. for C₁₆H₂₆FeO₂Sn: C, 45.22; H, 6.17. Found: C, 45.12; H, 6.08.

1.6.4 Synthesis of (η⁵-C₅H₅)Fe(CO)₂Sn^tBu₂(η⁵-C₅H₅)Mo(CO)₃: To 60 mL of a THF solution of (η⁵-C₅H₅)Fe(CO)₂⁻Na⁺ (prepared from 2.0 g (5.65 mmol) of [(η⁵-C₅H₅)Fe(CO)₂]₂ in a 250 mL Schlenk flask, was added slowly via a syringe 1.72 g (5.65 mmol) of di-*t*-

butyltin dichloride in 20 mL of THF at 0 °C. The reaction mixture was stirred at room temperature overnight. THF was evaporated and the orange residue was extracted with 100 mL of 80:20 hexane / CH₂Cl₂ mixtures and the solution was filtered over Celite. The solution was concentrated and chromatographed on silica gel column. The orange band was eluted with 80:20 hexanes / CH₂Cl₂ solvents were removed under vacuum. The orange residue was recrystallized from 4:1 hexanes/CH₂Cl₂ mixture. Yield: 3.1 g (93%). It was finally recrystallized from 1:1 mixture of hexanes/benzene. Yield 1.1 g (73 %). ¹H NMR (300 MHz) (C₆D₆): δ 1.54 (s, 18 H, ^tBu, ³J¹¹⁹Sn-¹H = 60 Hz;), 4.40 (s, 10 H, (η⁵-C₅H₅)). ¹³C NMR (75.4 MHz) (C₆D₆): δ 34.08 (^tBu), 38.44 C(CH₃)₃, 82.60 ((η⁵-C₅H₅)), 218.20 (CO). ¹¹⁹Sn NMR (111.93 MHz) (C₆D₆): δ 470.7. IR (ν̄ CO, cm⁻¹) (Hexane): 1986.8, 1974.7, 1939.6, 1931.4. Anal. Calcd. for C₂₂H₂₈Fe₂O₄Sn: C, 45.02; H, 4.80. Found: C, 45.16; H, 4.88.

1.6.5 Synthesis of [(η⁵-C₅H₅)Fe(CO)]₂ (μ-Sn^tBu₂)(μ-CO) (5): A solution of compound 7 (0.2 g, 0.34 mmol) in 1.0 mL of degassed C₆D₆ was sealed in a Pyrex NMR tube. The tube was placed at a distance of 5 cm from a 450-W medium-pressure mercury lamp and irradiated. The progress of the photoreaction was followed by ¹H, ¹³C, and ¹¹⁹Sn NMR spectroscopy. The starting material was completely disappeared in 18 h of irradiation with formation of trans/cis isomers in 2:1 ratio of stannylene-carbonyl bridged diiron complex 8 and no other tin compound was observed in the NMR spectra. The dark maroon complex 8 was recrystallized from hexane in 90 % yield. ¹H NMR (300 MHz) (C₆D₆): δ 1.39, 1.63 (cis), 1.50 (trans), (s, 18 H, ^tBu), 4.29 (cis) (s, 5 H, (η⁵-C₅H₅)), 4.39 (trans) (s, 5 H, (η⁵-C₅H₅)). ¹³C NMR (75.4 MHz) (C₆D₆): δ 33.00 (trans), 33.35, 33.71 (cis), (^tBu); 45.40 (trans), 45.77, 45.82 (cis), C(CH₃)₃; 81.38 (trans), 81.58 (cis) ((η⁵-C₅H₅)), 213.35, 213.50 (ter-CO), 278.50, 279.90 (bdg-CO). ¹¹⁹Sn NMR (111.93 MHz) (C₆D₆): δ 1067.2 (cis), 1073.8 (trans). IR (ν̄ CO, cm⁻¹) (Hexane): 1994, 1975, 1947, 1930, (ter-CO), 1794, 1769 (bdg-CO) cm⁻¹. HR

MS (CI): exact mass found 560.982533, calculated for [M+1] C₂₁H₂₉Fe₂O₃Sn 560.983748.

1.6.6 Synthesis of MpSn^tBu₂Cl: To 80 mL of THF solution of Mp⁻Na⁺ [Mp = (η⁵-C₅H₅)Mo(CO)₃] (prepared from 4.0 g (8.16 mmol) of [(η⁵-C₅H₅)Mo(CO)₃]₂) in a 250 mL Schlenk flask, was added slowly via a syringe 4.95 g (16.32 mmol) of di-tert-butyltin dichloride in 20 mL of THF at room temperature. The reaction mixture was stirred at room temperature overnight. The solvent was removed under vacuum and 80 mL hexanes were added and the solution was filtered over Celite. The filtrate was collected and the solvent was removed under vacuum. The yellow solid residue was recrystallized from hexane at -5°C. Yield: 6.69 g (80 %). m.p.: 136 °C. ¹H NMR (300 MHz) (C₆D₆): δ 1.43 (s, 18H, ^tBu, ³J¹¹⁹Sn-¹H = 81 Hz), 4.71 (s, 5 H, (η⁵-C₅H₅)). ¹³C NMR (75.4 MHz) (C₆D₆): δ 31.5 (^tBu), 42.6 C(CH₃)₃, 89.7 ((η⁵-C₅H₅)), 226.0 (CO), 230.5 (CO). ¹¹⁹Sn NMR (111.93 MHz) (C₆D₆): δ 328.6. IR (ν̄ CO, cm⁻¹) (THF): 2003.4, 1935.7, 1905.7, Anal. Calcd. for C₁₆H₂₃ClMoO₃Sn: C, 37.42; H, 4.52. Found: C, 37.26; H, 4.53.

1.6.7 Synthesis of MpSn^tBu₂Me: A flame dried three-necked 250 mL round-bottom flask equipped with reflux condenser and a dropping funnel was charged with 1.0 g (1.94 mmol) of (η⁵-C₅H₅)Mo(CO)₃Sn^tBu₂Cl in 40 mL ether. The temperature was maintained at -10 °C, and at this temperature was added slowly via a dropping funnel 0.217 g (2.0 mmol) of MeLi (1.5 M) in ether. The mixture was stirred for 2 hours and temperature was raised from -10 °C to room temperature. At this time ether was removed and the residue was extracted with 30 mL of hexane and filtered through Celite. The hexanes were removed under vacuum and the yellow solid was recrystallized from hexane at -10 °C. Yield: 0.46g (92 %). m.p. 86 °C. ¹H NMR (300 MHz) (C₆D₆): δ 0.44 (s, 3H, Me, ²J¹¹⁹Sn-¹H = 40 Hz), 1.30 (s, 18 H, ^tBu, ³J¹¹⁹Sn-¹H = 66 Hz; ³J¹¹⁷Sn-¹H = 40 Hz), 4.7 (s, 5 H, (η⁵-C₅H₅)). ¹³C NMR (75.4 MHz)

(C₆D₆): δ -6.48 (Me), 32.6 (^tBu), 32.91 C(CH₃)₃, 88.50 ((η^5 -C₅H₅)), 226.8, 230.1 (CO).

¹¹⁹Sn NMR (111.93 MHz) (C₆D₆): δ 132.3. IR (ν CO, cm⁻¹) (THF): 1985.99, 1910.50, 1890.80. Anal. Calcd. for C₁₇H₂₆MoO₃Sn: C, 41.41; H, 5.32. Found: C, 39.50; H, 5.02.

1.6.8 Synthesis of MpSn^tBu₂H : A flame dried three-necked 100 mL round-bottom flask equipped with reflux condenser and a dropping funnel was charged with 0.038 g (0.99 mmol) of LiAlH₄ in 20 mL of dry ether. The temperature was maintained at -20 °C and at this temperature was added slowly via a dropping funnel 20 mL solution of 0.5 g (0.97 mmol) of MpSn^tBu₂Cl in ether. The mixture was stirred for 1h maintaining the temperature of the bath between -20 to -10 °C. After 1h the mixture was filtered through Celite. The ether was removed under vacuum and the residue was extracted with 20 ml of hexane and again filtered through nylon acrodisc filter. The hexanes were removed under vacuum and the red residue was recrystallized from diethyl ether at -10 °C. Yield: 0.46g (92 %). m.p.: 84 °C. ¹H NMR (300 MHz) (C₆D₆): δ 1.39 (s, 18 H, ^tBu, ³J_{Sn-H} = 42 Hz;), 4.66(s, 5H, (η^5 -C₅H₅)), 5.51(1H, Sn-H, 1J119Sn-1H = 1298 Hz: 1J117Sn-1H = 1240 Hz). ¹³C NMR (75.4 MHz) (C₆D₆): δ 33.4 (^tBu), 33.1 C(CH₃)₃, 88.8 ((η^5 -C₅H₅)), 202.5 (CO), 234.0 (CO). ¹¹⁹Sn NMR (111.93 MHz) (C₆D₆): δ 90.6 . IR (ν CO, cm⁻¹) (Hexane): 1991.7, 1895.9, 1750 (w, Sn-H). Anal. Calcd. for C₁₆H₂₄MoO₃Sn: C, 40.12; H, 5.05. Found: C, 39.55; H, 5.02.

1.6.9 Photochemical reaction of (η^5 -C₅H₅)Mo(CO)₃Me, 2a with ^tBu₂SnH₂ : A solution of compound **2a** (0.25 g, 0.96 mmol) and ^tBu₂SnH₂, **3** (0.11 g, 0.47 mmol) in 1.0 mL of degassed C₆D₆ was sealed in a Pyrex NMR tube. The tube was placed at a distance of 5 cm from a 450 W medium-pressure mercury lamp and irradiated. The progress of the photoreaction was followed by ¹H, ¹³C, and ¹¹⁹Sn NMR spectroscopy. The starting material was completely disappeared after 80 min of irradiation with the formation of MpSn^tBu₂Me, **4a**, MpSn^tBu₂H, along with trace amounts of distannane, ^tBu₂HSn-SnH^tBu₂, ^tBu₂MeSnH and ^tBu₂SnMe₂. The photolysis was stopped and the solution was placed in 2.5 x

10 cm silica gel column, and yellow band was eluted with hexane. Upon removal of solvent in vacuum, 0.12 g (55 % yield) of $\text{MpSn}^t\text{Bu}_2\text{Me}$ was obtained.

1.7 Results and discussion

1.7.1 Synthesis of $(\eta^5\text{-C}_5\text{H}_5)\text{Mo}(\text{CO})_3^t\text{Bu}_2\text{Sn-Me}$ using $(\eta^5\text{-C}_5\text{H}_5)\text{Mo}(\text{CO})_3\text{Me}$ with $^t\text{Bu}_2\text{SnH}_2$ in benzene 3:1 ratio

Irradiation of a C_6D_6 solution of 3 mol excess of $^t\text{Bu}_2\text{SnH}_2(*)$ in the presence of 1 mol of $(\eta^5\text{-C}_5\text{H}_5)\text{Mo}(\text{CO})_3\text{Me}$ (**2a**), $\text{Cp} = \eta^5\text{-C}_5\text{H}_5$, in a sealed Pyrex NMR tube with a medium-pressure mercury lamp resulted in the progressive formation of a different set of products, including the expected $\text{H}^t\text{Bu}_2\text{SnSn}^t\text{Bu}_2\text{H}$ (Δ). The photochemical reaction was monitored by ^{119}Sn NMR spectroscopy, Fig. 1.16. showing the disappearance of $^t\text{Bu}_2\text{SnH}_2 (*)$ ^{119}Sn resonance at -118.2 ppm but only traces of the expected $\text{H}^t\text{Bu}_2\text{SnSn}^t\text{Bu}_2\text{H}$ at -83.4 ppm was observed. Thus, surprisingly a new set of signals were observed just by changing the concentration of the metal catalyst. After 4 hours of irradiation we decided to stop the reaction and try to analyze the products that were formed apart from the those we already knew such as -118 ppm ($^t\text{Bu}_2\text{SnH}_2$), -83 ppm ($\text{H}^t\text{Bu}_2\text{SnSn}^t\text{Bu}_2\text{H}$) and 90 ppm ($(\eta^5\text{-C}_5\text{H}_5)\text{Mo}(\text{CO})_3\text{Sn}^t\text{Bu}_2\text{-H}$).

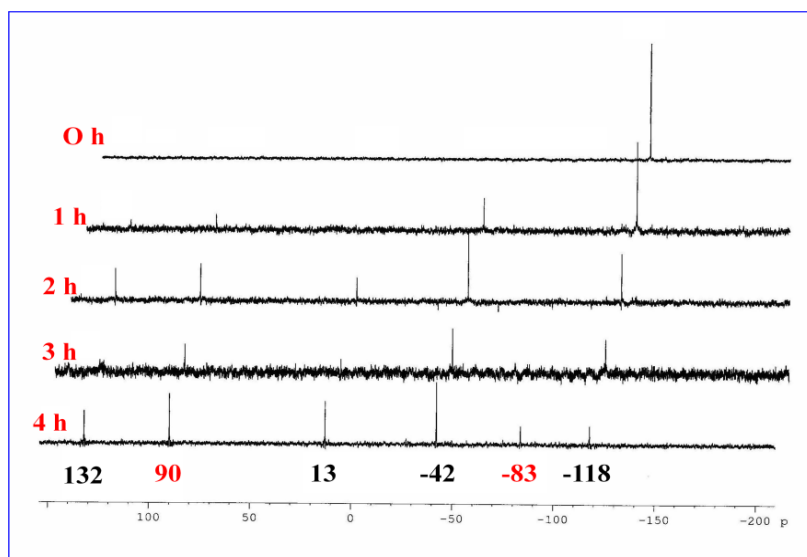


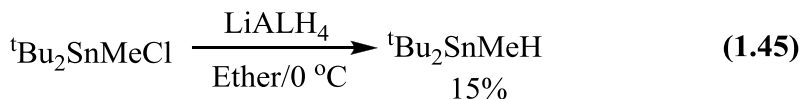
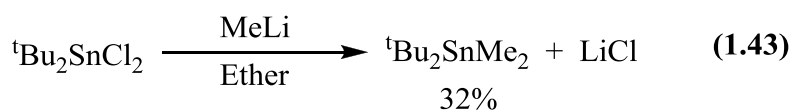
Figure 1.16 Photochemical irradiation of $t\text{Bu}_2\text{SnH}_2$ with $(\eta^5\text{-C}_5\text{H}_5)\text{Mo}(\text{CO})_3\text{Me}$ 3:1 ratio

We could isolate and identify the other signals present in the spectrum and these are presented Table. 1.9.

Table 1.9 ^{119}Sn NMR spectroscopy from the photochemical reaction 3:1 between $t\text{Bu}_2\text{SnH}_2$ and $(\eta^5\text{-C}_5\text{H}_5)\text{Mo}(\text{CO})_3\text{Me}$.

Observed Materials	$^{119}\text{Sn}/\text{C}_6\text{D}_6$ ppm
$t\text{Bu}_2\text{SnH}_2$	-118
$\text{H-}t\text{Bu}_2\text{Sn-Sn-}t\text{Bu}_2\text{-H}$	-83
$t\text{Bu}_2\text{SnMeH}$	-42
$t\text{Bu}_2\text{SnMe}_2$	13
$(\eta^5\text{-C}_5\text{H}_5)\text{Mo}(\text{CO})_3\text{Sn-}t\text{Bu}_2\text{-H}$	90
$(\eta^5\text{-C}_5\text{H}_5)\text{Mo}(\text{CO})_3\text{Sn-}t\text{Bu}_2\text{-Me}$	132

All these compounds were isolated but they can be synthetically prepared using the methodologies reported in the literature, eq. 1.43, 1.44, and 1.45.¹¹⁹⁻¹²¹



From these results we realized that a different type of chemistry was taking place that was in competition with the formation of distannanes (Δ), since only low traces of this product was formed, but the chemical shift at 132 ppm and 90 ppm for $(\eta^5\text{-C}_5\text{H}_5)\text{Mo}(\text{CO})_3\text{Sn}^t\text{Bu}_2\text{-Me}$ and $(\eta^5\text{-C}_5\text{H}_5)\text{Mo}(\text{CO})_3\text{Sn}^t\text{Bu}_2\text{-H}$ were present in higher concentrations.

The reaction between $(\eta^5\text{-C}_5\text{H}_5)\text{M}(\text{CO})_n\text{Me}$, and ${}^t\text{Bu}_2\text{SnH}_2$ (*),⁸³ in a stoichiometric ratio of 2 : 1 readily results in the formation of $(\eta^5\text{-C}_5\text{H}_5)\text{M}(\text{CO})_n\text{Sn}^t\text{Bu}_2\text{Me}$ (M = Fe, **1a**; M = Mo, **2a**), Figure.1.17. for M = Mo.

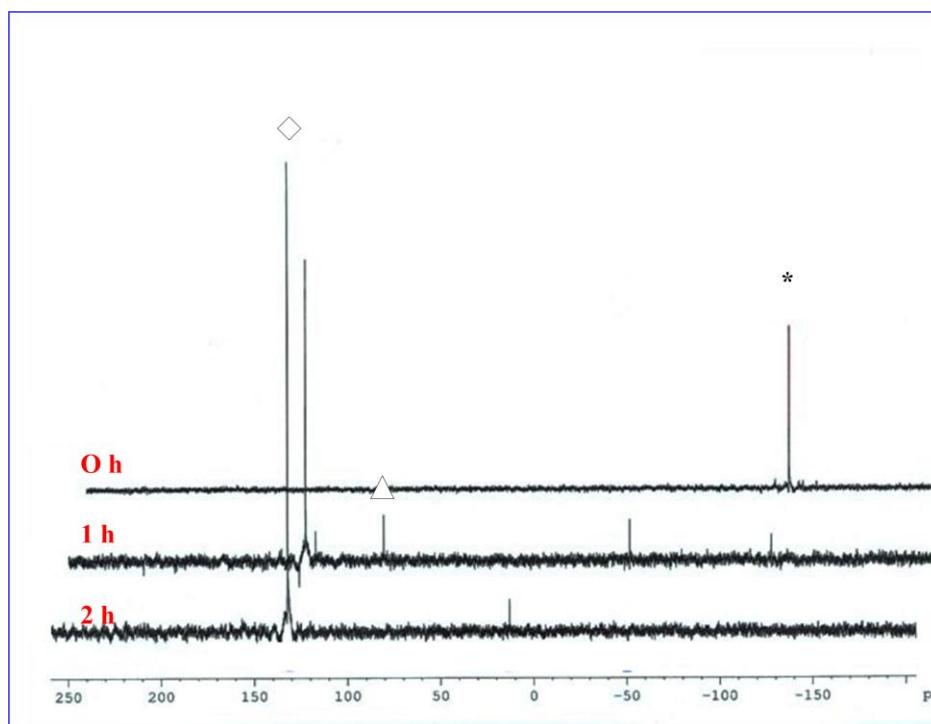


Figure 1.17 ^{119}Sn NMR spectroscopy showing the disappearance of ${}^t\text{Bu}_2\text{SnH}_2$ (*) into $(\eta^5\text{-C}_5\text{H}_5)\text{Mo}(\text{CO})_3\text{Sn}^t\text{Bu}_2\text{Me}$ (◊) under photochemical conditions.

As noted in Figure 1.17, ^{119}Sn monitoring illustrated that after 1 h of photolysis the formation of $(\eta^5\text{-C}_5\text{H}_5)\text{Mo}(\text{CO})_3\text{Sn}^t\text{Bu}_2\text{Me}(\diamond)$ (132 ppm), and $(\eta^5\text{-C}_5\text{H}_5)\text{Mo}(\text{CO})_3\text{Sn}^t\text{Bu}_2\text{-H}(\Delta)$, (90 ppm) at the expense of $^t\text{Bu}_2\text{SnH}_2(*)$ (-118ppm) can be observed. Continued irradiation (Fig. 1.17) resulted in the complete disappearance of $(\eta^5\text{-C}_5\text{H}_5)\text{Mo}(\text{CO})_3\text{Sn}^t\text{Bu}_2\text{-H}(\Delta)$, (^{119}Sn NMR, 90 ppm) and $^t\text{Bu}_2\text{SnH}_2(*)$ into $(\eta^5\text{-C}_5\text{H}_5)\text{M}(\text{CO})_3\text{Sn}^t\text{Bu}_2\text{Me}(\diamond)$ (^{119}Sn NMR (132 ppm). The reaction was stopped at this stage and the product was obtained as a yellow solid in 55% recovered yield.

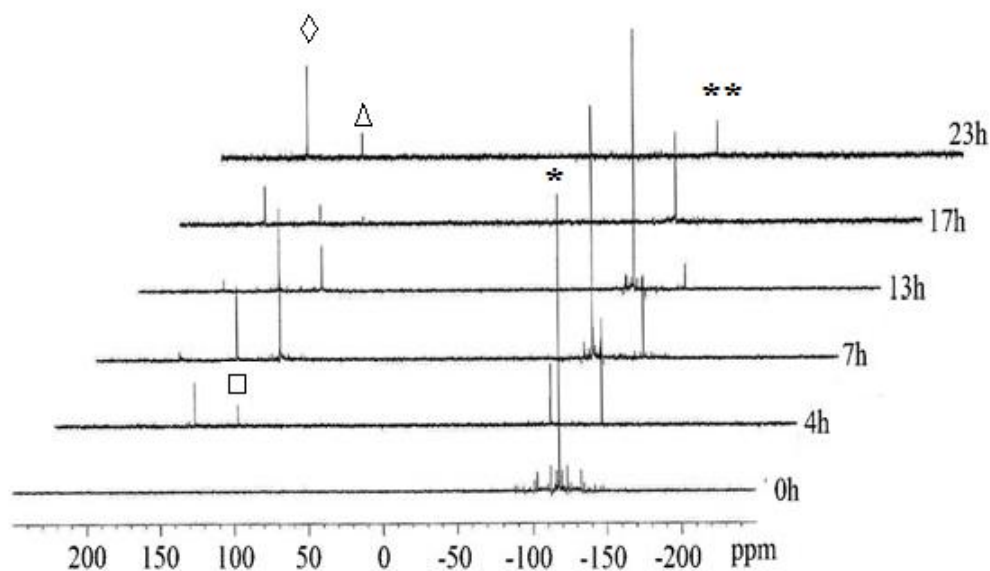
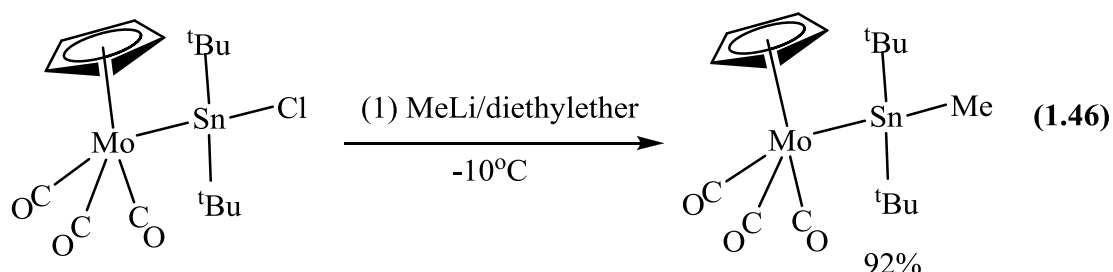


Figure 1.18 ^{119}Sn NMR spectroscopy showing the disappearance of $^t\text{Bu}_2\text{SnH}_2(*)$ into $(\eta^5\text{-C}_5\text{H}_5)\text{Fe}(\text{CO})_2\text{Sn}^t\text{Bu}_2\text{Me}(\diamond)$ under photochemical conditions.

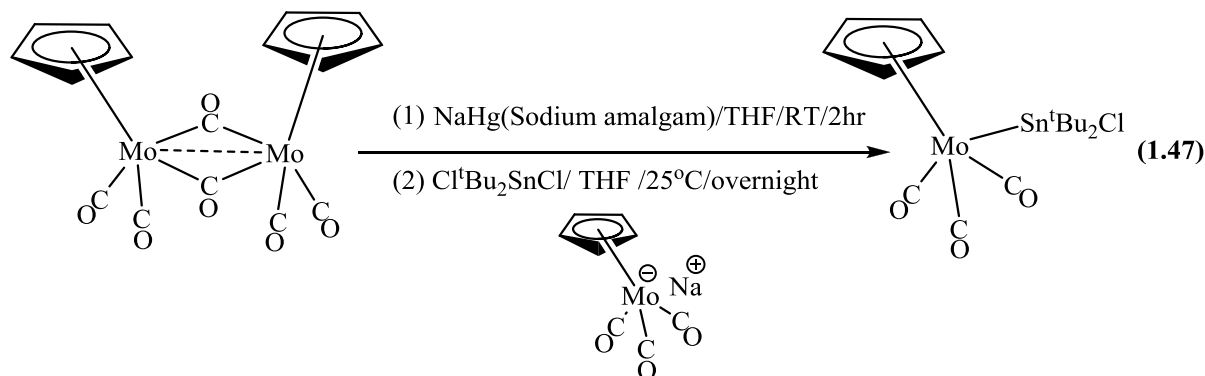
In a similar manner, the photolysis of a mixture of **1a** and $^t\text{Bu}_2\text{SnH}_2$ (in a 2 : 1 molar ratio in C_6D_6) produced $(\eta^5\text{-C}_5\text{H}_5)\text{Fe}(\text{CO})_2\text{Sn}^t\text{Bu}_2\text{Me}(\diamond)$ in 20% isolated yield, with a ^{119}Sn NMR at 192.4 ppm, Fig. 1.18. In this particular case the reaction was more complex and a series of other species could be observed by ^{119}Sn NMR spectroscopic analysis. Thus, in addition to $(\eta^5\text{-C}_5\text{H}_5)\text{Fe}(\text{CO})_2\text{Sn}^t\text{Bu}_2\text{H}(\Delta)$, (155.5 ppm) and $(\eta^5\text{-C}_5\text{H}_5)\text{Fe}(\text{CO})(\text{H})(\text{Sn}^t\text{Bu}_2\text{H})_2(\square)$, (126.4 ppm) we have tentatively assigned $\text{H}^t\text{Bu}_2\text{Sn-}$

$\text{Sn}^t\text{Bu}_2\text{H}^{**}$, -83.3 ppm). Additionally we could observe the formation of $(\eta^5\text{-C}_5\text{H}_5)\text{Fe}(\text{CO})_2\text{H}$,¹²⁴ by ^1H and ^{13}C NMR spectroscopy.

Both complexes $(\eta^5\text{-C}_5\text{H}_5)\text{M}(\text{CO})_n\text{Sn}^t\text{Bu}_2\text{Me}$ $\text{M} = \text{Fe}$, $n = 2$ (**S1**); Mo , $n = 3$ (**S2**) were independently synthesized from the reaction of MeLi with $(\eta^5\text{-C}_5\text{H}_5)\text{Fe}(\text{CO})_2\text{Sn}^t\text{Bu}_2\text{Cl}$ and $\text{MpSn}^t\text{Bu}_2\text{Cl}$, respectively, eq. 1.46.¹¹⁹ Full characterization data are in the experimental section.



The starting $\text{M-Sn}^t\text{Bu}_2\text{Cl}$ derivatives were prepared by the well-established salt-elimination reaction illustrated in eq. 1.47.⁸⁰ Full characterization data are in the experimental section.



1.7.2 Crystal structure characterization of $(\eta^5\text{-C}_5\text{H}_5)\text{M}(\text{CO})_n\text{Sn}^t\text{Bu}_2\text{Cl}$, ($\text{M} = \text{Fe}$, $n = 2$; Mo , $n = 3$)

Based on the structural geometry of $(\eta^5\text{-C}_5\text{H}_5)\text{M}(\text{CO})_n\text{Sn}^t\text{Bu}_2\text{Cl}$, Fig. 1.19, we can see the Mo atom adopts a four-legged piano-stool geometry and the Mo-Sn bond distance of

2.8841(4) Å is one of the longest such distances reported.¹²³ Presumably, this elongation is due to steric influence of two bulky ^tBu substituents at the Sn atom.

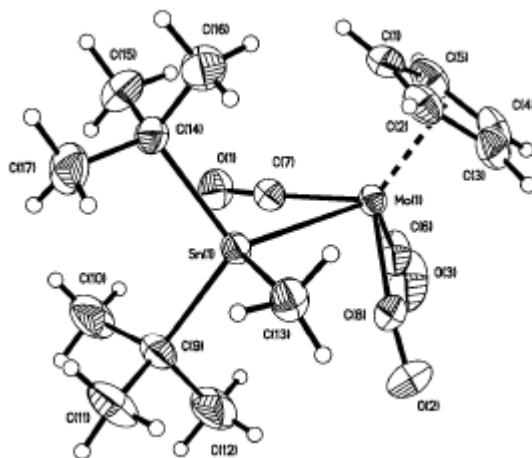


Figure 1.19 Molecular structure of $(\eta^5\text{-C}_5\text{H}_5)\text{Mo}(\text{CO})_3\text{Sn}^t\text{Bu}_2\text{Cl}$
(thermal ellipsoids are set at 50%).

Selected bond distances [Å] and angles [°]: Mo1–Sn1 = 2.8841(4),

C₉–Sn₁–Mo₁ = 115.57(10), C₁₃–Sn₁–Mo₁ = 108.81(9),

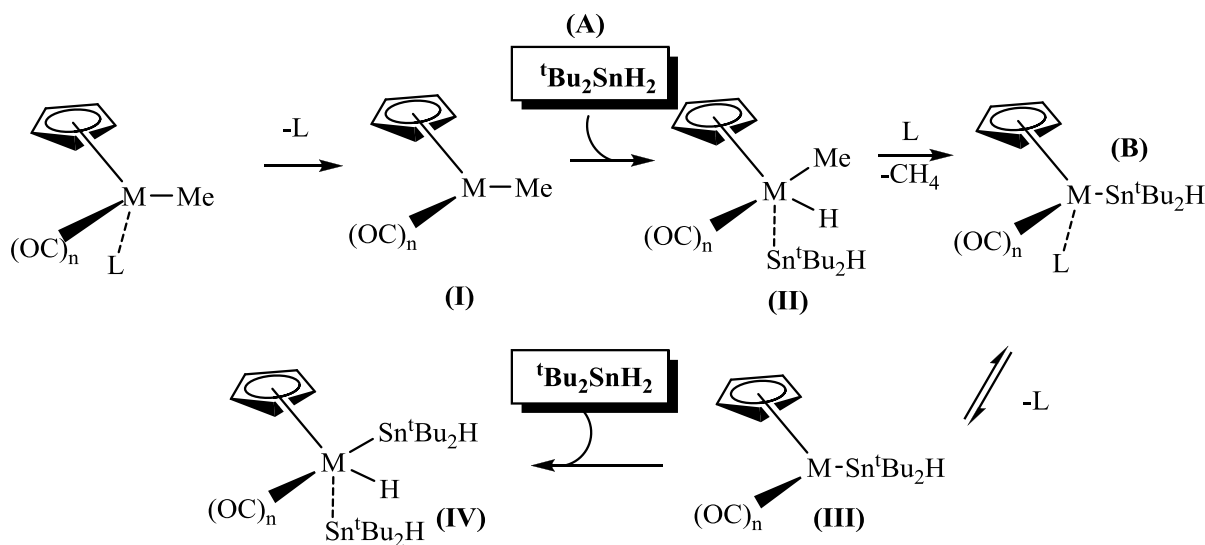
C₁₄–Sn₁–Mo₁ = 112.62(8), C₉–Sn₁–C₁₃ = 105.29(14),

C₁₄–Sn₁–C₉ = 110.86(13), C₁₄–Sn₁–C₁₃ = 102.57(13).

1.7.3 Proposed mechanism for the methyl transfer from metal to tin center

Analysis of the spectral changes (Fig. 1.17 and Fig. 1.18) during the formation of $(\eta^5\text{-C}_5\text{H}_5)\text{M}(\text{CO})_n\text{Sn}^t\text{Bu}_2\text{Me}$, indicates that build up of $(\eta^5\text{-C}_5\text{H}_5)\text{M}(\text{CO})_n\text{Sn}^t\text{Bu}_2\text{SnH}$ and $\text{H}^t\text{Bu}_2\text{Sn-Sn}^t\text{Bu}_2\text{H}$ are necessary for the formation of the product. The first step in the mechanism, as for the catalytic cycles associated with the chemistry in eq. 1.21.⁸³ involves the loss of CO from **1a(2a)** to form the 16e- transient $(\eta^5\text{-C}_5\text{H}_5)\text{M}(\text{CO})_{n-1}\text{Me}$ (M = Fe, n = 2; M = Mo, n = 3) (**I**). Oxidative addition of $\text{Sn}^t\text{Bu}_2\text{SnH}_2$ to this species produces $(\eta^5\text{-C}_5\text{H}_5)\text{MMe}(\text{H})(\text{CO})_{n-1}(\text{Sn}^t\text{Bu}_2\text{H})$ (**II**) which can undergo the reductive elimination of CH_4 ¹²⁴ to form another

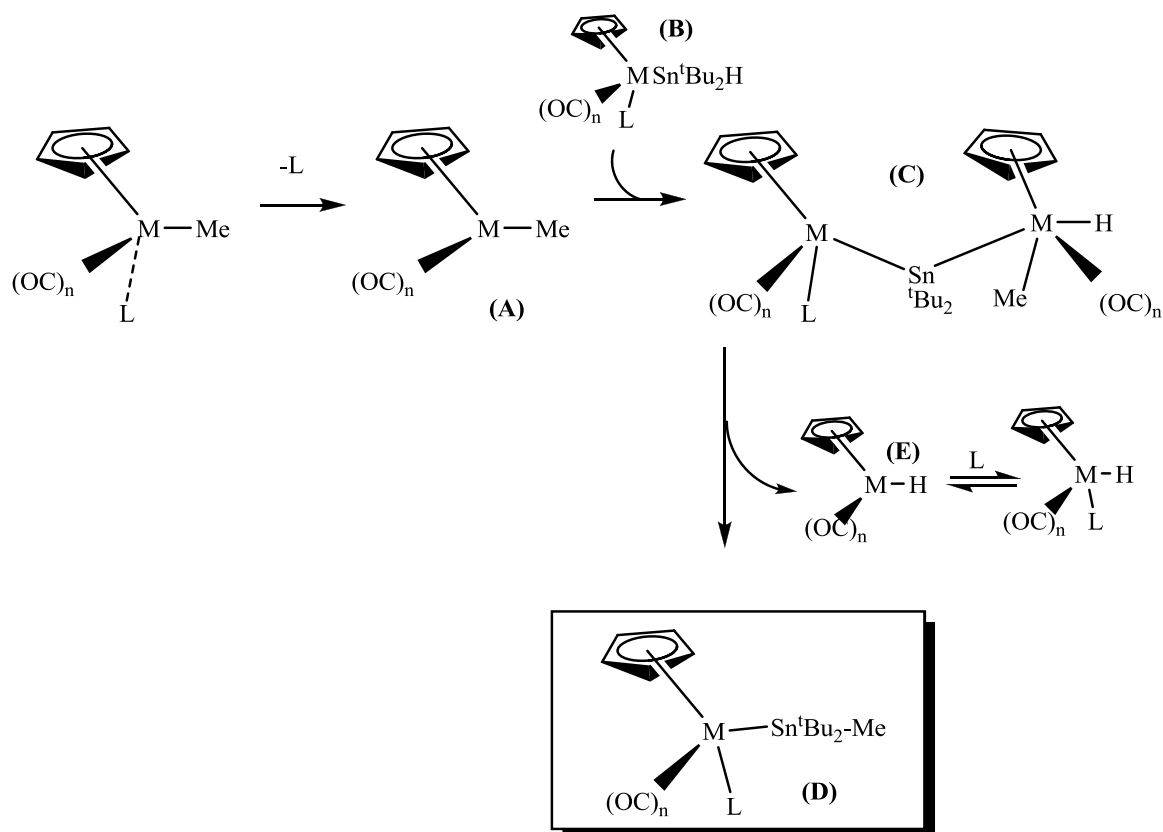
coordinatively unsaturated complex, $(\eta^5\text{-C}_5\text{H}_5)\text{M}(\text{CO})_{n-1}(\text{Sn}^t\text{Bu}_2\text{H})$ (**III**) that is the key intermediate in the initial segment of the process, Scheme. 1.8.⁸³



Scheme 1.8 Proposed mechanism for the formation of $(\eta^5\text{-C}_5\text{H}_5)\text{M}(\text{CO})_n\text{Sn}^t\text{Bu}_2\text{H}$

Transient (**III**) can undergo oxidative addition of another molecule of $t\text{Bu}_2\text{SnH}_2$ to form bis(hydrostannyl)iron(**IV**) complex, $(\eta^5\text{-C}_5\text{H}_5)\text{M}(\text{CO})_{n-1}(\text{H})(\text{Sn}^t\text{Bu}_2\text{H})_2$, (a well-established reaction involving R_3EH , $\text{E}=\text{Si}$,¹²⁵ Sn ¹²⁶ to form $(\eta^5\text{-C}_5\text{H}_5)\text{M}(\text{CO})_{n-1}(\text{H})(\text{ER}_3)_2$) that results in the formation of the distannane $\text{H}^t\text{Bu}_2\text{Sn-Sn}^t\text{Bu}_2\text{H}$ and $(\eta^5\text{-C}_5\text{H}_5)\text{M}(\text{CO})_{n-1}(\text{H})$.⁸³ Alternatively, recoordination of CO in the sealed system will lead to the formation of $(\eta^5\text{-C}_5\text{H}_5)\text{M}(\text{CO})_n\text{Sn}^t\text{Bu}_2\text{H}$ (**B**) in the same manner as Malisch et al. observed the formation of $(\eta^5\text{-C}_5\text{H}_5)\text{Fe}(\text{CO})_2\text{Si}^t\text{Bu}_2\text{H}$.¹²⁷ This overall process is similar to the catalytic formation of distannanes,⁸³ with the exception there is still an excess of $(\eta^5\text{-C}_5\text{H}_5)\text{M}(\text{CO})_{n-1}\text{Me}$ **1a**, (**2a**) present in the system for further reactions with $(\eta^5\text{-C}_5\text{H}_5)\text{M}(\text{CO})_n\text{Sn}^t\text{Bu}_2\text{H}$ (**III**) and $\text{H}^t\text{Bu}_2\text{Sn-Sn}^t\text{Bu}_2\text{H}$.

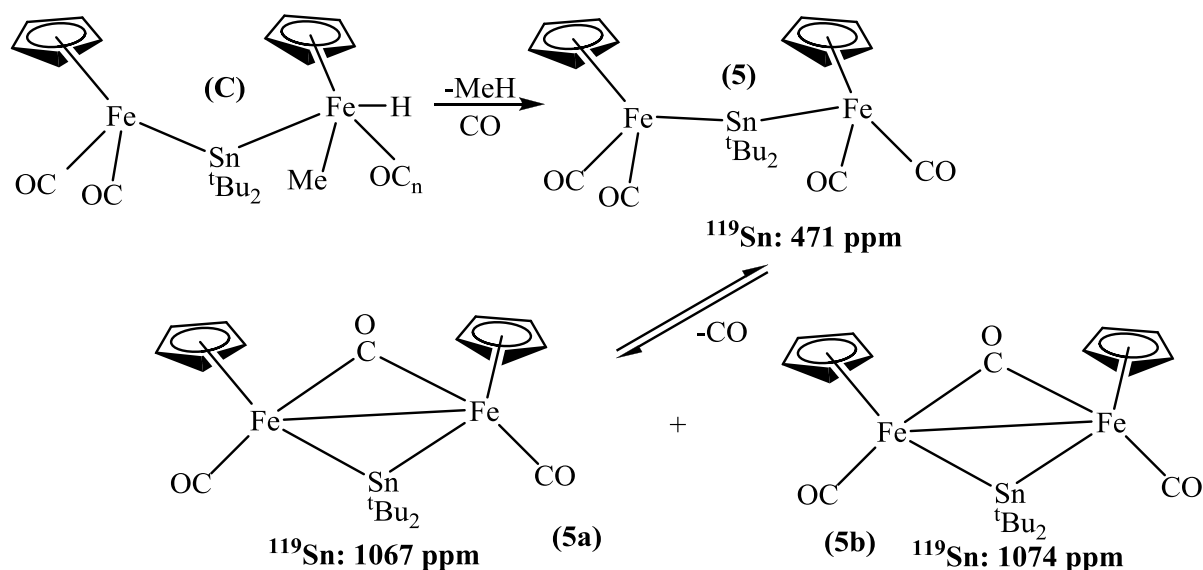
In separate reactions we have reacted both ($\text{M} = \text{Fe}$) and ($\text{M} = \text{Mo}$) $(\eta^5\text{-C}_5\text{H}_5)\text{M}(\text{CO})_n\text{Sn}^t\text{Bu}_2\text{H}$ with an excess of **1a** and **2a** and the progress of these reactions was monitored by ^{119}Sn NMR spectroscopy.¹²⁸ In both cases fast, high yield, reactions resulted in the formation of **S1(S2)** *via* a process suggested in Scheme. 1.6.



Scheme 1.6 : Proposed mechanism to explain Sn-CH₃ bond formation. M = Fe, n = 1, (**1a**) M = Mo, n = 2, L = CO (**2a**)

The key feature in this chemistry is the capacity of complex $(\eta^5-C_5H_5)M(CO)_nSn^tBu_2H$, (**B**) to react with the 16e- species $(\eta^5-C_5H_5)M(CO)_nMe$ (**A**) to produce a tin-bridged dimetal intermediate $(\eta^5-C_5H_5)MMe(H)(CO)_n-(Sn^tBu_2)(CO)_nLM(\eta^5-C_5H_5)$, (**C**). This intermediate can reductively eliminate the $(\eta^5-C_5H_5)M(CO)_nSn^tBu_2Me$ (**D**) resulting in the formation of the metal species $(\eta^5-C_5H_5)M(CO)_nH$ (**E**) which upon recoordination of CO forms $(\eta^5-C_5H_5)M(CO)_nLH$ (which we observe spectroscopically for the iron analogues).^{122a}

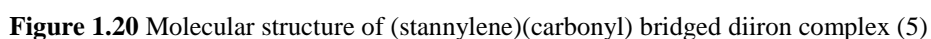
However, intermediate **C** can also eliminate methane to yield a (stannylene)(carbonyl) bridged diiron complex for example, (**5**), a type of product reported by Tobita *et al.* in the case of the reaction of **1a** with R_2SnH_2 (R = Mes, Tip), Scheme. 1.9 with ¹¹⁹Sn NMR resonances for each species.¹³⁵



Scheme 1.9 Proposed mechanism for the formation of bridging compounds of the type M-Sn-M bond

Using ^{119}Sn NMR spectroscopy we have been able to observe initial formation of **(5)** and its subsequent transformation to the *cis*- and *trans*-isomers **5a**, **5b** from our reaction mixture. It is clear that the competition between elimination of CH_4 or $(\eta^5\text{-C}_5\text{H}_5)\text{M}(\text{CO})_n\text{Sn}^t\text{Bu}_2\text{Me}$ is regulated by the combination of the steric and electronic impact of the substituents on tin: the electron-withdrawing mesityl groups drive MeH elimination whereas the strongly electron-donating ^tBu group more readily facilitates elimination of $\text{Me}^t\text{Bu}_2\text{Sn}(\text{CO})_n\text{M}(\eta^5\text{-C}_5\text{H}_5)$.

The molecular structure of **(5)** was determined by X-ray analysis and is depicted in Fig. 1.20. Only three crystal structures have been reported for $[(\eta^5\text{-C}_5\text{H}_5)\text{Fe}(\text{CO})_2]_2\text{SnR}_2$ complexes ($\text{R} = n^1\text{-cyclopentadienyl}$,¹²⁹ Ph ,¹³⁰ Me ¹³¹)¹²⁹⁻¹³¹. The Fe-Sn and Sn-C bond distances in **(5)** 2.6601(4) Å and 2.264(4) Å, respectively, are relatively longer than the bond distances in other $[(\eta^5\text{-C}_5\text{H}_5)\text{Fe}(\text{CO})_2]_2\text{SnR}_2$ complexes and Fe-Sn is the longest such bond reported.¹³²



5b = 1074 ppm
(Trans Isomer)

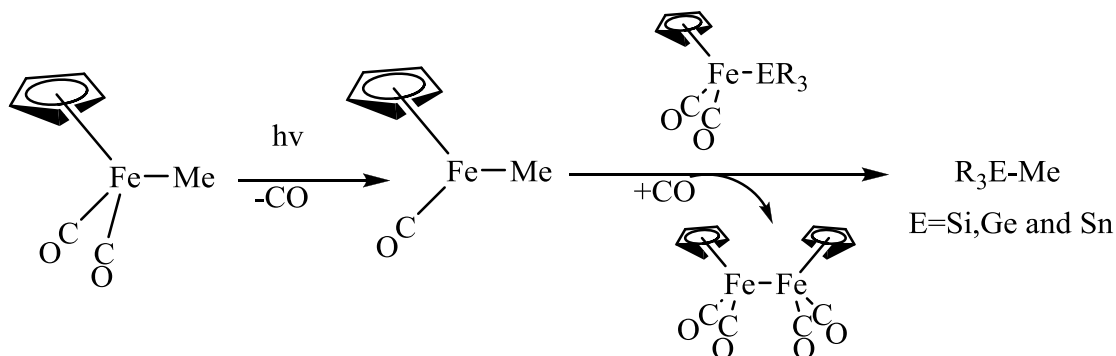
5a = 1067 ppm
(Cis Isomer)

Figure 1.21 ^{119}Sn NMR spectroscopy showing the isomerization of (stannylene)(carbonyl) bridged diiron complex (5) into (cis) 5a and (trans) 5b

An independent experiment involving solution photolysis of (**5**) by itself produced, cleanly and quantitatively, two geometrical isomers of **5a**, **5b**, *cis* and *trans* in 1 : 2 ratio, Fig. 1.21. The preliminary structure of the *trans* isomer **5b** was obtained by X-ray diffraction studies¹³³ in which the basic structural features are reliable and exhibit the *trans* arrangement of two Cp rings coordinated to two iron atoms and a *planar* four-membered ring comprising of Fe₂CSn atoms.

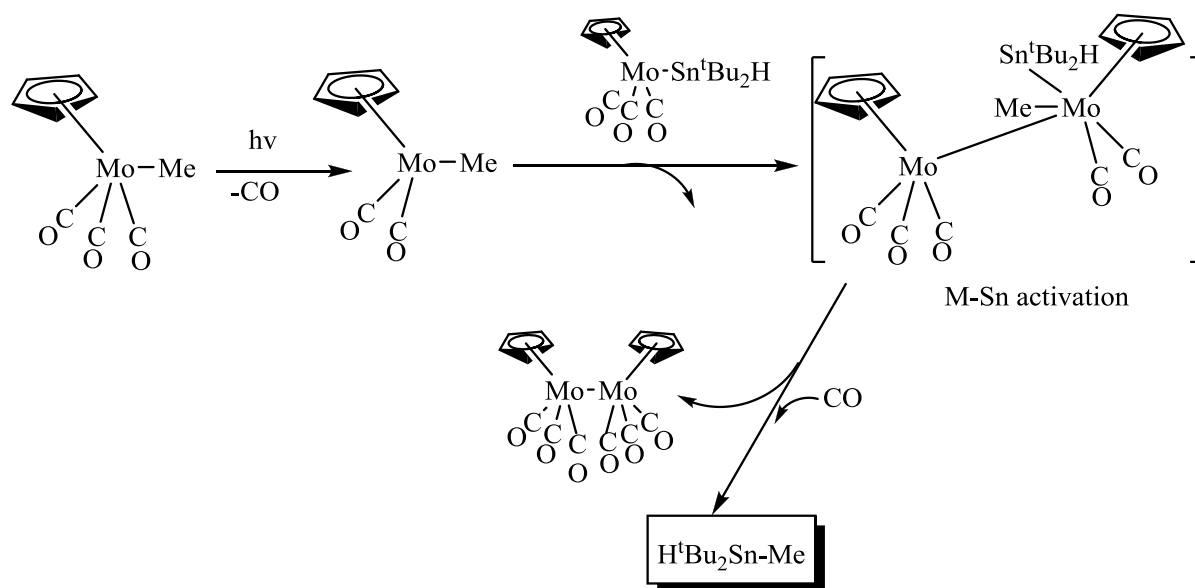
1.7.4 Observations related to the formation of ^tBu₂(H)Sn-Me

Small amounts of this side products have been observed in the process of the chemistry presented above. Interestingly the formation of such species are related to the chemistry associated with M-E bond activations, E = Si, Ge and Sn reported recently by the our own group,¹³⁴ Scheme. 1.10.



Scheme 1.10 Photochemical activation of Fe-E bond in the presence of (η^5 -C₅H₅)Fe(CO)₂Me, E = Si, Ge, Sn

By analogy we can suggest the formation of ^tBu₂(H)Sn-Me through the following proposed mechanism, Scheme 1.11.



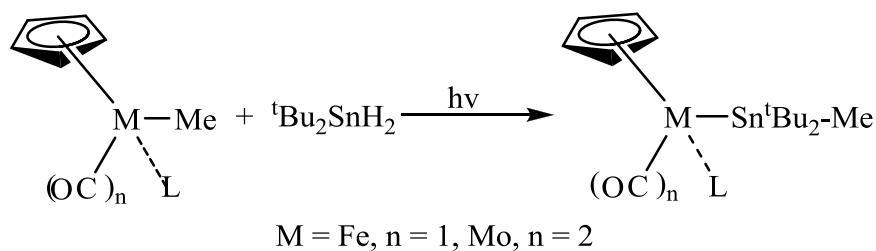
Scheme 1.11 Proposed mechanism for the M-E activation, E = Si, Ge, Sn

The low yields observed in this chemistry perhaps relate to the short reaction times (4 h) ($(\eta^5\text{-C}_5\text{H}_5)\text{Mo(CO)}_3\text{Me} + (\eta^5\text{-C}_5\text{H}_5)\text{M(CO)Sn}^t\text{Bu}_2\text{-H}$ 1:3 Ratio), Fig. 1.16, compared to that reported by Fortier, where only 20% react with longer periods of time >270 h. ($(\eta^5\text{-C}_5\text{H}_5)\text{Fe(CO)}_2\text{Me} + (\eta^5\text{-C}_5\text{H}_5)\text{Fe(CO)}_2\text{SnR}_3$ 1:1 Ratio).¹³⁴

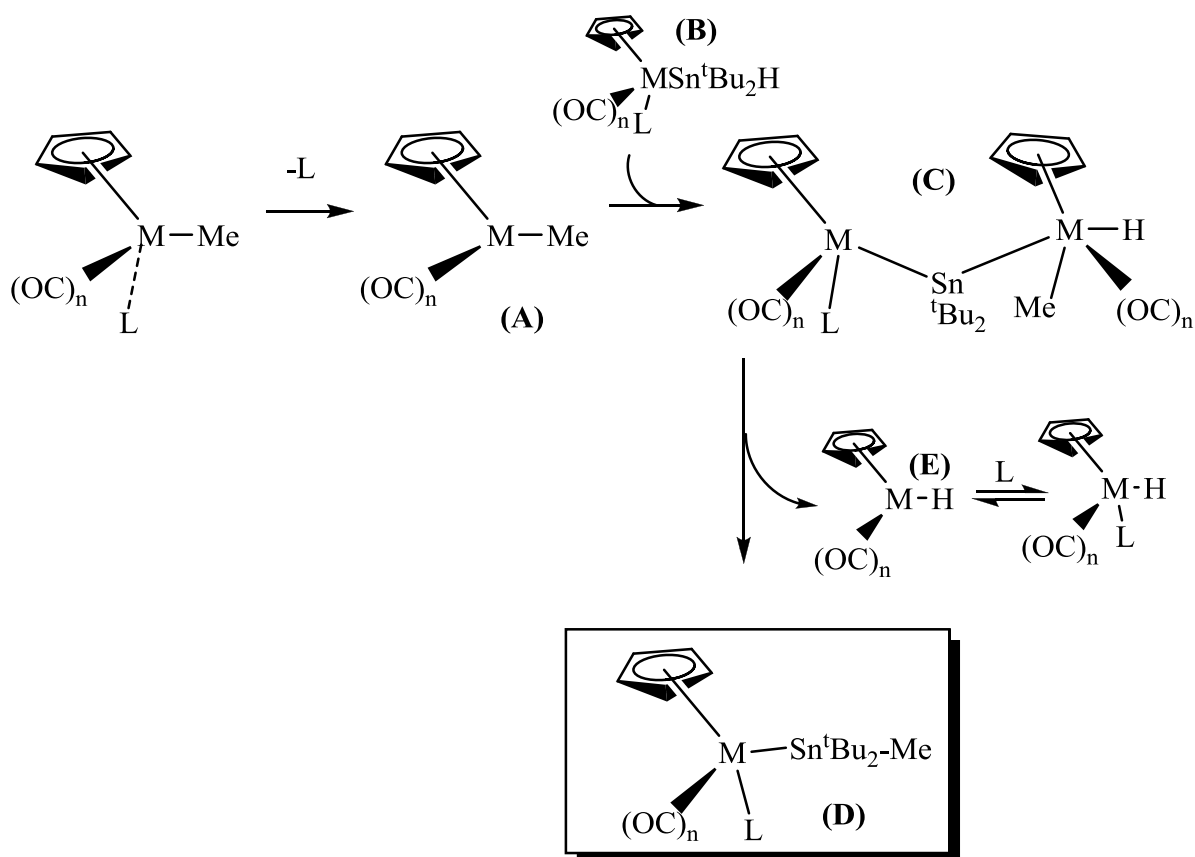
Clearly the activation of the Sn-H bond in $(\eta^5\text{-C}_5\text{H}_5)\text{M(CO)}_n(\text{}^t\text{Bu}_2\text{Sn-H})$ complex is favored over the M-Sn activation working in higher concentration of the of unsaturated metal complex $(\eta^5\text{-C}_5\text{H}_5)\text{Mo(CO)}_2\text{Me}$ (16e-), but at lower concentrations there an interesting competition between Sn-H and M-Sn activation (Fig. 1.16).

1.8 Conclusions

- 1 For the first time we established a new method for the photochemical formation of a Sn-C bond by the direct transfer of a methyl group from a transition metal to a tin center with concomitant formation of a Sn-transition metal bond.



- 2 A 2:1 ratio of $(\eta^5\text{-C}_5\text{H}_5)\text{M}(\text{CO})_n\text{Me}$ and ${}^t\text{Bu}_2\text{SnH}_2$ has been proposed as the optimum to the formation of methyl transfer product, $(\eta^5\text{-C}_5\text{H}_5)\text{M}(\text{CO})_n\text{Sn}^t\text{Bu}_2\text{Me}$.
- 2 The formation of the metal complex $(\eta^5\text{-C}_5\text{H}_5)\text{M}(\text{CO})_n\text{Sn}^t\text{Bu}_2\text{H}$ has been reported as the key intermediate in the proposed mechanism.



Scheme 1.10 : Proposed mechanism to explain the results on Sn-CH₃ bond formation. $\text{M} = \text{Fe}, n = 1$, (1a) $\text{M} = \text{Mo}, n = 2, \text{L} = \text{CO}$ (2a)

1.9 References

- 98) Van der Kerk. G.J.M.; Luijten. J.G.A., *Org. Synth.*, **1956**, 36, 86; (b) Glockling. F.; Lyle. M.A.; Stobart. R.S., *J. Chem. Soc., Dalton Trans.*, **1974**, 2537.
- 99) Bokranz. A.; Plum. H.; *Fortschr. Chem. Forshung*, **1971**, 16, 365; (b) Bokranz.; A.; Plum. H., *Industrial Manufacture and Use of Organotin Compounds*, Schering. A.G., Bergkamen, **1975**.
- 100) Schlenk. W., *Chem. Ber.* **1929**, 62,920; (b) Andersen. R. A.; Wilkinson. G., *Inorg. Synth.* **1979**,19, 262.
- 101) Kocheshkov. K.A.; *Ber. Deutsch. Chem. Gesell.*, **1926**, 62, 996.
- 102) Neumann, W.P., *The organic Chemistry of tin*, Wiley, London, **1970**; (b) Sawyer. A.K.; *Organotin Compounds*, New York, **1971**; (b) Thoonan. S.; Deelman. B.J.; Van Koten. G., *Chem. Comm.*, **2001**, 1840.
- 103) Van der Kerk. G.J.M.; Luijten. J.G.A.; Noltes. J.G., *Angew. Chem.*, **1958**, 70, 298.
- 104) Dang H. S.; Davies. A.G., *J. Chem. Soc., Perkin Trans.*, **1991**, 2, 2011
- 105) Owen. D. W.; Poller. R. C., *J. Organomet. Chem.*, **1983**, 255, 173
- 106) Hawker. D.W.; Wells. P.R., *J. Organomet. Chem.*, **1984**, 113, 1290
- 107) Meyer. N.; Seebach. D., *Chem. Ber.*, **1980**, 113, 1290
- 108) Ricci. A.; Taddei. M.; Seconi. G., *J. Organomet. Chem.*, **1986**, 306, 23
- 109) Rot. N.; Kanter. F.J.J.; Bickelhaupt, W.J.J.; Spek. A.L., *J. Organomet.Chem.*, **2000**, 369, 593-594.
- 110) Pearson. W.H.; Stevens. E.P.; *Synthesis*, **1994**, 904.
- 111) Frankland. E., *J. Chem. Soc.*, **1849**, 2, 263.
- 112) Holland. F.S., *Chem. Abstr.*, **1987**, 106, 21513, BP2169889.
- 113) Omae. I., *Organotin Chemistry*, vol 21, Elsevier, Amsterdam, **1989**

- 114) (a) Kuivila. H.G., *Adv. Organomet. Chem.* **1964**, *1*, 47; (b) Alwyn. D. G., *Organotin Chemistry*, Second Ed. Wiley-VCH Verlag GmbH & Co. KGaA, **2003**, Chap.4.
- 115) Leusink. A.J.; Noltes. J.G., *Tetrahedron Lett.*, **1966**, 335; (b) Neumann. W.P.; Nierman. H., Sommer. R., *Angew. Chem.* , **1961**, *73*, 768.
- 116) Burley. J.W.; Hutton. R.E.; Oakes. V., *J.Organomet. Chem.*, **1978**, *156*, 369; (b) Chopra. A.B.; Murray. A.P., *Main Group Metal Chem.*, **1998**, *21*, 347.
- 117) KiKuKawa. K.; UmeKawa. H.; Wada. F.; Matsuda. T., *Chem Lett.*, **1998**, 881; (b) Miyake. H.; Yamamura. K., *Chem Lett.*, **1989**, 981.
- 118) Lautens. M.; Kumanovic. S.; Meyer. C., *Angew. Chem. Int. Ed. Engl.*, **1996**, *35*, 1329.
- 119) Chadeayne. A.R.; Wolczanski. P.T.; Lobkovsky. E.B., *Inorganic Chemistry*, **2004**, *43*, 3421-3432.
- 120) Wolfgang E., *Zeitschrift fuer Naturforschung, B: Chemical Sciences*, **1990**, *45*, 25-30; (b) Chadeayne, A.R., *Inorganic Chemistry*, **2004**, *43*, 3421-3432.
- 121) Braia, N. et al., *Asian Journal of Chemistry*, **2009**, *21*, 4628-4634.
- 122) (a) $(\eta^5\text{-C}_5\text{H}_5)(\text{CO})_2\text{Fe-H}$ was characterized by ^1H NMR and IR spectroscopy. See: Shackleton. T. A.; Mackie, S. C.; Fergusson. S. B.; Johnson, L. J.; Baird. M. C., *Organometallics*, **1990**, *9*, 2248; (b) Okazaki, M.; Tobita H.; Ogino. H., *J. Chem. Soc., Dalton Trans.*, **1997**, 3531.
- 123) Whereas >80 reports of Mo-Sn bond containing complexes exist, with bond lengths in the range 2.652 to 3.073 Å, only 4 contains the $(\text{C}_5\text{H}_5)\text{Mo}(\text{CO})_3\text{Sn}(\text{C})_3$ system with a bond length range of 2.815 to 2.860 Å: (a) Tang. L.F.; Chai. J.F.; Zhao S.B.; Wang. J.T., *J. Organomet. Chem.*, **2003**, *669*, 57; (b) Tang. L.F.; Chai. J.F.; Zhao. S.B.; Wang. J.T.; Cao. X.Y.; Huaxue Xuebao, **2002**, *60*, 1298; (c) Fischer. P. J.; Krohn K. M.; Mwenda. E. T.; Young V. G., *Organometallics*, **2005**, *24*, 1776; (d) Chen. S.S.; Song. H.B.; Tang. L.F., *J. Organomet. Chem.*, **2007**, *692*, 5763.

- 124) Elimination of CH₄ was observed from the photolysis of 1a and ^tBu₂SnH₂ in C₆D₆ and after 30 minutes of irradiation, a resonance was observed at 0.16 ppm in ¹HNMR spectrum. See: Nakazawa. H.; Itazaki. M.; Kamata K.; Ueda. K., *Chem. Asian. J.*, **2007**, 2, 882.
- 125) (a) Kawano. Y.; Tobita. H.; Ogino. H., *J. Organomet. Chem.*, **1992**, 428, 125; (b) Sato. T.; Tobita. H.; Ogino. H., *Chem. Lett.*, **2001**, 854; (c) Randolph. C. L.; Wrighton. M. S., *J. Am. Chem. Soc.*, **1986**, 108, 3366.
- 126) (a) Akita. M.; Oku. T.; Tanaka. M.; Moro-oka. Y., *Organometallics*, **1991**, 10, 3080; (b) Zhang. S.; Brown. T., *Organometallics*, **1992**, 11, 2122; (c) Sharma. H. K.; Pannell. K. H., *Organometallics*, **2001**, 20, 7; (d) Itazaki. M.; Kamitani. M.; Ueda. K.; Nakazawa. H., *Organometallics*, **2009**, 28, 3601.
- 127) Adam. W.; Azzena. U.; Prechtel. V.; Hindahl. V., Malisch. W., *Chem. Ber.*, **1992**, 125, 1409.
- 128) The photolysis of 1a and (η⁵-C₅H₅)Fe(CO)₂Sn^tBu₂H, in 10 : 1 molar ratio in C₆D₆ in sealed NMR tube produced a mixture of (η⁵-C₅H₅)Fe(CO)₂Sn^tBu₂-Me (40%), (η⁵-C₅H₅)Fe(CO)₂Sn^tBu₂(η⁵-C₅H₅)Mo(CO)₃ (15%), (η⁵-C₅H₅)Mo(CO)₃H (15%) along with of diiron complexes 5a,b (30%).
- 129) Biryukov. B. P.; Struchkov. Y. T., *Zh. Strukt. Khim.*, **1969**, 10, 95.
- 130) Parkanyi. L; Pannell. K. H.; Hernandez. C., *J. Organomet.Chem.*, **1988**, 347, 295.
- 131) Biryukov. B. P.; Struchkov. Y. T., *Zh. Strukt. Khim.*, **1968**, 9, 488.
- 132) The range of Fe–Sn bond distances in 24 acyclic structures of the type (η⁵-C₅H₅)Fe(CO)₂Sn is between 2.453 to 2.620 Å ° , which makes the bond distance as the larger reported

133) The structure of (5) was not refined and only the isotropic refinement was finished because of the high R values. The molecular structure of (5) is depicted below CCDC 742972

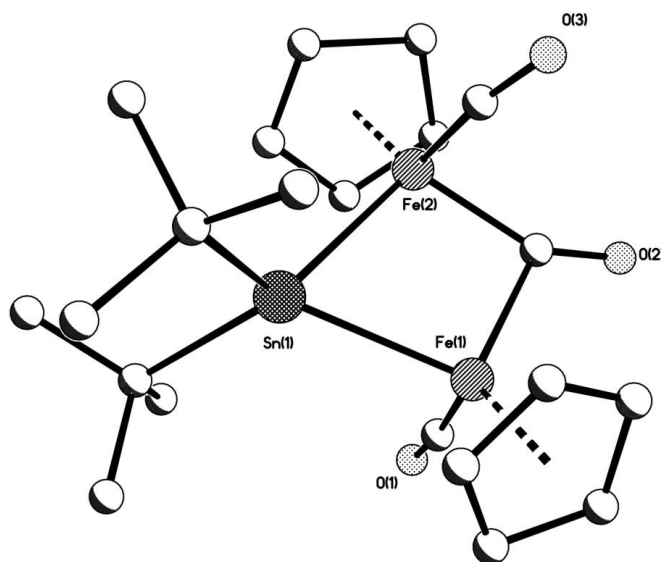


Figure (s): Molecular structure of (stannylene)(carbonyl) bridged diiron complex (5). The structure is not refined satisfactorily. The R parameters are very high.

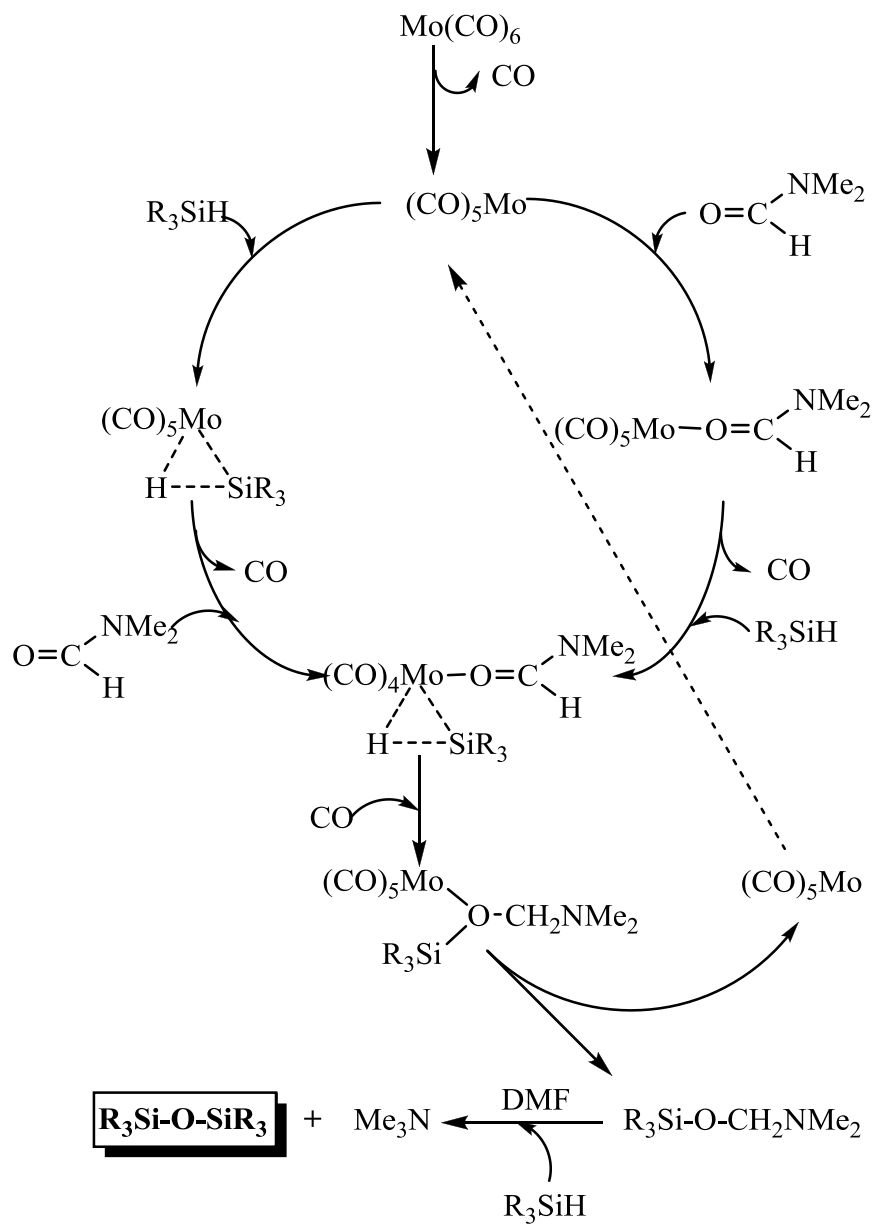
134) Fortier. S., Zhang. Y.; Sharma. H. K.; Pannell. K. H., *Organometallics*, **2010**, 29, 1041.

135) Mohamed. B. A. S.; Kikuchi. M.; Hashimoto. H.; Ueno. K.; Tobita. H.; Ogino. H., *Chem. Lett.*, **2004**, 33, 112.

Metal-catalyzed reduction of HCONR₂, R = Me (DMF); Et (DEF), by silanes to produce R₂NMe and disiloxanes: A mechanism unraveled

Abstract

The reduction of amides by silanes (R₃SiH) to form amines and disiloxanes catalyzed by a variety of transition metal catalysts is a well-established and important process. However, the mechanism of the process is unclear. In this work we demonstrate that using Mo(CO)₆, Mo(CO)₅NMe₃, and (η⁵-C₅H₅)Mn(CO)₃ as catalysts for the reduction of N,N-dimethylformamide (DMF), and N,N-diethylformamide (DEF), we can observe, intercept, and isolate, the important intermediates R₃SiOCH₂NR₂, R = Me, Et, for the first time. In the presence of excess amide such intermediates further react with a variety of silanes to form the disiloxanes while germanes and stannanes also react to form the appropriate R₃SiOER₃ oxides, E = Ge, Sn. We also show that the germanium hydrides, Et₃GeH and Bu₃GeH, can reduce DMF to form trimethylamine and the corresponding digermoxane; Bu₃SnH also reduces DMF, but along with the low yields of Bu₃SnOSnBu₃, significant side products are obtained including (Bu₃Sn)₂ and Bu₄Sn. The proposed mechanism of the process is presented in Scheme. 2.1.



Scheme 2. 1 Proposed mechanism for the reduction of amides to amines in the presence of M(CO)_6 as catalyst, $\text{M} = \text{Mo}, \text{Cr}, \text{and W}$.

Statement of the problem

The general area of investigation involves the study of the chemistry associated with the silane reduction of amides to amines using transition metal catalysts.¹⁻⁹ Even though the process has been widely studied, and hydrosilylation of aldehydes, ketones,¹⁰ and esters;¹¹ is well-reported, the mechanism associated with the amide reductions is not understood. Since there is still a pressing need for better and more general methods based on simple and inexpensive starting materials such as hydrosilanes,¹²⁻¹⁴ mechanistic studies are needed. Several important questions can be addressed to understand this chemistry: Is it true the transition metal activates Si-H bond, and does the metal also activate the amide? Or, maybe the basicity of the amide is enough to activate the Si-H bond? Will other reducing agents such as Ge-H or Sn-H exhibit the same reactivity or not?

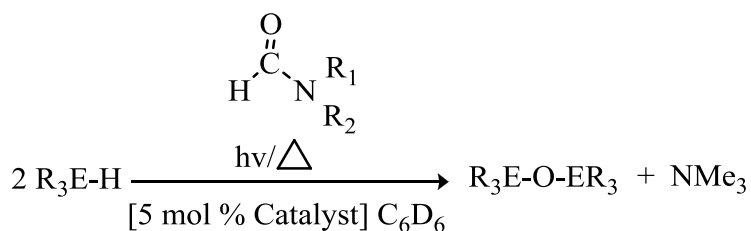
Justification of importance

Amides are among the most stable carboxylic acid derivatives,¹⁵ and it is not a trivial task to perform simple reduction transformations with these molecules, unless harsh conditions of high temperature and pressure, or strong reducing agents are used, e.g. Al-H,¹⁶ B-H.^{16,17} In spite of the utility of these reducing reagents, clear drawbacks associated with air and moisture sensitivity as well as costly purification of the products is not desired. Due to these problems, the development of catalytic reductions of amides is of high current interest.¹⁸ Amines are produced at almost 100,000 tons per year, and constitute an important class of compounds in bulk chemistry, but they are also high-value intermediates in organic synthesis, and used in the manufacture of plastics, surfactants, textiles, dyes, drugs, agrochemicals and in the paper industry.¹⁹ Though there have been important synthetic approaches in the metal catalytic reduction of amides to amines using silanes, R_3SiH ,¹⁻⁸ it is still necessary to find

mild and more environmentally friendly and inexpensive. Furthermore the mechanistic aspects related to this chemistry is still unclear. The development of new catalytic systems will provide not only new mild methodologies but also will allow us to understand the correct pathway to extend the selectivity of the systems.

Research objectives

- ❖ Determine the ability of different metal carbonyl complexes to catalyze the reduction of amides in the presence of tertiary silanes, germanes and stannanes, photochemically or thermally.



[Catalyst] : (η^5 -C₅H₅)M(CO)_nMe, Fe: n = 2, (**1a**), Mo, n = 3 (**2a**);

(η^5 -C₅H₅)M(CO)_{n-1}Ph₃PMe, Fe: n = 2, (**1b**); Mo, n = 3 (**2b**)

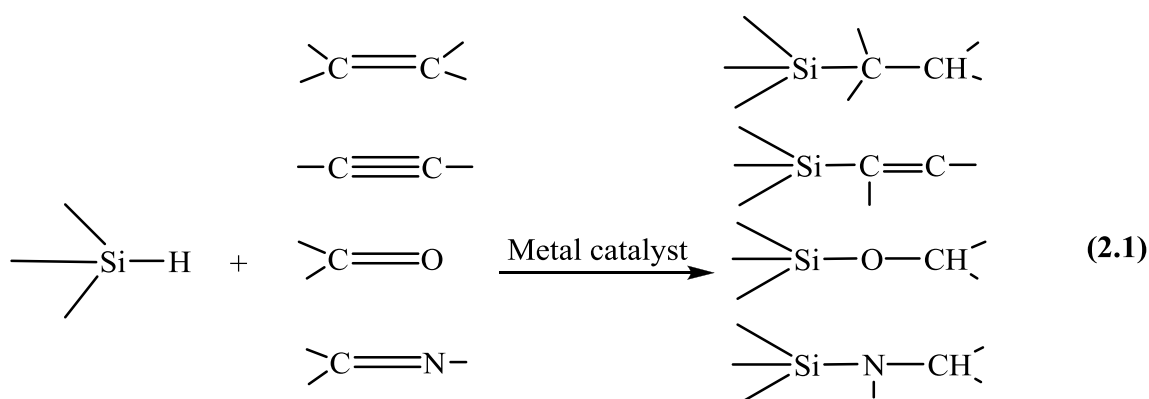
M(CO)₆, M = Mo (**3a**), Cr(**5**), W(**7**) and (η^5 -C₅H₅)Mn(CO)₃ (**6**)

- ❖ To determine the most important synthetic aspects of the mechanism associated with this chemistry.
- ❖ To extend the chemistry to the catalytic reduction of thioformamides.

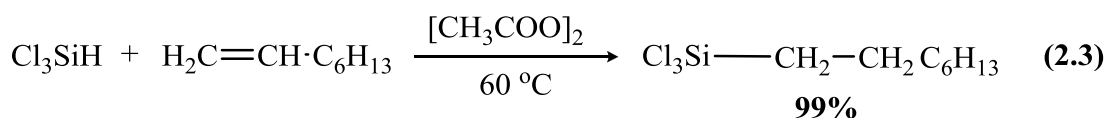
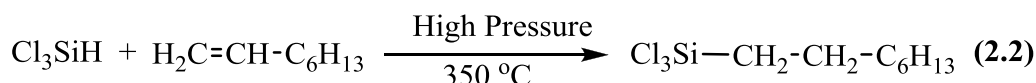
2.1 Introduction

2.1.1 Hydrosilylation

Hydrosilylation is the process of addition of one or more Si-H bonds to a range of unsaturated groups.^{20,21} The most commonly utilized reagents are SiR₃H, (R = halogen, H, OR, alkyl and aryl groups) and the unsaturated substrates are olefins, acetylenes, ketones, etc. eq. 2.1



This addition reaction is important not only as a method of reduction, but also as a major route to complex organosilanes.²¹ The first important approach was derived by Barry in 1947,²² who showed that Cl₃SiH would add to olefin under pressure above 350 °C, eq. 2.2. At the same time Sommer showed that the addition was accelerated by free radical initiators, with improved yields, eq. 2.3, and Burkhard published many examples of free radical additions.^{23,24}

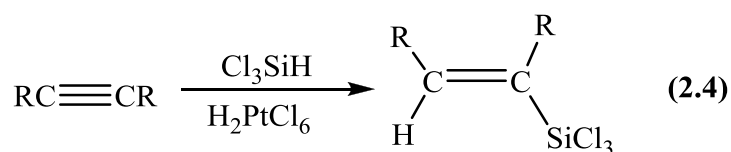


At that time Speier made an exhaustive study of these reactions and found that the

efficiency was highly dependent upon the structures of the reagents, establishing an important trend on reactivity for silanes: $\text{Cl}_3\text{SiH} \sim \text{Br}_3\text{SiH} \sim \text{PhSiH}_3 \gg \text{CH}_3\text{Cl}_2\text{SiH} > \text{O}[\text{SiMe}_2\text{H}]_2 > \text{R}_3\text{SiH}$, ($\text{R} = \text{alkyl}$).²⁵

A related order for the unsaturated substrate was $\text{CH}_2=\text{CHR} \sim \text{hexene} \sim \text{pentene} \gg \text{CH}_2=\text{CHPh}$; and use of initiators such as peroxides (R-O-O-R) and azo compounds (R-N=NR), $\text{R} = \text{alkyls}$; was found to be more useful than photolysis by itself.

However, in 1953 a patent reported by Wagner,²⁶ established the use of Pt on carbon as an efficient catalyst above 130°C for addition of Cl_3SiH to ethylene, acetylene, butadiene, vinyl chloride or vinyl fluoride. Later, in 1957, Speier reported for the first time the use of hexachloroplatinic acid (H_2PtCl_6) as a efficient soluble catalyst for the addition of Si-H bonds to alkenes and alkynes, eq. 2.4.²⁷



This was the starting point for the synthesis of the most effective and elegant method to form organosilicon and related compounds.²⁸ In the chemistry associated with the platinum catalyst, it was reported that terminal alkenes undergo hydrosilylation in preference to internal alkenes and such hydrosilylations proceed in an anti-Markovnikov fashion, where the R_3Si group is connected to the more electronegative bonding partner. On the other hand Lewis²⁹ suggested that the reactions needed a long induction period due to the reduction of the pre-catalyst H_2PtCl_6 to form a catalytically active Pt^0 species. The mechanistic studies suggest a Pt-induced Si-H activation, Fig. 2.1.

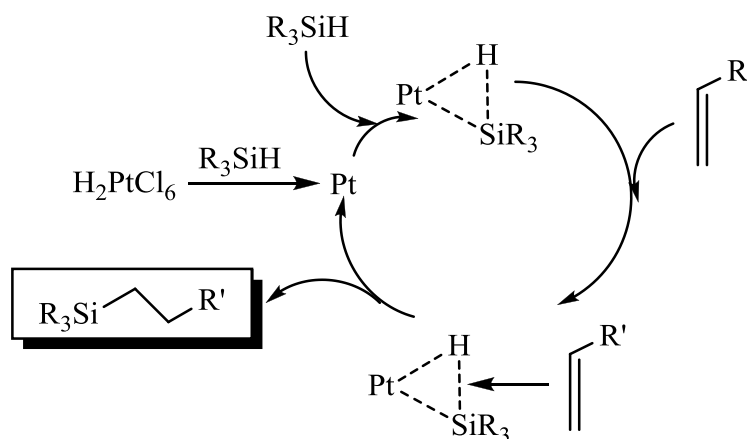


Figure 2. 1 Hydrosilylation of alkenes

2.1.2 Silicon hydrogen bond activation by transition metals

Several complexes of organosilanes, $\text{R}_n\text{SiH}_{4-n}$, with laterally bound $\eta^2\text{-Si-H}$ have been reported by Schubert³⁰ and a more recent example of $\text{L}_n\text{M}-(\eta^2\text{-SiH}_4)$ by Kubas³¹ lends some credibility to our mechanistic proposal. In addition to the Speier catalyst, $(\text{Ph}_3\text{P})_3\text{RhCl}$, $(\text{R}_3\text{P})_2(\text{CO})\text{RhX}$, and other Rh^{I} and Rh^{III} complexes have also been used for hydrosilylation reactions.³² In fact a considerable range of hydrosilylation catalysts are available using a range of metals, Co, Ti, Pt, Pd, Ni, and Fe.³³

Different hydrosilylation mechanisms have been shown to operate, dependent on the nature of the catalyst. For example, late transition metal catalysts typically proceed through a “Chalk-Harrod” pathway, in which the key step involves the activation of Si-H bond through the oxidative addition of the silane to a low-valent metal center, Fig. 2.2.³⁴


$$\begin{array}{c}
 \text{Complete oxidative addition} \\
 \text{LnM} + \text{HSiR}_3 \left[\begin{array}{l} \text{L}_{n-1}\text{M} \begin{array}{l} \text{H} \\ \text{SiR}_3 \end{array} \\ \text{L}_{n-1}\text{M} \begin{array}{c} \text{H} \\ | \\ \text{SiR}_3 \end{array} \end{array} \right. \\
 \text{Incomplete Oxidative addition}
 \end{array}$$

Figure 2. 3 Mechanism for the Si-H bond activation

84

Lichtenberger's group,³⁶ using photoelectron spectroscopy of $(\eta^5\text{-C}_5\text{H}_5)\text{Mn}(\text{CO})_2(\text{H})\text{SiR}_3$, suggested a nearly complete oxidative addition to manganese for $\text{R} = \text{Cl}$ (**A**), and incomplete oxidative addition (**B**) for the phenyl derivatives, indicating a three-center two-electron bonding for less electron-withdrawing R such as phenyl groups, Fig. 2.4.

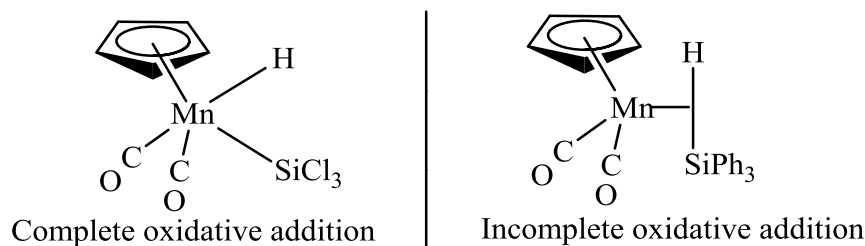
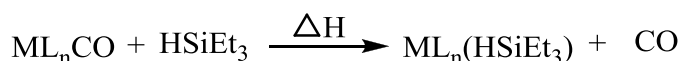


Figure 2. 4 Si-H Bond activation by oxidative addition and three center two electron bonding

Likewise Burkey has determined the activation of SiH bond by group 6 metal carbonyl complexes (Cr, W, Mo).³⁷ By making use of photoacoustic calorimetry, they were able to calculate the enthalpy of CO substitution with HSiEt_3 , outlined in Table 2.1., confirming the studies performed by Lichtenberger.

Table 2. 1 Enthalpies of reaction of metal carbonyls with triethylsilane (ΔH)



Metal complex	$\Delta\text{H} = \text{Kcal/Mol}$
$\text{Cr}(\text{CO})_6$	15.7 +/- 1.1
$\text{Mo}(\text{CO})_6$	18.5 +/- 0.5
$\text{W}(\text{CO})_6$	18.2 +/- 0.5
$(\eta^6\text{-C}_6\text{H}_6)\text{Cr}(\text{CO})_3$	17.1 +/- 2.5
$(\eta^5\text{-C}_5\text{H}_5)\text{Mn}(\text{CO})_3$	30.9 +/- 1.0

Clearly the process of CO substitution is an endothermic process requiring energy to remove the CO and activate the Si-H bond. The most fundamental explanation to these

changes are related to the presence of d-orbitals and the ability of the transition metal to undergo sigma bonding or π back donation to the ligand, Fig. 2.5.

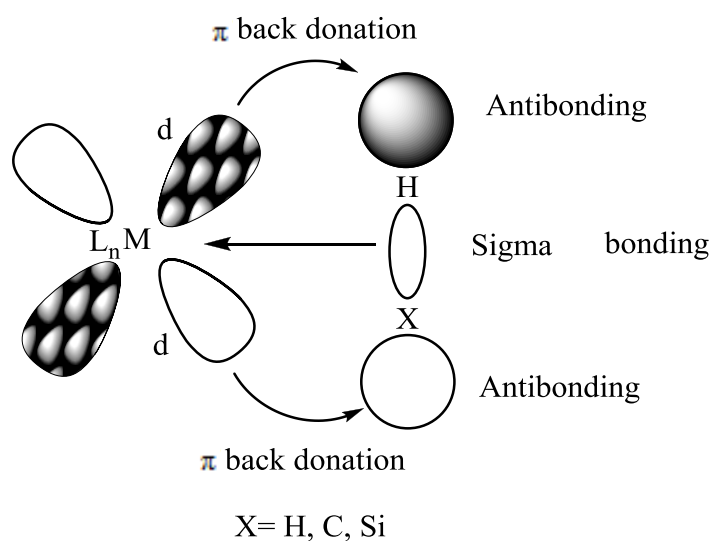
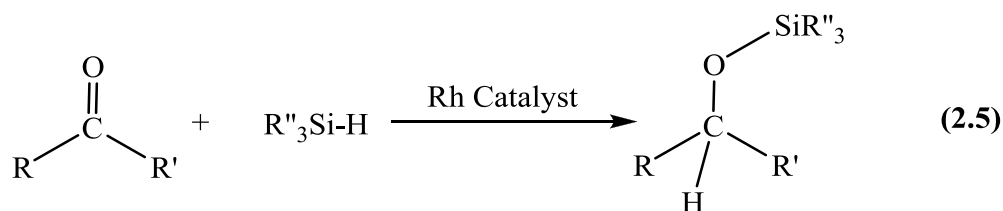


Figure 2. 5 Sigma bond and π backbonding for the Si-H activation

The M-CO bond strengths depend greatly on the ability of the metal to backbond, and the low oxidation states of these complexes favor backbonding.³⁷ For metal-alkane sigma (σ) complexes, backbonding is believed to be of secondary importance and sigma (σ) donation to the metal dominates.³⁷ For silane adducts, both sigma(σ) donation to the metal and backbonding to the silane can be important.³⁷ A recent report by Buzar. S. et al.³⁸ showed strong evidence for the activation of the Si-H bond through a two electron three center bond: $^1\text{H NMR: } \text{W(CO)}_6/\text{Et}_3\text{SiH}/h\nu \text{ } ^1\text{H/Pentane (-8.58 ppm) : } (\text{CO})_5\text{W}(\eta^2\text{-H-SiR}_3).$

2.1.3 Hydrosilylation of carbonyl derivatives by transition metals

Nagai and Ojima discovered that $\text{Rh(PPh}_3)_3\text{Cl}$ (Wilkinson's catalyst) catalyzes the hydrosilylation of ketones, eq. 2.5.,³⁹ and a year later, Kagan et al. reported the first example of an asymmetric version of this reaction.⁴⁰



Few investigations of the mechanism involved have been reported.³⁴ Of note are those differing mechanisms of Chan³⁸ and Ojima,⁴¹ Fig. 2.6. Even though the first step involves the Si-H bond activation as suggested by Burkey, Ojima suggested that the metal ketone complex **(c)** is favored in the second step, followed by the insertion of ketone carbonyl into the Rh-Si bond to form the silyloxyalkyl-rhodium **(d)**. Finally, reductive elimination liberates the silyl ether and recovers the Rh^I species **(a)**.

Contrarily, the Chan mechanism suggests that the ketone interacts with the silicon atom and form complex **(c')**, followed by insertion into the Si-H bond to give the alkoxysilylrhodium species **(d')**. After reductive elimination, the product is obtained and the active species **(a')** is recovered.

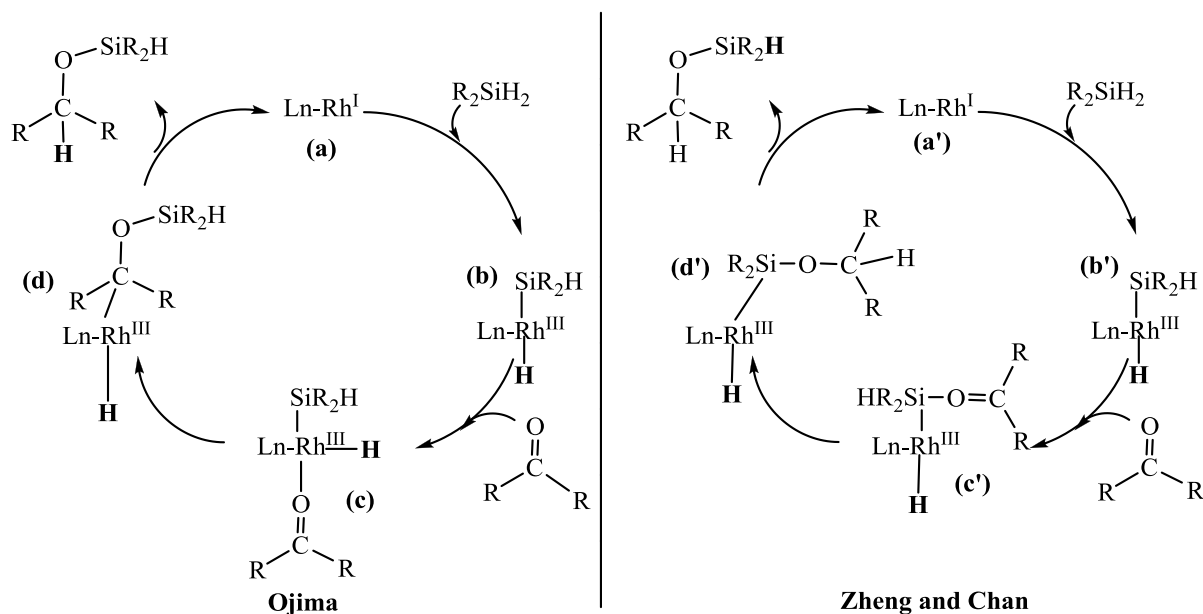


Figure 2. 6 Mechanism of the Rh-catalyzed hydrosilylation of ketones

Evidence concerning ketone-metal interactions have been reviewed by Brookhart and coworkers,⁴² who reported that an iridium acetone complex **(a)**, acts as a precatalyst and exists in rapid equilibrium with the silane complex **(b)**, Fig. 2.7. Further kinetic studies revealed that the ketone complex **(a)** is strongly favored and can be viewed as the resting state,⁴² which disagrees with the previous mechanism of Ojima and Chan, where the Si-H bond is primarily formed in the first step of the reaction.

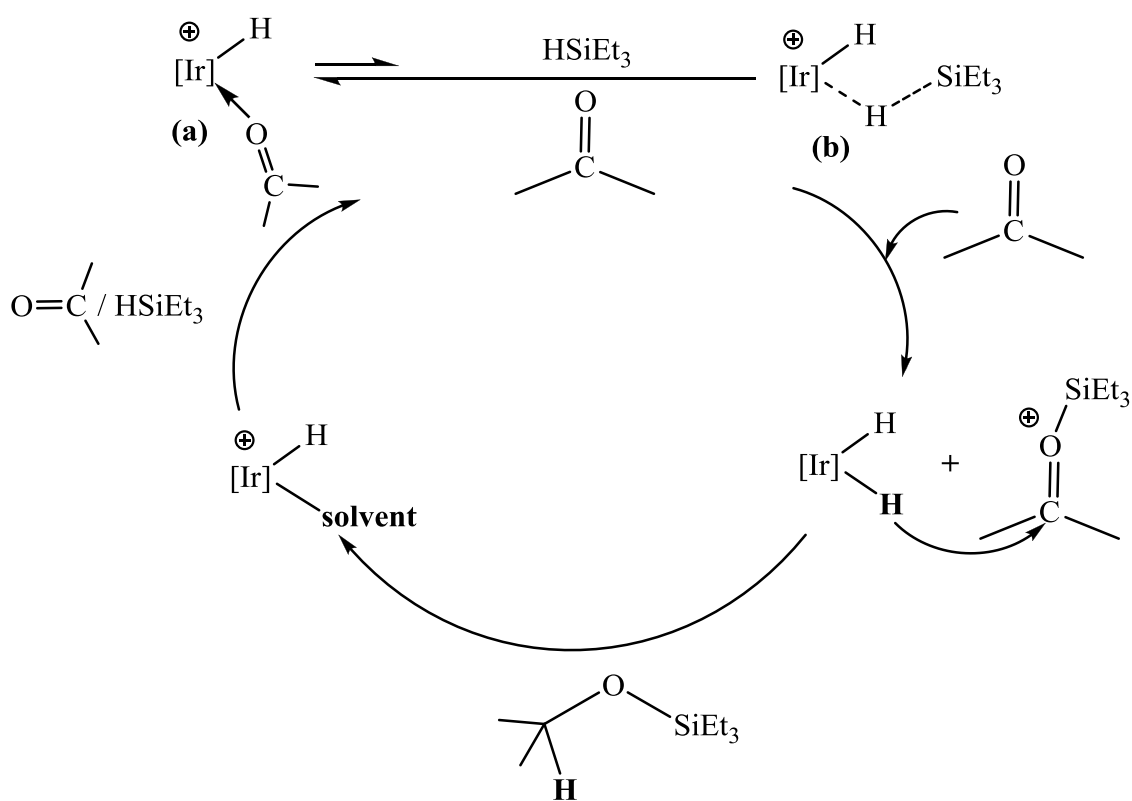


Figure 2. 7 Iridium catalyzed hydrosilylation of ketones

Recently Nikonov,⁴³ has reported the use of PhSiH_3 and $(\text{ArN})\text{Mo}(\text{Cl})-(\text{H})(\text{PMe}_3)_3$ as a catalyst, for the hydrosilylation of benzaldehyde, $\text{PhHC}=\text{O}$, and ethanol, $\text{CH}_3\text{CH}_2\text{OH}$ to form $\text{PhH}_2\text{COSiPhH}_2$ and $\text{CH}_3\text{CH}_2\text{OSiPhH}_2$ in a very good yields, Fig. 2.8.

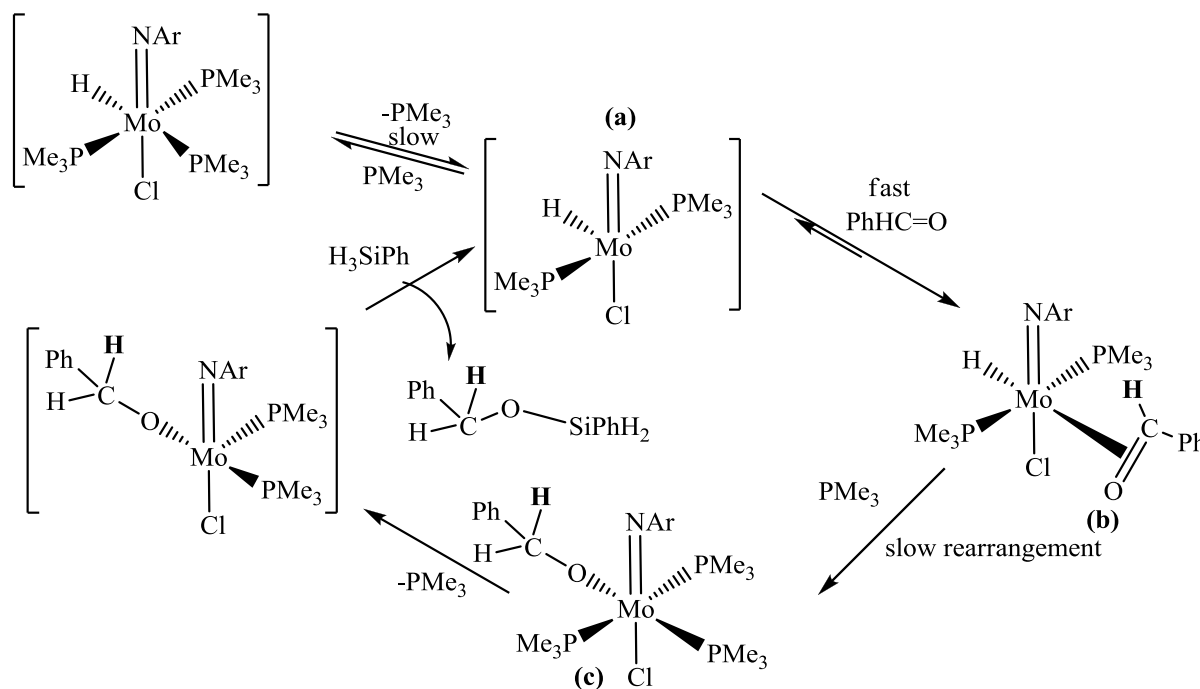


Figure 2. 8 Molybdenum catalyzed hydrosilylation of aldehydes

In this case the hydrosilylation of aldehydes mediated by $(\text{ArN})\text{Mo}(\text{Cl})-(\text{H})(\text{PMe}_3)_3$ is different from the previously established Ojima, Chan, and Chalk-Harrod mechanisms, as we have seen (Fig. 2.2. and Fig. 2.6), but in agreement with the Brookhart studies observed above (Fig. 2.7").⁴²

Consequently the catalyst (a) does not react in the presence of H_3SiPh , on the contrary the catalyst (a) easily reacts with $\text{PhHC}=\text{O}$ affording the benzoxy derivative $(\text{ArN})\text{Mo}(\text{Cl})(\text{OCH}_2\text{Ph})(\text{PMe}_3)_3$ (c) in a very good yields. Complex (b) has been determined as an important intermediate that has been characterized by proton NMR spectroscopy. A fast

reaction of (c) with H_3SiPh regenerates the hydride (a) and closes the cycle. Further calculations have also been reported.⁴⁴

2.1.4 Use of Si-H bonds for M-Si bond formation

Silicon transition-metal chemistry is now a mature area of study and many complexes have been prepared, often due to their applications in industry,⁴⁵ such as hydrosilylation, dehydrogenative silylation, and polysilane production.^{45,47,48} One of the most effective methods for the synthesis of these complexes is the reaction of transition-metal complexes with hydrosilanes via Si-H activation, Fig. 2.9.^{45,46}

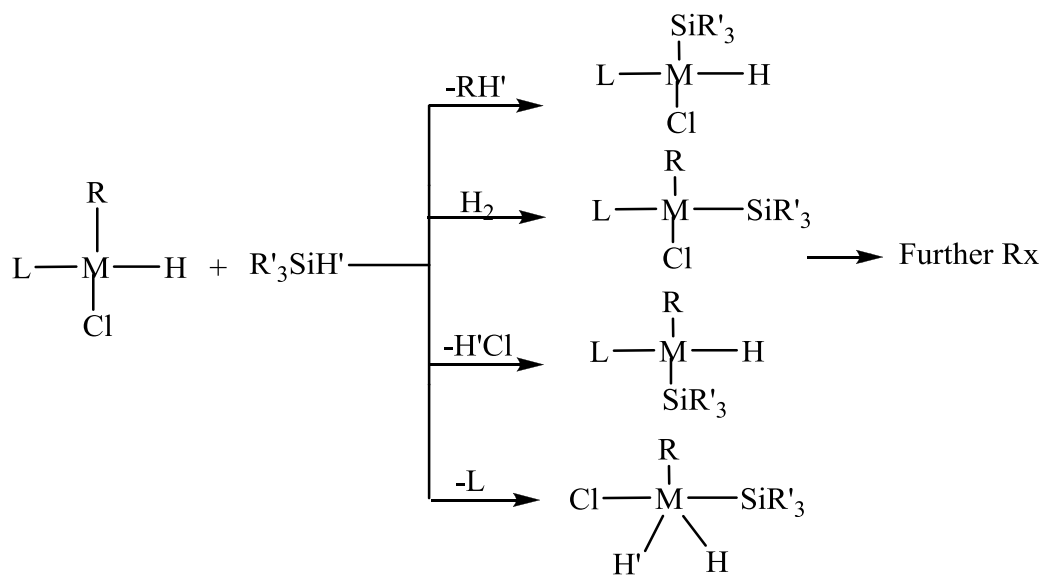
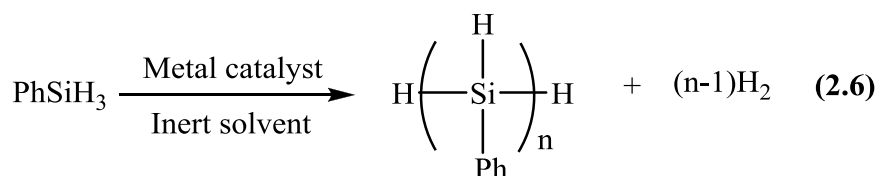
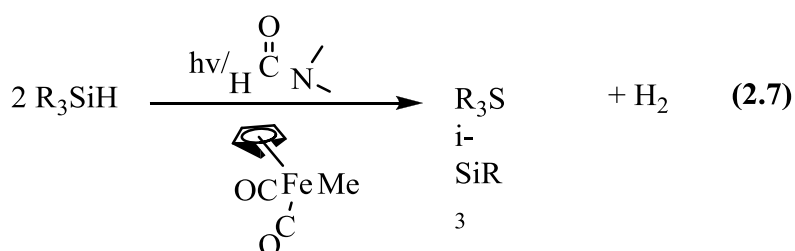


Figure 2. 9 Formation of metal-silicon bonds using SiH compounds

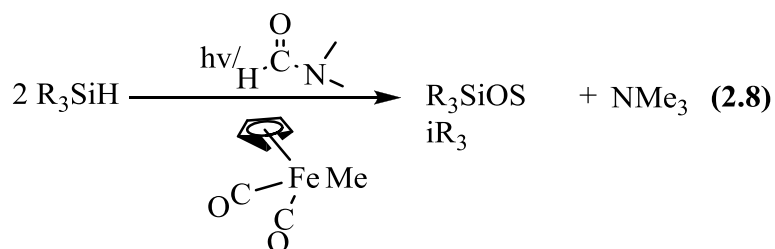
An important example of metal activation of Si-H bonds is the dehydrogenative-coupling formation of polysilanes, eq. 2.6.^{49–53}



Recently Masumi and Nakazawa reported that the photochemical irradiation of R_3SiH in the presence of a catalytic amount of $[(\eta^5\text{-C}_5\text{H}_5)\text{Fe}(\text{CO})_2\text{CH}_3]$ led to the efficient synthesis of the disilanes, $\text{R}_3\text{Si-SiR}_3$; however, the reaction only proceeded in DMF as solvent, eq. 2.7.⁵⁴



This seemed a strange result and upon repetition our group showed that these conditions led to the sole formation of disiloxanes, eq. 2.8.⁵⁵



This important finding was the beginning of this specific area of research. The current study will be concerned primarily with investigating the generality and mechanism of the chemistry. Further extension of the chemistry to other potential metal catalysts, $\text{M}(\text{CO})_6$, $\text{M} = \text{Mo}, \text{Cr}, \text{W}$ and $(\eta^5\text{-C}_5\text{H}_5)\text{Mn}(\text{CO})_3$, will allow us to look for potential intermediates in this catalytic cycle. Important trends associated with the reactivity of the E-H bonds, $\text{E} = \text{Si}, \text{Ge}$ and Sn will be studied as well as extension to thioamides, $\text{HC}(\text{S})\text{NR}_2$.

2.1.5 Synthesis of siloxanes

Symmetrical disiloxanes are an important class of compounds and some are known to have important applications as liquid crystals,⁵⁶ and pharmacologically active compounds, Fig. 2.10.⁵⁷

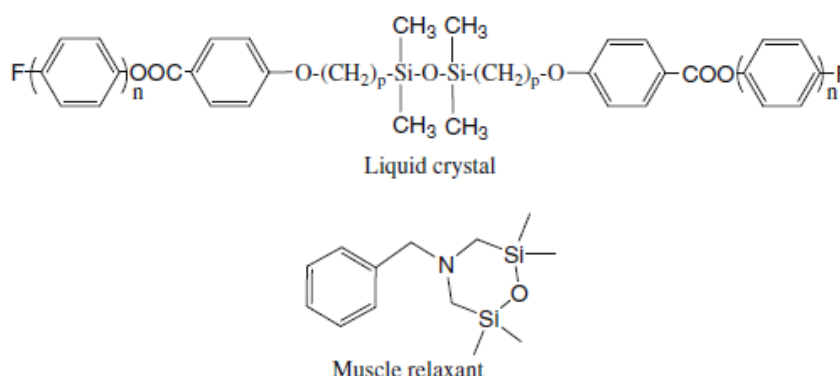
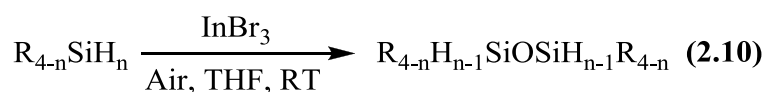
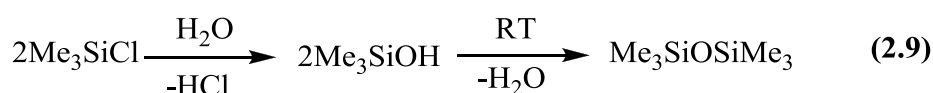
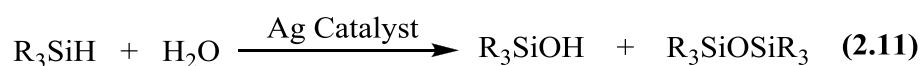


Figure 2. 10 Important symmetrical siloxanes

The general methods available in the literature for the preparation of symmetrical disiloxanes involve intermolecular condensation of silanols, eq. 2.9,⁵⁸ and the recently reported non-aqueous method by Lewis acid-catalyzed air oxidation, eq. 2.10.⁵⁹



Supported silver-nanoparticles have also been used as important catalytic materials for the oxidation of tertiary silanes, giving mostly silanols in very good yields; however, small amounts of siloxanes have also been reported, eq. 2.11.⁶⁰



2.2 Experimental

All manipulations were carried out under Argon atmosphere using Schlenk or vacuum line techniques. THF was distilled under nitrogen from benzophenone ketyl prior to use. Other solvents, hexanes, benzene and toluene were dried over sodium metal and distilled before use. DMF was distilled over BaO. Iron dimer $[(\eta^5\text{-C}_5\text{H}_5)\text{Fe}(\text{CO})_2]_2$, Mo dimer, $[(\eta^5\text{-C}_5\text{H}_5)\text{Mo}(\text{CO})_3]_2$ and $\text{Mo}(\text{CO})_6$ were purchased from Strem Chemicals. Group 14 hydrides, R_3EH were purchased either from Aldrich or Gelest. The metal complexes $(\eta^5\text{-C}_5\text{H}_5)\text{M}(\text{CO})_n\text{CH}_3$ and $(\eta^5\text{-C}_5\text{H}_5)\text{M}(\text{CO})_{n-1}(\text{PPh}_3)\text{-CH}_3$ ($\text{M} = \text{Fe}$, $n = 2$; $\text{M} = \text{Mo}$, $n = 3$) were synthesized by the reported method. NMR spectra were recorded on 300 MHz Bruker spectrometer in C_6D_6 . GC/MS were recorded on Thermo Fisher Scientific GC/mass spectrometer. All column chromatography was performed on small columns (5 x 60 mm) of Silica Gel (Aldrich), 700-230 mesh, 60Å^o Pore Volume 0.75 cm³/g.

2.2.1 Isolation of siloxymethylamines (4a-d) $\text{R}_3\text{SiOCH}_2\text{NMe}_2$ from the catalytic cycle:

In a typical experiment, a Pyrex NMR tube was charged with 1 mmol of R_3SiH ($\text{R}_3 = \text{PhMe}_2$, Ph_2Me , Ph_3), 2 mmol of DMF, 5 mol % of $\text{Mo}(\text{CO})_6$ and 0.5 mL of C_6D_6 . The tube was sealed under vacuum and heated at 90 °C in an oil bath under which conditions the catalyst completely dissolved. The reaction was monitored by ^{29}Si and ^{13}C NMR spectroscopy and after 2-5 h of heating, the concentration of siloxymethylamines reached a maximum with only a trace of the disiloxane present. The reaction was stopped at this stage and the NMR tube was opened and the solution was filtered through an acrodisc filter to remove the catalyst that had precipitated upon cooling. The volatiles and DMF were removed by flash distillation (into liquid nitrogen cooled receptacles) at ambient temperature (0.5mm of Hg) to leave the siloxymethylamines as colorless liquids which were further purified by distillation under vacuum.

Et₃SiOCH₂NMe₂: b.pt. 70-72 °C at 20mm of Hg. Yield: 90%. ¹H NMR: δ 0.55 (q, 6 H, CH₂), 0.97 (t, 9H, CH₃), 2.31, (s, 6 H, Me-N), 4.28 (s, 2 H, CH₂). ¹³C NMR: δ 5.03, 7.15 (Et), 41.1 ((CH₃)₂N), 82.3 (CH₂). ²⁹Si NMR: δ 15.3; HRMS(ESI): Calcd. for C₉H₂₂SiNO: (M⁺-1): 188.1470, Found 188.1445. Anal. Calcd. for C₁₁H₁₉NOSi: C, 63.11; H, 9.15. Found: C, 63.6; H, 9.42.

PhMe₂SiOCH₂NMe₂: b.pt. 60-62 °C at 0.07 mm of Hg. Yield: 30%. ¹H NMR: δ 0.7 (s, 6 H, Me), 2.6, (s, 6 H, Me-N), 4.6 (s, 2 H, CH₂), 7.6, 7.9 (m, 5H, Ph). ¹³C NMR: δ -1.4 (SiMe), 41.1 ((CH₃)₂N), 82.4 (CH₂), 128.1, 129.7, 133.7, 138.5 (Ph). ²⁹Si NMR: δ 5.4; HRMS(ESI): Calcd. for C₁₁H₂₀NOSi: (M⁺+1): 210.1314, Found 210.1314. Anal. Calcd. for C₁₁H₁₉NOSi: C, 63.11; H, 9.15. Found: C, 63.6; H, 9.42.

Ph₂MeSiOCH₂NMe₂: b.pt. 110-112 °C at 0.07 mm of Hg. Yield: 20%. ¹H NMR δ 0.5 (s, 3 H, MeSi), 2.2 (s, 6 H, Me-N), 4.3 (s, 2 H, CH₂), 7.1, 7.5 (m, 10 H, Ph). ¹³C NMR: δ -3.0 (SiMe), 40.8 (N(CH₃)₂), 82.5 (CH₂), 128.1, 129.9, 134.6, 136.9 (Ph). ²⁹Si NMR δ -5.1; HRMS(ESI): Calcd. for C₁₆H₂₂NOSi: (M⁺+1): 272.1470, Found 272.1417.

Ph₃SiOCH₂NMe₂: Yield: 10%. ¹H NMR: δ 2.28 (s, 6H, Me-N), 4.38 (s, 2 H, CH₂), 7.41, 7.46, 7.65 (m, 15 H, Ph). ¹³C NMR: δ 40.87 (N(CH₃)₂), 81.8 (CH₂), 128.0, 130.2, 135.5, 135.6(Ph). ²⁹Si NMR: δ -14.8; HRMS(ESI): Calcd. for C₂₁H₂₄NOSi: 334.1627:(M⁺+1): Found: 334.1479.

2.2.2 Isolation of siloxyethylamine, PhMe₂SiOCH₂NEt₂ using DEF from the catalytic cycle:

In a typical experiment, a Pyrex NMR tube was charged with 1 mmol of R₃SiH (R₃= PhMe₂) and 1.5 mmol of DEF and 5 mol % of (η⁵-C₅H₅)Mn(CO)₃ in 0.5 mL of C₆D₆ and was sealed under vacuum. Sealed tube was irradiated 4 cm from a 400 W medium-pressure

mercury lamp and the reaction was monitored by ^{29}Si and ^{13}C NMR spectroscopy. After 16 h of irradiation, the concentration of siloxymethylamine was reached to maximum and only small traces of siloxane was observed. The reaction was stopped at this stage and NMR tube was opened and the solvents were removed under reduced pressure and $\text{PhMe}_2\text{SiOCH}_2\text{NEt}_2$ was obtained in 95% yield.

$\text{PhMe}_2\text{SiOCH}_2\text{NEt}_2$: Yield: 95%. ^1H NMR : δ 0.39(s, 6 H, (Me)), 1.10(t, 6 H, (Me) CH_2N), 2.74(q, 4 H, $(\text{CH}_2)\text{NMe}$), 4.55(s, 2 H, $(\text{CH}_2)\text{NEt}_2$); 7.31, 7.66(m, 5 H, Ph). ^{13}C NMR : δ -1.64 (Me), 13.30, 44.80 $(\text{Et})_2\text{N}$, 76.56 $(\text{CH}_2)\text{N}$. ^{29}Si NMR : δ . 3.64. HRMS(ESI): Calcd. for $\text{C}_{13}\text{H}_{23}\text{NOSi}$: (M^+): 237.1540, Found 237.1463.

2.2.3 The reaction of $\text{PhMe}_2\text{SiOCH}_2\text{NMe}_2$ with PhMe_2SiH using $\text{Mo}(\text{CO})_6$ as a catalyst:

In a typical experiment, a Pyrex NMR tube was charged with 1 mmol of R_3EH ($\text{E} = \text{Si}$, $\text{R}_3 = \text{PhMe}_2$), 1.5 mmol of $\text{PhMe}_2\text{SiOCH}_2\text{NMe}_2$, 5 mol % of $\text{Mo}(\text{CO})_6$ and 0.5 mL of C_6D_6 . The tube was sealed under vacuum and heated at 90 °C in an oil bath. The reaction was monitored by ^{29}Si and ^{13}C NMR spectroscopy and shown to be complete in 1 day to yield $(\text{PhMe}_2\text{Si})_2\text{O}$ and NMe_3 (^{13}C 47 ppm) and $\text{Mo}(\text{CO})_5\text{NMe}_3$ (^{13}C 58 ppm). The disiloxane, $(\text{PhMe}_2\text{Si})_2\text{O}$ was purified by column chromatography eluting with hexanes and was isolated in 80% yield.

2.2.4 Synthesis of symmetrical disiloxanes: Reaction of siloxymethylamines $\text{R}_3\text{SiOCH}_2\text{NR}'_2$ and R_3SiH in the presence of either $\text{Mo}(\text{CO})_6$, or $(\eta^5\text{-C}_5\text{H}_5)\text{Mn}(\text{CO})_3$ or $(\eta^5\text{-C}_5\text{H}_5)\text{Mo}(\text{CO})_3\text{Me}$ as a catalyst:

In a typical experiment, a Pyrex NMR tube was charged with 1 mmol of R_3SiH ($\text{R}_3 = \text{Et}_3$, PhMe_2), 1.5 mmol of $\text{R}_3\text{SiOCH}_2\text{NR}'_2$ ($\text{R}'_2 = \text{Me}$, Et) and 5 mol % of catalyst in 0.5 mL of C_6D_6 and sealed under vacuum. Sealed NMR tube was either heated at 90 °C in an oil bath or photo chemically irradiated with a medium pressure mercury lamp. The reaction was monitored by ^{29}Si and ^{13}C NMR spectroscopy. The reaction

was stopped (Table.2.2) when all the $R_3SiOCH_2NR'_2$ was consumed to yield symmetrical siloxanes, $(R_3Si)_2O$ and R'_3N .

Table 2. 2 Synthesis of $R_3SiOSiR_3$ in the presence of $R_3SiOCH_2NR'_2$ and R_3SiH using $(\eta^5-C_5H_5)Mn(CO)_3$, $(\eta^5-C_5H_5)Mo(CO)_3$, $Mo(CO)_6$ as catalyst.

R_3	R'_2	Cat	$h\nu/\Delta$	Time	Yield (NMR) ^b
Et ₃	Me ₂	2a	h ν	12 h	(100)
Et ₃	Me ₂	2a	Δ	12 h	(100)
Et ₃	Me ₂	3a	Δ	2d	TR
Et ₃	Me ₂	3a	Δ	2d	(80) ^c
Et ₃	Me ₂	3a	h ν	4d	(20)
PhMe ₂	Et ₂	4a	Δ	5 h	(100) ^c

^bYields based upon ¹H NMR; ^c reaction performed at 120 °C.

$(\eta^5-C_5H_5)Mo(CO)_3Me$ (**2a**); $Mo(CO)_6$ (**3a**); $(\eta^5-C_5H_5)Mn(CO)_3$ (**4a**).

2.2.5 Synthesis of digermoxanes using $Mo(CO)_6$ as a catalyst: In a typical experiment a Pyrex NMR tube was charged with 1 mmol of R_3GeH ($R = Et, Bu, Ph$), 3 mmol of DMF, 5 mol % of $Mo(CO)_6$ and 0.5 mL of C_6D_6 . The tube was sealed under vacuum and heated at 90 °C in an oil bath. The reaction was monitored by ¹H and ¹³C NMR spectroscopy. The reaction was complete in 3-7 days to yield the corresponding digermoxanes. No germoxymethylamines, $R_3GeOCH_2NMe_2$ were observed in the reaction. The ¹³C NMR spectra of the reaction mixture showed a small resonance at 58 ppm which is assigned to the $Mo(CO)_5NMe_3$ complex. The digermoxanes were purified by column chromatography eluting with hexanes.

2.2.6 Synthesis of digermoxanes using $(\eta^5-C_5H_5)Mo(CO)_2(PPh_3)Me$, **2b, as a catalyst:** In a typical experiment, a Pyrex NMR tube was charged with 1 mmol of R_3GeH ($R = Et, Bu$), 3 mmol of DMF, 5 mol % of $(\eta^5-C_5H_5)Mo(CO)_2Ph_3PMe$ and 0.5 mL of C_6D_6 . The tube was sealed under vacuum and heated at 90 °C in an oil bath. The reaction was monitored by ¹H

and ^{13}C NMR spectroscopy. The reaction was 90% complete in 5-8 days to yield digermoxanes which were purified by column chromatography eluting with hexanes. The yields of digermoxanes were relatively lower than $\text{Mo}(\text{CO})_6$ catalytic reaction.

2.2.7 Synthesis of unsymmetrical disiloxanes, and mixed siloxy-germanes, siloxy-stannanes using $(\eta^5\text{-C}_5\text{H}_5)\text{Mo}(\text{CO})_3\text{Me}$ as a catalyst: In a typical experiment, a Pyrex NMR tube was charged with 1 mmol of R_3EH ($\text{E} = \text{Si}$, $\text{R}_3 = \text{Ph}$, Ph_2Me , PhMe_2 ; $\text{E} = \text{Ge}$, $\text{R}_3 = \text{Ph}$, Et ; $\text{E} = \text{Sn}$, $\text{R}_3 = \text{Bu}$), 1.2 mmol of $\text{Me}_3\text{SiOCH}_2\text{NMe}_2$, 5 mol % of $(\eta^5\text{-C}_5\text{H}_5)\text{Mo}(\text{CO})_3\text{Me}$ and 0.5 mL of C_6D_6 and sealed under vacuum. The tube was irradiated with a 450 W medium pressure mercury lamp. The progress of the reactions were monitored by ^{13}C , ^{29}Si or ^{119}Sn NMR spectroscopy. After 2-18 h of irradiation, the siloxyproducts were maximized and the reaction was stopped. The volatiles were removed by flash distillation, ambient temperature 0.5 mm Hg, and the disiloxanes, siloxygermanes or siloxystannanes were purified by column chromatography eluting with hexanes and isolated in 60-83 % yield.

2.2.8 Reactions of $\text{Me}_3\text{SiOCH}_2\text{NMe}_2$ with R_3ECl to form unsymmetrical disiloxanes, and mixed siloxy-germanes, siloxy-stannanes: In a typical experiment, a Pyrex NMR tube was charged with 1 mmol of R_3ECl ($\text{E} = \text{Si}$, $\text{R}_3 = \text{Ph}$, Ph_2Me , PhMe_2 ; $\text{E} = \text{Ge}$, $\text{R}_3 = \text{Ph}$, Me ; $\text{E} = \text{Sn}$, $\text{R}_3 = \text{Bu}$, Ph), 1.2 mmol of $\text{Me}_3\text{SiOCH}_2\text{NMe}_2$ and 0.5 mL of C_6D_6 and the tube was sealed under vacuum. The tube was heated from 20 to 80 $^\circ\text{C}$ depending upon the R_3ECl in an oil bath. The progress of the reaction was monitored by ^{13}C , ^{29}Si or ^{119}Sn NMR spectroscopy. After 1-12 h of heating, the reaction was stopped and the volatiles were removed by flash distillation and the disiloxanes, siloxygermanes, siloxystannanes were purified by column chromatography eluting with hexanes and were isolated in 58-90 % yield.

$\text{Ph}_3\text{SiOSiMe}_3$: Yield: 83%. ^1H NMR: δ 0.20 (s, 9 H, Me), 7.26, 7.44, 7.82 (m, 15 H, Ph). ^{13}C

NMR: δ 2.08 Me, 128.1, 130.1, 135.4, 136.6 Ph. ^{29}Si NMR δ -20.2 Si(Ph), 11.1 Si(Me).
GC/Mass: m/z : 348 (M^+ , 10%); 333(M^+ -Me, 54%); 255(M^+ -1-PhMe, 100%); 193(M^+ -1-Ph₂, 45%) 179(M^+ -Ph₂Me, 45%).

Ph₂MeSiOSiMe₃: Yield: 60%. ^1H NMR : δ 0.2 (s, 9 H, Me), 0.7 (s, 3H, Me), 7.2, 7.3, 7.8 (m, 12 H, Ph). ^{13}C NMR : δ -0.3 Me, 2.0 Me, 128.1, 129.9, 134.4, 138.4 Ph). ^{29}Si NMR : δ -11.2 Si(Ph), 10.2 Si(Me); GC/Mass: m/z : 286(M^+ , 1%); 271(M^+ -Me, 63%); 193 (M^+ -1-PhMe, 100%); 179(M^+ -PhMe₂, 1%).

PhMe₂SiOSiMe₃: Yield: 70%. ^1H NMR : δ 0.2 (s, 9 H, Me), 0.4 (s, 6 H, Me), 7.2, 7.3, 7.6 (m, 5 H, Ph). ^{13}C NMR : δ 0.9 Me, 2.0 Me, 128.0, 129.6, 133.3, 140.1 (Ph). ^{29}Si NMR : δ -1.6 Si(Ph), 9.2 Si(Me). GC/Mass: m/z : 224 (M^+ , 1%); 209 (M^+ -Me, 100%); 193(M^+ -1-Me₂, 50%), 179 (M^+ -Me₃, 4%); 135(PhMe₂Si⁺, 4%); 107(M^+ -SiOSiMe₃, 2%).

Ph₃GeOSiMe₃: Yield: 91%. ^1H NMR : δ 0.3 (s, 9 H, Me), 7.2, 7.3, 7.8 (m, 15 H, Ph). ^{13}C NMR : δ 2.9 (Me), 128.6, 130.1, 134.5, 137.1 Ge(Ph). ^{29}Si NMR : δ 8.3 . GC/Mass: m/z : 394 (M^+); 379.0(M^+ -Me, 100%); 318(M^+ +1-Ph, 33%); 301(M^+ -1-PhMe, 75%); 241(M^+ +1-Ph₂, 7%).

Et₃GeOSiMe₃: Yield: %. ^1H NMR : δ 0.1 (s, 9H, (Me)₃Si), 0.7 (q, 6H, CH₂), 0.9 (t, 9 H, (Me)Ge). ^{13}C NMR : δ 2.9 (Me)₃Si, 7.9, 8.6 (Et)₃Ge. ^{29}Si NMR : δ 6.8.

Me₃GeOSiMe₃: Yield: 50%. ^1H NMR : δ 0.2 (s, 9 H, Si(Me)₃), 0.3 (s, 9 H, Me). ^{13}C NMR : δ 2.8 Si(Me), 2.9 Ge(Me). ^{29}Si NMR : δ 7.9. GC/Mass: m/z : 207 (M^+ -1, 4%); 193(M^+ -Me, 25%), 119 (Me₃Ge⁺, 100%); 89(MeGe⁺, 20%); 74(Ge⁺ 1%).

PhMe₂GeOSiMe₃: Yield: 90%. ^1H NMR : δ 0.2 (s, 9 H, SiMe), 0.6 (s, 6 H, GeMe), 7.2, 7.3, 7.7 (m, 5H, Ph). ^{13}C NMR : δ 1.1 SiMe 2.88 GeMe, 128.4, 129.6, 132.8, 141.5 (Ph). ^{29}Si

NMR : δ 5.9. GC/Mass: m/z : 272($M^+ + 2$, 5%); 255($M^+ - \text{Me}$, 100%); 239($M^+ - 1 - \text{Me}_2$, 30%); 181(PhMe_2Ge^+ , 66%); 151(PhGe^+ , 8%); 73(SiMe_3^+ , 1,3%).

Bu₃SnOSiMe₃: Yield: 80%. ¹H NMR: δ 0.3 (s, 9 H, Me), 0.9, 1.1, 1.4, 1.7 (m, 27H, ⁿBu). ¹³C NMR: δ 3.7 Me, 13.8, 16.2, 27.4, 28.2 Bu. ²⁹Si NMR: δ 5.6, (²J^{119/117}Sn-O-²⁹Si = 37.0 Hz). ¹¹⁹Sn NMR 76.44. HRMS(ESI): Calcd. for C₁₅H₃₆OSiSn: 381.1635 ($M^+ + 1$), Found: 381.1550.

Ph₃SnOSiMe₃: Yield: 84%. ¹H NMR : δ 0.30 (s, 9 H, Me), 7.24, 7.25, 7.75 (m, 15H, Ph). ¹³C NMR: δ 3.62 Si(CH₃)₃, 129.15, 130.19, 136.65, 139.32 Sn(Ph)₃. ²⁹Si NMR: δ 11.04, (²J^{119/117}Sn-O-²⁹Si = 32 Hz). ¹¹⁹Sn NMR : -107.5. HRMS(ESI): Calcd. for C₂₁H₂₅OSiSn: 441.06996 ($M^+ + 1$), Found: 441.2524.

Bu₃GeOGeBu₃: Yield: 70%. ¹H NMR : δ 0.8, 0.9, 1.3, 1.5 (m, 54H, ⁿBu). ¹³C NMR : δ 14.1, 18.2, 26.8, 27.0, Ge(ⁿBu). GC/Mass: m/z : 506(M^+ , 1%); 447($M^+ - 2 - \text{Bu}$, 15%); 391 ($M^+ - 1 - 2\text{Bu}$, 83%); 335.0($M^+ - 3\text{Bu}$, 100%); 277($M^+ - 1 - 4\text{Bu}$, 42%); 221($M^+ - 5\text{Bu}$, 15%); 163($M^+ - 1 - 6\text{Bu}$, 4%); 75(Ge^+ , 1%).

Et₃GeOGeEt₃: Yield: 70%. ¹H NMR: δ 0.8, 1.0 (m, 30H, Et). ¹³C NMR: δ 8.3, 9.3, Et. GC/Mass: m/z : 338(M^+ , 1%); 309($M^+ - \text{Et}$, 100%); 280($M^+ - 2\text{Et}$, 49%); 252($M^+ - 1 - 3\text{Et}$, 57%); 222($M^+ - 4\text{Et}$, 53%); 195($M^+ + 2 - 5\text{Et}$, 50%); 75(Ge^+ , 9 %).

Ph₃GeOGePh₃: Yield: 60%. Found: ¹³C NMR: δ 128.5, 129.9, 134.4, 137.6 (Ph). Reported in CDCl₃: ¹³C NMR: δ 128.0, 129.3, 134.3, 137.4 (Ph). M. pt found: 184-185°C. Mp: Reported: 184°C.

PhMe₂SiOSiMe₃: Yield: 30%. ¹H NMR : δ 0.2 (s, 9 H, Me), 0.4 (s, 6 H, Me), 7.2, 7.3, 7.6 (m, 5 H, Ph). ¹³C NMR : δ 0.9 Me, 2.0 Me, 128.0, 129.6, 133.3, 140.1 (Ph). ²⁹Si NMR : δ -1.6 Si(Ph), 9.2 Si(Me).

2.2.9 The Reaction of $\text{Me}_3\text{SiOCH}_2\text{NMe}_2$ with PhMe_2SiH and $\text{Mo}(\text{CO})_5\text{THF}$ complex: In a typical experiment, a solution of $\text{Mo}(\text{CO})_6$ (0.6 g) (2.3 mmol) in 50 mL of dry THF, in a quartz tube, was degassed twice. The solution was irradiated by Hanovia 450-W medium pressure mercury lamp at a distance of 4 cm for 12h under nitrogen atmosphere as has been reported.^{3b} To the yellow solution formed, was added 0.4 g (2.3 mmol) of $\text{Me}_3\text{SiOCH}_2\text{NMe}_2$ and stirred at room temperature for 1 h. To this solution was added 0.36 g (2.6 mmol) of PhMe_2SiH for 2 h. The solvent was removed under vacuum and passes through a column in hexanes to give isolated yields of 30% for the disiloxane, $\text{PhMe}_2\text{SiOSiMe}_3$ and 35% of $\text{Mo}(\text{CO})_5\text{NMe}_3$ complex.

$\text{Mo}(\text{CO})_5\text{NMe}_3$ (3b): Yield: 35%. ^1H NMR : δ 1.9(s,9H, Me_3) . ^{13}C NMR : δ 58.8(Me_3), 204.3(CO_{eq}), 213.8(CO_{ax}).

2.2.10 Reaction of $\text{Mo}(\text{CO})_6$ with Et_3SiH and DMF: A Pyrex NMR tube was charged with 0.15 g (1.3 mmol) of Et_3SiH , 0.06 g (0.22 mmol) of $\text{Mo}(\text{CO})_6$ and 0.4 mL of C_6D_6 and sealed under vacuum. The tube was irradiated with a 450 W medium pressure mercury lamp. After 20 minutes of photolysis, the color of solution turned yellow and in the ^1H NMR spectrum a resonance appeared at -8.4 ppm due to the formation of $(\text{CO})_5\text{Mo}(\eta^2\text{-H-SiEt}_3)$ complex. At this time 0.4 mL DMF was added and the NMR tube was resealed after two freeze-pump-thaw cycles and ^1H NMR spectrum was recorded immediately which exhibited that the resonance at -8.9 ppm is decreasing and a new resonance at 4.28 ppm is appearing which is assigned to the CH_2 group of the $\text{Et}_3\text{SiOCH}_2\text{NMe}_2$. The NMR tube was left at room temperature for 48 h, the ^1H , ^{13}C and ^{29}Si NMR spectra showed that all the Et_3SiH is completely consumed and reacted with DMF to form $\text{Et}_3\text{SiOCH}_2\text{NMe}_2$.

2.2.11 Synthesis of unsymmetrical disiloxanes using excess DMF without a catalyst: In a

typical experiment, a Pyrex NMR tube was charged with 1.5 mmol of PhMe_2SiH , 1 mmol of $\text{Et}_3\text{SiOCH}_2\text{NMe}_2$ and 5 mmol of DMF in C_6D_6 and sealed under vacuum. The tube was heated at 90°C . The progress of the reaction was monitored by ^{13}C , ^{29}Si NMR spectroscopy. After 3 h of heating, the resonance at 47 ppm due to the formation of Me_3N in the ^{13}C NMR was reached to maximum, the reaction was stopped and the volatiles removed. Unsymmetrical disiloxane $\text{Et}_3\text{SiOSiPhMe}_2$ was formed in 90 % yield along with trace amount of symmetrical disiloxane, $\text{PhMe}_2\text{SiOSiMe}_2\text{Ph}$.

$\text{Et}_3\text{SiOSiPhMe}_2$: Yield: 90%. ^1H NMR : δ 0.35 (s, 3 H, (Me)PhSi), 0.55 (q, 6 H, $(\text{CH}_2)\text{Si}$), 0.98 (t, 9 H, (Me)Si), 7.24, 7.62 (m, 5 H, Ph). ^{13}C NMR : δ 1.00 (Me), 6.66, 7.03 (Et), 128.33, 129.56, 133.27, 140.30 (Ph). ^{29}Si NMR : δ 10.90 (Si)Et₃, -3.21 (Si)PhMe₂. HRMS(ESI): Calcd. for $\text{C}_{14}\text{H}_{26}\text{Si}_2\text{O}$: (M^++1): 267.1600, Found 267.1573.

Table 2. 3 Synthesis of $\text{R}_3\text{SiOSiR}_3$: Reaction of $\text{R}_3\text{SiOCH}_2\text{NR}'_2$ and R_3SiH using excess of DMF/DEF without a catalyst

R_3	R'_2	$\text{h}\nu/\Delta$	Time	Yield (NMR) ^b
Et_3	Me_2	Δ	3 h	(100)
Et_3	Me_2	$\text{H}\nu$	1d	(100)
PhMe_2	Et_2	Δ	5 h	(100) ^c

^bYields based upon ^1H NMR; ^c reaction performed at 120°C .

2.2.12 Synthesis of $\text{PhMe}_2\text{SiOSiPhMe}_2$ from a catalytic cycle using $\text{M}(\text{CO})_6$, ($\text{M} = \text{Cr}, \text{W}$) Catalysts.

In a typical experiment, a Pyrex NMR tube was charged with 1 mmol of PhMe_2SiH and 8 mmol of DMF and 5 mol % of $\text{M}(\text{CO})_6$ in 0.5 mL of C_6D_6 and was sealed under vacuum. Sealed tube was either heated at 90°C in an oil bath or photochemically irradiated. The reaction was monitored by ^{29}Si and ^{13}C NMR spectroscopy. After 1-7 h of heating or

irradiation, the formation of products disiloxanes, $\text{PhMe}_2\text{SiOSiPhMe}_2$ and NMe_3 were reached to maximum. The reaction was stopped at this stage and NMR tube was opened and the solution was filtered with acrodisc filter to remove the traces of the catalyst, $\text{M}(\text{CO})_6$. The volatiles were removed under high vacuum and the disiloxane obtained was passed through a small silica gel column (0.4cm x 2 cm) eluting with hexanes to yield 70-90% of disiloxane, $\text{PhMe}_2\text{SiOSiPhMe}_2$.

2.2.13 Synthesis of R_3ESER_3 , E = Si, Ge, Sn with $\text{Mo}(\text{CO})_6$ as catalyst: In a typical experiment, a Pyrex NMR tube was charged with 1 mmol (150mg) of R_3EH , E = Si, $\text{R}_3 = \text{Me}_2\text{Ph}$, MePh_2 , Et_3 ; E = Ge, $\text{R}_3 = \text{Et}_3$, Bu_3 , Ph_3 ; E = Sn, $\text{R}_3 = \text{Bu}_3$, Ph_3 and 3 mmol excess of $\text{HC}(\text{S})\text{NMe}_2$, 5 mol % of $\text{Mo}(\text{CO})_6$ and 0.5 mL of C_6D_6 and sealed under vacuum. The tube was heated to 120 °C in an oil bath. The progress of the reaction was monitored by ^{13}C , ^{29}Si or ^{119}Sn NMR spectroscopy. After 1-3 days of heating, the reaction was stopped and the volatiles were removed by pumping nitrogen to the solution and the respective derivatives R_3ESER_3 were purified by column chromatography eluting with hexanes and were isolated in 53-90 % yield.

$\text{PhMe}_2\text{SiSSiMe}_2\text{Ph}$: Yield: 87%. ^1H NMR : δ 0.42(s,12H,Me), 7.3, 7.5, 7.6(m,10H,Ph). ^{13}C NMR : δ 2.6 (Me), 128.1, 129.8, 133.8, 138.6(Ph). ^{29}Si NMR : δ 7.1. GC/Mass: m/z : 301(M^+ -1,1%), 287(M^+ -Me,42%), 209(M^+ -1-PhMe,100%), 135(M^+ -PhMe₂SiS,10%), 105(SiPh^+ ,7%).

$\text{Ph}_2\text{MeSiSSiMePh}_2$: Yield: 63%. ^1H NMR : δ 0.4(s,6H,Me), 7.1, 7.2, 7.3(m,20H,Ph). ^{13}C NMR : δ 0.5 (Me), 127.8, 129.8, 134.2, 136.4 (Ph). ^{29}Si NMR : δ 1.5. GC/Mass: m/z : 427(M^+ +1,1%), 411(M^+ -Me,37%), 333(M^+ -1-PhMe,100%), 271(M^+ -1-Ph₂,9%), 181(M^+ -1-Ph₂MeSiS-Me,12%).

$\text{Et}_3\text{SiSSiEt}_3$: Yield: 62%. ^1H NMR : δ 0.6(q,12H, CH_2), 0.9(t,18H, CH_3). ^{13}C NMR : δ 7.3,

8.0(Et)₃. ²⁹Si NMR : δ 22.5. GC/Mass: *m/z*: 261(M⁺-1,1%), 233(M⁺-Et,58%), 205(M⁺+1-2Et,100%), 177(M⁺+2-3Et,75%), 149(Et₃SiH₂⁺,26%), 87(M⁺-1-6Et,10%), 115(Et₃Si⁺,8%), 59(SiS⁺,24%).

Et₃GeSGeEt₃: Yield: 63%. ¹H NMR : δ 0.9(q,12H,CH₂), 1.0(t,18H,CH₃). ¹³C NMR : δ 8.7, 10.1(Et)₃. GC/Mass: *m/z*: 354(M⁺,15%), 325(M⁺-3-Et,90%), 295(M⁺-1-2Et,100%), 267(M⁺-3Et,55%), 239(M⁺-1-4Et,6%), 161(M⁺-Et₃GeS,70%), 133(M⁺+1-Et₃GeS-Et,70%), 103(EtGe⁺,45%), 75(GeH⁺,33%).

Bu₃GeSGeBu₃: Yield: 67%. ¹H NMR : δ 0.8, 1.0, 1.3, 1.5(m,54H,Bu). ¹³C NMR : δ 13.6, 18.7, 26.4, 27.3(Bu)₃. GC/Mass: *m/z*: 521(M⁺-1,1%), 407(M⁺-1-2Bu,61%), 351(M⁺-3Bu,100%), 295(M⁺+1-4Bu,70%), 189(M⁺+1-Bu₃GeS-Bu,25%), 105(M⁺-1-Bu₃Ge-3Bu,12%), 89(GeMe⁺,25%).

Ph₃GeSGePh₃: Yield: 53%. ¹H NMR : δ 7.1, 7.2, 7.3. ¹³C NMR : δ 128.1, 129.4, 134.7, 136.8. MP: 121-123°C. Reported MP: 130°C. Found HRMS(DART): Calcd. for C₃₆H₃₁Ge₂S: (M⁺

+1): 641.05791, Found 641.0670

Bu₃SnSSnBu₃: Yield: 80%. ¹H NMR : δ 0.7, 0.9, 1.2, 1.4(m,54H,Bu). ¹³C NMR : δ 13.9, 15.9, 27.4, 28.9(Bu)₃. ¹¹⁹Sn NMR : δ 80.6. Found HRMS(DART): Calcd. for C₂₄H₅₃Sn₂S: (M⁺-1): 611.19061, Found 611.2218.

Ph₃SnSSnPh₃: Yield: 60%. CDCl₃: ¹H NMR : δ 7.1, 7.2, 7.3. ¹³C NMR : δ 128.5, 129.3, 136.5, 138.9. ¹¹⁹Sn NMR : δ -53.7. MP: 141-143°C. Reported MP: 141-143°C. Found HRMS(DART): Calcd. for C₃₆H₃₁Sn₂S: (M⁺+1): 733.01846, Found 733.0561.

2.2.14 Synthesis of $R_3SiSSiR_3$ with $Mo(CO)_5(S=CHNMe_2)$ as catalyst: In a typical experiment, a Pyrex NMR tube was charged with 1 mmol(150mg) of $PhMe_2SiH$, and 3 mmol excess of $HC(S)NMe_2$, 7 mol % of $Mo(CO)_5(S=CHNMe_2)$ and 0.3 mL of C_6D_6 and sealed under vacuum. The tube was heated to 120 °C in an oil bath. The progress of the reaction was monitored by ^{13}C , ^{29}Si NMR spectroscopy. After 3 h of heating, the reaction was stopped, and the respective derivative $PhMe_2SiSSiPhMe_2$ were purified by column chromatography eluting with hexanes and were isolated.

2.2.15 Synthesis of $R_3SiSSiR_3$ with $Mo(CO)_5NMe_3$ as Catalyst: In a typical experiment, a Pyrex NMR tube was charged with 1 mmol(150mg) of $PhMe_2SiH$, and 3 mmol excess of $HC(S)NMe_2$, 5 mol % of $Mo(CO)_5(S=CHNMe_2)$ and 0.3 mL of C_6D_6 and sealed under vacuum. The tube was heated to 120 °C in an oil bath. The progress of the reaction was monitored by ^{13}C , ^{29}Si NMR spectroscopy. After 1 d of heating, the reaction was stopped, and the respective derivative $PhMe_2SiSSiPhMe_2$ were purified by column chromatography eluting with hexanes and were isolated.

2.2.16 Synthesis of $Mo(CO)_5(S=CHNMe_2)$ (3c) with $Mo(CO)_5NMe_3$ (3b) and thioformamide: In a typical experiment, a Pyrex NMR tube was charged with 1 mmol(100mg) of **3b**, and 3 mmol excess of $HC(S)NMe_2$, and 0.3 mL of C_6D_6 and sealed under vacuum. The tube was heated to room temperature. The progress of the reaction was monitored by ^{13}C , ^{29}Si NMR spectroscopy. After 14 h of heating, the reaction was stopped, and the respective derivative $Mo(CO)_5(S=CHNMe_2)$ (**3c**) was observed together with thioformamide still present, but non **3b**. (Clearly thioformamide displayed the NMe_3 really fast in comparison to the DMF).

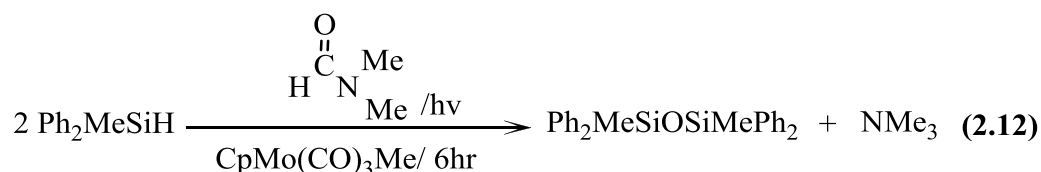
2.2.17 Synthesis of $R_3SiSSiR_3$ with $Mo(CO)_5(S=CHNMe_2)$ (3c) and $PhMe_2SiH$: In a typical experiment, a Pyrex NMR tube was charged with 4 mmol(100 mg) of $PhMe_2SiH$,

and 1 mmol of HC(S)NMe₂, and 0.5 mL of C₆D₆ and sealed under vacuum. The tube was heated to 120 °C in an oil bath. The progress of the reaction was monitored by ¹³C, ¹H, and ⁹Si NMR spectroscopy. After 2 d of heating, the reaction was stopped, and the respective derivative PhMe₂SiSSiPhMe₂ were purified by column chromatography eluting with hexanes and were isolated in 40% yield.

2.3 Results and discussion

2.3.1 Reduction of amides by R₃EH in the presence of iron and molybdenum complexes

The initial studies concerning the photochemical formation of disiloxanes,⁵⁵ were associated with the use of the Fe catalyst [(η⁵-C₅H₅)Fe(CO)₂CH₃], (η⁵-C₅H₅)Fe(CO)₂Me, (**1a**). We have extended these studies to related Mo complexes: [(η⁵-C₅H₅)Mo(CO)₃CH₃], (**2a**) and [(η⁵-C₅H₅)Mo(CO)₂(PPh₃)CH₃], (**2b**) and shown them also to be active. In the case of the Mo phosphine complex, the reaction occurs thermally at 70 °C. The reactions are monitored by ²⁹Si NMR as noted in Fig. 2.11, and the Mo catalysts are far superior than the Fe analogs, eq. 2.12.



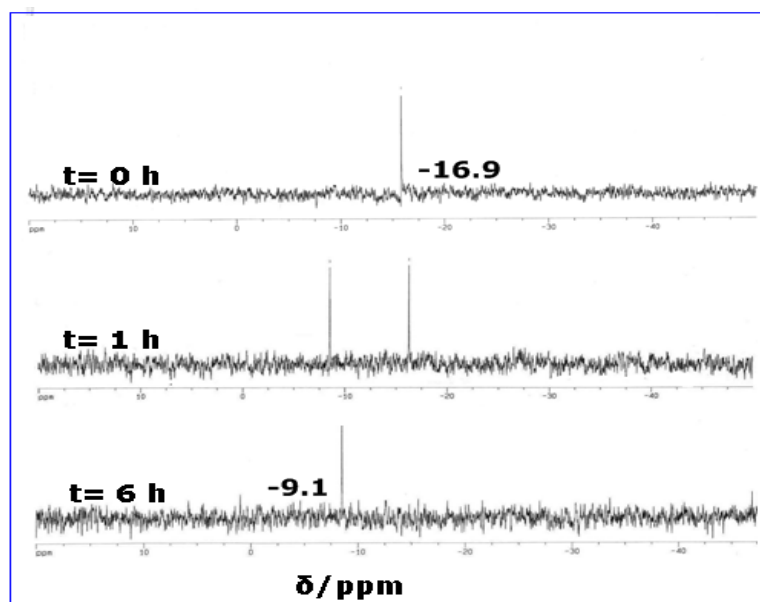
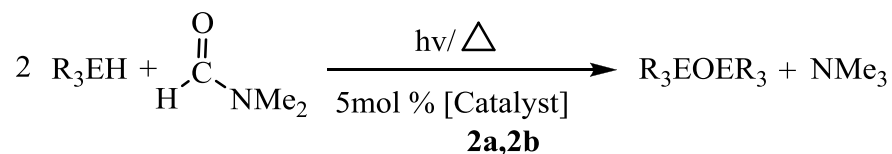


Figure 2. 11 ^{29}Si NMR spectroscopic monitoring showing the disappearance of Ph_2MeSiH in the presence a 5 mol% **2a** catalyst in $\text{DMF-C}_6\text{D}_6$, photochemically irradiated

We have also extended the study to include the use of $[(\eta^5\text{-C}_5\text{H}_5)\text{Mo}(\text{CO})_3\text{CH}_3]$ (**2a**) and $[(\eta^5\text{-C}_5\text{H}_5)\text{Mo}(\text{CO})_2(\text{PPh}_3)\text{CH}_3]$ (**2b**) for the hydrogermylation and hydrostannylation of dimethylformamide. These reactions were successful and the results of this work are presented in Table. 2.4.

Table 2. 4 Catalytic reduction of DMF with R₃E-H, (E = Si, Ge, Sn) in the presence of 5 mol% Mo catalyst **2a** or **2b*** in C₆D₆



Tertiary hydrides	Reaction Time	Reaction Product	Yield
R ₃ E-H	hr/day		%
PhMe ₂ SiH	3h	PhMe ₂ SiOSiMe ₂ Ph	80(100)
Ph ₂ MeSiH	6h	Ph ₂ MeSiOSiMePh ₂	70(100)
Ph ₃ SiH	48h	Ph ₃ SiOSiPh ₃	<5
Et ₃ GeH	5d	Et ₃ GeOGeEt ₃	80(100)
Bu ₃ GeH	5d	Bu ₃ GeOGeBu ₃	70(100)
Ph ₃ GeH	7d	Ph ₃ GeOGePh ₃	<5
Bu ₃ SnH	12h	Bu ₃ SnOSnBu ₃	<5(15)
Ph ₃ SnH	12h	Ph ₃ SnOSnPh ₃	<15

* Both catalysts **2a** and **2b** were used for the photochemical and thermal reactions (70 °C), respectively. **The reaction does not take place in the absence of the catalyst.** Yields based on proton NMR in parentheses.

A few examples to illustrate these findings are reported in the Figures 2.12, and 2.13.

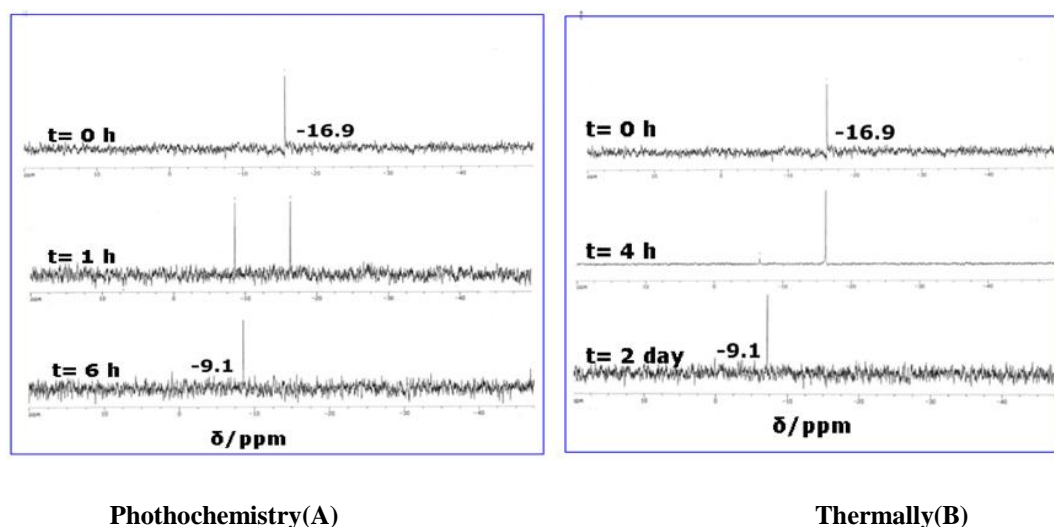


Figure 2.12 ²⁹Si NMR spectroscopic monitoring showing the disappearance of Ph₂MeSiH in the presence a 5 mol% Mo-catalyst (**2a**) UV-light and (**2b**) Thermally 70°C in DMF-C₆D₆.

Here we can see how both catalysts **2a** and **2b** can be used successfully for the catalytic reduction of DMF into Ph₂MeSi-O-SiMePh₂ and NMe₃.

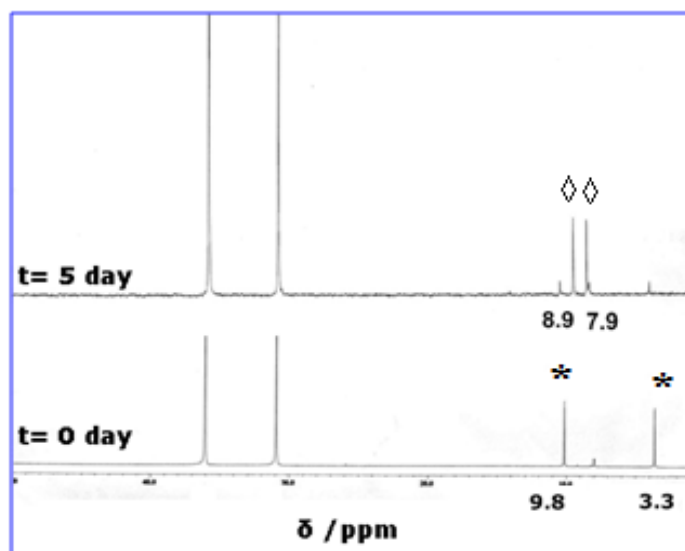
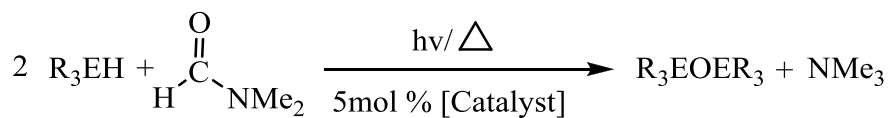


Figure 2.13 ^{13}C NMR spectroscopic monitoring showing the disappearance of Et_3GeH^* and the appearance of $\text{Et}_3\text{Ge-O-GeEt}_3(\diamond)$ in the presence of **2b** at 70 °C.

In the case of the germanium transformations, followed by ^{13}C NMR spectroscopy, we can see the disappearance of Et_3GeH^* and the appearance of 2 new signals associated with the formation of the $\text{Et}_3\text{GeOGeEt}_3(\diamond)$ but a longer period of time was required. Interestingly the reaction is not quite effective under photochemical conditions, and only 30% is transformed (entry 12 and 15) from Table. 2.5.

Table 2. 5 Synthesis of disiloxanes, digermoxanes and distannoxanes using Fe, Mo catalysts with excess DMF 2 -8 fold.



Entry	R ₃	E	Cat	hν/Δ	Time	Yield ^a /% (NMR) ^b
1	PhMe ₂	Si	1a	Hv	14 h	(100)
2	PhMe ₂	Si	1b	Δ	2d	TR
3	PhMe ₂	Si	2a	Hv	3 h	65(100)
4	PhMe ₂	Si	2b	Δ	6 h	75(100)
5	Ph ₂ Me	Si	1a	hν	18 h	(100)
6	Ph ₂ Me	Si	1b	hν	2d	TR
7	Ph ₂ Me	Si	2 ^a	hν	3 h	60(100)
8	Ph ₂ Me	Si	2b	Δ	2d	65(100)
9	Ph ₃	Si	1a,1b,2a	hν/Δ	2d	NR
10	Ph ₃	Si	2b	Δ	1d	TR
11	Et ₃	Ge	1a,1b	hν/Δ	5d	TR
12	Et ₃	Ge	2a	hν	1d	(30)
13	Et ₃	Ge	2b	Δ	5d	55(80)
14	Bu ₃	Ge	1a,1b	hν/Δ	7d	TR
15	Bu ₃	Ge	2a	hν	1d	(30)
16	Bu ₃	Ge	2b	Δ	7d	45(55)
17	Ph ₃	Ge	1a,1b	hν/Δ	7d	NR
18	Ph ₃	Ge	2a,2b	hν/Δ	7d	TR
19	Bu ₃	Sn	1a,2a	hν	12 h	TR
20	Bu ₃	Sn	1b	Δ	2d	5(15)

^a Isolated yields; ^bYields based upon ¹H NMR; ^c reaction performed at 120 °C. TR: traces; NR: no reaction.

(η⁵-C₅H₅)Fe(CO)₂Me (**1a**); (η⁵-C₅H₅)Fe(CO)₂Ph₃PMe(**1b**); (η⁵-C₅H₅)Mo(CO)₃Me (**2a**); (η⁵-C₅H₅)Mo(CO)₂Ph₃PMe (**2b**)

On the other hand, we found that $\text{Bu}_3\text{Sn-H}$ also reduces DMF, but along with low yields of $\text{Bu}_3\text{SnOSnBu}_3$, significant side products are obtained including $(\text{Bu}_3\text{Sn})_2$ and Bu_4Sn , Fig. 2.14.

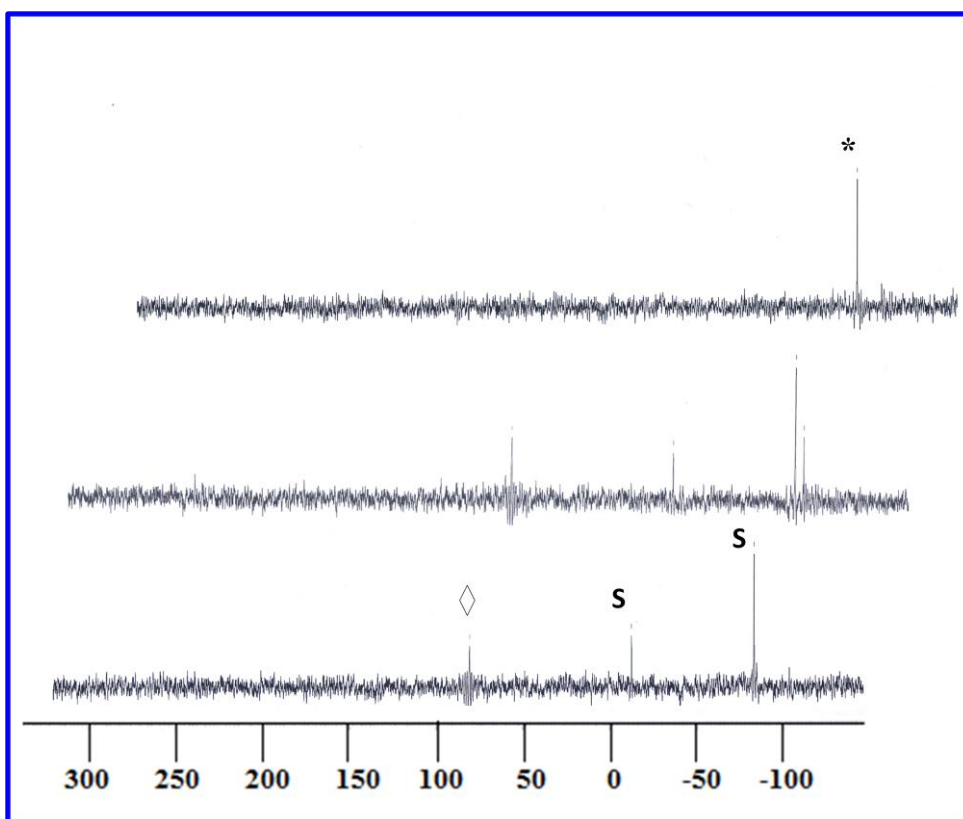
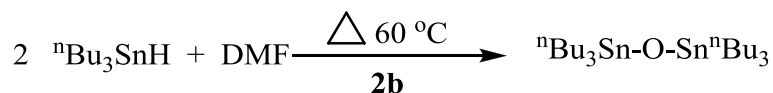
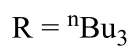
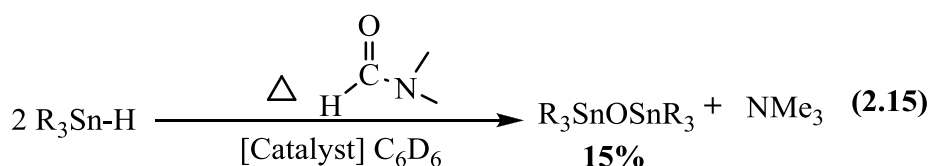
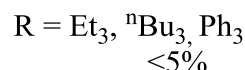
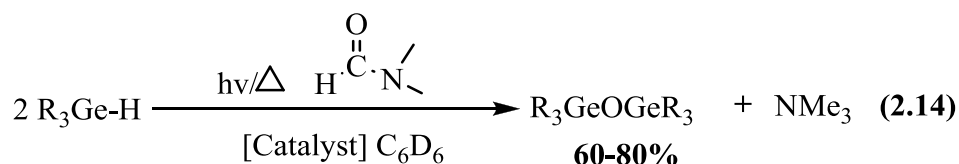
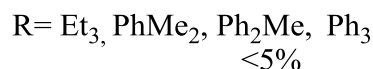
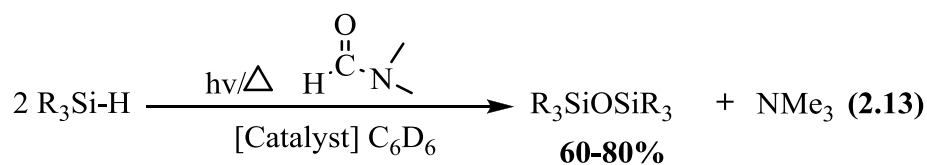


Figure 2. 14 ^{119}Sn NMR spectroscopy showing the disappearance of Bu_3SnH (*) and the formation of $\text{Bu}_3\text{SnOSnBu}_3$ (◊) in the presence of (2b) catalyst.

^S Along with the reaction we can see the formation of Bu_4Sn (-13ppm) and $\text{Bu}_3\text{SnSnBu}_3$ (-83ppm)

From the above results, we found an interesting trend in reactivity associated with the metal carbonyl catalyst and the respective reducing agent used, eqs. 2.13, 2.14 and 2.15.



Based upon the results obtained, we observe that germanium hydrides, Et_3GeH and Bu_3GeH , also reduce DMF to form trimethylamine and the corresponding digermoxane; but with longer periods of time compared to the silicon hydrides, R_3SiH . (See Table. 2.5, entry 11-18). In this series of experiments we were able to determine the higher reactivity associated with silicon hydrides compared to the hydrogermanes and hydrostannanes based in reaction times and yields obtained.



In terms of the catalytically active species, we found a higher reactivity on the molybdenum analogues associated with $(\eta^5\text{-C}_5\text{H}_5)\text{Mo}(\text{CO})_3\text{Me}$ (**2a**) and $(\eta^5\text{-C}_5\text{H}_5)\text{Mo}(\text{CO})_2\text{Ph}_3\text{PMe}$ (**2b**) compared to the iron analogues, $(\eta^5\text{-C}_5\text{H}_5)\text{Fe}(\text{CO})_2\text{Me}$ (**1a**) and

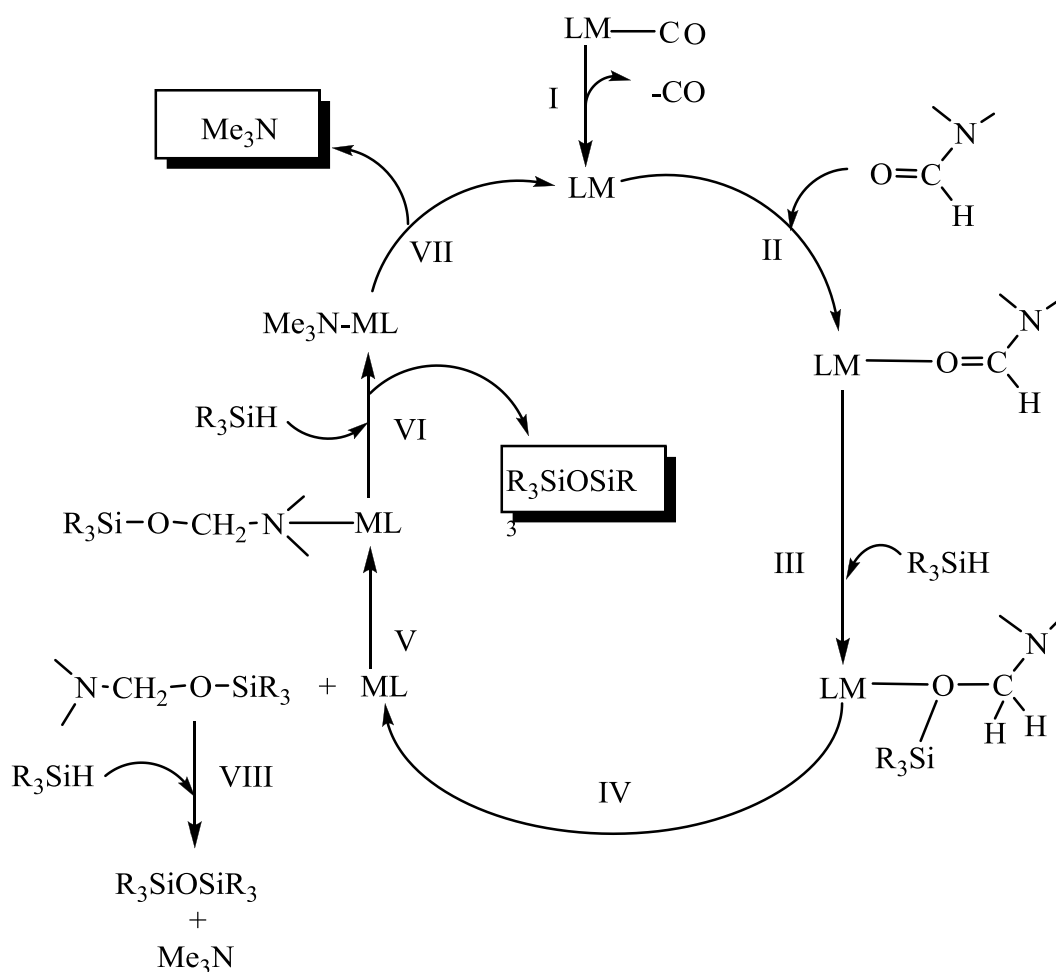
(η^5 -C₅H₅)Fe(CO)Ph₃PMe (**1b**), in terms of shorter reactions times and more stability, meaning the presence of the catalyst at the end of the reaction:

(η^5 -C₅H₅)Mo(CO)₂Ph₃PMe (**2b**) ~ (η^5 -C₅H₅)Mo(CO)₃Me (**2a**) > (η^5 -C₅H₅)Fe(CO)Ph₃PMe (**1b**) ~ (η^5 -C₅H₅)Fe(CO)₂Me (**1a**).

Additionally we found that reactions associated with bulky substituents such as triphenyl silanes (R₃SiH) produce low yields for all cases (entry 9, 10, 17 and 18, Table. 2.5). This signifies a reduced utility of these particular catalysts for bulky substituents at the silicon atom.

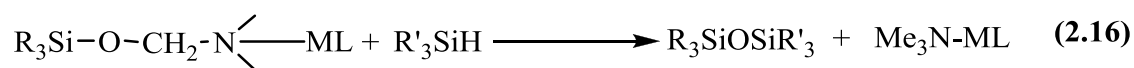
Initial proposed mechanism

Initially we proposed that the mechanism for the formation of reduction of amides from the reaction of SiH compounds and DMF in the presence of transition metal catalysts proceeds as outlined in Scheme 2.2, via multiple steps **I – VII**



Scheme 2. 2 Initial proposed mechanism for siloxane formation

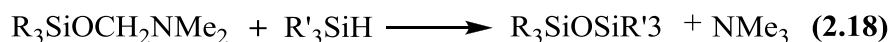
The initial formation of DMF complexes, step **II**, has precedent in the literature.⁴²⁻⁴⁴ One of the key steps has to be the formation of $R_3SiOCH_2NMe_2$ for the first hydrosilylation, step **III**. There are also several reports concerning the activation of ketones to form alkoxysilanes,^{19,38,41-44} *via* molybdenum catalysts which is similar to our proposed step.^{42,43,61-64} We suggested that the O-bound siloxymethylamine rearranges to the more energetically favorable N-bound isomer, steps **IV-V**. The metal-nitrogen bond can activate the C-O bond to allow the second Si-H bond addition to form the respective siloxanes and trimethyl amine complex, step **VI**. eq. 2.16



The trimethylamine complex can undergo a ligand dissociation, and release the trimethyl amine to reform the metal catalyst into the cycle, step **VII**, eq. 2.17.



However, it is also possible that the hydrosilylated product $\text{R}_3\text{SiOCH}_2\text{NMe}_2$ could be eliminated and itself react with R_3SiH to form the disiloxane and Me_3N , step **VIII**, eq. 2.18.



This suggestion comes from a related precedent from Mironov and coworkers involving disiloxane elimination reactions of the only representative molecule of this kind with **chlorosilanes** and related species, eq. 2.19, $\text{X} = \text{Cl}, \text{NR}_2$ etc.⁶⁵



Unfortunately in the presence of catalyst **1a**, **1b**, **2a** and **2b** there was no evidence for the formation of the proposed intermediate, “ the hydrosilylation product”, Fig. 2.15, even with low concentration of the amide and low temperatures we were not able to see any intermediate.

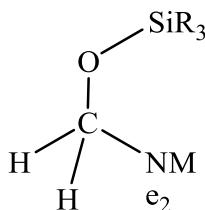
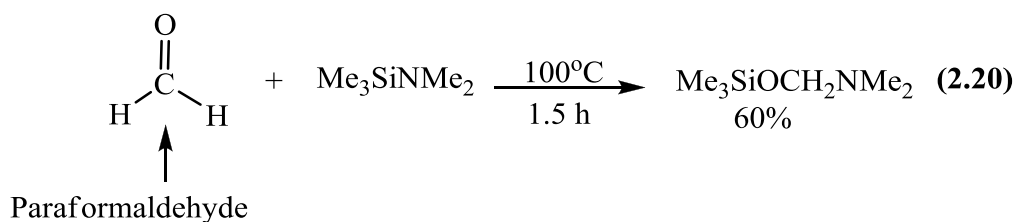


Figure 2. 15 Proposed hydrosilylation product in the first step of the catalytic reduction of amide

Credibility of the initial proposed mechanism

Using a literature procedure we were able to synthesize $\text{Me}_3\text{SiOCH}_2\text{NMe}_2$,⁶⁵ the only reported compound of this kind through the insertion of formaldehyde into Si-N bond from

Me₃Si-NMe₂, eq. 2.20.



This material was properly characterized by NMR Spectroscopy outlined in Fig. 2.16.

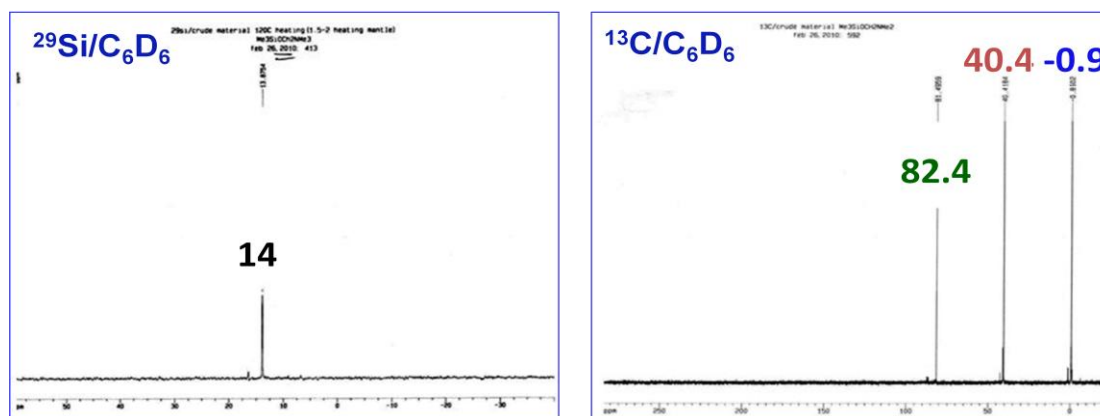
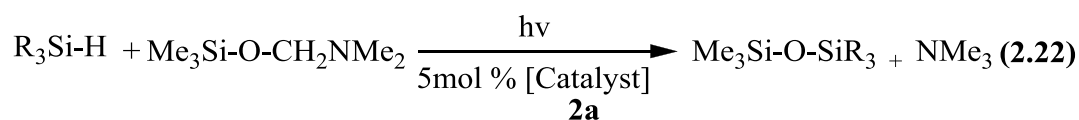


Figure 2.16 Characterization by ²⁹Si and ¹³C NMR spectroscopy of Me₃Si-O-CH₂NMe₂

We reacted Me₃Si-O-CH₂NMe₂ with a variety of silanes and observed no reaction even increasing the temperature to 120°C, eq. 2.21. However, upon addition of the Mo catalysts (**2a**) the desired chemistry occurred, eq. 2.22.

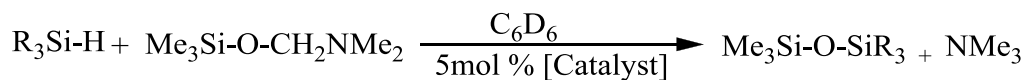


At this point we concluded that the catalyst was necessary for the whole cycle and the formation of R₃EOCH₂NMe₂ in the first stage of the process was important at least for the silane case.

We extended the chemistry to generalize these findings with germanium and tin hydrides to see if the same proposed intermediate Me₃SiOCH₂NMe₂ can react with

germanium and tin hydrides R₃E-H, E = Ge, Sn, and the results are outlined in Table 2.6.

Table 2. 6 Photochemical reaction of Me₃SiOCH₂NMe₂ with R₃E-H, (E = Si, Ge, Sn) in the presence of 5mol% Mo (2a) catalyst in C₆D₆.



R	E	Time	Yield ^a /% (NMR) ^b	NMR data for	
				²⁹ Si	¹¹⁹ Sn
Ph ₃	Si	6	83(100)	11.07	-20
Ph ₂ Me	Si	4	60(100)	10.18	-11
PhMe ₂	Si	4	70(100)	9.18	-1.6
PhMe ₂	Si	24	80(100) ^c		-0.5
Ph ₃	Ge	12	40(80)	8.25	
Et ₃	Ge	18	(100)	6.8	
Bu ₃	Sn	2	80(100)	5.56	76.44

^a Isolated yield; ^b Yield based upon ¹H NMR. ^c 5 mol% Mo(CO)₆ as catalyst and PhMe₂SiOCH₂NMe₂ at 90 °C

The reaction of Me₃SiOCH₂NMe₂ with all group 14 hydrides occurs smoothly, but for E = Si and Ge it needs the presence of the catalyst. The reactions with tributyltinhydride without catalyst, occur thermally but with a low yield of Bu₃SnOSiMe₃ (30%) together with Bu₃Sn-SnBu₃. See Fig. 2.17.

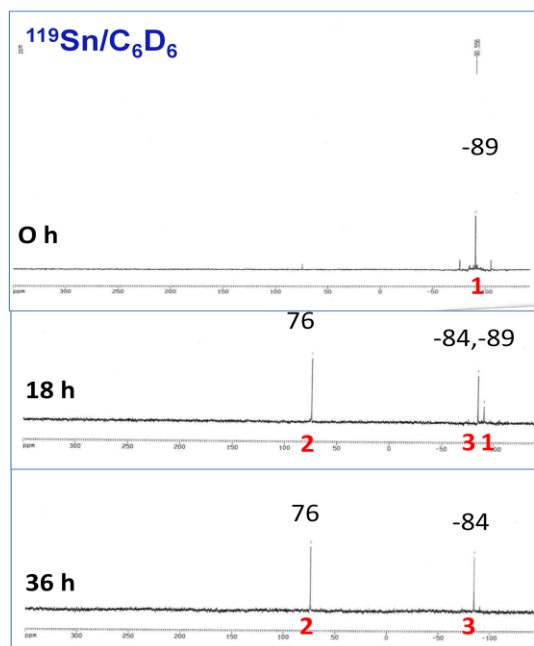
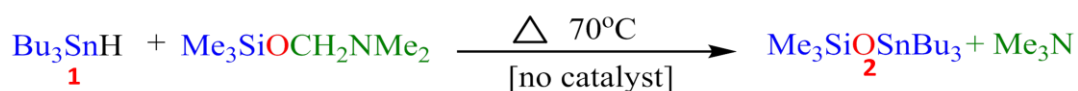
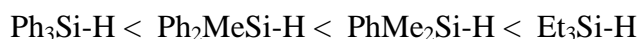
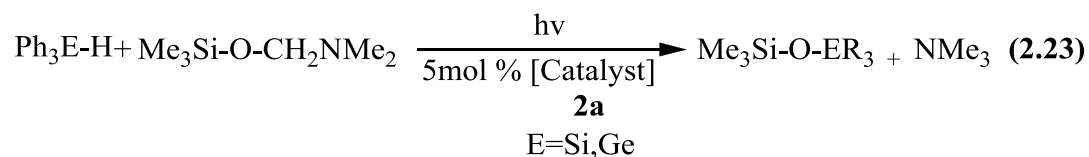


Figure 2. 17 ^{119}Sn NMR spectroscopic monitoring the disappearance of Bu_3SnH (1) and $\text{Me}_3\text{SiOCH}_2\text{NMe}_2$ into $\text{Bu}_3\text{SnOSiMe}_3$ (2) in C_6D_6 .

Note: The signal (3), Fig. 2.17, correspond to the formation of $\text{Bu}_3\text{Sn-SnBu}_3$, and the reaction was stopped since further heating does not create new, or continued chemistry. It seems that the weakness of the Sn-H bond is higher and it can easily undergo activation and form other series of products.

An important finding in this chemistry was the ability of $\text{Me}_3\text{SiOCH}_2\text{NMe}_2$ to react with $\text{Ph}_3\text{E-H}$, $\text{E} = \text{Si, Ge}$, Figure 2.18, 2.19. Since this intermediate, does not participate in the original metal catalyzed reduction of DMF, It seems that the energy required to activate the Si-H bond for the initial hydrosilylation is higher for bulky substituents such as $\text{Ph}_3\text{Si-H}$ or $\text{Ph}_3\text{Ge-H}$ compared with less bulky substituents, whereas for the second step, eq. 2.23 this is not a problem.



A clear example to illustrate how the presence of the proposed intermediate helps to overcome the initial state is presented here, Figures 2.18, 2.19, and 2.20.

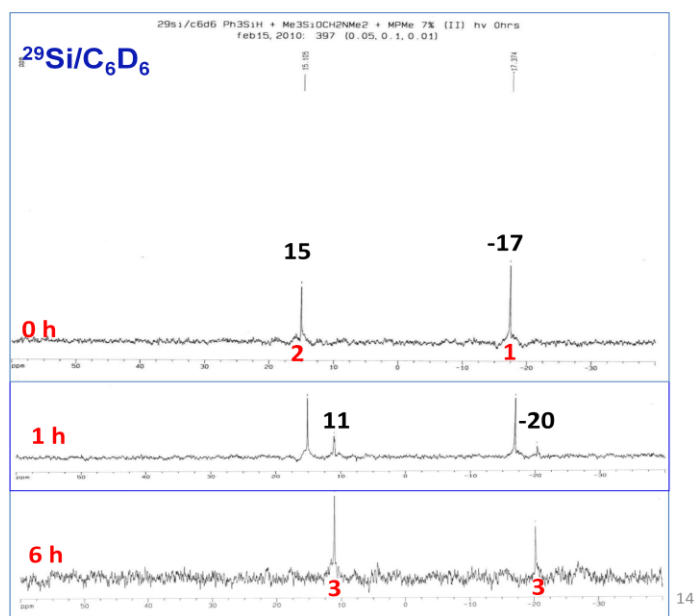
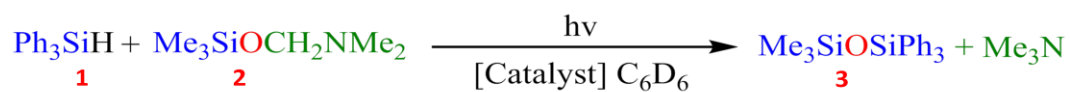


Figure 2.18 ^{29}Si NMR Spectroscopic monitoring the disappearance of Ph_3SiH (1) and $\text{Me}_3\text{SiOCH}_2\text{NMe}_2$ (2) into $\text{Ph}_3\text{SiOSiMe}_3$ (3) in the presence a 5 mol % Mo-Catalyst (2a) in C_6D_6 .

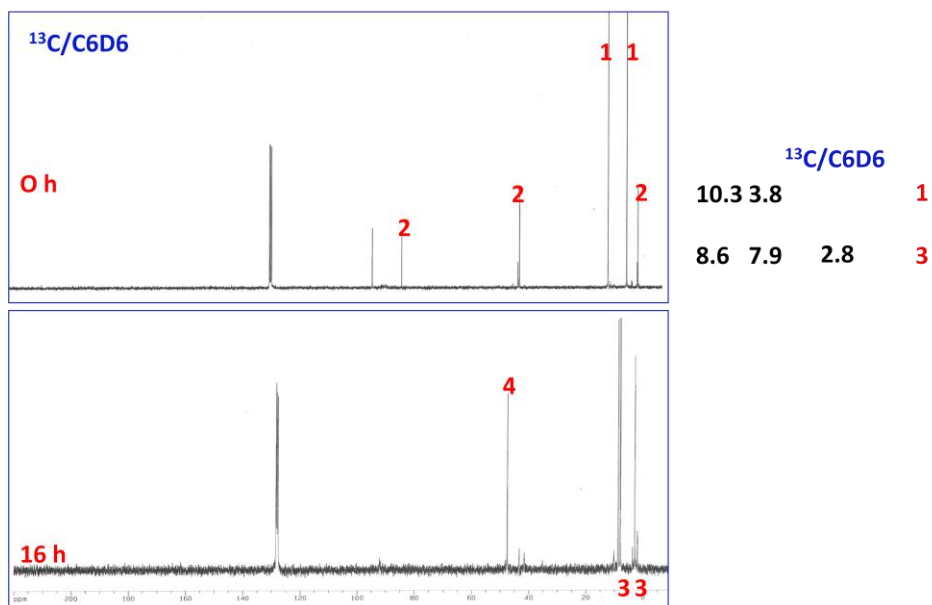
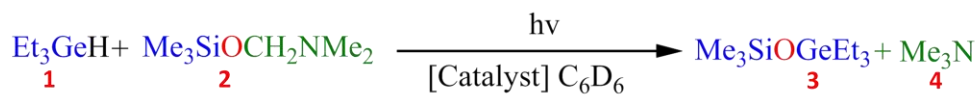


Figure 2.19 ¹³C NMR spectroscopic monitoring the disappearance of Et₃GeH(1) and Me₃SiOCH₂NMe₂(2) into Et₃GeOSiMe₃(3) in the presence a 5 mol % Mo-catalyst (2a) in C₆D₆.

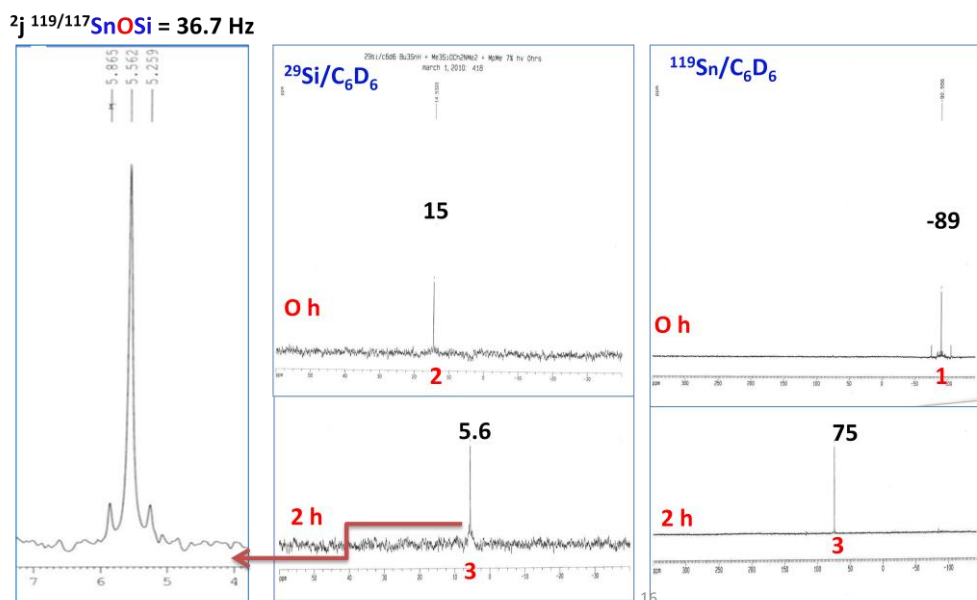
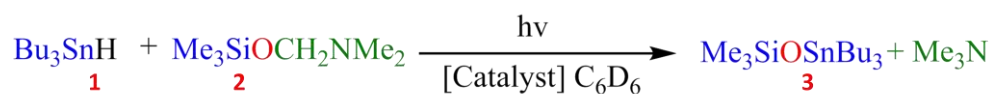
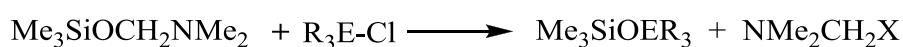


Figure 2.20 ¹³C NMR spectroscopic monitoring the disappearance of Bu₃SnH(1) and Me₃SiOCH₂NMe₂(2) into Bu₃SnOSiMe₃(3) in the presence a 5 mol % Mo-catalyst (2a) in C₆D₆.

The last illustration (Fig. 2.20) is another example that clarifies the viability of the proposed intermediate $\text{R}_3\text{SiOCH}_2\text{NMe}_2$ shown in Scheme 2.2.

The synthesis of the unsymmetrical siloxanes, siloxy-germanes and siloxy-stannanes noted above was confirmed by their independent synthesis using the Mironov reaction between $\text{Me}_3\text{SiOCH}_2\text{NMe}_2$ and the appropriate group 14 chloride, R_3ECl , Table 2.7.

Table 2. 7 Thermal reaction of $\text{Me}_3\text{SiOCH}_2\text{NMe}_2$ with R_3ECl , (E = Si, Ge, Sn) in C_6D_6 .

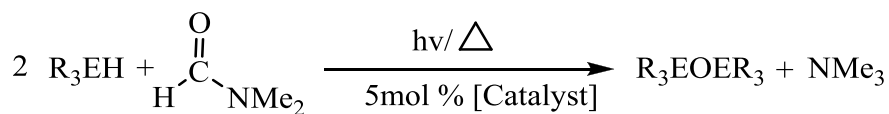


Reactant	Reaction Time	Reaction Product	Temperature	Yield
$\text{R}_3\text{E-H}$	hr/day		$^{\circ}\text{C}$	%
PhMe_2SiCl	0.5	$\text{PhMe}_2\text{SiOSiMe}_3$	25	70
Ph_2MeSiCl	1	$\text{Ph}_2\text{MeSiOSiMe}_3$	25	70
Ph_3SiCl	6	$\text{Ph}_3\text{SiOSiMe}_3$	25	60
Me_3GeCl	1	$\text{Me}_3\text{GeOSiMe}_3$	25	50
PhMe_2GeCl	1	$\text{PhMe}_2\text{GeOSiMe}_3$	25	90
Ph_3GeCl	12	$\text{Ph}_3\text{GeOSiMe}_3$	90	90
Bu_3SnCl	2	$\text{Bu}_3\text{SnOSiMe}_3$	90	90
Ph_3SnCl	12	$\text{Ph}_3\text{SnOSiMe}_3$	90	84

2.3.2 Isolation of the intermediates $\text{R}_3\text{SiOCH}_2\text{NMe}_2$ in the presence of $\text{M}(\text{CO})_6$, M = Mo, Cr, W

Our initial usage of $\text{Mo}(\text{CO})_6$ (**3a**) as catalyst for the silane reduction of DMF involved using 8 to 10 time excess fold of the amide and, as noted we did not observe the formation of any intermediate. The same applied to our study on the utility of the Cr and W analogs, $\text{M}(\text{CO})_6$, M = Cr (**4**), W (**5**). The results are noted in Table 2.8.

Table 2.8 Synthesis of disiloxanes, and digermoxanes using M(CO)₆, M = Mo (3a), Cr(4), W(5) catalysts with excess 2 -8 fold of DMF.



R ₃	E	Cat	hν/Δ	Time	Yield ^a /% (NMR) ^b
Et ₃	Si	3a	hν	1h	85(100)
Et ₃	Si	3a	Δ	3h	85(100)
PhMe ₂	Si	3a	hν	2h	80(100)
PhMe ₂	Si	3a	Δ	6 h	80(100)
PhMe ₂	Si	4	hν	4h	93(100)
PhMe ₂	Si	4	Δ	1h	93(100)
PhMe ₂	Si	5	hν	7h	81(100)
PhMe ₂	Si	5	Δ	7h	81(100)
Ph ₂ Me	Si	3a	Δ	12 h	65(100)
Ph ₃	Si	3a	Δ	2d	50(100) ^c
Et ₃	Ge	3a	Δ	3d	70(100)
Bu ₃	Ge	3a	Δ	5d	70(100)
Bu ₃	Ge	3a	hν	5d	TR
Ph ₃	Ge	3a	Δ	7d	60(100) ^c

^a Isolated yields; ^bYields based upon ¹H NMR; ^c reaction performed at 120 °C. ^dDEF. TR: traces; NR: no reaction. Mo(CO)₆ (**3a**), Cr(CO)₆ (**4**); W(CO)₆ (**5**).

Metal hexacarbonyl systems are as good as the previous catalyst (**1**, **2**), however they offer some advantages:

- Higher selectivity: Ph₃SiH and Ph₃GeH could be used as effective reducing agents.
- Easy to recycle from the reaction mixture.
- Commercially available

Changing the ratio of silane:DMF to 1:2 ratio resulted in a new discovery. Monitoring the reaction between PhMe₂SiH and DMF ([SiH] : [DMF] = 1:2) catalyzed by **3a** in C₆D₆ using ²⁹Si NMR, clearly illustrated the efficient transformation of the silane to the corresponding disiloxane (PhMe₂Si)₂O; however, it is clear that a transient silicon-containing

compound is formed with a ^{29}Si NMR resonance at 5.4 ppm, Figure 2.21a. Similar monitoring of the same reaction by ^{13}C NMR also indicates the formation of a transient species with three ^{13}C NMR resonances at 82.4 (CH_2), 41.1 (Me_2N) and -1.41 (Me_2Si) ppm, Figure 2.21b. Isolation of this transient by stopping the overall reaction prior to completion permitted us to identify it as $\text{PhMe}_2\text{SiOCH}_2\text{NMe}_2$ (**4a**) and for the first time, observe the initial hydrosilylation product of DMF, and illustrate it as a key intermediate in the overall DMF reduction process, eq. 2.24.

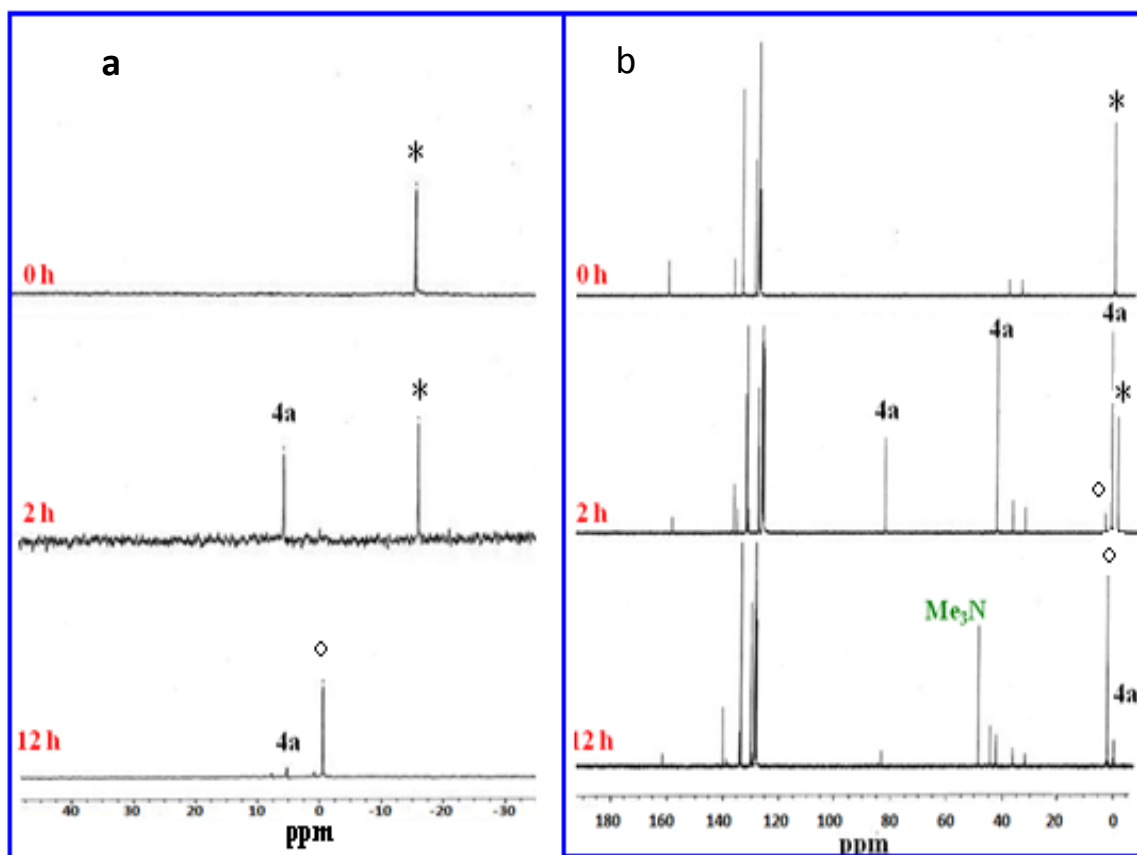
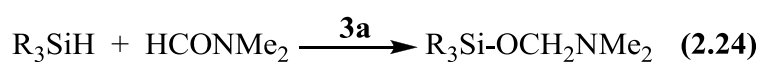


Figure 2.21 Left, ^{29}Si NMR showing the disappearance of PhMe_2SiH (-17.3 ppm) and transient formation of **4a** (5.4 ppm) en route to $(\text{PhMe}_2\text{Si})_2\text{O}$ (0.6ppm): Right, ^{13}C spectra illustrating formation of $\text{PhMe}_2\text{SiOCH}_2\text{NMe}_2$ (**4a**), in the presence of $\text{Mo}(\text{CO})_6$.

Full experimental details for the isolation of **4a** are provided in the experimental part and we also isolated and characterized Ph₂MeSiOCH₂NMe₂ (**4b**), Ph₃SiOCH₂NMe₂ (**4c**) and Et₃SiOCH₂NMe₂ (**4d**) (Table 2.2). The ¹³C NMR data for **4a-d** are almost equivalent to that of Me₃SiOCH₂NMe₂ (**4f**) the only previously reported member of this family.⁶⁶

Table 2.9 Synthesis of R₃SiOCH₂NMe₂ using **3a**.

Entry	R ₃	Time/h	Yield ^a /%(NMR) ^b	Spectral data for R ₃ SiOCH ₂ NMe ₂			
				²⁹ Si	¹³ C (CH ₂)	(Me) ₂ N	(Me)Si
1	Me ₃			13.87	81.49	40.42	-0.86
2	Et ₃	2	90(100)	15.30	82.34	41.11	
3	PhMe ₂	2	30(60)	5.35	82.43	41.1	-1.42
4	Ph ₂ Me	5	10(25)	-5.08	82.54	40.84	-3.04
5	Ph ₃ Si	5	(10)	-15.2	82.92	40.94	

^a Isolated yield; ^b Yields based upon ¹H NMR.

Extension to the use of Cr(CO)₆ (**4**) and W(CO)₆ (**5**) resulted in the same type of chemistry in similar time periods, Table 2.8. We observed that for all the group 6 catalysts the ratio [R₃SiH]:[DMF] was important in determining the relative yields of siloxymethylamine vs disiloxane. The lower the amount of DMF the less disiloxane was obtained, and in the reactions with a large excess of DMF, we could not usually observe the intermediate **4**, an initially puzzling observation.

We have examined the thermal reactivity of **4** in the presence of various silanes and observed no apparent chemical reaction when the reaction was performed in deuterobenzene, the solvent of choice for monitoring the reaction progress using NMR spectroscopy. However, upon addition of excess DMF to these same C₆D₆ solutions, under the thermal conditions similar to those used for the chemistry observed in Figure 2.21, but without the metal catalyst, the appropriate disiloxane and Me₃N were formed in high yield, eq. 2.25 and Fig. 2.22.

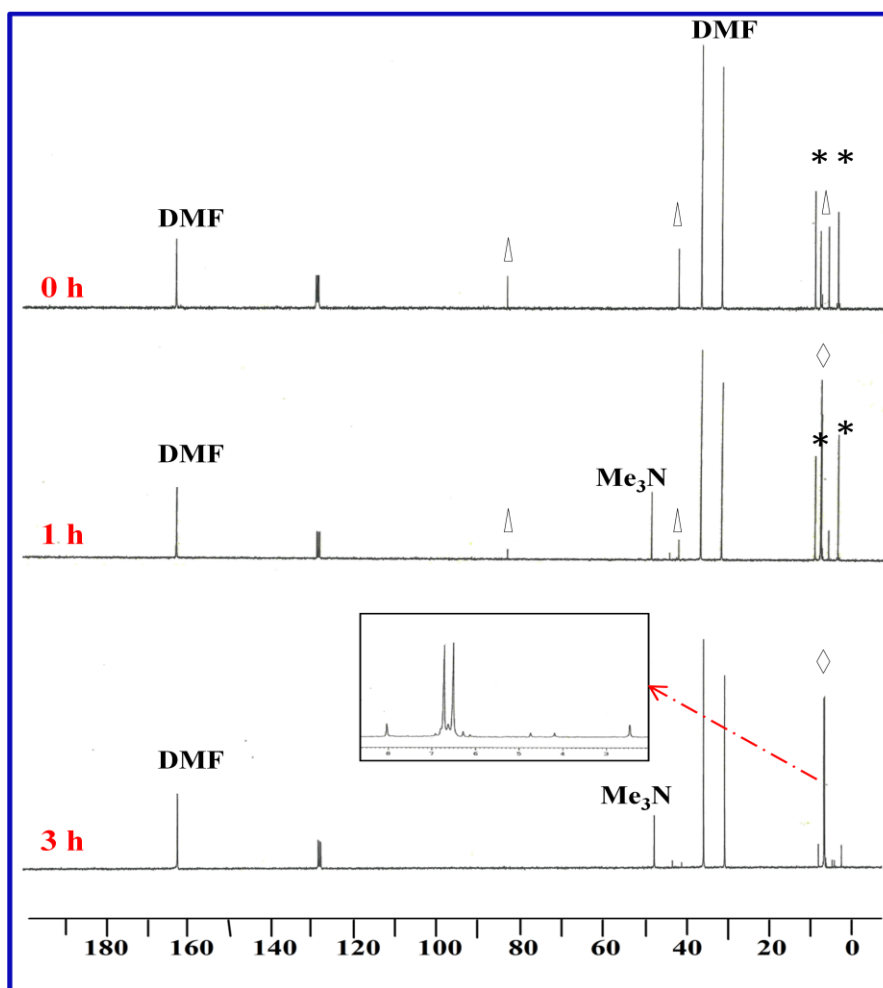
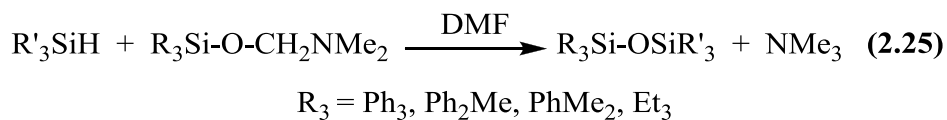


Figure 2.22 ^{13}C NMR spectroscopy showing the disappearance of $\text{Et}_3\text{SiOCH}_2\text{NMe}_2(\Delta)$ and $\text{Et}_3\text{SiH}(\ast)$ into $(\text{Et}_3\text{Si})_2\text{O}(\diamond)$ with concomitant formation of Me_3N at 90°C in the presence excess DMF.

This new reaction is reminiscent of similar reactions of silanes with hydroxylic reagents and related systems where activation of the Si-H bond *via* DMF coordination to form 5- and 6-coordinated transients has been proposed and in some cases observed.⁶⁷ So in this particular case we are proposing that the amide (DMF) is helping to activate the Si-H, through the coordination with the $\text{R}_3\text{Si-H}$. It is well known that silicon compound can extend their coordination number to 5 or even 6.⁶⁷ That increase in coordination number could increase the Lewis acidity of the silicon,⁶⁸ and consequently a good nucleophile can interact

and release the hydrogen, as I have proposed in the Fig. 2.23.

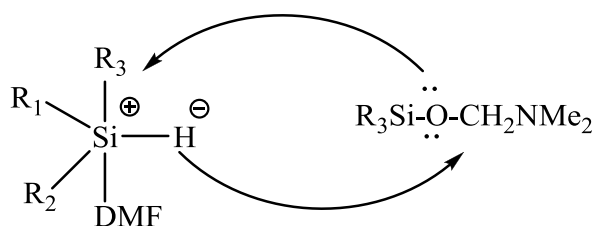


Figure 2.23 Proposed activation of the Si-H bond by DMF coordination.

2.3.3 Final proposed mechanism

From the above results we can now propose that the thermal reduction of amides to amines occurs *via* the cycle noted in Scheme 2.1. Initially the ligand bond dissociation to generate the unsaturated metal center (**i**) The dynamics of the hexacarbonyls of Cr, Mo, and W after photolysis have been extensively studied in low-temperature matrices. Upon photolysis, a CO is ejected, and an excited metal pentacarbonyl is formed that rearranges to a trigonal-bipyramidal geometry. The trigonal bipyramid relaxes to a ground-state square-pyramidal geometry, each involving **two** equatorial COs opening to nearly 180°, but only in one direction is the vacant site facing the ejected CO.³⁷ Then the hydrosilylation reaction can proceed either *via* initial amide coordination to molybdenum as has been reported,⁶⁹ followed by η^2 -silane coordination after further loss of CO, or *vice versa*, initial coordination of the η^2 -SiH, followed by the amide (**ii**), Fig. 2.24.

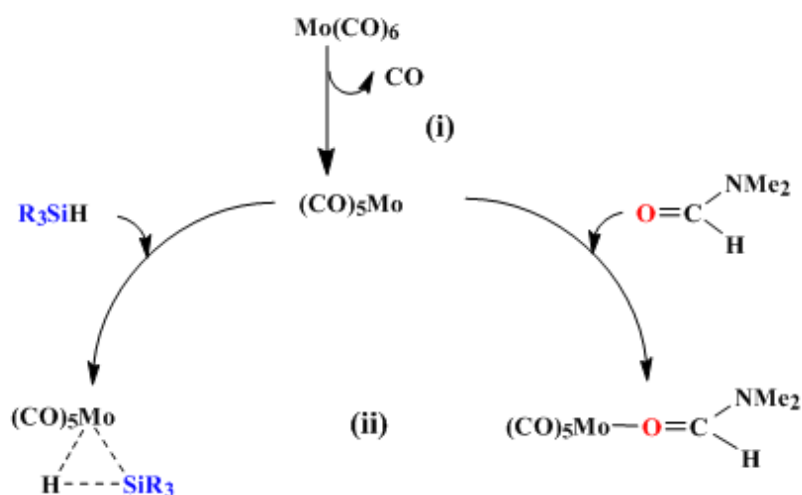


Figure 2.24 Metal carbonyl dissociation and metal coordination or Si-H activation.

Molybdenum η^2 -silane σ -complexes, $(\text{CO})_5\text{Mo}(\eta^2\text{-H-SiR}_3)$ have been detected by ^1H NMR spectroscopy in the photochemical reaction of group 6 metal carbonyls and R_3SiH .⁷⁰

Further substitution on the metal carbonyl complex can generate another di-substituted complex (**X**), Fig. 2.25 (iii).

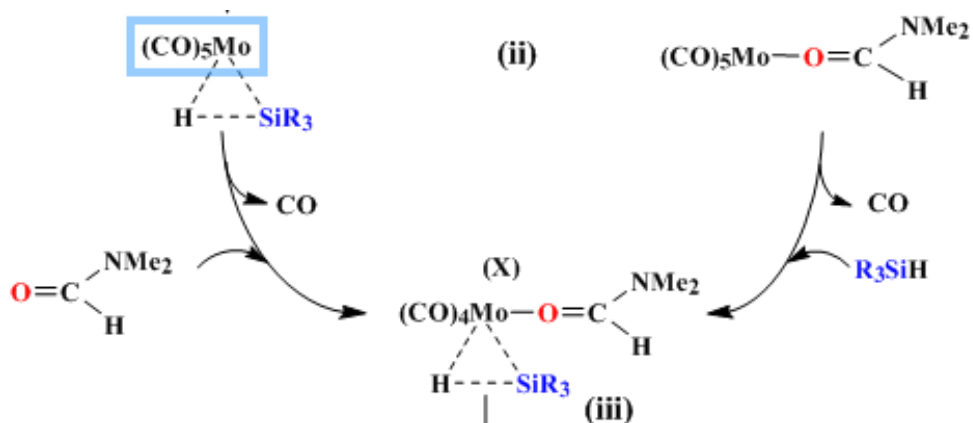


Figure 2.25 Metal coordination and Si-H activation (ii,iii)

The ability of metal carbonyl complexes to undergo 1, 2 or even 3 carbonyl substitutions is known and has been reported by Szymanska,⁷⁰ as for example illustrated in Fig. 2.26

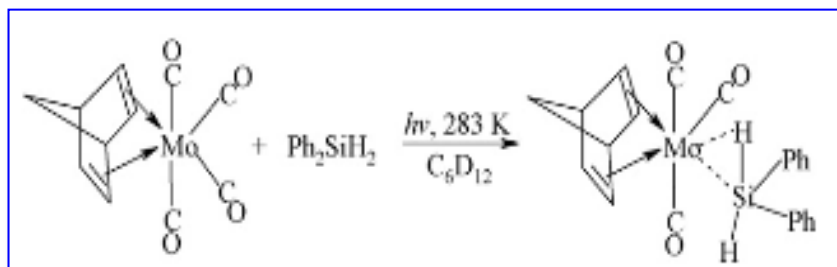


Figure 2.26 Molybdenum carbonyl tri-substituted complex

Migration of the the R_3Si group to oxygen can thus lead to the reductive elimination of the siloxymethyl amines $R_3SiOCH_2NMe_2$ **4**, and the generation of the unsaturated metal center back to the cycle (**iv**).

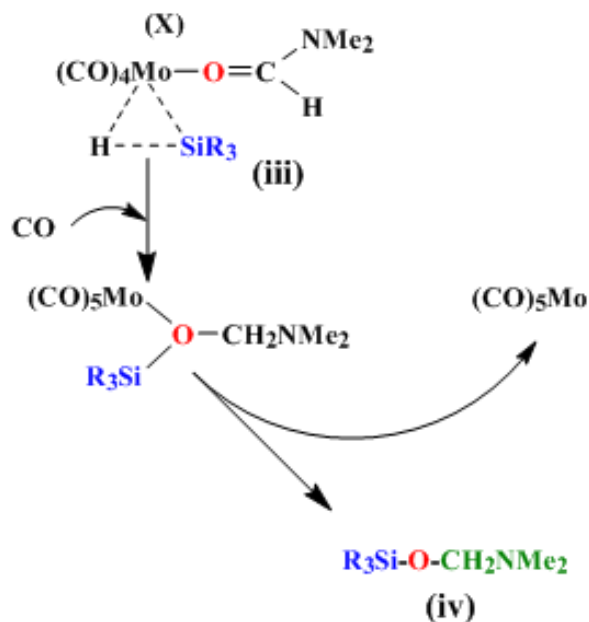
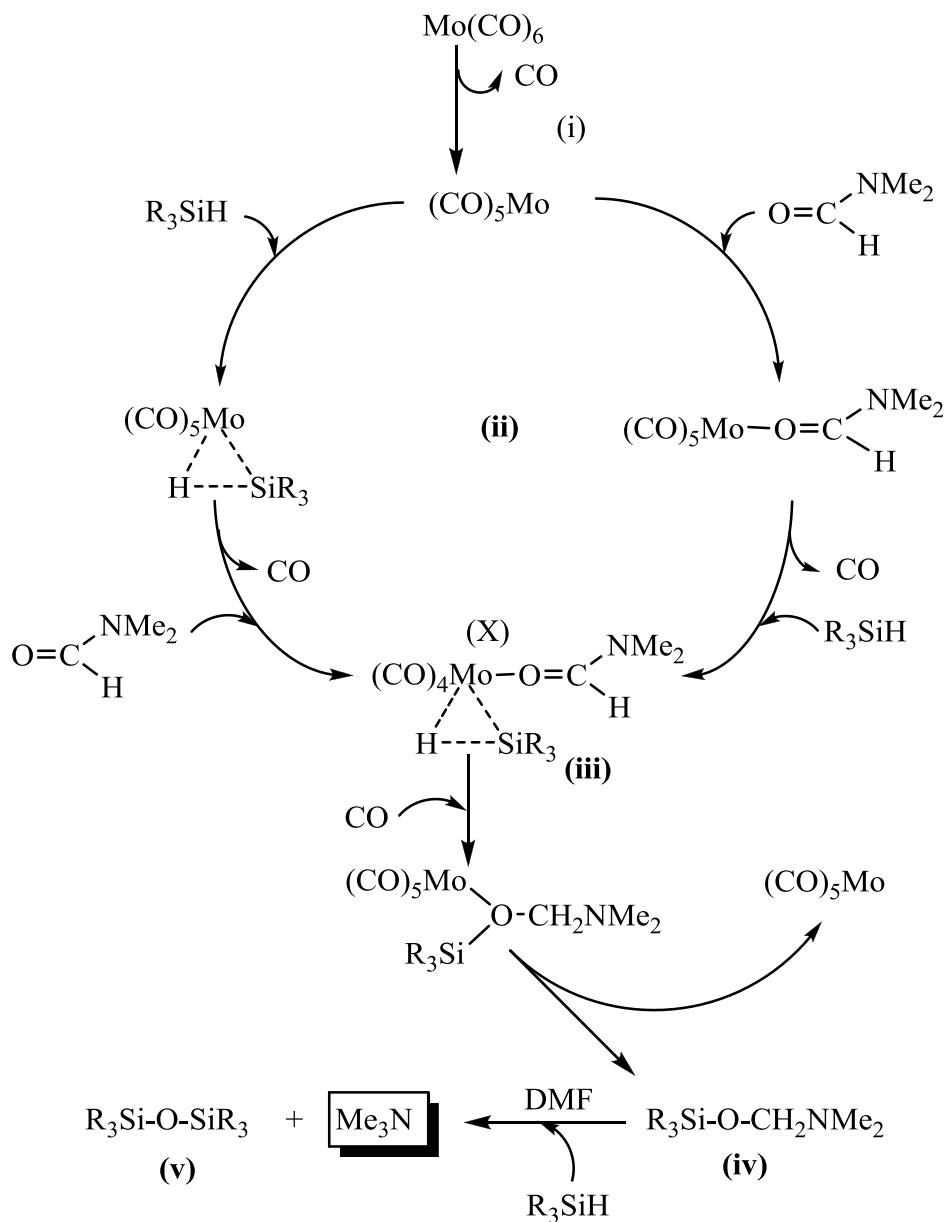


Figure 2.27 Reductive elimination of intermediate $R_3SiOCH_2NMe_2$ (iii,iv)

The final step as we have found is the reaction of the siloxymethylamines $R_3SiOCH_2NMe_2$ (**4**) with the R_3SiH but in the presence of DMF (amide) to complete the cycle and form the trimethylamine and the corresponding disiloxanes. (**V**), Scheme 2.1.



Scheme 2.1 Proposed mechanism for the reduction of amides to amines in the presence of $M(CO)_6$ as catalyst, $M = Mo, Cr, \text{ and } W$.

Our observation that the reaction between **4f** and R_3EH yields Me_3SiOER_3 in the absence of DMF signifies that the metal catalysts are useful in this latter reaction in “inert”

solvent, e.g. C₆D₆ and thus a separate mechanism is operating. We have attempted to form molybdenum complexes of **4f** from reactions with **3a** but these attempts have, to date, proven unsuccessful and led to unrelated chemistry. We suggest that the thermal and photochemical metal-catalyzed reactions outlined in eq. 2.23. involve the metal-silane transient (CO)₅Mo(η^2 -R₃SiH) we have noted above and studies on this aspect of the work continue.

Careful examination of the ¹³C NMR spectra from monitoring the reactions between R₃SiH and DMF catalyzed by **3a** illustrated trace amount of (CO)₅MoNMe₃, **3b**. Clearly it is part of the metal-catalyzed cycle. We have independently synthesized **3b**⁷¹ and in a separate experiments shown that, as expected in light of the chemistry noted above, it acts as a catalyst for the overall reaction of the transformation of R₃SiH to R₃SiOSiR₃ in the presence of DMF, Table 2.10.

Table 2.10 Catalytic reduction of DMF with R₃E-H, (E = Si, Ge) in the presence of 5mol% Mo Catalyst* in C₆D₆

R ₃	E	Cat	hν/Δ	Time	Yield ^a /% (NMR) ^b
Et ₃	Si	3b	hν	1h	(100)
Et ₃	Si	3b	Δ	3h	(100)
Et ₃	Si	6	hν	28h	(90)
PhMe ₂	Si	3b	hν	2h	80(100)
PhMe ₂	Si	3b	Δ	8 h	80(100)
PhMe ₂	Si	6	hν	18 h	(80)
PhMe ₂	Si	6	Δ	24 h	(100) ^c
PhMe ₂	Si ^d	6	hν	12h	(85)
PhMe ₂	Si ^d	6	Δ	24h	(90) ^c
Et ₃	Ge	3b	Δ	2d	(100)
Bu ₃	Ge	3b	hν	5d	TR

^a Isolated yields; ^bYields based upon ¹H NMR; ^c reaction performed at 120 °C. ^dDEF. TR: traces; NR: no reaction. Mo(CO)₅NMe₃ (**3b**); (η^5 -C₅H₅)Mn(CO)₃ (**6**)

Another metal system that has been reported to activate R₃SiH and where DMF coordination can play a rôle is (η^5 -C₅H₅)Mn(CO)₃, **6**.^{72, 73} Use of this material as a catalyst for the above thermal chemistry was also successful and the intermediacy of organosilicon compounds **4** was observed, (Experimental section). In the case of the germane and stannane

chemistry we have, to date, been unable to observe any $R_3EOCH_2NMe_2$ ($E = Ge, Sn$) intermediates when using either **2a**, **3a**, **3b**, **4**, **5** or **6** as catalysts. It is possible that these group 14 substituted amines react more rapidly under the reaction conditions than their silicon analogs, preventing their observation.

2.3.4 Extension to the catalytic reduction of thioformamide

I extended our studies to the attempted reduction of N,N-dimethylthioformamides, DMTF, by group 14 hydrides. Thus, using a range of group 14 hydrides R_3EH , $E = Si$, $R_3 = Me_2Ph$, $MePh_2$, Et_3 ; $E = Ge$, $R_3 = Et_3$, Bu_3 , Ph_3 ; $E = Sn$, $R_3 = Bu_3$, coupled to a range of catalysts **3a** and **3b**, we obtain good to excellent yields of the appropriate group 14 sulfides, eq. 2.26, Table 2.11, together with Me_3N . A typical monitoring of the reaction between $PhMe_2SiH$ and $HC(S)NMe_2$ is presented in Figure 2.28.

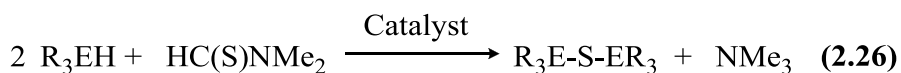


Table 2.11 Synthesis of disila-, digerma-, and distanna-thianes.

	R	E	Cat	$\Delta/h\nu$	Time	Yield %^a (NMR)^b
1	PhMe ₂	Si	3b	Δ	18h	(100)
2	PhMe ₂	Si	3a	Δ	18h	87(100)
3	PhMe ₂	Si	3a	Hv	2d	TR
4	Ph ₂ Me	Si	3a	Δ	3d	63(100)
5	Et ₃	Si	3a	Δ	2d	62(100)
6	PhMe ₂	Si	3c	Δ	3h	(80)
7	Et ₃	Ge	3a	Δ	2d	63(100)
8	Bu ₃	Ge	3a	Δ	2d	67(100)
9	Ph ₃	Ge	3a	Δ	2d	53(90)
10	Bu ₃	Sn	3a	Δ	3h	80(100)
11	Ph ₃	Sn	3a	Δ	3h	60(100)
12	PhMe ₂	Si	-	Δ	2d	NR
13	Et ₃	Ge	-	Δ	2d	NR
14	Bu ₃	Sn	-	Δ	3h	(100)
15	Ph ₃	Sn	-	Δ	3h	(100)
16	PhMe ₂	Si	benzoyl peroxide	Δ	4d	NR
17	Et ₃	Ge	benzoyl peroxide	Δ	4d	NR
18	PhMe ₂	Si	AIBN	Δ	2d	NR

[a] Isolated yields; [b] Yields based upon ¹H NMR; NR: no reaction; TR: traces

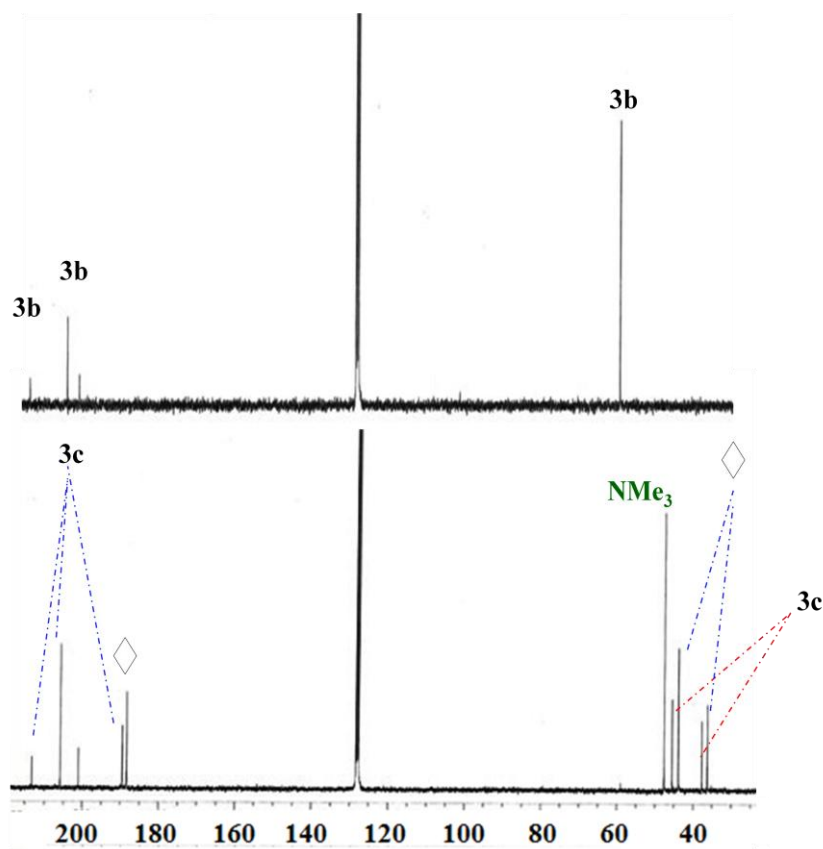
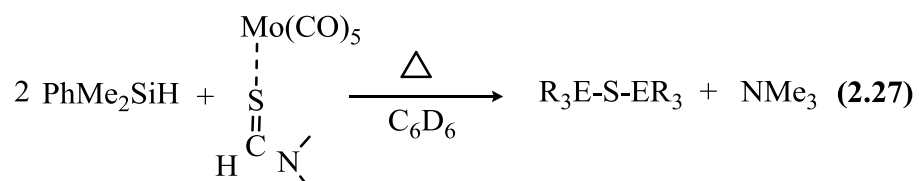


Figure 2.29 NMR monitoring of the reaction between $\text{Mo(CO)}_5\text{NMe}_3$ (**3b**) and HC(=S)NMe_2 (\diamond) showing the complete disappearance of (**3b**) to form $\text{Mo(CO)}_5(\text{S=CHNMe}_2)$ (**3c**) and Me_3N at room temperature (14h) : ^{13}C spectra

We have independently synthesized complex **3c** using a literature procedure by Ishaq et al.⁷⁴ and confirmed that the spectral data noted in the catalytic process was indeed that of the proposed intermediate. Complex **3c**, is also an efficient catalyst as we expected for the reduction process, (Table 2.11 entry 6).

In this chemistry we have also studied the direct reaction of **3c** with silanes, R_3SiH , eq. 2.27, Fig. 2.30.



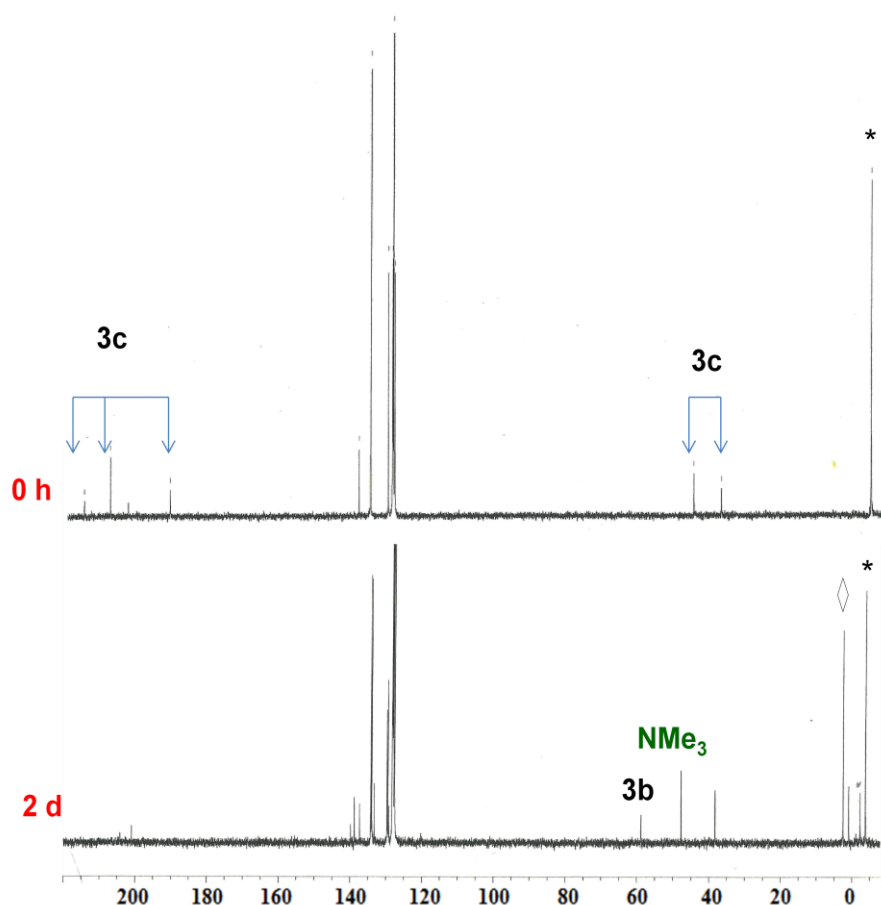
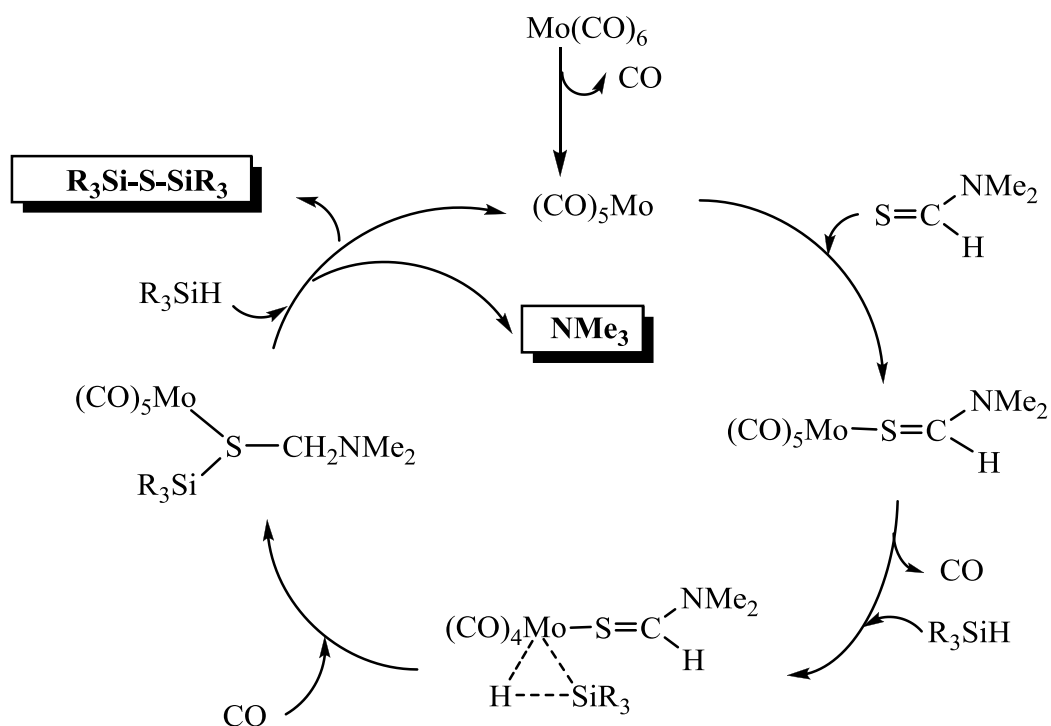


Figure 2.30 ^{13}C spectra NMR monitoring of the reaction between $\text{Mo}(\text{CO})_5(\text{S}=\text{CHNMe}_2)$ (**3c**) and PhMe_2SiH (*) showing the complete disappearance of **3c** to form $\text{PhMe}_2\text{SiSSiPhMe}_2$ (◊) and Me_3N at 120°C .

From this experiment we could observe the formation of the sulfur compound $\text{PhMe}_2\text{Si-S-SiPhMe}_2$ but also the formation of complex $\text{Mo}(\text{CO})_5\text{NMe}_3$ **3b** that has been pointed out as potential intermediate in this catalytic cycle and some side products associated with the formation of $\text{PhMe}_2\text{Si-NMe}_2$ (^{13}C NMR 38.2 ppm (Me) and -2.3 ppm (Me_2)N).

With all these approaches the overall mechanism is similar to that we have proposed for the reduction of DMF,⁷⁵ but still further investigations are required to determine the complete difference between amides and thioamides, Scheme 2.3.



Scheme 2.3 Proposed catalytic cycle for the formation of Me_3N and $\text{R}_3\text{SiSSiR}_3$ from the reaction between R_3EH and thioformamide.

The thermal reaction between Bu_3SnH and dimethylthioformamide, Table 2.11, suggests a possible radical process is important, since it works without the presence of any catalyst; however, attempts to induce the silane and germane reductions in a radical manner by introduction of benzoyl peroxide, or AIBN, were totally unsuccessful (Table 2.11, entry 16, 17 and 18).

2.4 Conclusions

1 I have determined the ability of different metal carbonyl complexes to catalyze the reduction of amides in the presence of tertiary silanes, germanes and stannanes, photochemically or thermally.

2 For the first time we have been able to isolate the hydrosilylation product $R_3SiOCH_2NMe_2$ as the main intermediate in this catalytic cycle using $M(CO)_6$ systems.

3 We have found that the DMF (amide) is required in the second step to undergo the complete thermal reduction to trimethylamine and the corresponding disiloxanes.

4 Extension to the treatment of N,N-dimethylthioformamide with a variety of silanes, germanes, and stannanes, R_3EH , $E = Si, Ge, Sn$, in the presence of transition metal complexes leads to facile reduction to trimethylamine and the corresponding group 14 thioethers, $(R_3E)_2S$.

2.5 References

- 1) Kopylova, L. I.; Ivanova, N. D.; Voronkov, M. G. *Zhur. Obshch. Khim.* **1985**, *55*, 1649-51.
- 2) Zhou, S.; Junge, K.; Adis, D.; Das, S.; Beller, M. *Angew. Chem. Int. Ed.* **2009**, *48*, 9507-9510.
- 3) (a) Das, S.; Addis, D.; Zhou, S.; Junge, K.; Beller, M. *J. Amer. Chem. Soc.* **2010**, *132*, 1770-1771. (b) Das, S.; Addis, D.; Junge, K.; Beller, M. *Chem. Eur. J.* **2011**, *17*, 12186-12192.
- 4) (a) Motoyama, Y.; Mitsui, K.; Ishida, T.; Nagashima, H. *J. Amer. Chem. Soc.* **2005**, *127*, 13150-13151. (b) Hanada, S.; Motoyama, Y.; Nagashima, H. *Tetrahedron Lett.* **2006**, *47*, 6173-6177. (c) Miles, D.; Ward, J.; Foucher, D. A. *Macromolecules*, **2009**, *42*, 9199-9203.
- 5) Matsubara K.; Iura, T.; Maki, T.; Nagashima, H. *J. Org. Chem.* **2002**, *67*, 4985-4988.
- 6) (a) Sunada, Y.; Kawakami, H.; Imaoka, T.; Motoyama, Y.; Nagashima, H. *Angew. Chem. Int. Ed.* **2009**, *48*, 9511-9514. (b) Motoyama, Y.; Aoki, M.; Takaoka, N.; Aoto, R. *Chem. Commun.* **2009**, 1574-1576.
- 7) (a) Sakai, N.; Fujii, K.; Konokahara, T. *Tetrahedron Lett.* **2008**, *49*, 6873-75.
- 8) (a) Barbe, G.; Charette, A. B. *J. Amer. Chem. Soc.*, **2008**, *130*, 18-19. (b) Pelletier, G.; Bechara, W. S.; Charette, A. B. *J. Amer. Chem. Soc.*, **2010**, *132*, 12817-12819.
- 9) (a) Ojima, I. *In The Chemistry of Organosilicon Compounds*; Patai, S.; Rappoport, Z.; Eds.; John Wiley & Sons: New York, **1989**; Part 2, Chapter 25, 1479-1526, (b) Marciniak, B.; Ed *Comprehensive Handbook on Hydrosilylation*; Pergamon Press: Oxford, **1992**.

- 10) (a) Ojima, I.; Nihonyanagi, M.; Nagai, Y., *J. Chem. Soc., Chem. Commun.* **1972**, 938,
(b) Cavanaugh, M.D.; Gregg, B.T.; Cutler, A.R. *Organometallics*, **1996**, *15*, 2764-2769.
- 11) (a) Ryoichi K.; Massotoshi T., Yoshihiko. I., *Tetrahedron. Lett.*, **1998**, *39*, 1017-1020,
(b) Berk. S.C.; Kreutzer, K.A.; Buchwald, S.L., *J. Am. Chem. Soc.* **1991**, *113*, 5093-5095, (c) Berk, S.C.; Buchwald, S.L., *J. Org. Chem.* **1992**, *57*, 3751-3753, (d) Barr, K. J.; Berk, S.C.; Buchwald, S.L. *J. Org. Chem.* **1994**, *59*, 4323.
- 12) (a) Yang. M.S.; Xu. W.L.; Qiu. H.Y.; Lai. G.Q.; Jiang, J.X., *Tetrahedron Lett*, **2008**, *49*, 253; (b) Simon. M.O.; Martinez. R.; Genet. J.P.; Darse. S., *Adv. Synth. Catal*, **2009**, *351*, 153, (c) Sakamoto, S.; Shimojima. A.; Miyasaka, K.; Ruan, J.; Terasaki. O.; Kuroda. K., *J. Am. Chem. Soc.* **2009**, *131*, 9634.
- 13) Thompson, D.B.; Brook. M.A., *J. Am. Chem. Soc.* **2008**, *130*, 32, (b) Naga. N.; Kihara. Y.; Miyanaga. T.; Fukukawa. H., *Macromolecules.*, **2009**, *42*, 3454.
- 14) (a) Lamac, M.; Spannenberg, W.; Baumann, J. H.; Fischer, C.; Hansen. S.; Arndt. P.; Rosenthal, *J. Am. Chem.Soc.* **2010**, *132*, 4369.
- 15) (a) Breneman. C.M.; Martinov. M.; in the Linkage: Structural Significance in Chemistry, Biochemistry and Materilas Science(Eds: Greenberg, A. , Breneman, C.M., Liebman, J.F.) Wiley-VCH, Hoboken, **2003**, 1-33; (b) Robin. M.B.; Bovey. F.A.; Basch in The Chemistry of Amides(Ed.; Zabicky. J.), Interscience, New York, **1970**, 1-72
- 16) (a) Seyden-Penne. J., Reductions by the alumino and Borohydrides in Organic Synthesis, 2nd Ed., Wiley-VCH, Weinheim, **1997**, Gribble. G.W., *Chem. Soc. Rev.*, **1998**, *27*, 395.
- 17) (a) Young, I.S.; Kerr, A.M., *J. Am. Chem. Soc.* **2007**, *129*, 1465 (b) Nagata, T.; Nakazawa. M.; Nishida. A., *J.Am.Chem. Soc.* **2003**, *125*, 7484, (c) Cushing, D.T.; Sanz-Cervera, F.J.; Williams. M.R., *J. Am. Chem. Soc.* **1993**, *115*, 9323, (d)

- Sugimoto, H.; Limura. I.; Yamanishi. Y.; Yamatsu. K.J. *Med. Chem.* **1995**, 38, 4821,
(e) Greshock, J.T.; Grubbs, W.A.; Williams. M.R., *Tetrahedron*, **2007**, 4, 2577.
- 18) Barbe. G.; Charette. A.B., *J. Am. Chem. Soc.* **2008**, 130, 18, (b) Hanada, S.; Tsutsumi. E.; Motoyama. Y.; Nagashima. H., *J. Am. Chem. Soc.* **2009**, 131, 15032.
- 19) (a) Eller. K.; Henkes. E.; Rossbacher R.; Hoke. H., *Ullman's Encyclopedia of Industrial Chemistry*, Wiley-VCH, Weinheim, **2000**.
- 20) Pruchnik, F., "*Organometallic chemistry of the transition elements*", Ed. Plenum Press., p. 703-704, New York, **1990**; Colvin. E. W. "*Silicon in Organic Synthesis*", **1981**
- 21) Lukevics, E.; Russ. *Chem. Rev.*, **1977**, 46, 264; Lukevics, E.; Belyakova, Z.; Pomerantseva, M. G.; Voronkov, M. G. *Organometal. Chem. Rev.*, **1977**, 5, 1.
- 22) Barry, A. J.; Depree, L., Gilkey, J. W., Hook, D. E. *J. Am. Chem. Soc.*, **1947**, 69, 2916.
- 23) Sommers, L. H.; Pietrusza, E. W.; Whitmore, F. C. *J. Am. Chem. Soc.*, **1947**, 69, 188.
- 24) Burkhard, C. A.; Krieble, R. H. *J. Am. Chem. Soc.*, **1947**, 69, 2687.
- 25) Speier, J. L.; Zimmerman, R.; Webster, J. *J. Am. Chem. Soc.*, **1956**, 78, 2278.
- 26) Wagner, G. H., U. S. Pat. **1953**, 2, 637, 738.
- 27) Speier, J. L.; Webster, J. A.; Barnes, G. H. *J. Am. Chem. Soc.*, **1957**, 79, 974.
- 28) Speier, J. L.; "*Homogeneous Catalyst of Hydrosilation by Transition Metals*", *Advances in Organometallic Chemistry*, Vol. 17, Academic Press, New York, **1979**
- 29) Lewis, L. N. *J. Am. Chem. Soc.*, **1990**, 112, 5998.
- 30) Schubert, A. *Adv. Organomet. Chem.*, **1990**, 30, 151.
- 31) Kubas, G. J. *J. Am. Chem. Soc.*, **1995**, 117, 1159.
- 32) Faltynek, R. A. *Inorg. Chem.*, **1981**, 20, 1357–1362.
- 33) Harrod, J. F.; Chalk. A. J., *J. Am. Chem. Soc.*, **1965**, 87, 1133; Takahashi, T.; Bao, F.; Gao, G.; Ogasawara, M. *Org. Lett.*, **2003**, 5, 3479–3481; Adams, J. J.; Arulsamy, N.;

- Roddick, D. M. *Organometallics*, **2009**, 28, 1148–1157; Ura, Y.; Gao, G.; Bao, F.; Ogasawara, M.; Takahashi, T. *Organometallics*, **2004**, 23, 4804–4806; Archer, A. M.; Bouwkamp, M. W.; Cortez, M.; Lobkovsky, E.; Chirik, P. J. *Organometallics*, **2006**, 25, 4269–4278.
- 34) Chalk, A. J.; Harrod, J. F. *J. Am. Chem. Soc.* **1965**, 87, 16; Ojima, I.; Nihonyanagi, M.; Nagai, Y. *J. Chem. Soc., Chem. Commun.*, **1972**, 938a; Ojima, I.; Nihonyanagi, M.; Kogure, T.; Kumagai, M.; Horiuchi, S.; Nakatsugawa, K.; Nagai, Y. *J. Organomet. Chem.* **1975**, 94, 449; Kobayashi, M.; Koyama, T.; Ogura, K.; Seto, S.; Ritter, Brueggemann-Rotgans, F. J. *J. Am. Chem. Soc.*, **1980**, 102, 6602; Semmelhack, M. F.; Misra, R. N. *J. Org. Chem.*, **1982**, 47, 2469; Ojima, I.; Kogure, T. *Organometallics*, **1982**, 1, 1390; Brunner, H.; Becker, R.; Riepl, G. *Organometallics*, **1984**, 3, 1354; Brunner, H.; Kurzinger, A. *J. Organomet. Chem.* **1988**, 346, 413; Ohkuma, T.; Hashiguchi, S.; Noyori, R. *J. Org. Chem.*, **1994**, 59, 217; Zheng, G. Z.; Chan, T. H. *Organometallics*, **1995**, 14, 70; Wright, M. E.; Cochran, B. B. *Organometallics*, **1996**, 15, 317; Nagashima, H.; Suzuki, A.; Iura, T.; Ryu, K.; Matsubara, K. *Organometallics*, **2000**, 19, 3579; Tao, B.; Fu, G. C. *Angew. Chem. Int. Ed.*, **2002**, 41, 3892; Gade, L. H.; Cesar, V.; Bellemin-Laponnaz, S. *Angew. Chem. Int. Ed.*, **2004**, 43, 1014.
- 35) Jetz, W.; Graham, W. A. G. *Inorg. Chem.*, **1971**, 10, 4; Lichtenberger, D. L.; Rai-Chaudhuri, A. *J. Am. Chem. Soc.* **1989**, 111, 358; Lichtenberger, D. L.; Rai-Chaudhuri, A. *Inorg. Chem.* **1990**, 29, 975; Lichtenberger, D. L.; Rai-Chaudhuri, A. *J. Am. Chem. Soc.* **1990**, 112, 2492; Young, K. M.; Wrighton, M. S. *Organometallics*, **1989**, 8, 106; Schubert, U.; Muller, J.; Alt, H. G. *Organometallics*, **1987**, 6, 469; Hill, R. H.; Wrighton, M. S. *Organometallics*, **1987**, 6, 63; Carre, F.; Colomer, E.; Corriu, R. J. P.; Vioux, A. *Organometallics*, **1984**, 3, 1272.

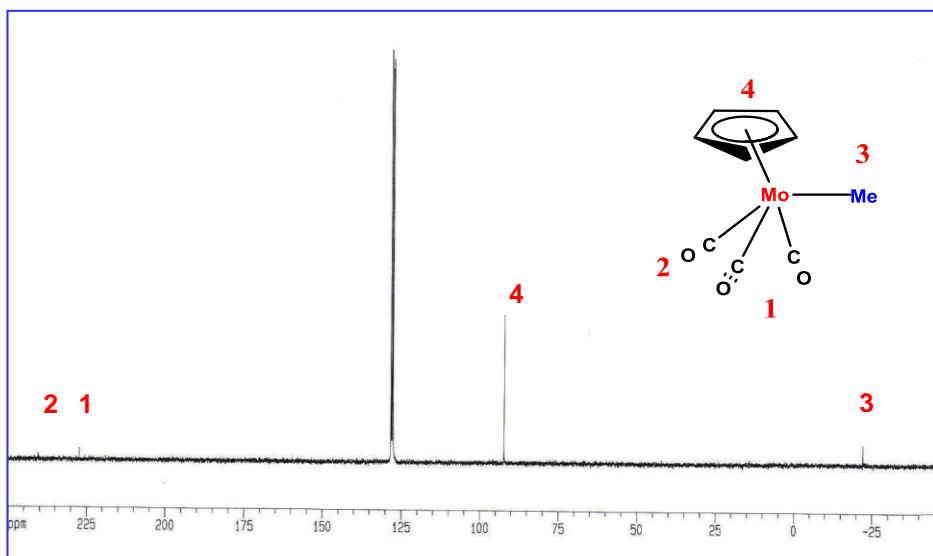
- 36) Lichtenberger, D. L.; Rai-Chaudhuri, A. *J. Am. Chem. Soc.*, **1989**, *111*, 3583;
Lichtenberger, D. L.; Rai-Chaudhuri, A. *Inorg. Chem.*, **1990**, *29*, 975; Lichtenberger,
D. L.; Rai-Chaudhuri, A. *J. Am. Chem., Soc.* **1990**, *112*, 2492.
- 37) Burkey, *J. Am. Chem. Soc.*, **1990**, *112*, 8329.
- 38) Zheng, G. Z.; Chan, T. H. *Organometallics*, **1995**, *14*, 70; Imao, D.; Hayama, M.;
Ishikawa, K.; Ohta, T.; Ito, Y. *Chem. Lett.*, **2007**, *36*, 366.
- 38,) Gadek. A.; Szyman´ska-Buzar. T., *Polyhedron.*, **2006**, *25*, 1441.
- 39) Ojima, I.; Kogure, T.; Nihonyanagi, M.; Nagai, Y. *J. Chem. Soc., Chem. Commun.*,
1972, 938a; Ojima, I.; Nihonyanagi, M.; Nagai, Y. *Bull. Chem. Soc. Jpn.*, **1972**, *45*,
3506; Ojima, I.; Nihonyanagi, M.; Kogure, T.; Kumagai, M.; Horiuchi, S.;
Nakatsugawa, K. *J. Organomet. Chem.* **1975**, *94*, 449.
- 40) Dummont, W.; Poulin, J.-C.; Dang, T.-P.; Kagan, H.B. *J. Am. Chem. Soc.*, **1973**, *95*,
8295.
- 41) Ojima, I.; Kogure, T.; Kumagai, M.; Horiuchi, S.; Sato, T. *J. Organomet. Chem.*,
1976, *122*, 83.
- 42) Park, S.; Brookhart, M., *Organometallics*, **2010**, *29*, 6057–6064.
- 43) Peterson, E.; Khalimon, A. Y.; Simionescu, R.; Kuzmina, L. G.; Howard, J. A. K.;
Nikonov, G. *J. Am. Chem. Soc.*, **2009**, *131*, 908–909.
- 44) Shirobokov, O. G.; Gorelsky, S. I.; Simionescu, R.; Kuzminac, L. G.; Nikonov, G. I.
Chem. Commun., **2010**, *46*, 7831–7833.
- 45) Ogino, H.; Tobita, H. *Adv.. Organomet. Chem.*, **1998**, *42*, 223; Harrod, J. F. *Coord.*
Chem. Rev., **2000**, *493*, 206; Kang, S. O.; Lee, J.; Ko. J. *Coord. Chem. Rev.*, **2002**,
231, 47; Chandrasekhar, V.; Boomishankar, R.; Nagendran, S. *Chem. Rev.*, **2004**, *104*,
5847; Marciniac, B. *Coord. Chem. Rev.*, **2005**, *249*, 2374; Shimada, S.; Tanaka, M.
Coord. Chem. Rev., **2006**, *250*, 991; Lachaize, S.; Sabo-Etienne, S. *Eur. J. Inorg.*

- Chem.*, **2006**, *11*, 2115.
- 46) Watanabe, T.; Hashimoto, H.; Tobita, H. *Angew. Chem. Int. Ed.*, **2004**, *43*, 218; Tobita, H.; Matsuda, A.; Hashimoto, H.; Ueno, K.; Ogino, H. *Angew. Chem. Int. Ed.*, **2004**, *43*, 221; Chen, W.; Shimada, S.; Tanaka, M.; Kobayashi, Y.; Saigo, K. *J. Am. Chem. Soc.*, **2004**, *126*, 8072; Suzuki, E.; Okazaki, M.; Tobita, H. *Chem. Lett.*, **2005**, *34*, 1026; Hashimoto, H.; Matsuda, A.; Tobita, H. *Chem. Lett.*, **2005**, *34*, 1374; Koshikawa, H.; Okazaki, M.; Matsumoto, S.; Ueno, K.; Tobita, H.; Ogino, H. *Chem. Lett.*, **2005**, *34*, 1412; Sakaba, H.; Yoshida, M.; Kabuto, C.; Kabuto, K. *J. Am. Chem. Soc.*, **2005**, *127*, 7276; Adams, R. D.; Smith, J. L. Jr. *Organometallics*, **2005**, *24*, 4489; Shimada, S.; Rao, M. L. N.; Li, Y. H.; Tanaka, M. *Organometallics*, **2005**, *24*, 6029; Hayes, P. G.; Beddie, C.; Hall, M. B.; Waterman, R.; Tilley, T. D. *J. Am. Chem. Soc.*, **2006**, *128*, 428; Watanabe, T.; Hashimoto, H.; Tobita, H. *J. Am. Chem. Soc.*, **2006**, *128*, 2176.
 - 47) Brook, M. A. “*Silicon in Organic, Organometallic, and Polymer Chemistry*”, Wiley: New York, **2000**, Chapter 12.8, p 401; Kim, B. H.; Woo, H. G. *Adv. Organomet. Chem.*, **2005**, *52*, 143; Varchi, G.; Ojima, C., *Org. Chem.*, **2006**, *10*, 1341.
 - 48) Seitz, F.; Wrighton, M. S. *Angew. Chem., Int. Ed. Engl.*, **1988**, *27*, 289; Cleary, B. P.; Mehta, R.; Eisenberg, R. *Organometallics*, **1995**, *14*, 2297; Turculet, L.; Feldman, J. D.; Tilley, T. D. *Organometallics*, **2004**, *23*, 2488.
 - 49) Goldslager, B. A.; Clarson, S., J. *Journal of Inorganic and Organometallic Polymers.*, **1999**, *9*, 2.
 - 50) Ojima, I.; Inaba, S.; Kogure, T.; Nagai, Y. *J. Organomet. Chem.*, **1973**, *55*, C7.
 - 51) Yamashita, H.; Tanaka, M. *Bull. Chem. Soc. Jpn.*, **1995**, *68*, 403.
 - 52) Corey, J. Y. *Adv. Organomet. Chem.*, **2004**, *51*, 1 – 52.
 - 53) Herzig, C. “*Organosilicon Chemistry*”, Eds. N. Auner, J. Weis.; VCH; Weinheim.,

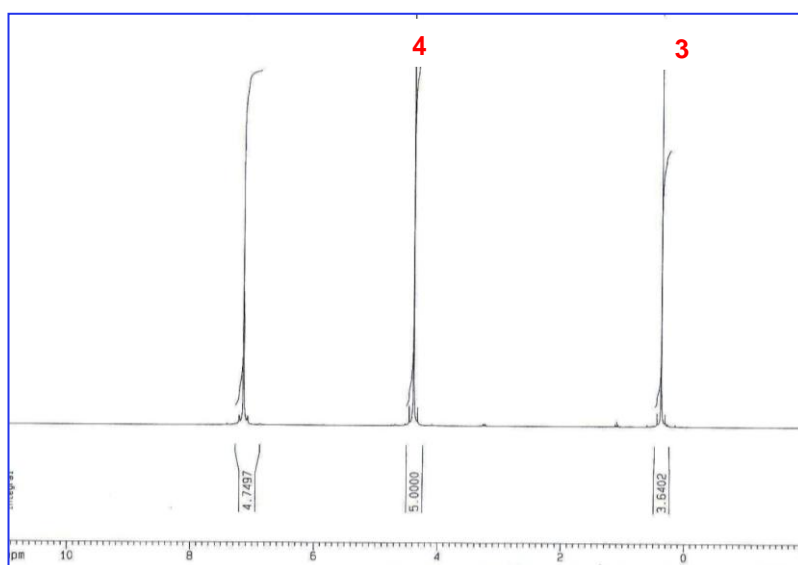
- 1994**, pp. 253 – 260.
- 54) Itazaki, M.; Ueda, K.; Nakazawa, H., *Angew. Chem. Int. Ed.*, **2009**, 48, 3313.
 - 55) Sharma, H. K.; Pannell, K. H. *Angew. Chem. Int. Ed.*, **2009**, 48, 7052.
 - 56) Engel, M.; Hisgen, B.; Keller, R.; Kreuder, W.; Reck, B.; Ringsdorf, H.; Schmidt, H.-W.; Tschirner, P. *Pure Appl. Chem.* **1985**, 57, 1009.
 - 57) Cory, J. Y.; Corey, E. R. “*New Directions of Silicon Chemistry for Obtaining Bioactive Compound In Silicon Chemistry*”, Eds. Ellis Horwood Ltd: England., **1988**, pp 135–144. Chapter 13.
 - 58) Grubb, W. T. *J. Am. Chem. Soc.*, **1954**, 76, 3408.
 - 59) Sridhar, M.; Ramanaiah, B. C.; Narsaiah, C.; Mudam, K. S., Bellam, M.; Mallu, K.; Kumar, R. *Tetrahedron Letters.*, **2009**, 50, 7166.
 - 60) Mitsudome, T.; Arita, S.; Mori, H.; Mizugaki, T.; Jitsukawa, K.; Kaneda, K. *Angew. Chem. Int. Ed.*, **2008**, 47, 7938 .
 - 61) Stolz, I. W.; Dobson, G. R.; Sheline, R. K. *Inorg. Chem.*, **1963**, 2, 323
 - 62) Da Costa, A. P.; Reis, P. M.; Gamelas, C.; Romao, C. C.; Royo, B., *Inorg. Chimica Acta.*, **2008**, 361, 1915
 - 63) Reis, P. M.; Romao, C. C.; Royo, B. *Dalton Trans.*, **2006**, 1842–1846
 - 64) Schmidt, T. *Tetrahedron.*, **1994**, 35, 3513.
 - 65) Kozyukov, V. P.; Mironov, V. F. *Zh. Obshch. Khim.*, **1983**, 53, 119(100).
 - 66) We have synthesized the new materials $R_3SiOCH_2NMe_2$, in good yields for $R_3 = Ph_3$, Ph_2Me , $PhMe_2$, Et_3 and the procedure can be readily extended to a wide variety of silyl groups. Previously only the Me_3Si compound had been reported by the Mironov group by a different route. Kozyukov, V. P.; Kozyukov, V. P.; Mironov, V. F. *Zh. Obshch. Khim.* **1983**, 53, 119-126. Full experimental and characterization data are in the experimental part.

- 67) (a) Chruściel, J. J. *Can. J. Chem.* **2005**, 83, 508-516. (b) Weinmann, M.; Walter, G.; Huttner, G.; Heinrich, J. *J. Organomet. Chem.* **1998**, 561, 131-141. (c) Marciniec, B.; Gulińska, H. *J. Organomet. Chem.* **1978**, 146, 1-5.
- 68) Corriu. R. J .P.; Perz. R.; Eye. C., *Tetrahedron*, **1983**, **39**, 999-1009.
- 69) Stolz, I.; Dobson, G. R.; Sheline, R. K. *Inorg. Chem.* **1963**, 2, 322-6.
- 70) (a) Mathews, S. L.; Pons, V.; Heinekey, D. M. *Inorg. Chem.* **2006**, 45, 6453-6459. (b) Stosur, M.; Kochel, A.; Keller, A.; Szymańska-Buzar, T. *J. Organometallics*, **2006**, 25, 3791-3794. (c) Adrjan, B.; Szymańska-Buzar, T. *J. Organomet. Chem.* **2008**, 693, 2163-2170. (d) Gadek, A.; Szymańska-Buzar, T. *Polyhedron*, **2006**, 25, 1441-1448. We have photolyzed Mo(CO)₆ in the presence of Et₃SiH and observed the formation of (CO)₅Mo(η^2 -H-SiEt₃), ¹H NMR resonance at - 8.4 ppm for Mo-H. Addition of DMF to this solution at room temperature results in the formation of Et₃SiOCH₂NMe₂.
- 71) Strohmeier, W.; Guttenberger, J. F.; Blumenthal, H.; Albert, G. *Chem. Ber.* **1966**, 99, 3419-3424.
- 72) (a) Palmer, B. J.; Hill, R. H. *Can. J. Chem.* **1996**, 74, 1959-1967. (b) Schubert, U.; Grubert, S. *Monats. Chemie* **1998**, 129, 437-443.
- 73) Sheng, T.; Dechert, S.; Hyla-Kryspin, I.; Winter, R. F.; Meyer, F. *Inorg. Chem.* **2005**, 44, 3863-3874.
- 74) Baghlaf. A. O.; Al-Shaikh. A. H.; Ishaq. M., *J. Chem. Soc. Pakistan*, **1987**, 9, 555-558.
- 75) Arias Ugarte. R.; Morris A.; Cervantes. E.; Sharma. H. K.; Pannell. K.H., *J. Am. Chem. Soc.* **2011**, In Press.

Appendices

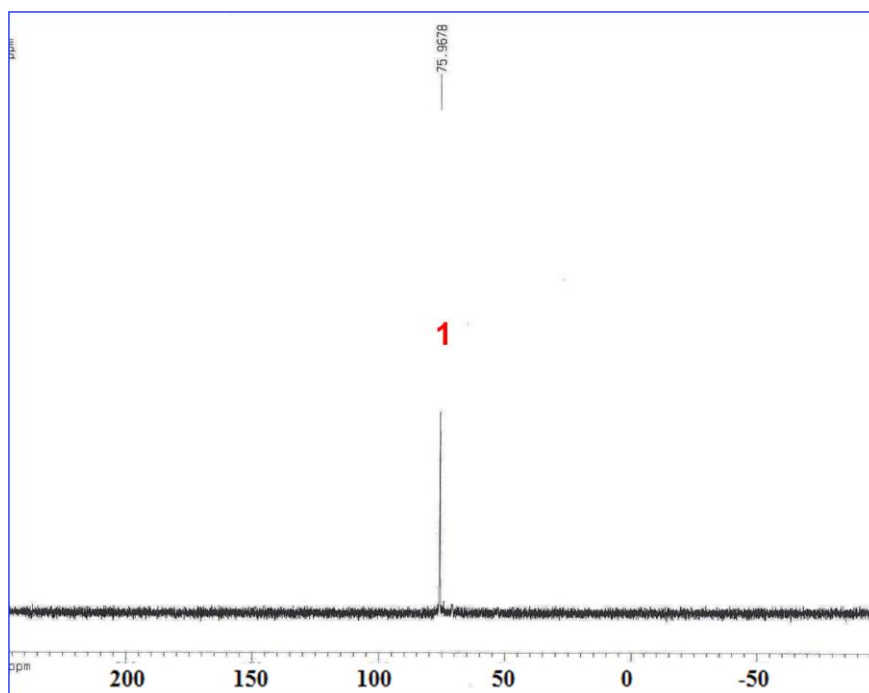
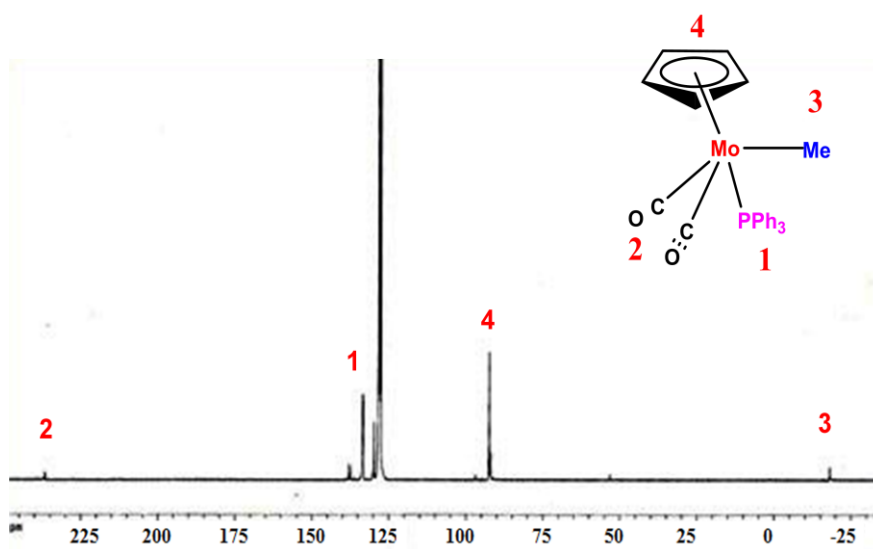


Appendix 1.1 : $^{13}\text{C}/\text{C}_6\text{D}_6$ NMR spectroscopy for $(\eta^5\text{-C}_5\text{H}_5)\text{Mo}(\text{CO})_3\text{Me}$ (**2a**)



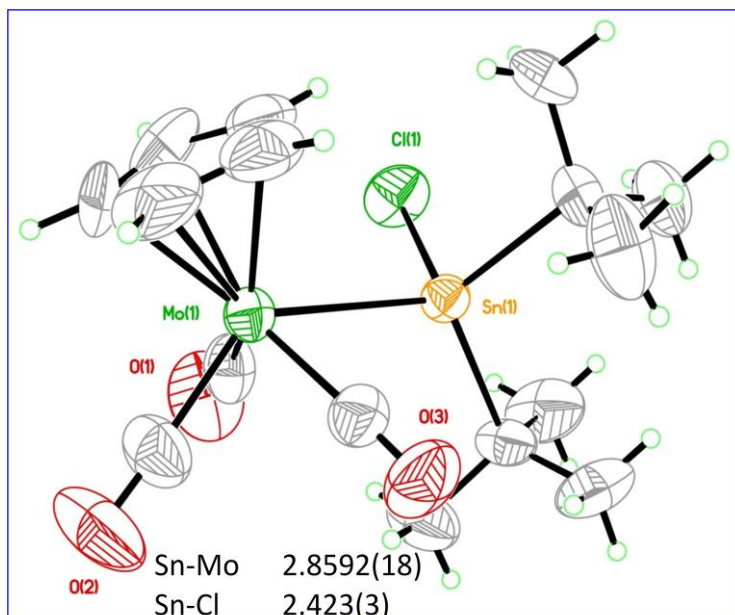
Appendix 1.2 : $^{13}\text{C}/\text{C}_6\text{D}_6$ NMR spectroscopy for $(\eta^5\text{-C}_5\text{H}_5)\text{Mo}(\text{CO})_3\text{Me}$ (**2a**)

^1H NMR(C_6D_6 , 300MHz) 4.39(s,5H, C_5H_5), 0.38(Me); ^{13}C NMR(C_6D_6 ,300MHz) 240.32, (CO), 227.18(2CO), 92.41($(\eta^5\text{-C}_5\text{H}_5)$), -21.98(Me); IR(THF) 2016.11, 1926.81(3CO)

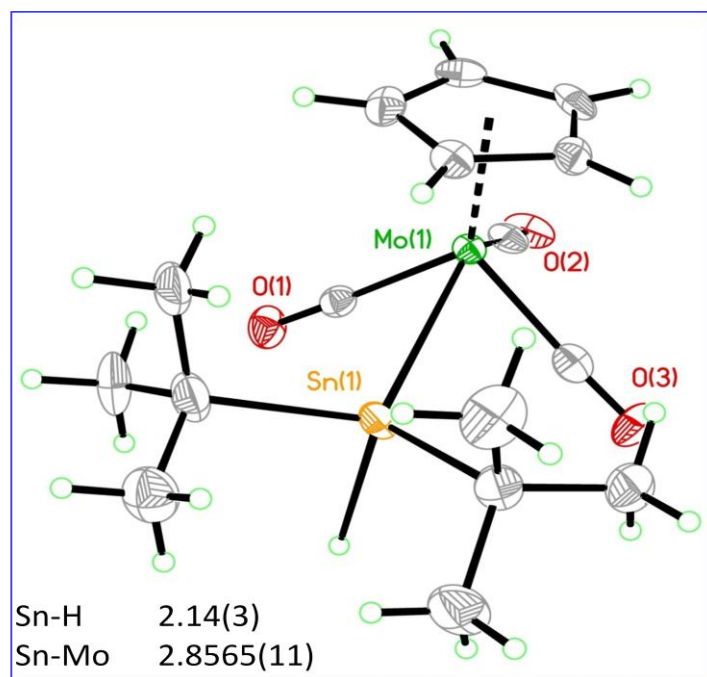


Appendix 1.3 : $^{13}\text{C}/\text{C}_6\text{D}_6$ and ^{31}P NMR spectroscopy for $(\eta^5\text{-C}_5\text{H}_5)\text{Mo}(\text{CO})_2(\text{Ph}_3\text{P})\text{Me} (**2b**)$

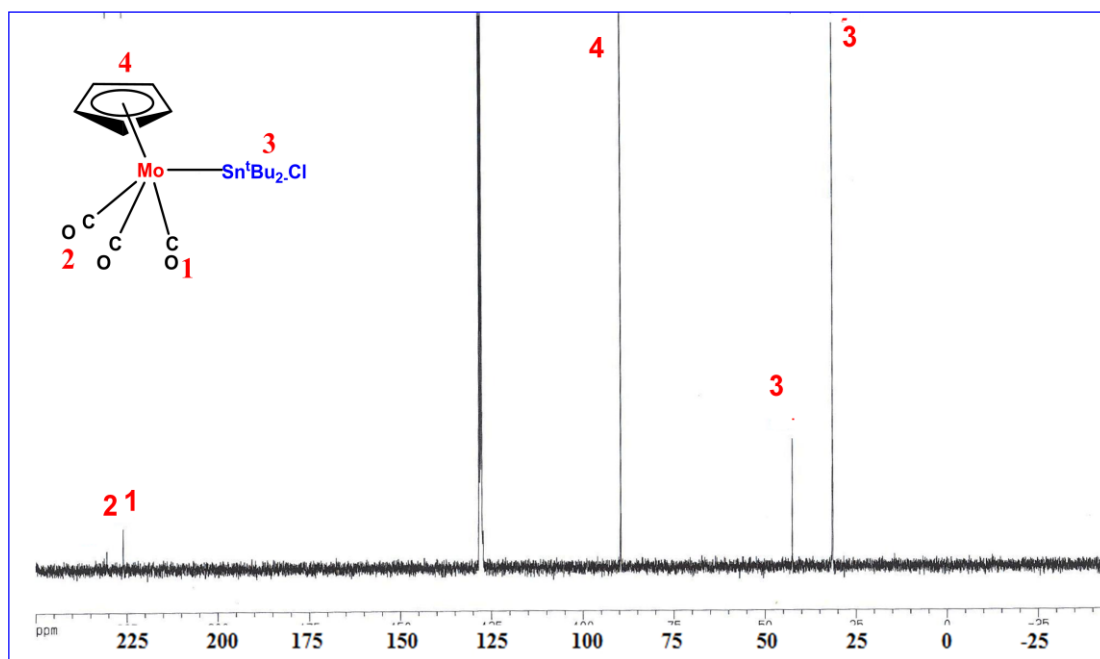
^{13}C NMR (75.4 MHz) (C_6D_6): δ -18.0, 18.13 (d, Me), 92.54 ($(\eta^5\text{-C}_5\text{H}_5)$), ^{31}P NMR (MHz): δ 75.9.



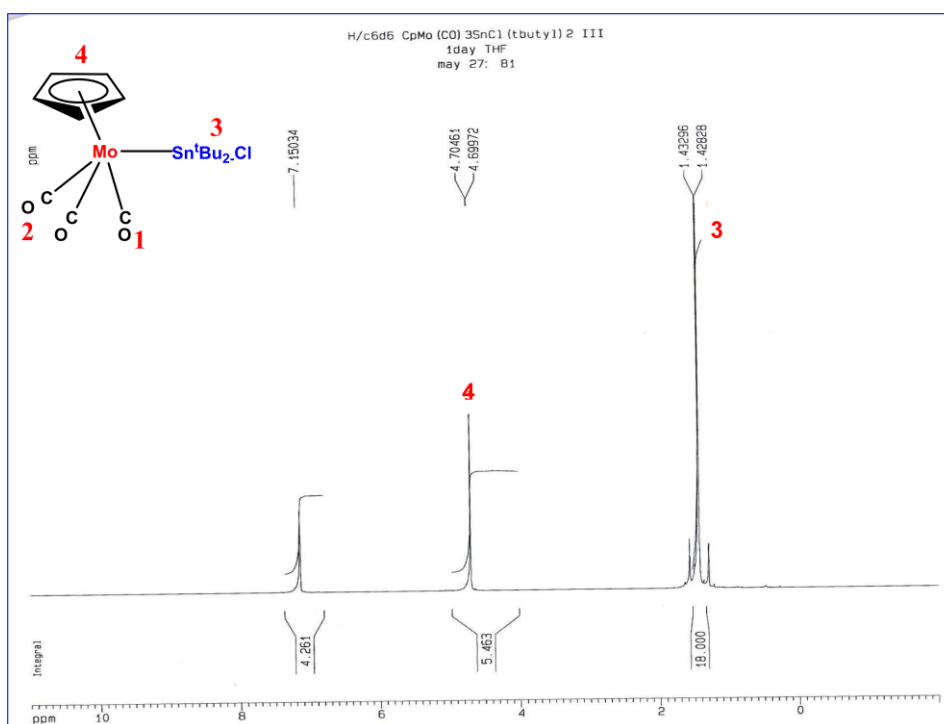
Appendix 1.4: Crystal structure of $(\eta^5\text{-C}_5\text{H}_5)\text{Mo}(\text{CO})_3\text{Sn}^t\text{Bu}_2\text{Cl}$



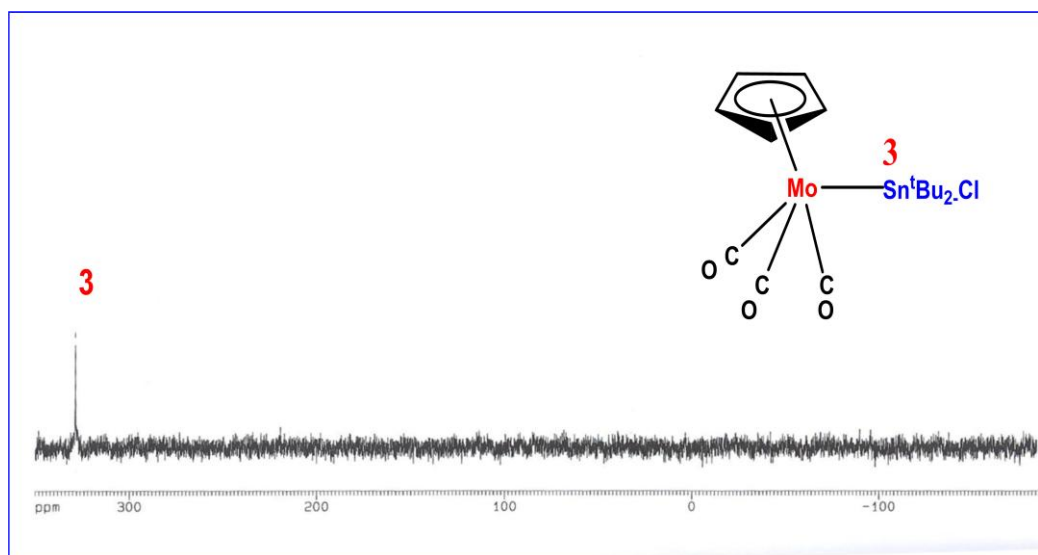
Appendix 1.5: Crystal structure of $(\eta^5\text{-C}_5\text{H}_5)\text{Mo}(\text{CO})_3\text{Sn}^t\text{Bu}_2\text{H}$



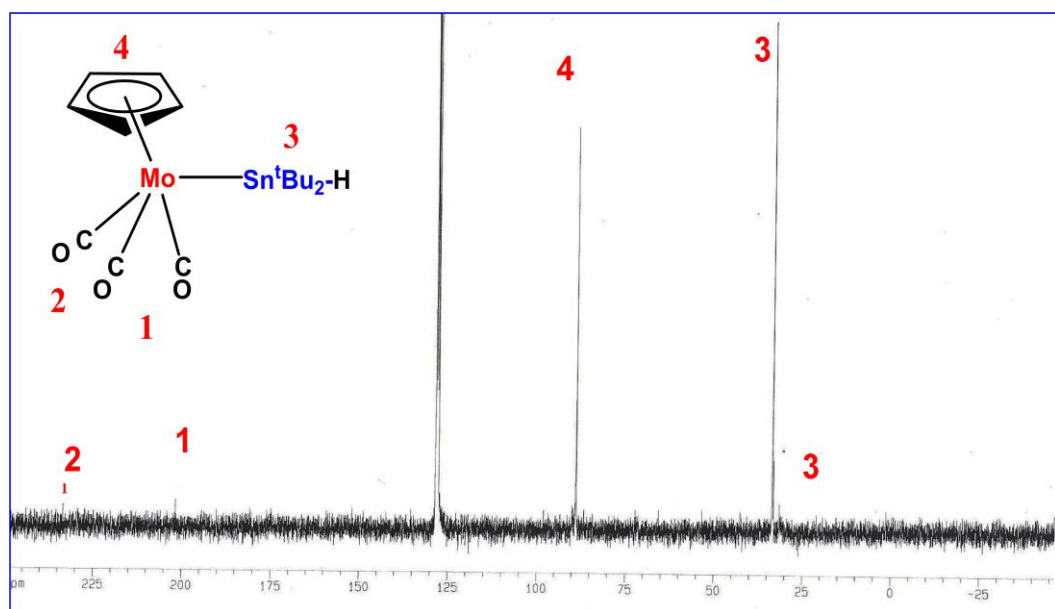
Appendix 1.6: ¹³C/C₆D₆ NMR spectroscopy for $(\eta^5\text{-C}_5\text{H}_5)\text{Mo}(\text{CO})_3\text{Sn}^t\text{Bu}_2\text{Cl}$



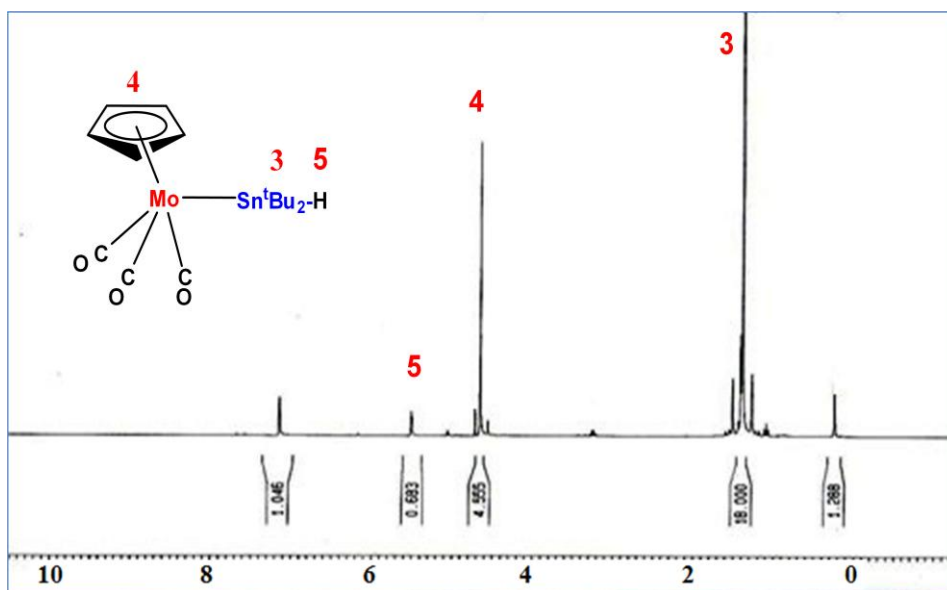
Appendix 1.7: ¹H/C₆D₆ NMR spectroscopy for $(\eta^5\text{-C}_5\text{H}_5)\text{Mo}(\text{CO})_3\text{Sn}^t\text{Bu}_2\text{Cl}$



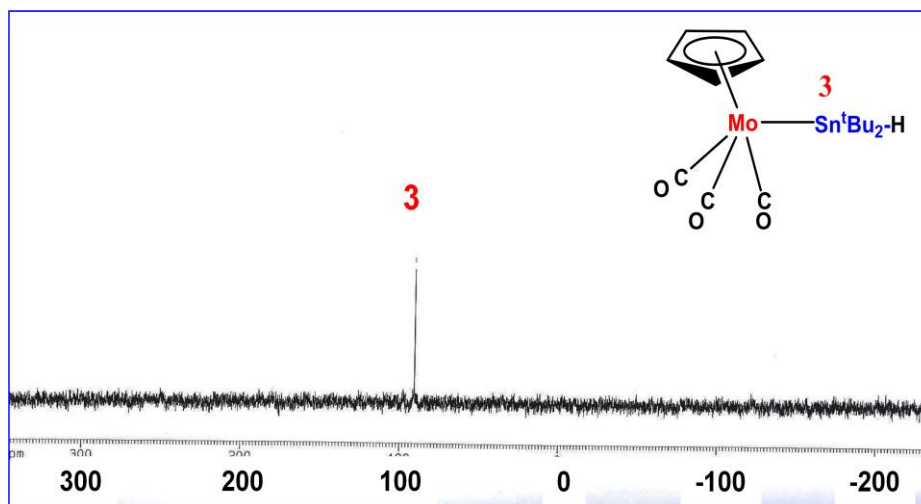
Appendix 1.8: $^{119}\text{Sn}/\text{C}_6\text{D}_6$ NMR spectroscopy for $(\eta^5\text{-C}_5\text{H}_5)\text{Mo}(\text{CO})_3\text{Sn}^t\text{Bu}_2\text{Cl}$



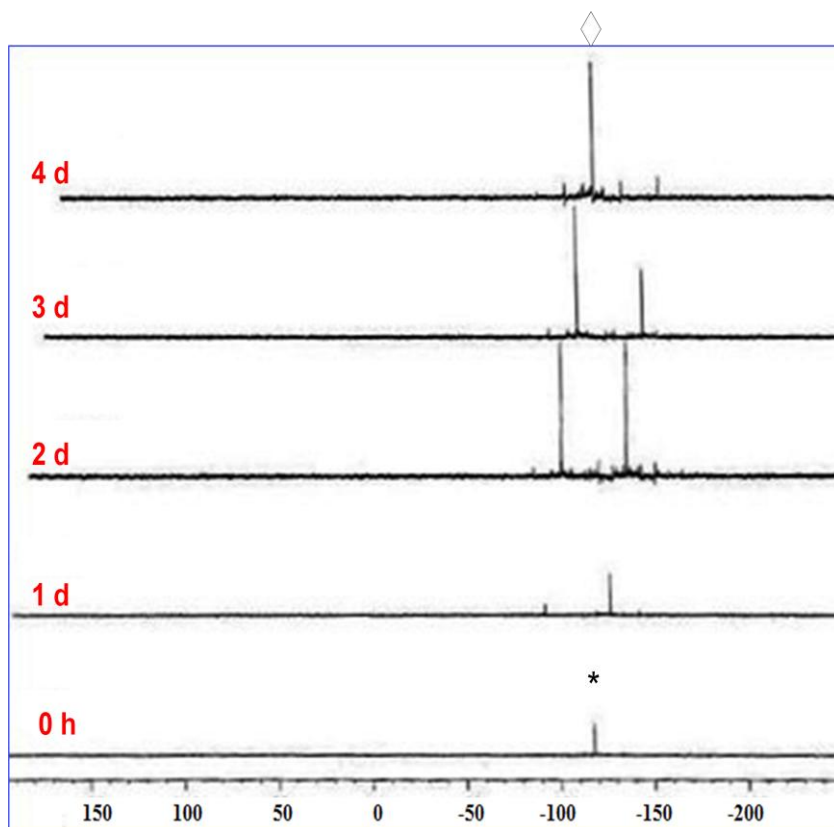
Appendix 1.9: $^{13}\text{C}/\text{C}_6\text{D}_6$ NMR spectroscopy for $(\eta^5\text{-C}_5\text{H}_5)\text{Mo}(\text{CO})_3\text{Sn}^t\text{Bu}_2\text{H}$



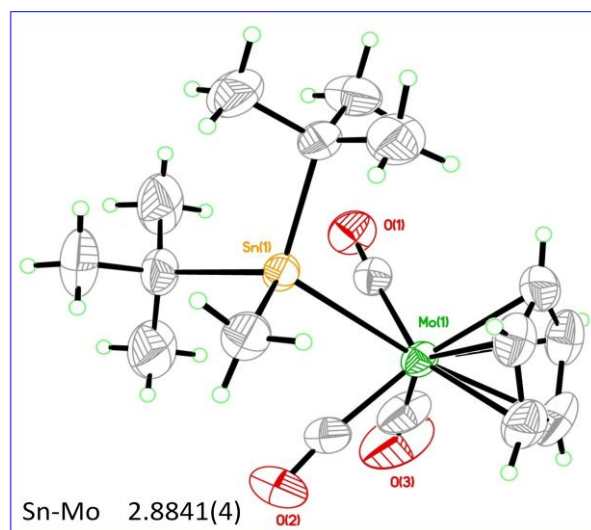
Appendix 1.10: $^1\text{H}/\text{C}_6\text{D}_6$ NMR spectroscopy for $(\eta^5\text{-C}_5\text{H}_5)\text{Mo}(\text{CO})_3\text{Sn}^t\text{Bu}_2\text{H}$



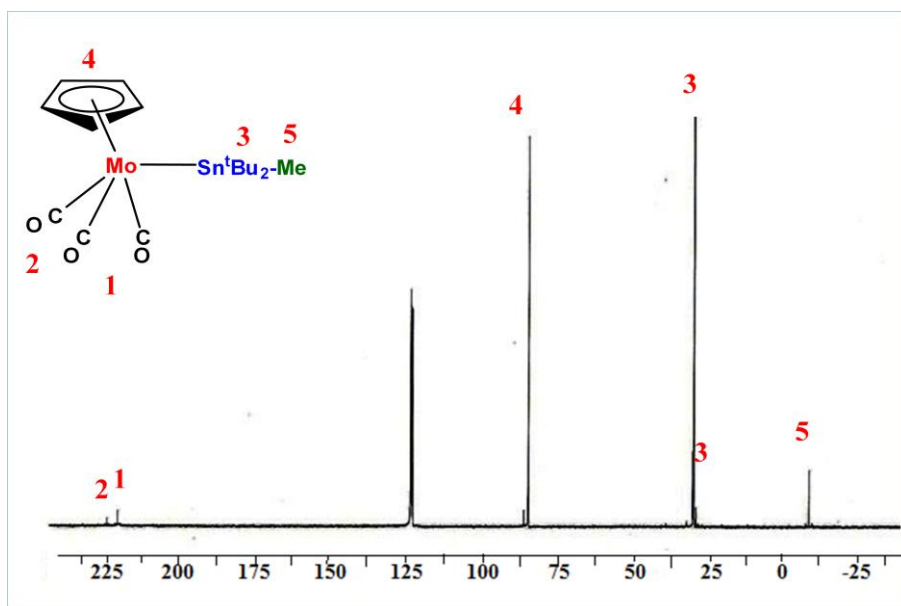
Appendix 1.11: $^{119}\text{Sn}/\text{C}_6\text{D}_6$ NMR spectroscopy for $(\eta^5\text{-C}_5\text{H}_5)\text{Mo}(\text{CO})_3\text{Sn}^t\text{Bu}_2\text{H}$



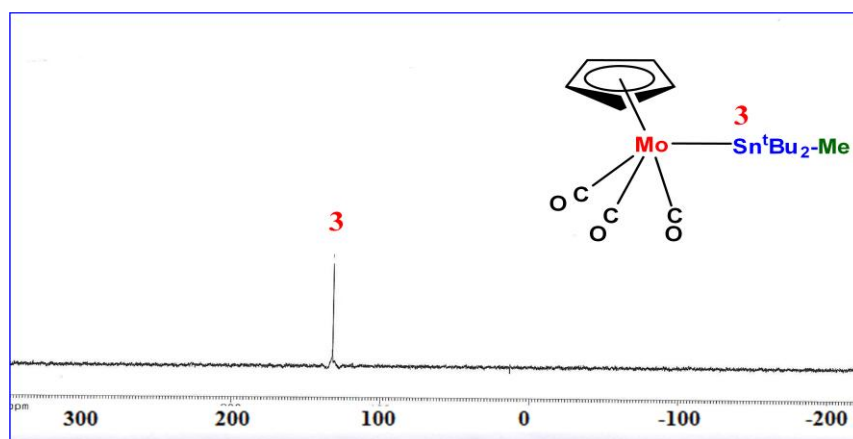
Appendix 1.12: ^{119}Sn NMR spectroscopy monitoring the disappearance of $^t\text{Bu}_2\text{SnH}_2$ (*) into $\text{H}^t\text{Bu}_2\text{Sn-Sn}^t\text{Bu}_2\text{H}$ (◊) in the presence of $(\eta^5\text{-C}_5\text{H}_5)\text{Fe}(\text{CO})(\text{PPh}_3)\text{Me}$ (**1b**) in C_6D_6 , 60°C



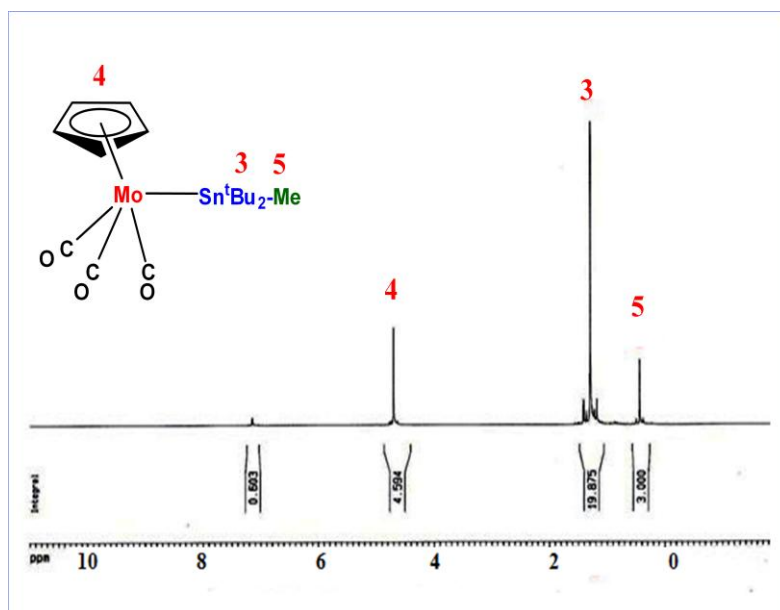
Appendix 1.13: Crystal structure of $(\eta^5\text{-C}_5\text{H}_5)\text{Mo}(\text{CO})_3\text{Sn}^t\text{Bu}_2\text{Me}$



Appendix 1.14: $^{13}\text{C}/\text{C}_6\text{D}_6$ NMR spectroscopy for $(\eta^5\text{-C}_5\text{H}_5)\text{Mo}(\text{CO})_3\text{Sn}^t\text{Bu}_2\text{Me}$

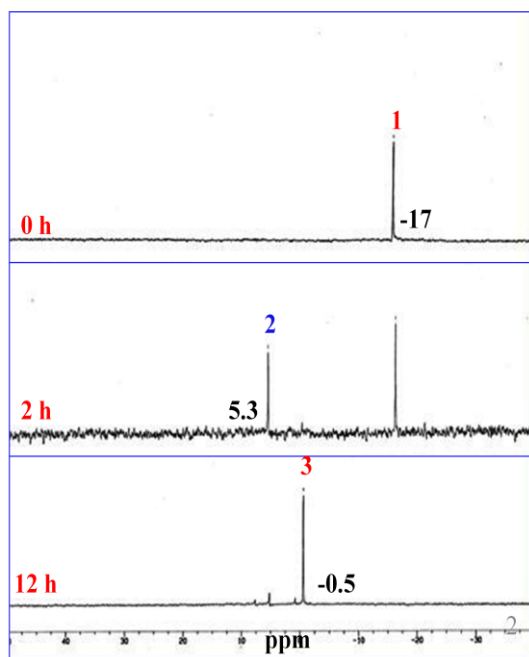


Appendix 1.15: $^{119}\text{Sn}/\text{C}_6\text{D}_6$ NMR spectroscopy for $(\eta^5\text{-C}_5\text{H}_5)\text{Mo}(\text{CO})_3\text{Sn}^t\text{Bu}_2\text{Me}$

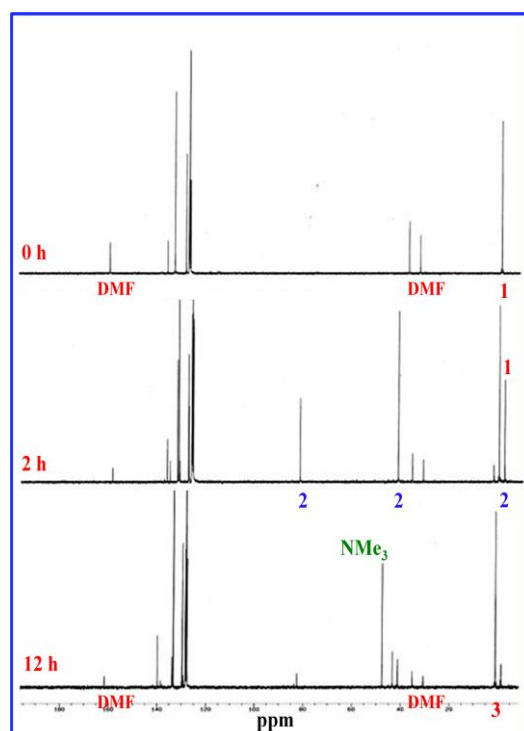


Appendix 1.16: $^1\text{H}/\text{C}_6\text{D}_6$ NMR spectroscopy for $(\eta^5\text{-C}_5\text{H}_5)\text{Mo}(\text{CO})_3\text{Sn}^t\text{Bu}_2\text{Me}$

Synthesis and characterization of $R_3SiOCH_2NMe_2$



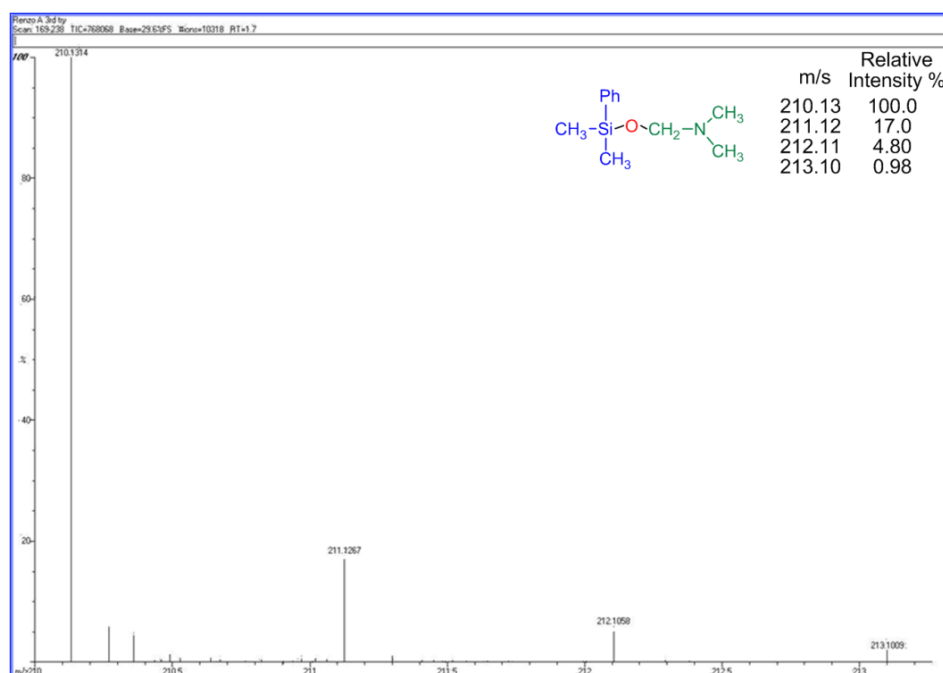
Appendix 2.1: ^{29}Si NMR spectroscopy monitoring the disappearance of 1 mol of $PhMe_2SiH$ (1) into $PhMe_2SiOCH_2NMe_2$ (2) and then the reaction continues to form $PhMe_2SiOSiMe_2Ph$ (3) in the presence a 5 mol% catalyst $Mo(CO)_6$ and 2 mol of DMF in C_6D_6 at $90^\circ C$.



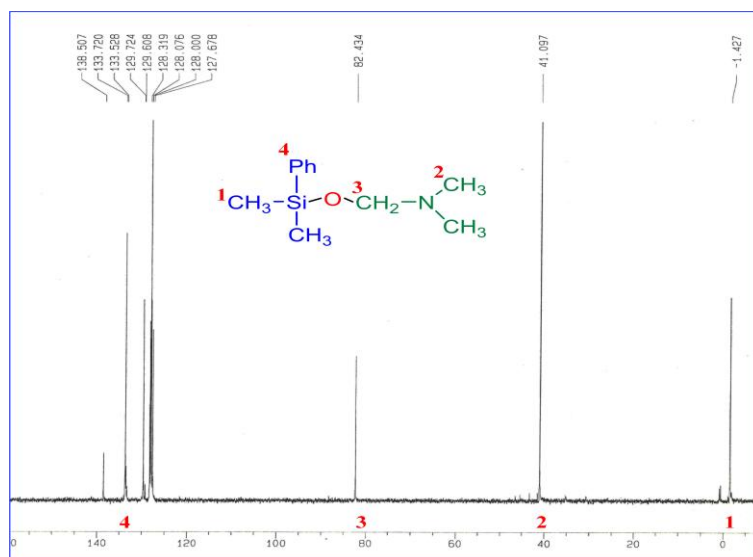
Appendix 2.2: ^{13}C NMR spectroscopy monitoring the disappearance of 1 mol of $PhMe_2SiH$ (1) into $PhMe_2SiOCH_2NMe_2$ (2) and then the reaction continues to form $PhMe_2SiOSiMe_2Ph$ (3) in the presence a 5 mol% catalyst $Mo(CO)_6$ and 2 mol of DMF in C_6D_6 at $90^\circ C$.



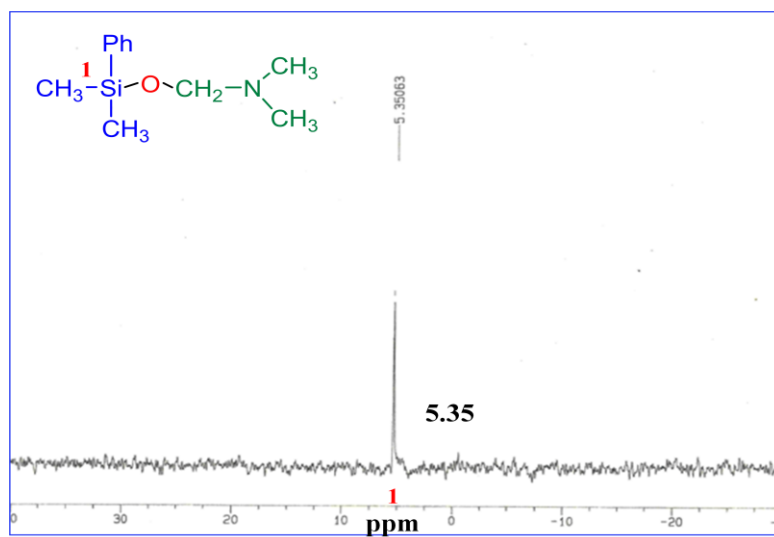
Appendix 2.3: ¹³C 135 DEPT NMR spectroscopy to identify the CH₂ from PhMe₂SiOCH₂NMe₂



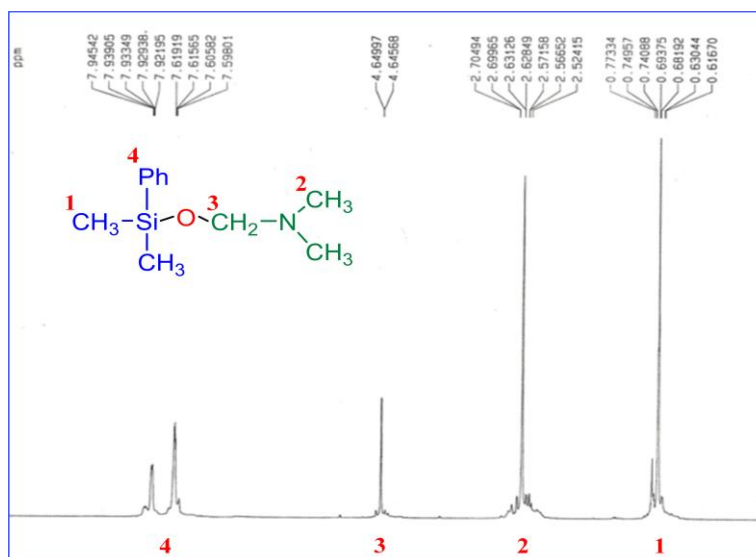
Appendix 2.4: Mass spectrum (ESI) m/s: data for PhMe₂SiOCH₂NMe₂ in hexanes.



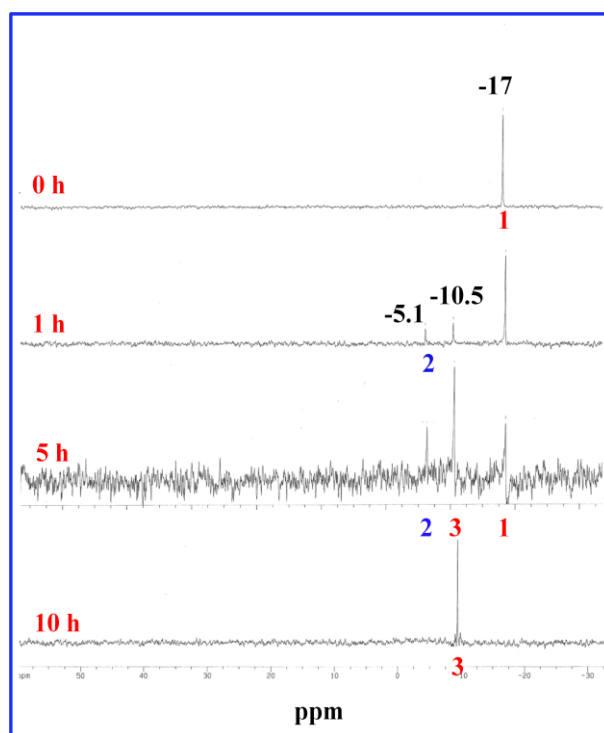
Appendix 2.5: ^{13}C NMR spectroscopic of $\text{PhMe}_2\text{SiOCH}_2\text{NMe}_2$ in C_6D_6



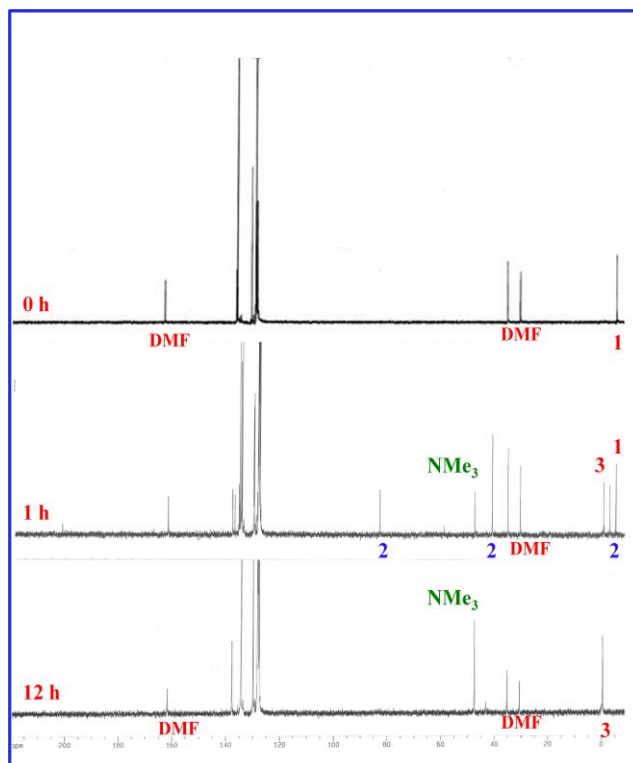
Appendix 2.6: ^{29}Si NMR spectroscopic of $\text{PhMe}_2\text{SiOCH}_2\text{NMe}_2$ in C_6D_6



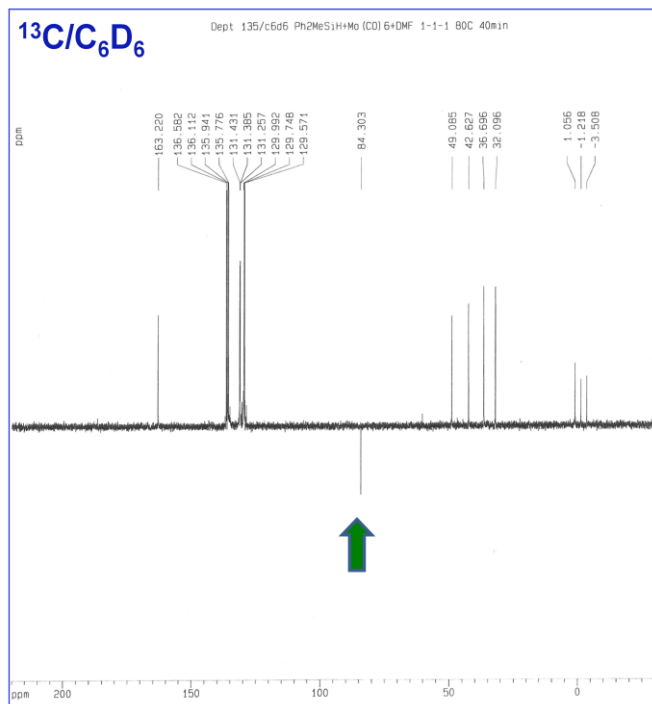
Appendix 2.7: ^1H NMR spectroscopic of $\text{PhMe}_2\text{SiOCH}_2\text{NMe}_2$ in C_6D_6



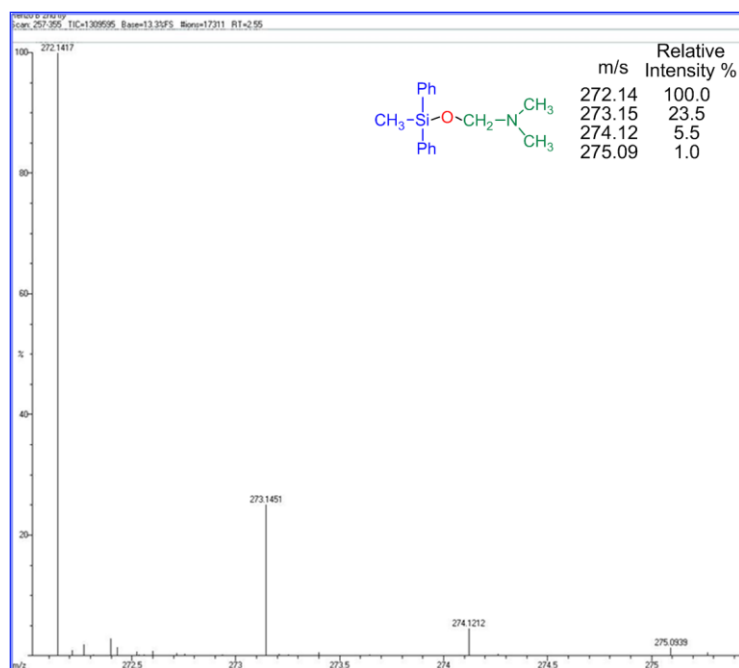
Appendix 2.8: ^{29}Si NMR spectroscopy monitoring the disappearance of 1 mol of Ph_2MeSiH (1) into $\text{Ph}_2\text{MeSiOCH}_2\text{NMe}_2$ (2) and then the reaction continues to form $\text{Ph}_2\text{MeSiOSiMePh}_2$ (3) in the presence a 5 mol% catalyst $\text{Mo}(\text{CO})_6$ and 2 mol of DMF in C_6D_6 at 90°C .



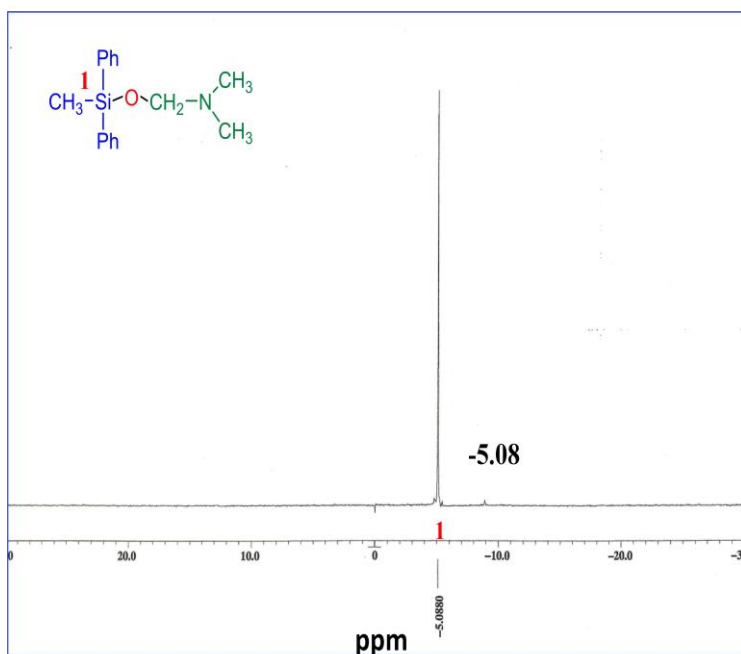
Appendix 2.9: ^{13}C NMR spectroscopy monitoring the disappearance of 1 mol of Ph_2MeSiH (1) into $\text{Ph}_2\text{MeSiOCH}_2\text{NMe}_2$ (2) and then the reaction continues to form $\text{Ph}_2\text{MeSiOSiMePh}_2$ (3) in the presence a 5 mol% catalyst $\text{Mo}(\text{CO})_6$ and 2 mol of DMF in C_6D_6 at 90°C .



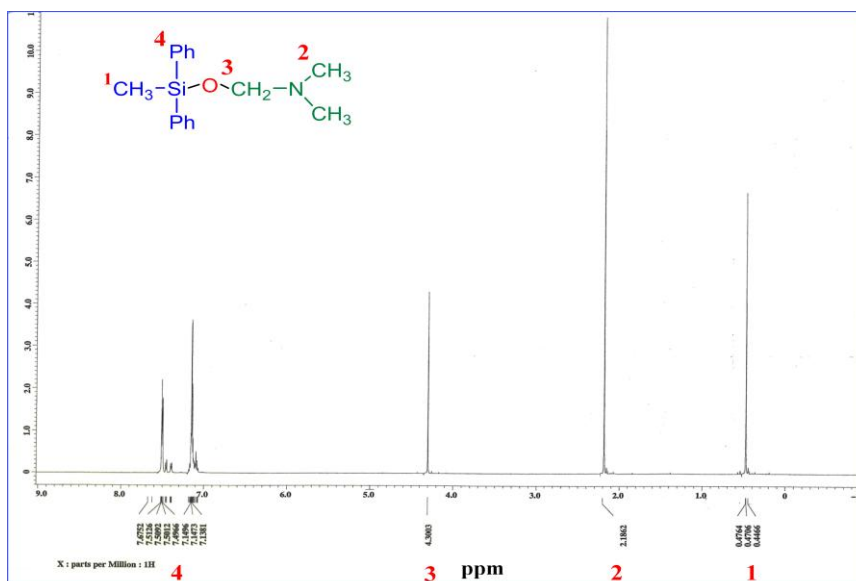
Appendix 2.10: ^{13}C 135 DEPT NMR spectroscopy to identify the CH_2 from $\text{Ph}_2\text{MeSiOCH}_2\text{NMe}_2$



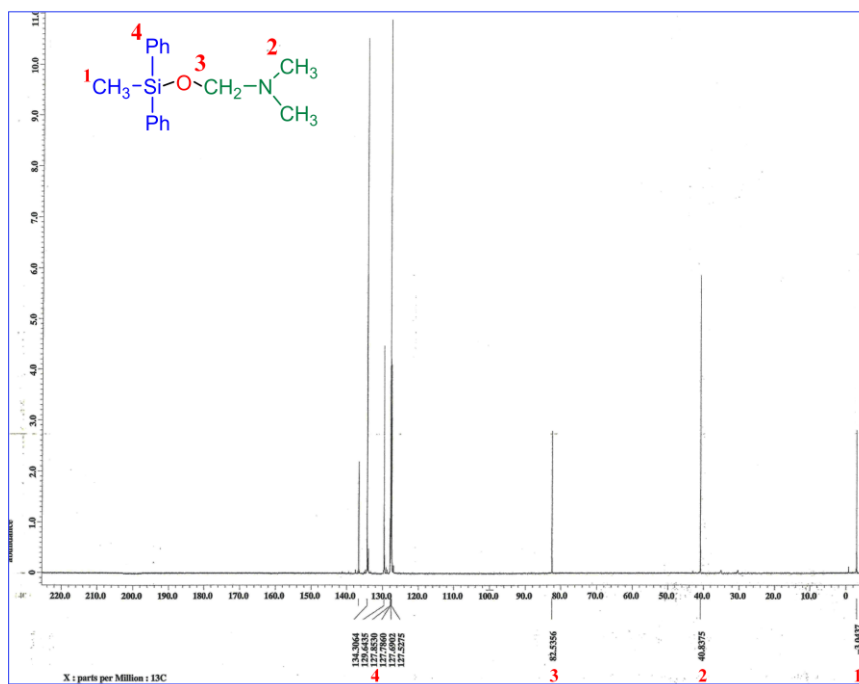
Appendix 2.11: Mass spectrum (ESI) m/z : data for $\text{Ph}_2\text{MeSiOCH}_2\text{NMe}_2$ in hexanes.



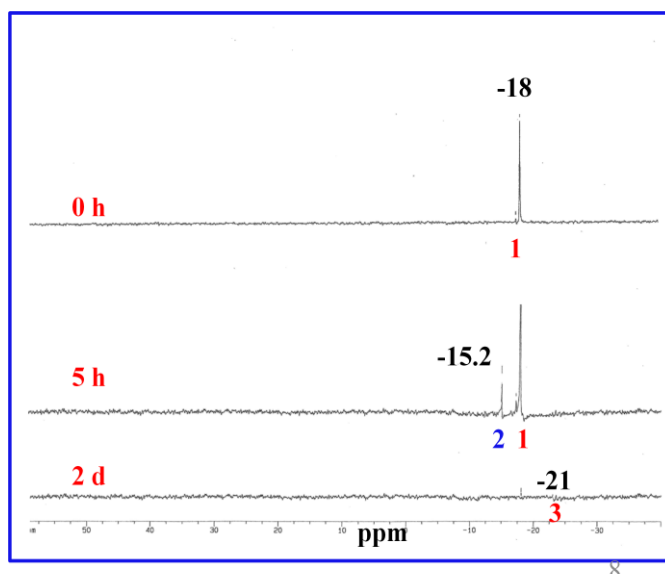
Appendix 2.12: ^{29}Si NMR spectroscopic of $\text{Ph}_2\text{Me}_2\text{SiOCH}_2\text{NMe}_2(1)$ in C_6D_6



Appendix 2.13: ¹H NMR spectroscopic of Ph₂Me₂SiOCH₂NMe₂ in C₆D₆

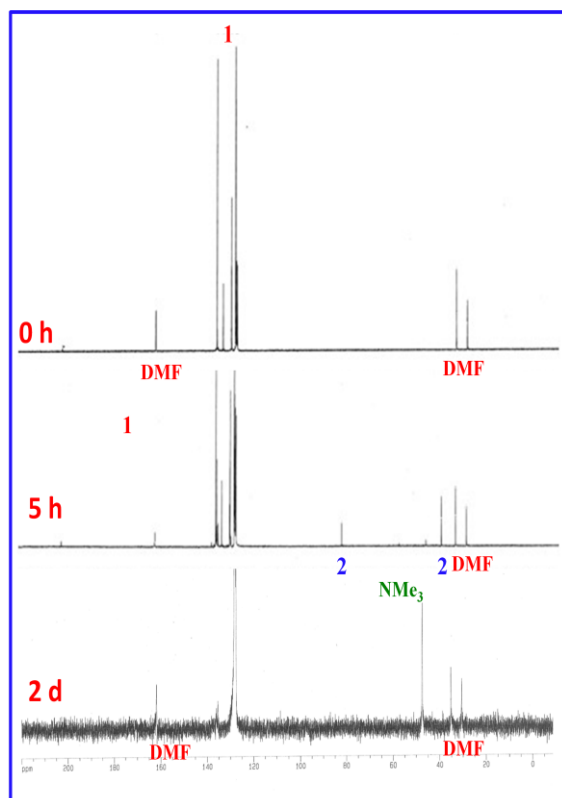


Appendix 2.14: ¹³C NMR spectroscopic of Ph₂Me₂SiOCH₂NMe₂ in C₆D₆

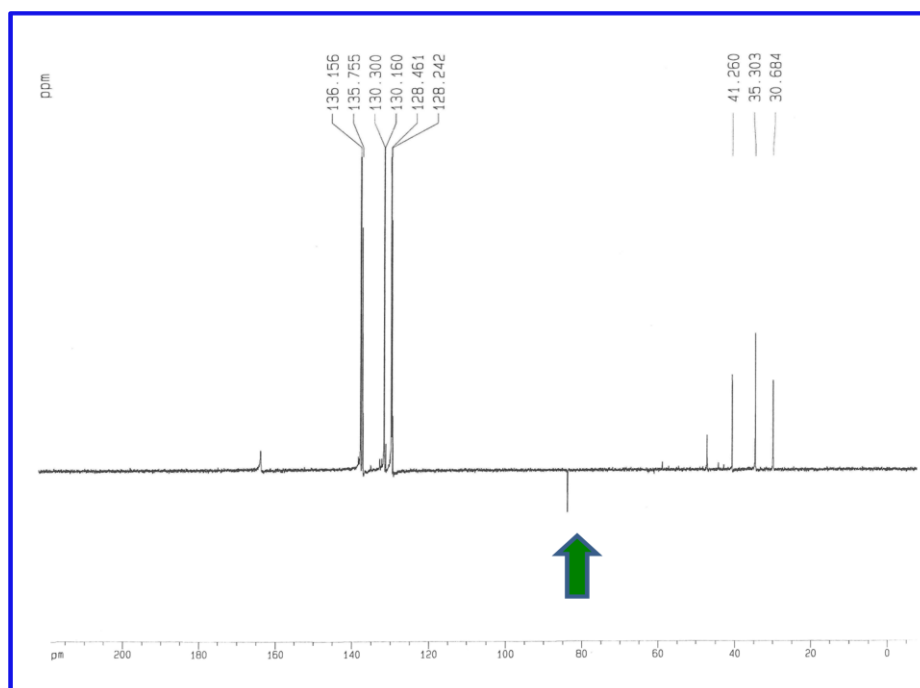


Appendix 2.15: ^{29}Si NMR spectroscopy monitoring the disappearance of 1 mol of Ph_3SiH (1) into $\text{Ph}_3\text{SiOCH}_2\text{NMe}_2$ (2) and then the reaction continues to form $\text{Ph}_3\text{SiOSiPh}_3$ (3) in the presence a 5 mol% catalyst $\text{Mo}(\text{CO})_6$ and 2 mol of DMF in C_6D_6 at 90°C .

Note: The siloxane formed precipitated in the course of the reaction but in the $^{29}\text{Si}/\text{CDCl}_3$ the signal is observed at -21ppm.

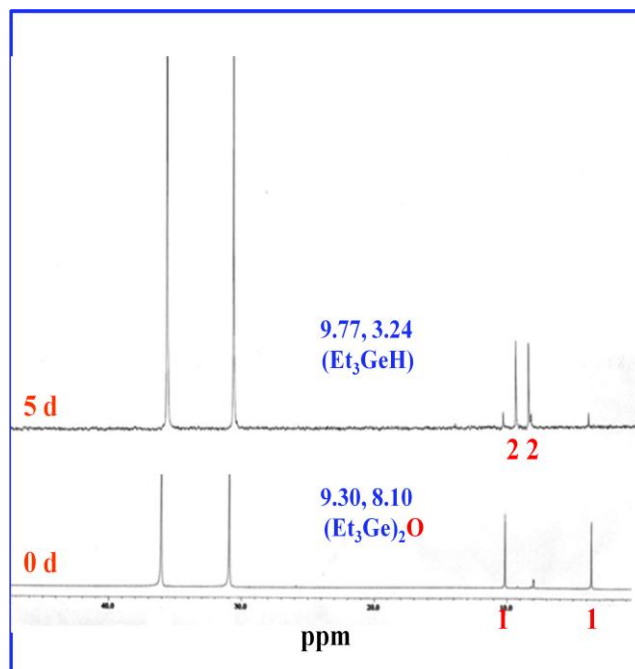


Appendix 2.16: ^{13}C NMR spectroscopy monitoring the disappearance of 1 mol of Ph_3SiH (1) into $\text{Ph}_3\text{SiOCH}_2\text{NMe}_2$ (2) and then the reaction continues to form $\text{Ph}_3\text{SiOSiPh}_3$ (3) in the presence a 5 mol% catalyst $\text{Mo}(\text{CO})_6$ and 2 mol of DMF in C_6D_6 at 90°C . Note: The siloxane formed precipitated in the course of the reaction but in the $^{29}\text{Si}/\text{CDCl}_3$ the signal is observed at -21ppm.

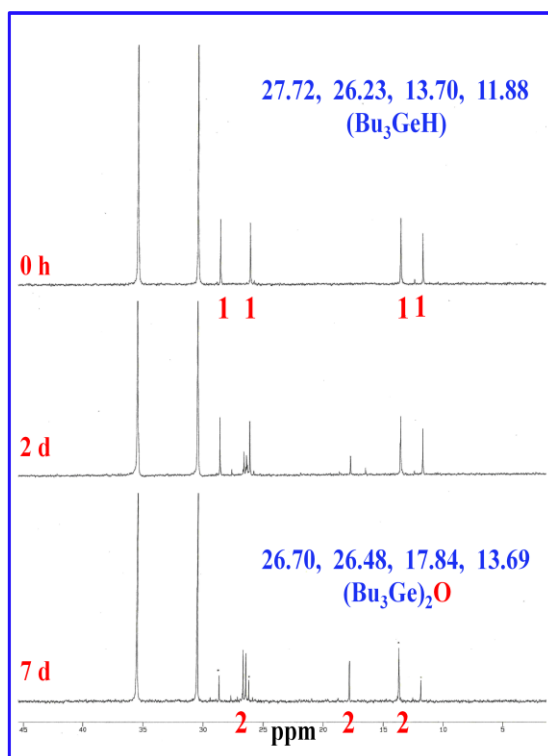


Appendix 2.17: ^{13}C 135 DEPT NMR spectroscopy to identify the CH_2 from $\text{Ph}_3\text{SiOCH}_2\text{NMe}_2$

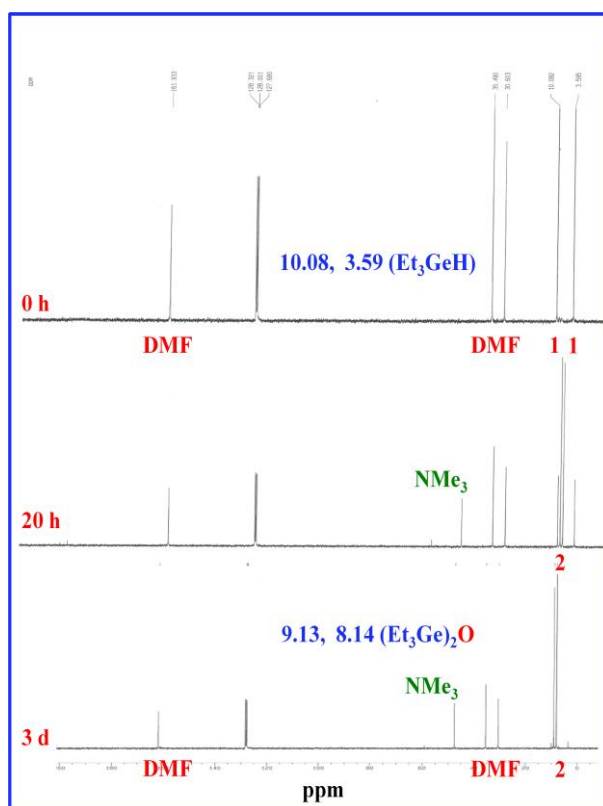
Synthesis and characterization of $\text{R}_3\text{Ge-O-GeR}_3$ using 2b, 3a



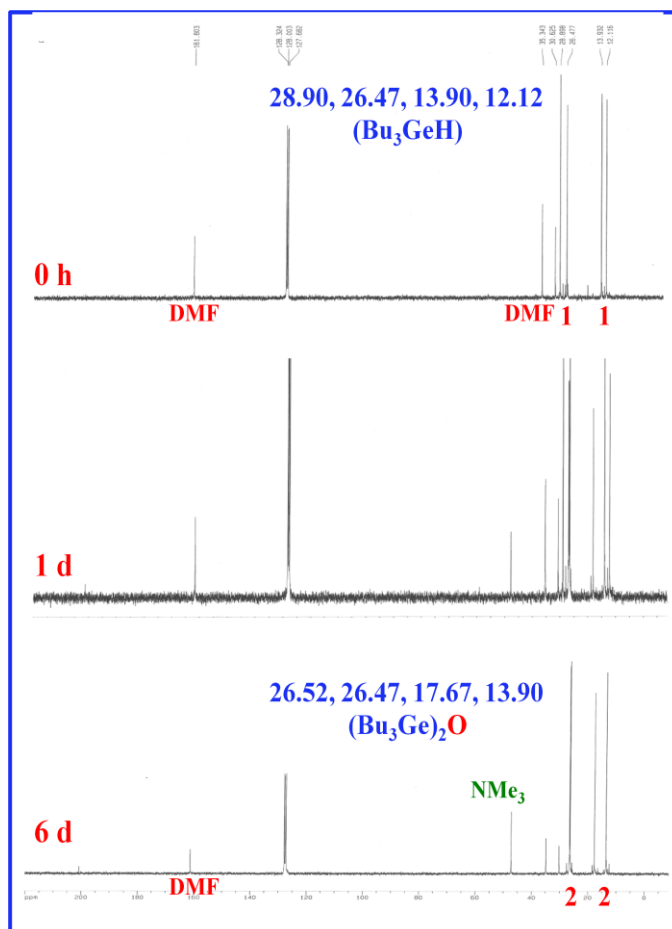
Appendix 2.18: ^{13}C NMR spectroscopy monitoring the disappearance of 1 mol of Et_3GeH (1) into $\text{Et}_3\text{GeOGeEt}_3$ (2) in the presence of a 5 mol% catalyst ($\eta^5\text{-C}_5\text{H}_5$) $\text{Mo}(\text{CO})_2\text{Ph}_3\text{PMe}$ and 3 mol of DMF in C_6D_6 at 90°C .



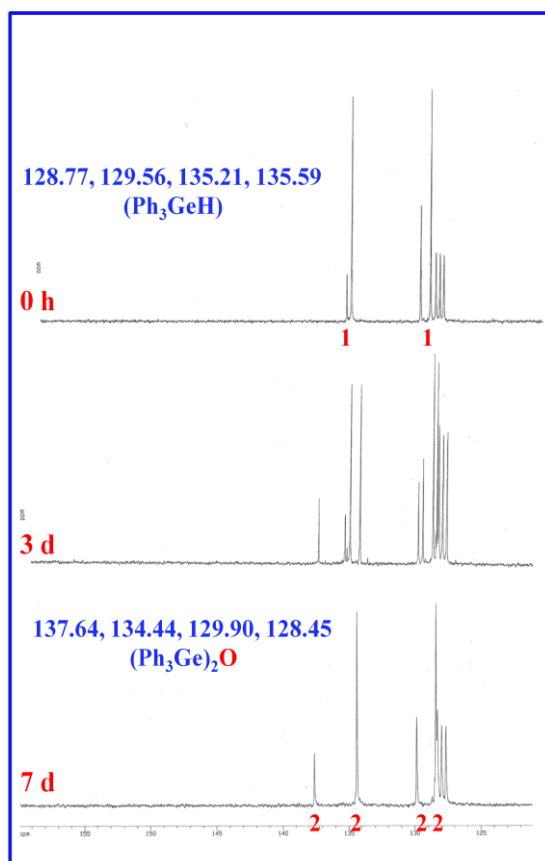
Appendix 2.19: ^{13}C NMR spectroscopy monitoring the disappearance of 1 mol of Bu_3GeH (1) into $\text{Bu}_3\text{GeOGeBu}_3$ (2) in the presence a 5 mol% catalyst $(\eta^5\text{-C}_5\text{H}_5)\text{Mo}(\text{CO})_2\text{Ph}_3\text{PMe}$ and 3 mol of DMF in C_6D_6 at 90°C .



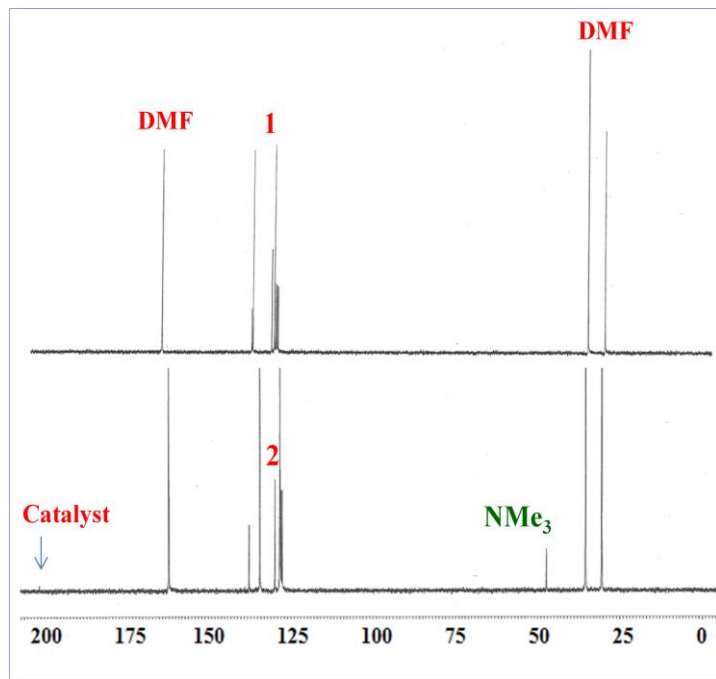
Appendix 2.20: ^{13}C NMR spectroscopy monitoring the disappearance of 1 mol of Et_3GeH (1) into $\text{Et}_3\text{GeOGeEt}_3$ (2) and NMe_3 at 47ppm in the presence a 5 mol% catalyst $\text{Mo}(\text{CO})_6$ and 3 mol of DMF in C_6D_6 . At 90°C



Appendix 2.21: ¹³C NMR spectroscopy monitoring the disappearance of 1 mol of Bu₃GeH (1) into Bu₃GeOGeBu₃ (2) and NMe₃ at 47ppm in the presence a 5 mol% catalyst Mo(CO)₆ and 3 mol of DMF in C₆D₆.
At 90°C

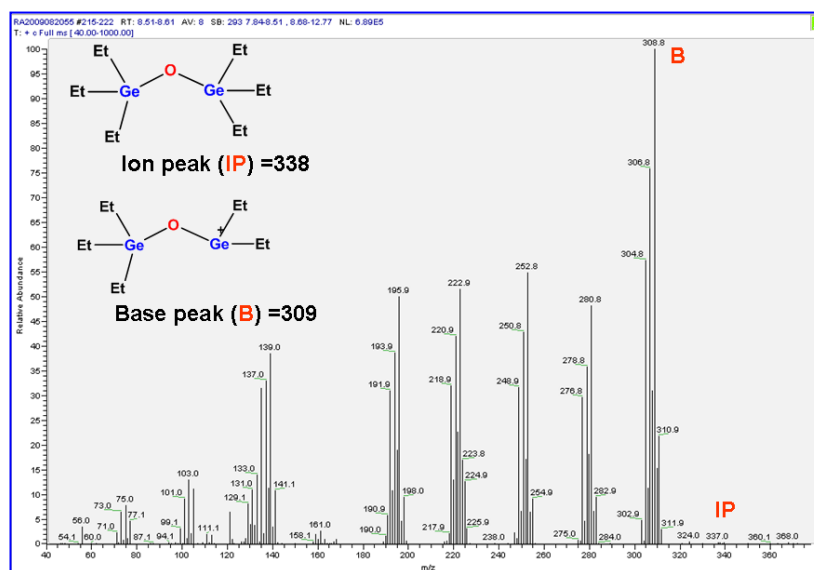


Appendix 2.22: ^{13}C NMR spectroscopy monitoring the disappearance of 1 mol of Ph_3GeH (1) into $\text{Ph}_3\text{GeOGePh}_3$ (2) in the presence a 5 mol% catalyst $\text{Mo}(\text{CO})_6$ and 3 mol of DMF in C_6D_6 at 120°C .

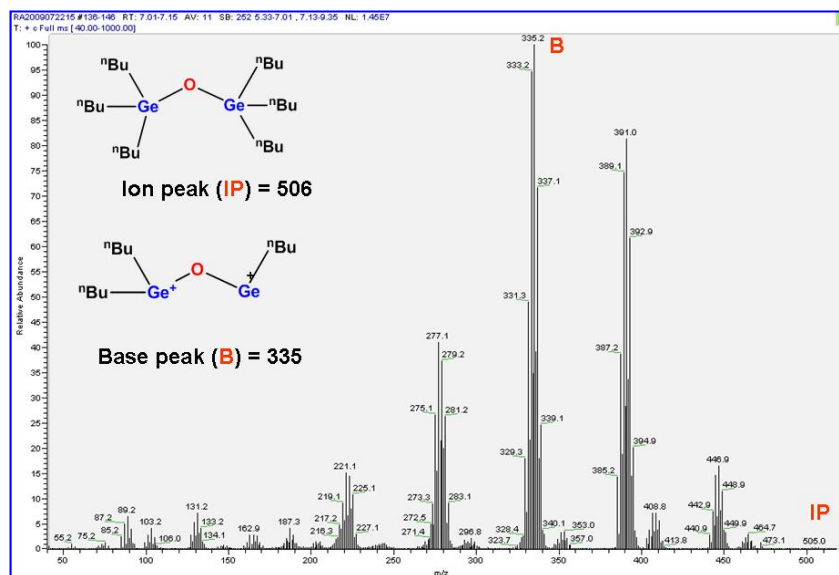


Appendix 2.23: ^{13}C NMR spectroscopy monitoring the disappearance of 1 mol of Ph_3GeH (1) into $\text{Ph}_3\text{GeOGePh}_3$ (2) in the presence a 5 mol% catalyst $\text{Mo}(\text{CO})_6$ and 3 mol of DMF in C_6D_6 at 120°C .

a)



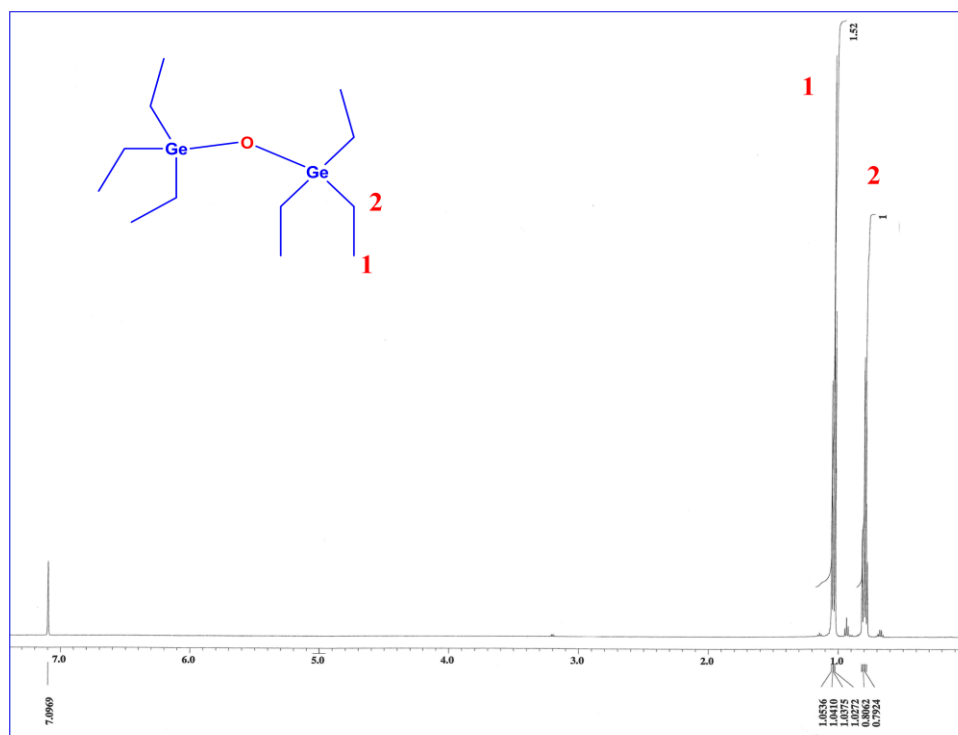
b)



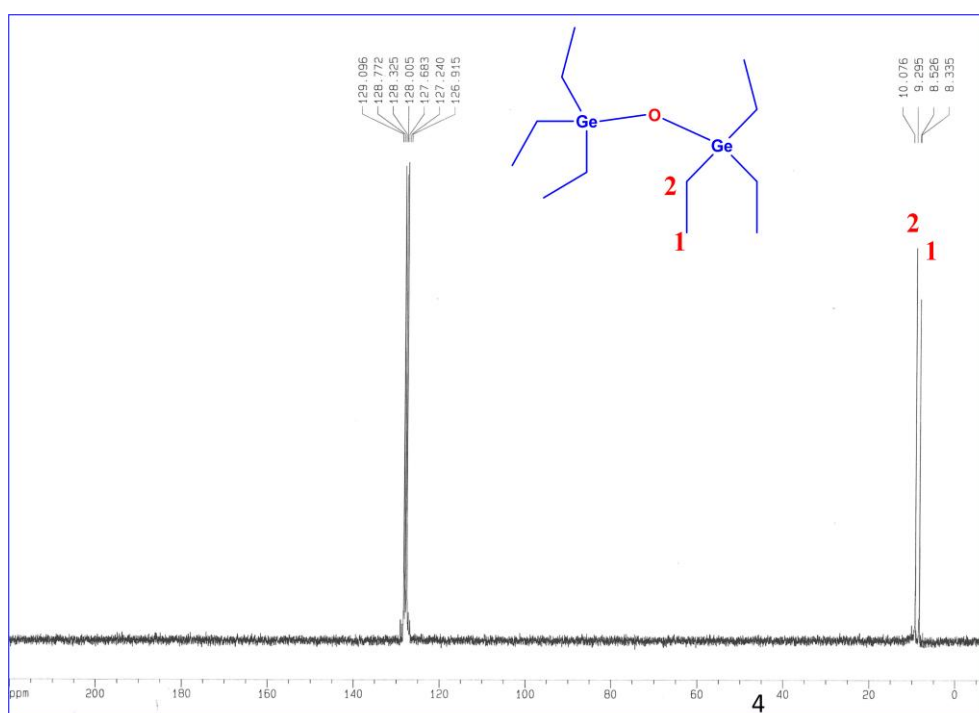
Appendix 2.24: Mass spectra of (a) $\text{Et}_3\text{GeOGeEt}_3$ (b) $\text{Bu}_3\text{GeOGeBu}_3$

The use of GC to distinguish the germanoxane products resulted in retention times of 8.58 min for $\text{Et}_3\text{GeOGeEt}_3$ (a), and 7.11 min for $\text{Bu}_3\text{GeOGeBu}_3$ (b), in Hexanes solution.

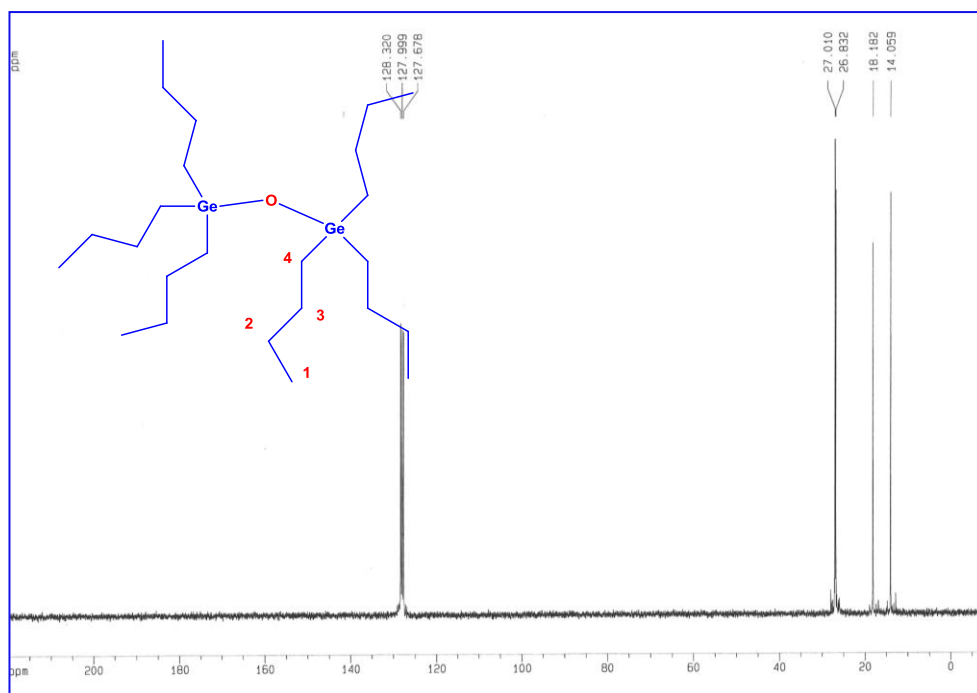
The molecular ion (IP) and base peak (B) at 338 and 309 belong to the $\text{Et}_3\text{GeOGeEt}_3$ (3), and the 506 and 335 for the $\text{Bu}_3\text{GeOGeBu}_3$ (4), respectively



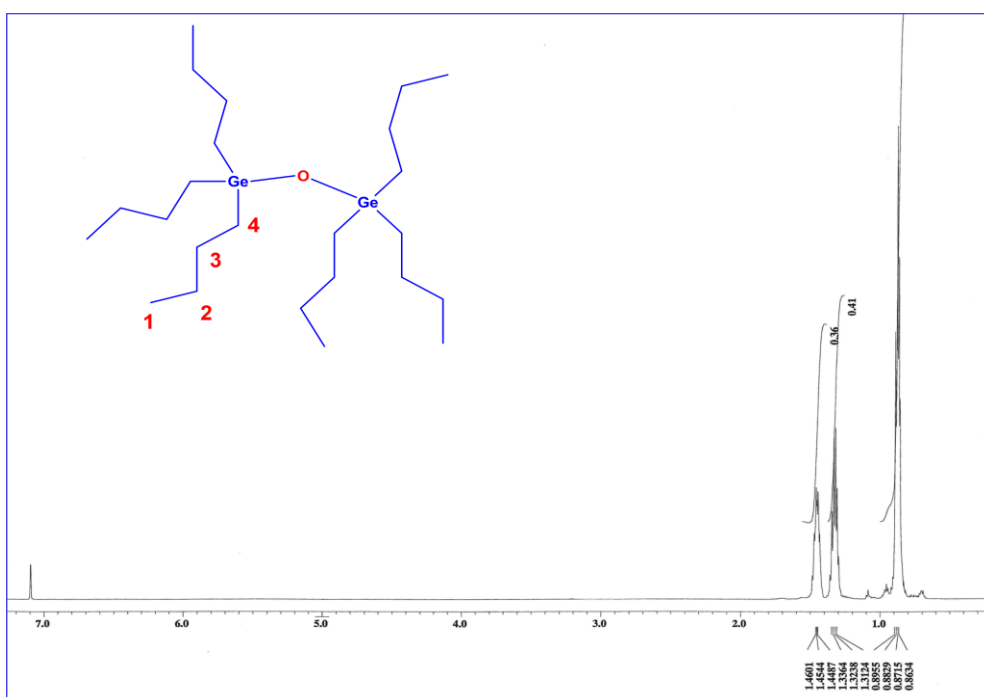
Appendix 2.25: ¹H NMR spectroscopy for Et₃GeOGeEt₃



Appendix 2.26: ¹³C NMR spectroscopy for Et₃GeOGeEt₃

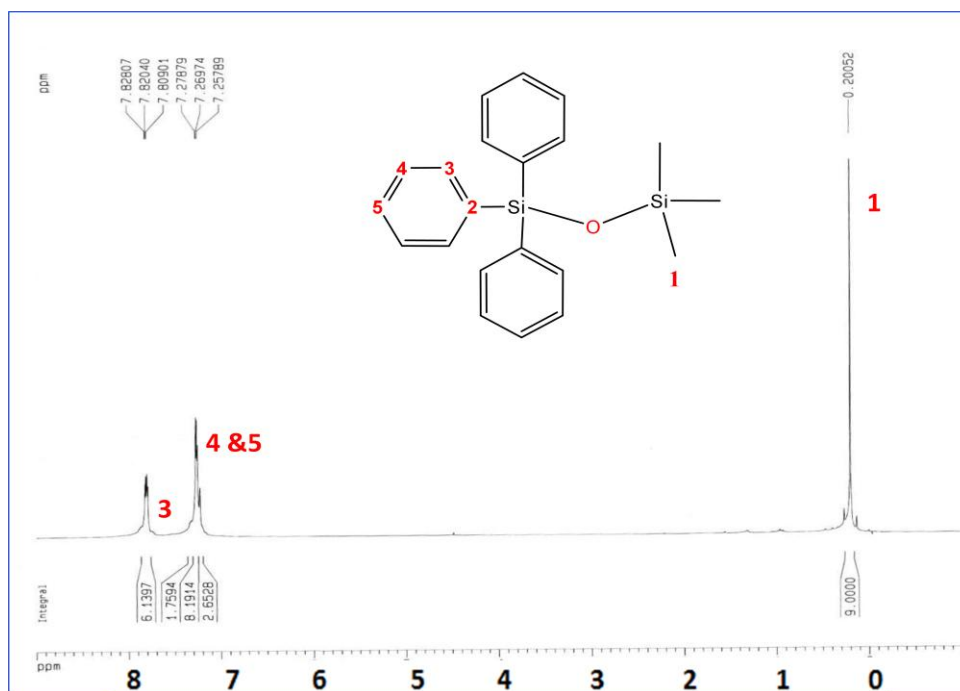


Appendix 2.27: ¹³C NMR spectroscopy for $\text{Bu}_3\text{GeOGeBu}_3$

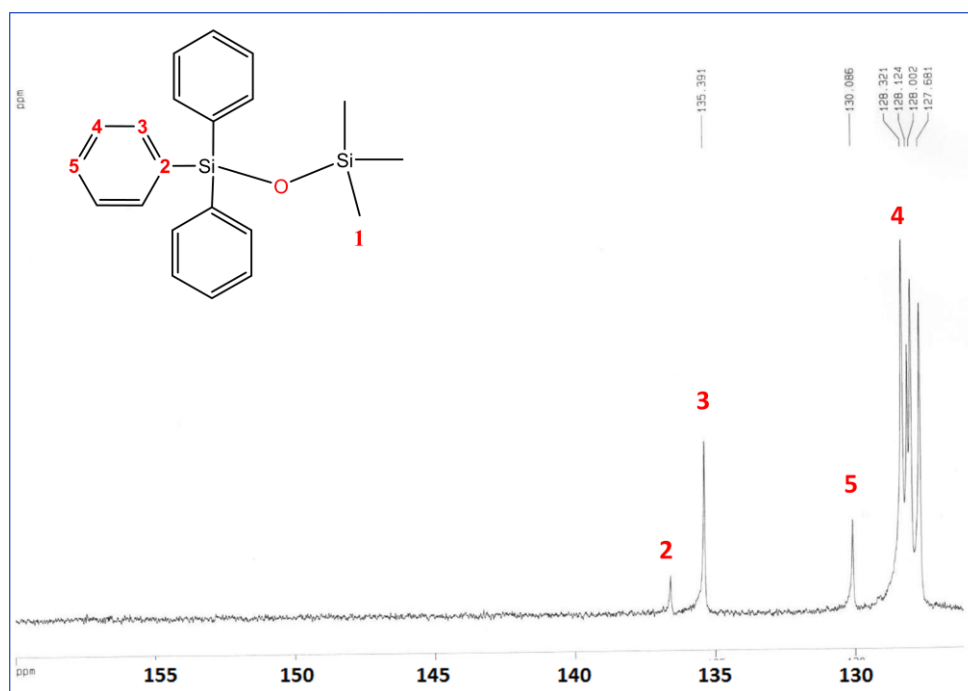


Appendix 2.28: ¹H NMR spectroscopy for $\text{Bu}_3\text{GeOGeBu}_3$

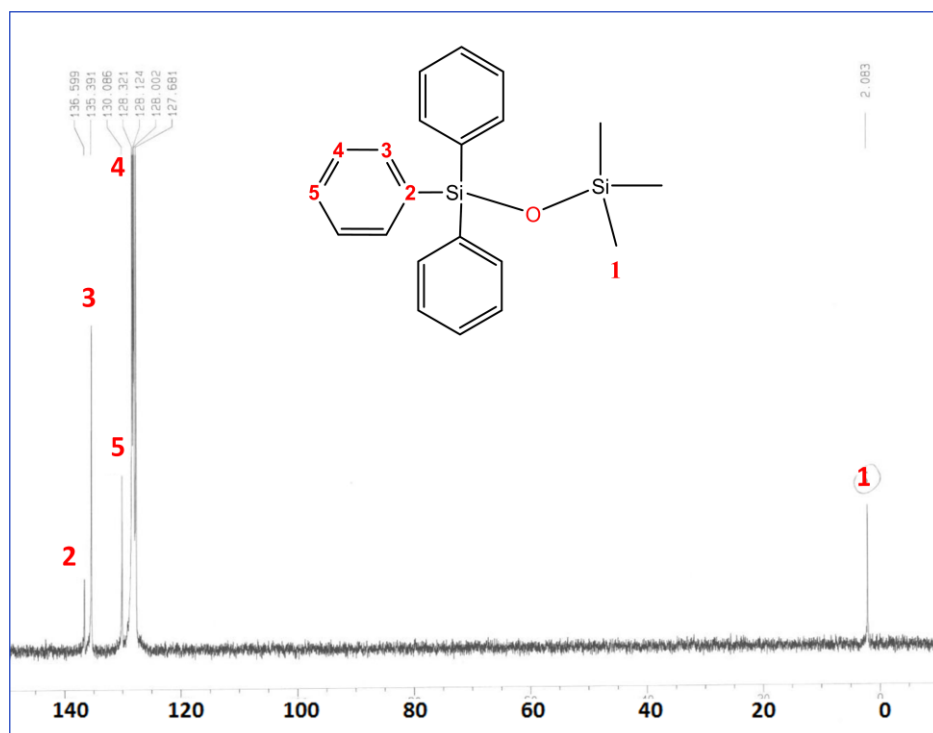
Synthesis of mixed siloxanes $\text{Me}_3\text{SiOER}_3$



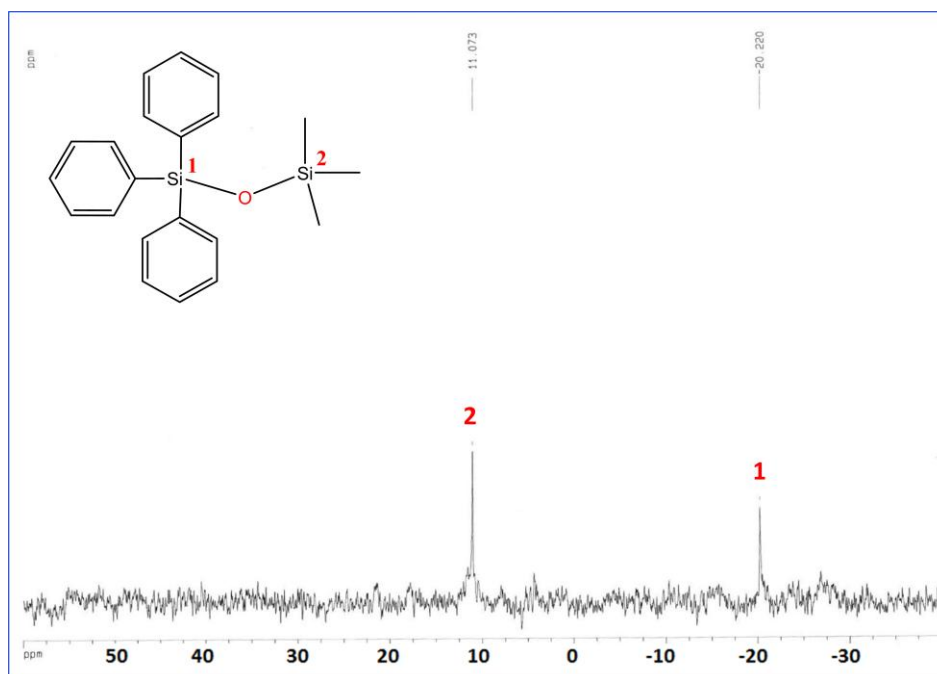
Appendix 2.29: ^1H NMR spectroscopy for $\text{Ph}_3\text{Si-O-SiMe}_3$



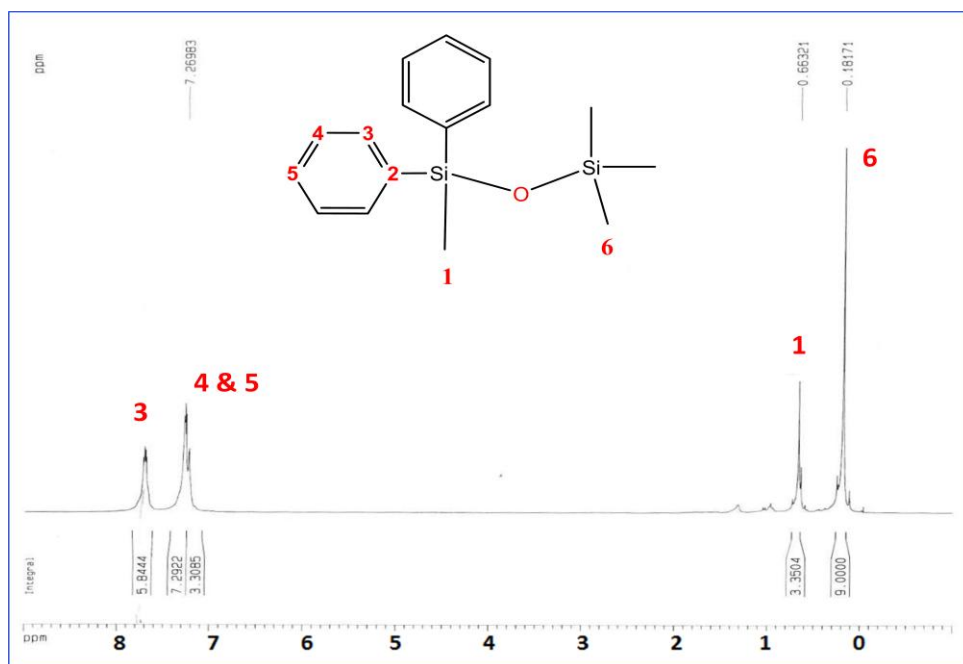
Appendix 2.30: ^{13}C NMR spectroscopy for $\text{Ph}_3\text{Si-O-SiMe}_3$



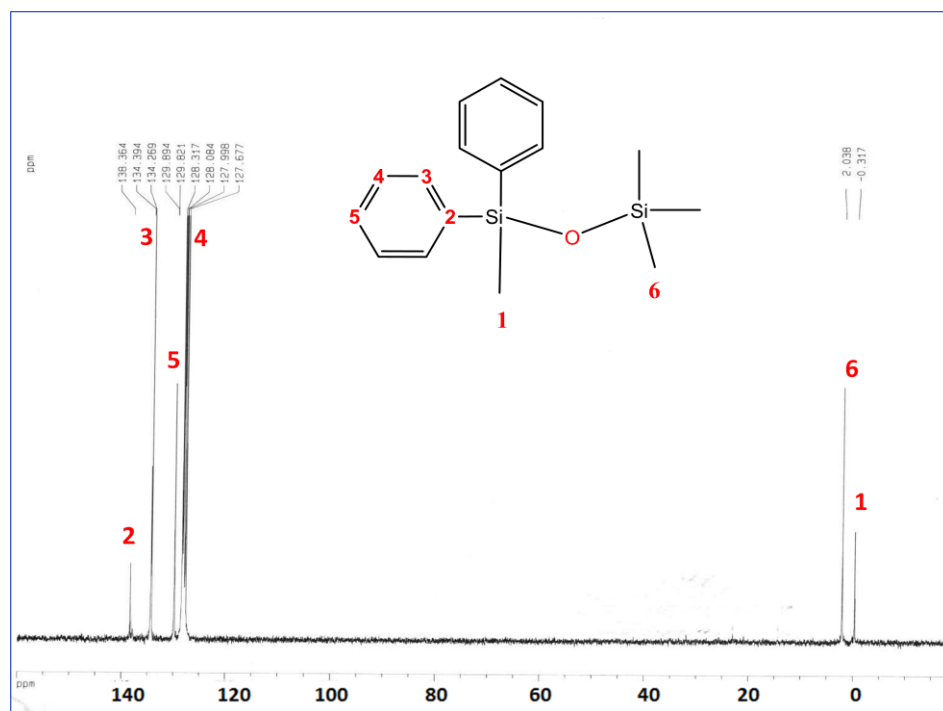
Appendix 2.31: ¹³C NMR spectroscopy for $\text{Ph}_3\text{Si-O-SiMe}_3$



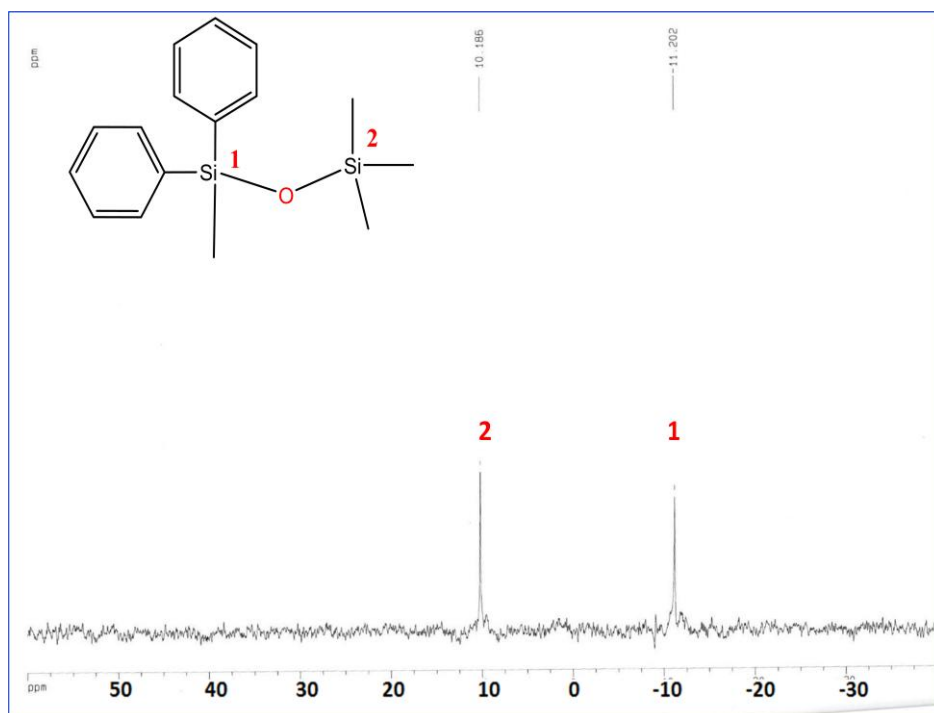
Appendix 2.32 ²⁹Si NMR spectroscopy for $\text{Ph}_3\text{Si-O-SiMe}_3$



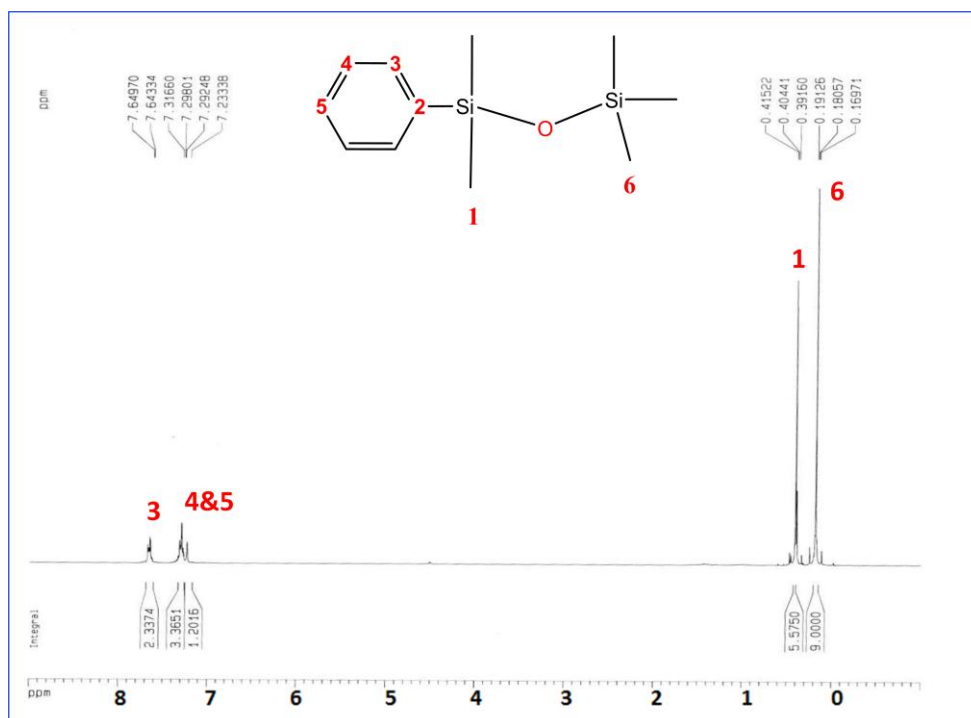
Appendix 2.33: ¹H NMR spectroscopy for Ph₂MeSi-O-SiMe₃



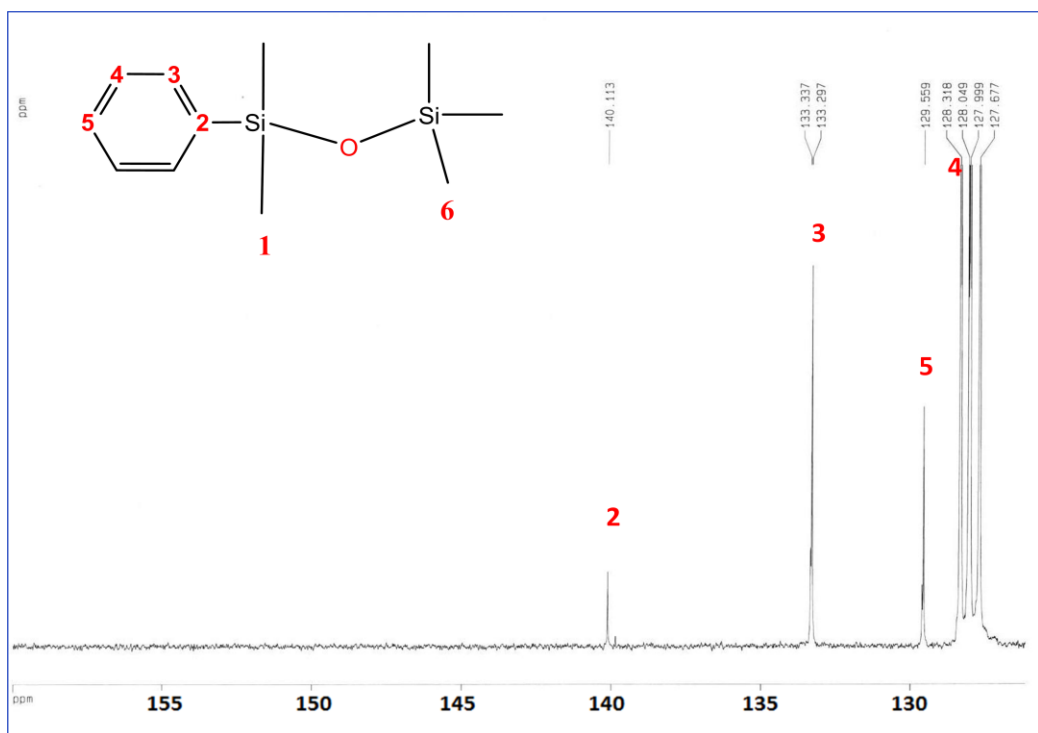
Appendix 2.34: ¹³C NMR spectroscopy for Ph₂MeSi-O-SiMe₃



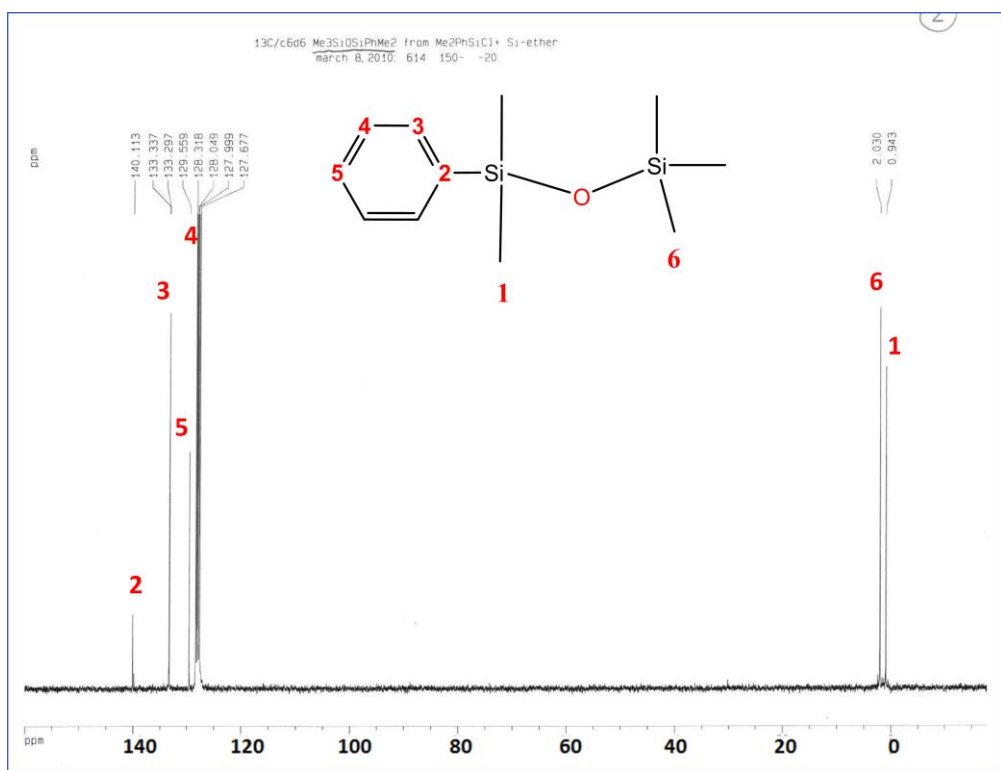
Appendix 2.35: ²⁹Si NMR spectroscopy for Ph₂MeSi-O-SiMe₃



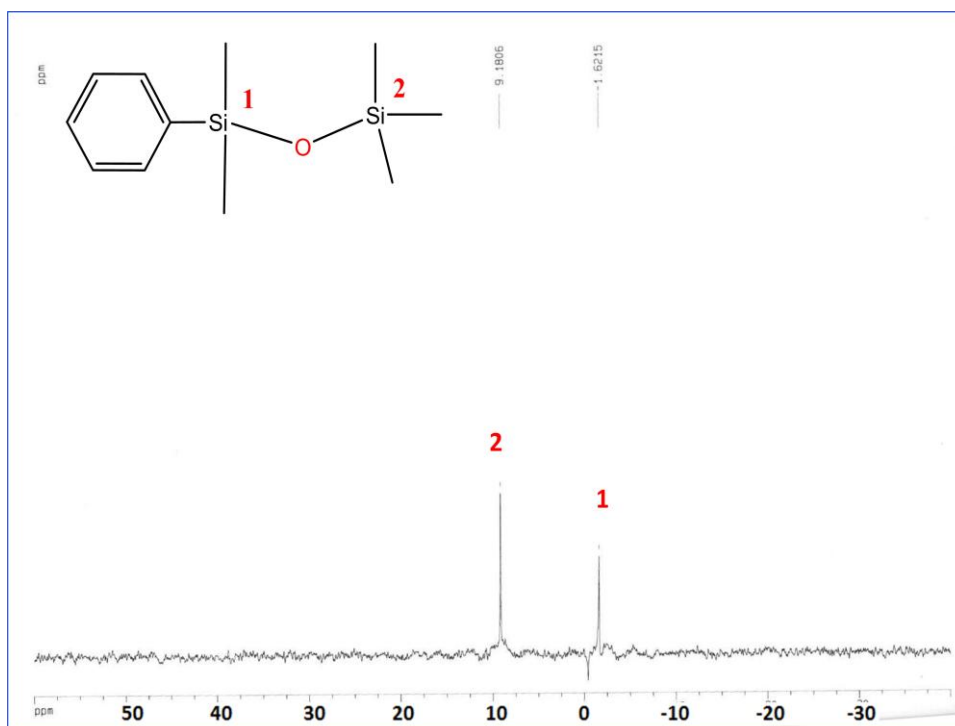
Appendix 2.36: ¹H NMR spectroscopy for PhMe₂Si-O-SiMe₃



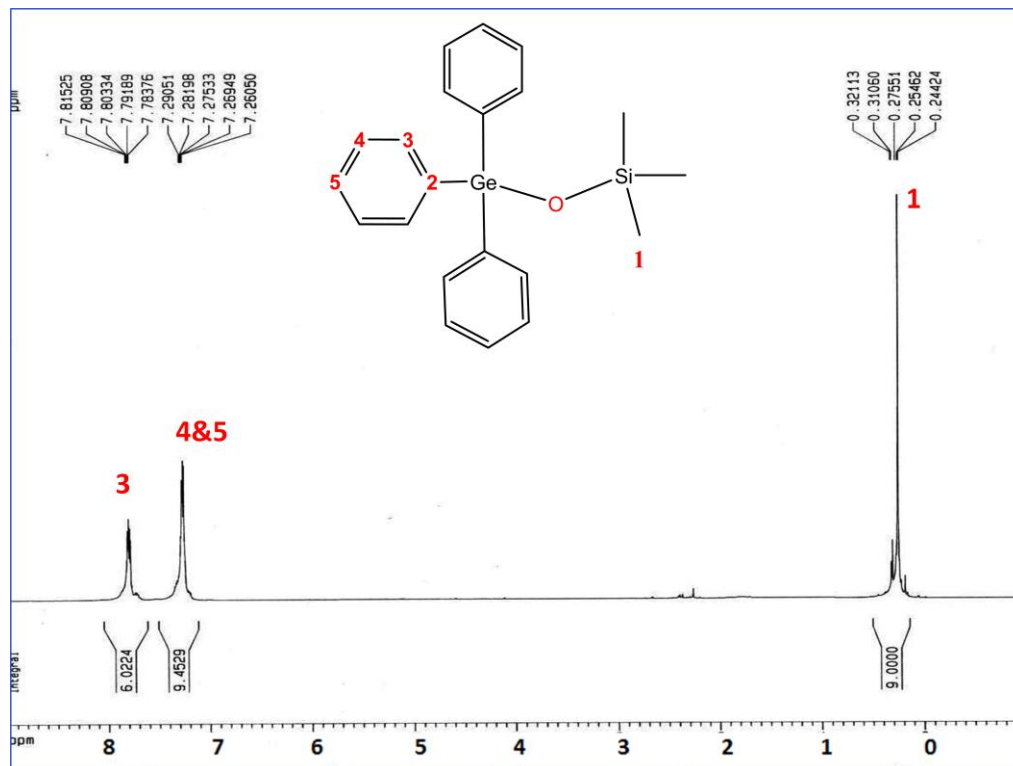
Appendix 2.37: ^{13}C NMR spectroscopy for $\text{PhMe}_2\text{Si-O-SiMe}_3$



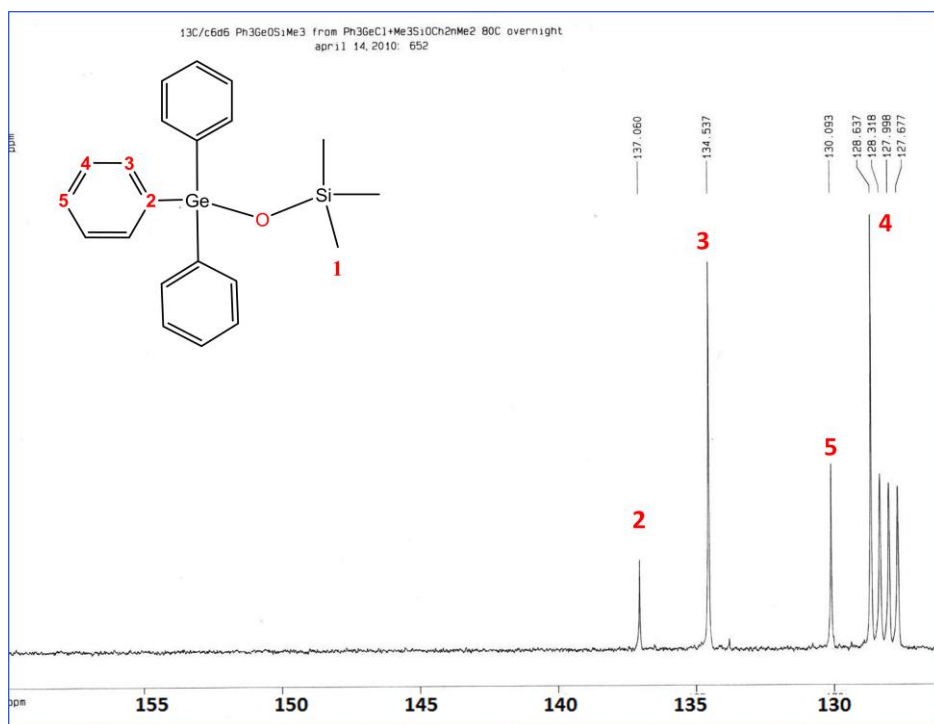
Appendix 2.38: ^{13}C NMR spectroscopy for $\text{PhMe}_2\text{Si-O-SiMe}_3$



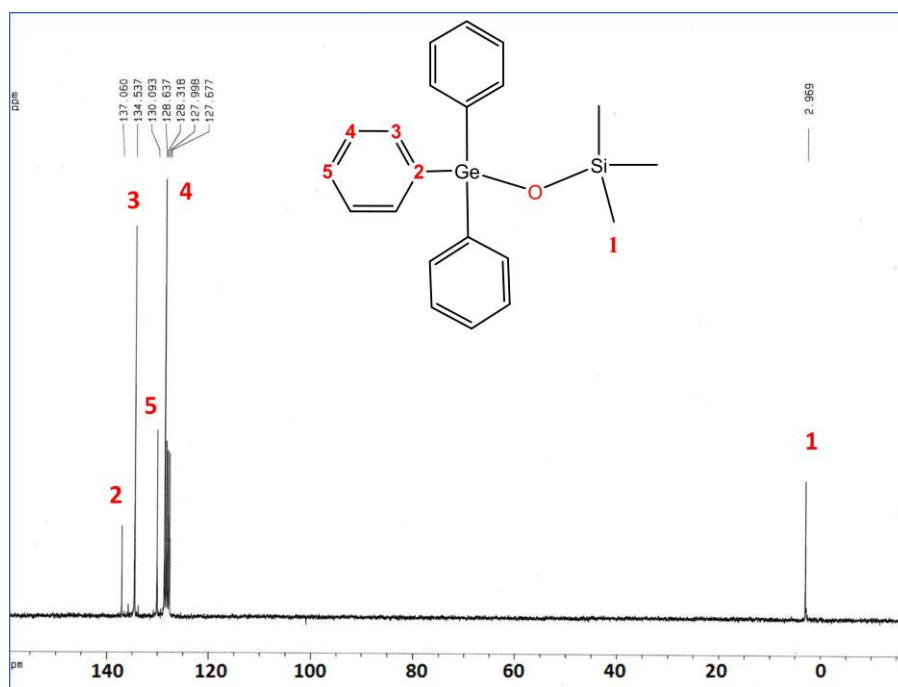
Appendix 2.39: ²⁹Si NMR spectroscopy for PhMe₂Si-O-SiMe₃



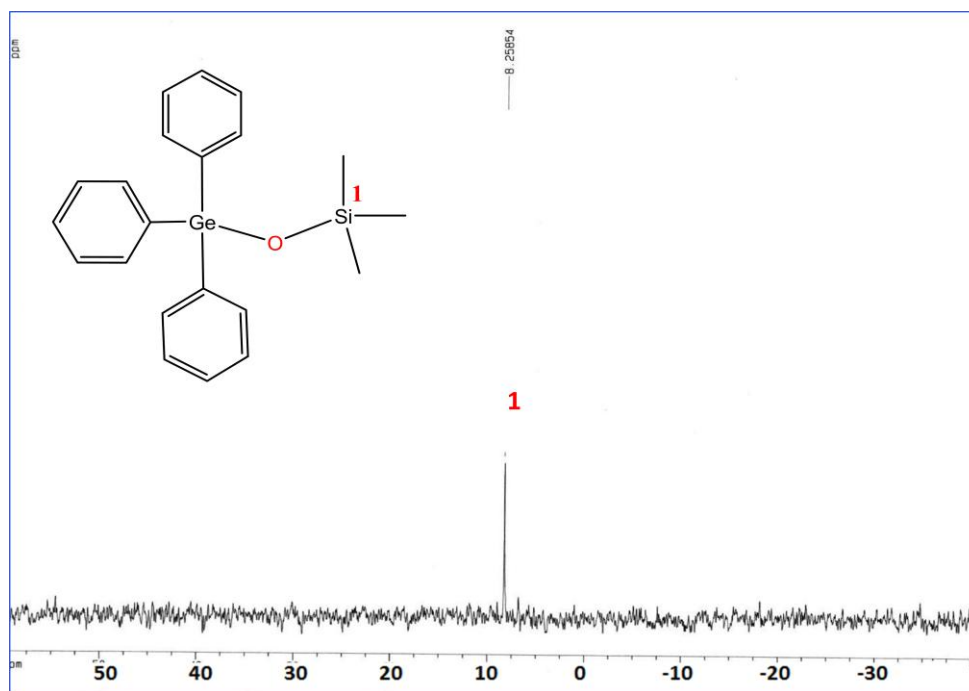
Appendix 2.40: ²⁹Si NMR spectroscopy for Ph₃Ge-O-SiMe₃



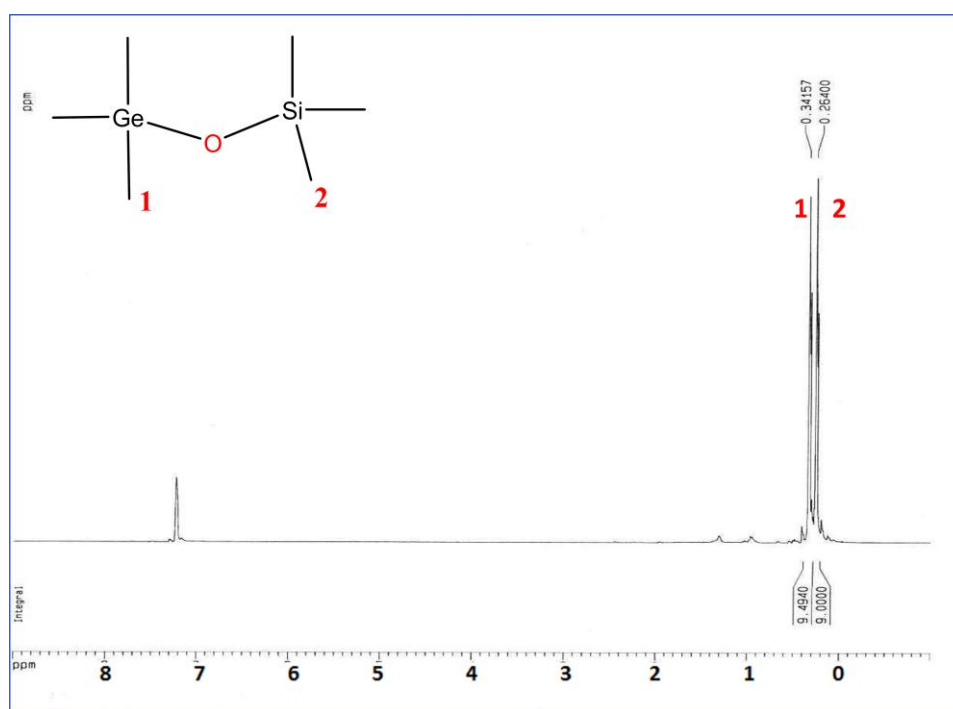
Appendix 2.41: ^{13}C NMR spectroscopy for $\text{Ph}_3\text{Ge-O-SiMe}_3$



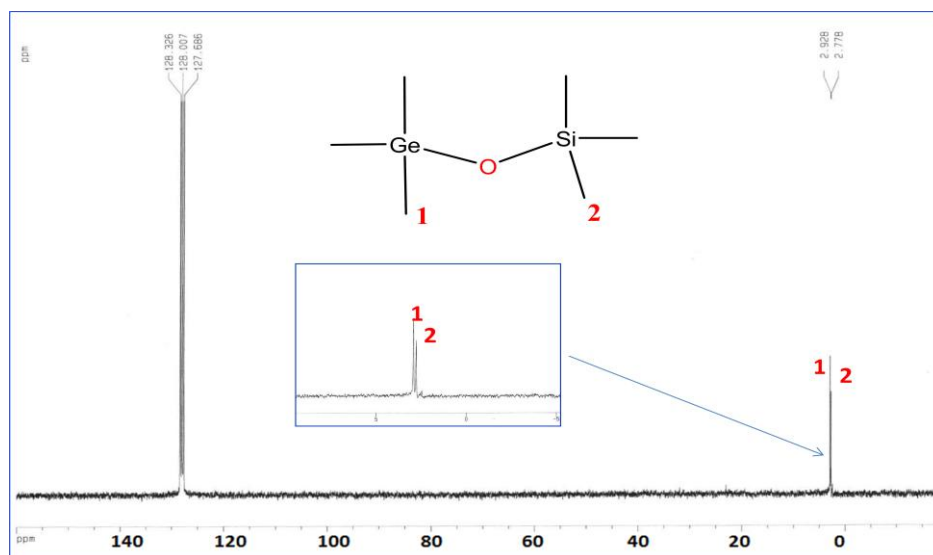
Appendix 2.42: ^{13}C NMR spectroscopy for $\text{Ph}_3\text{Ge-O-SiMe}_3$



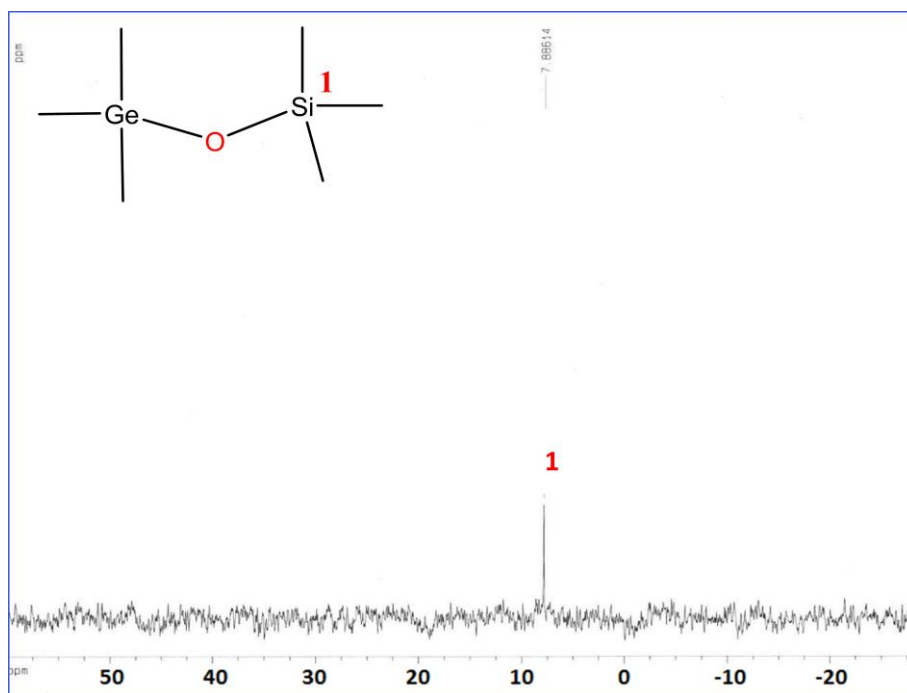
Appendix 2.43: ^{29}Si NMR spectroscopy for $\text{Ph}_3\text{Ge-O-SiMe}_3$



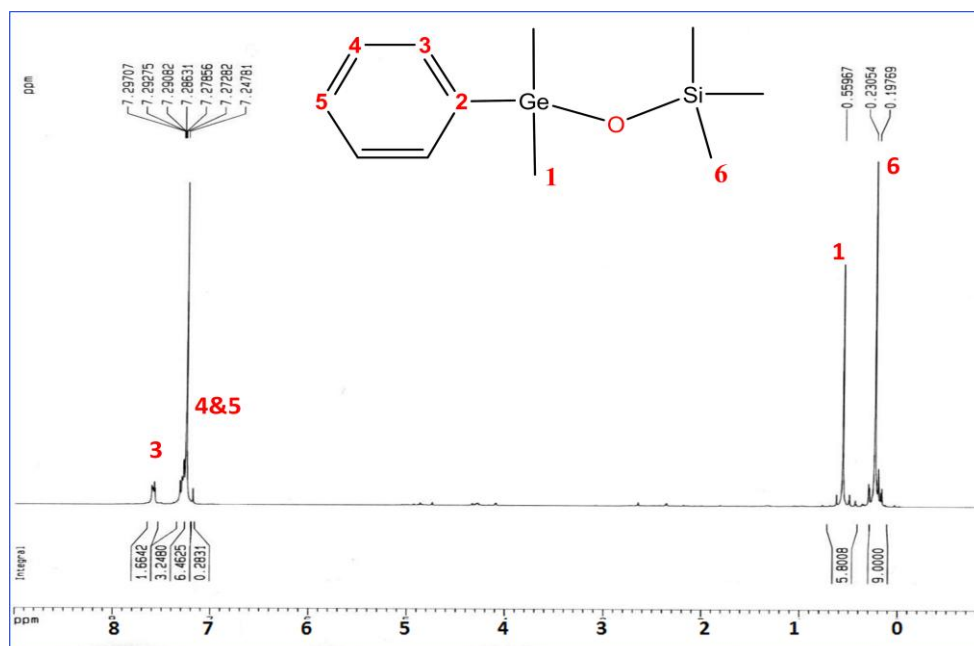
Appendix 2.44: ^1H NMR spectroscopy for $\text{Me}_3\text{Ge-O-SiMe}_3$



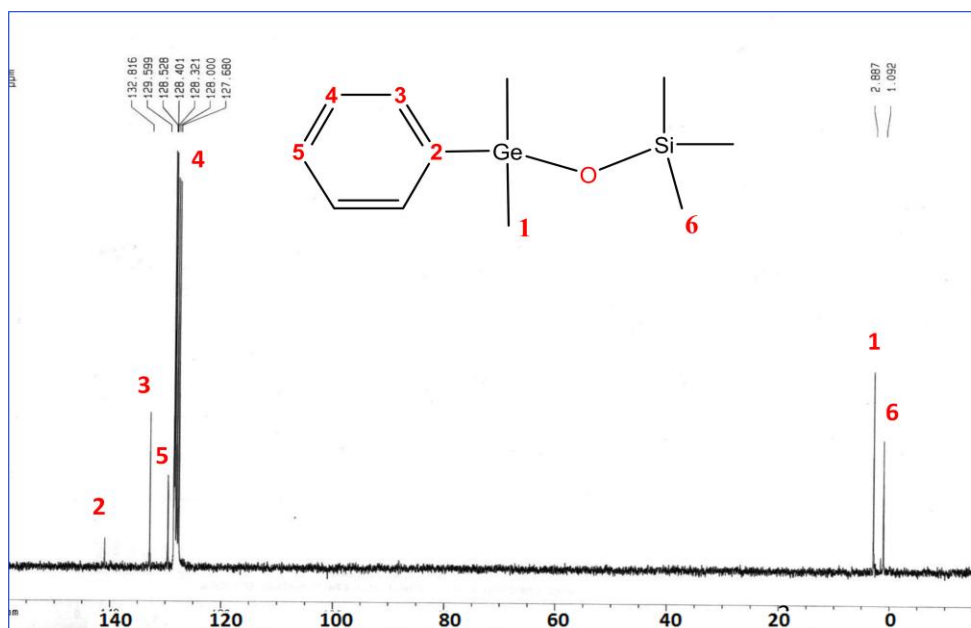
Appendix 2.45: ¹H NMR spectroscopy for Me₃Ge-O-SiMe₃



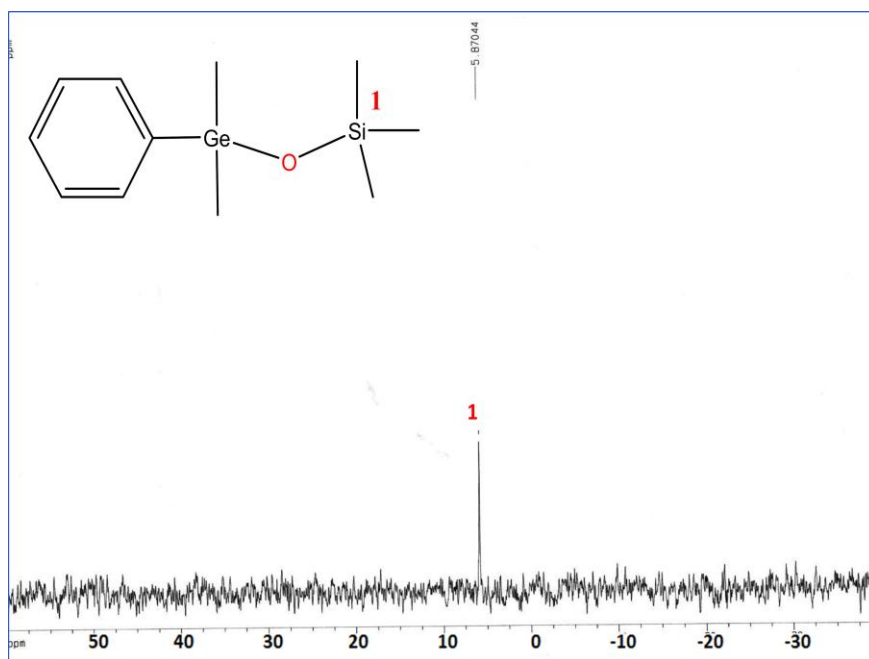
Appendix 2.46: ²⁹Si NMR spectroscopy for Me₃Ge-O-SiMe₃



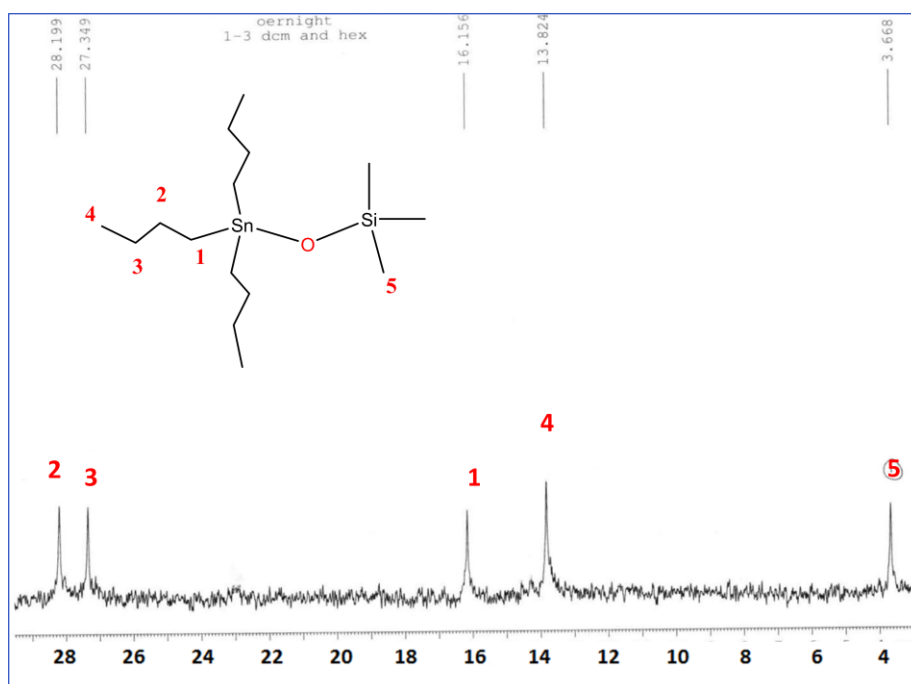
Appendix 2.47: ¹H NMR spectroscopy for Me₃Ge-O-SiMe₃



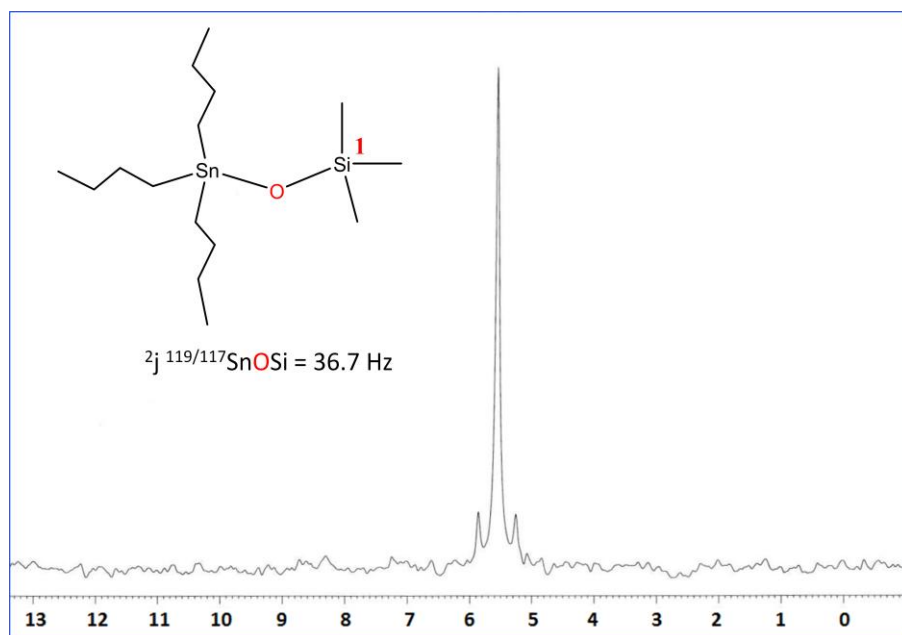
Appendix 2.48: ¹³C NMR spectroscopy for PhMe₂Ge-O-SiMe₃



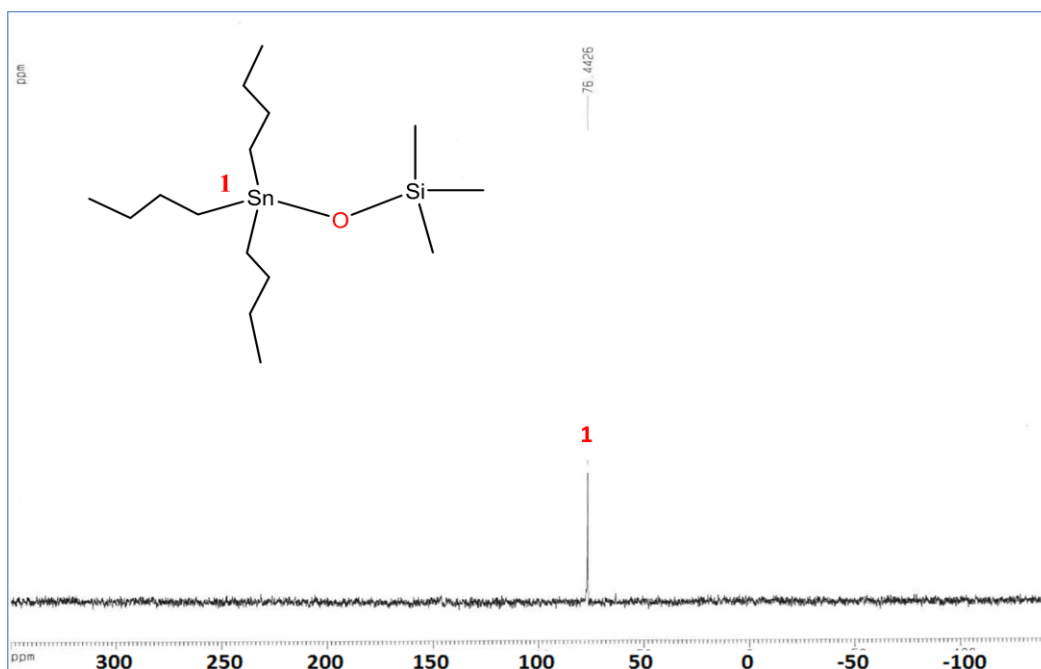
Appendix 2.49: ^{13}C NMR spectroscopy for $\text{PhMe}_2\text{Ge-O-SiMe}_3$



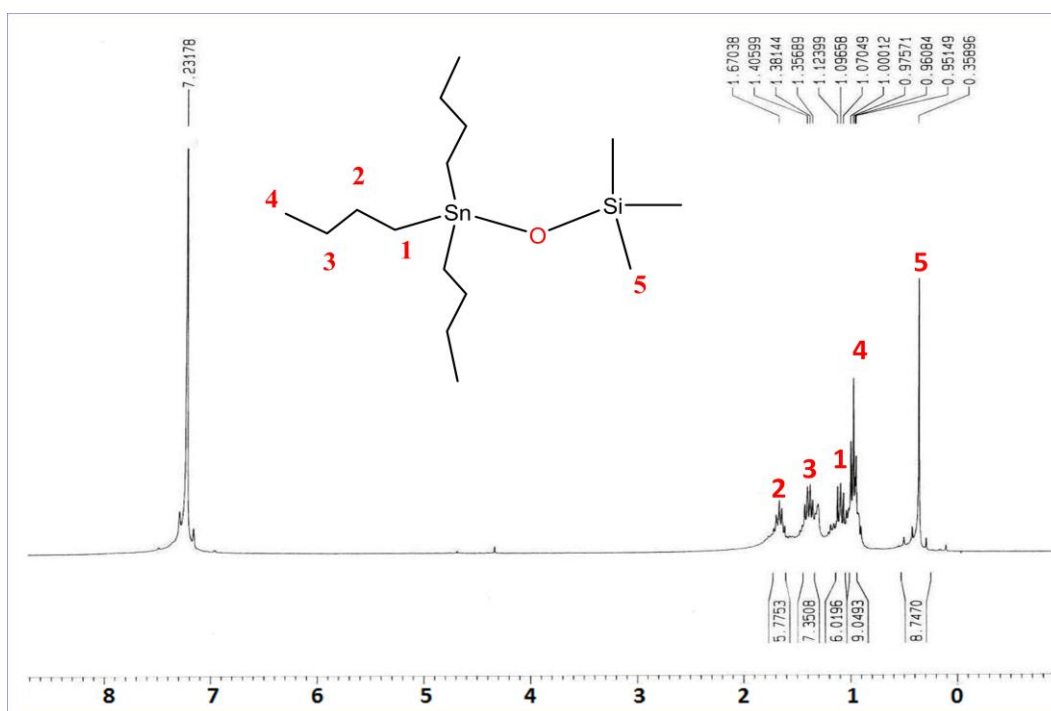
Appendix 2.50: ^{13}C NMR spectroscopy for $\text{Bu}_3\text{Sn-O-SiMe}_3$



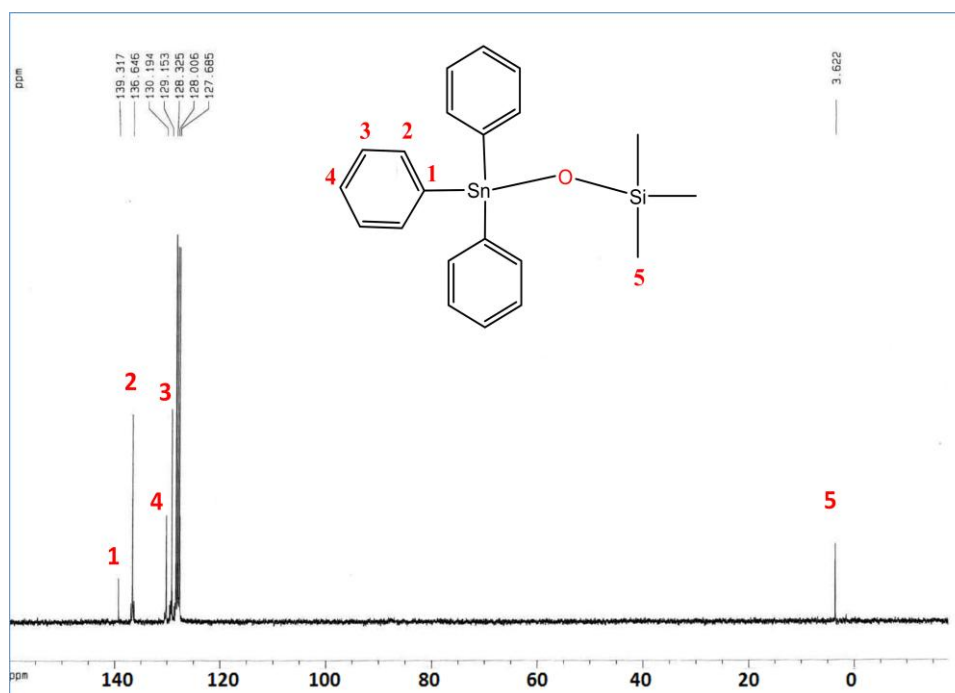
Appendix 2.51: ^{29}Si NMR spectroscopy for $\text{Bu}_3\text{Sn-O-SiMe}_3$



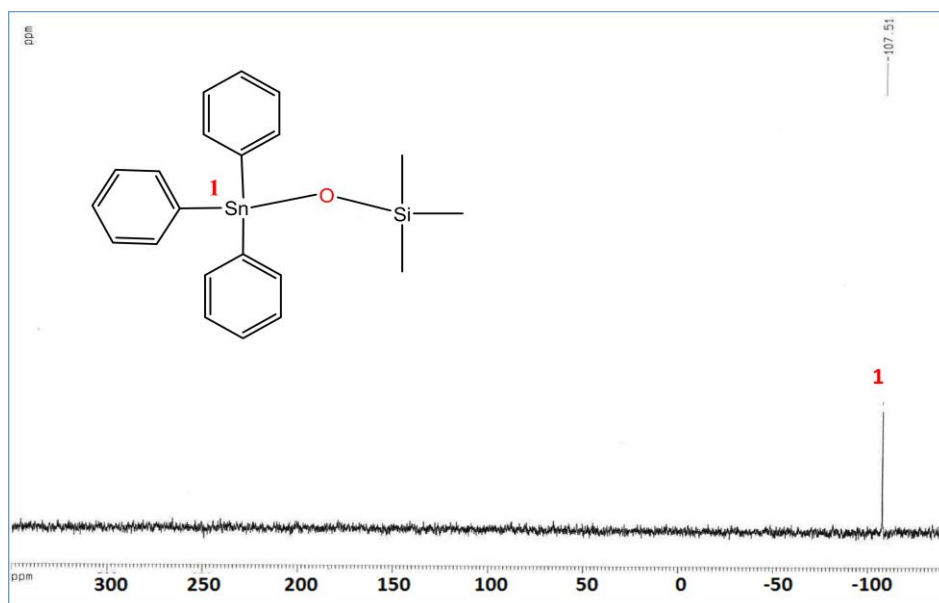
Appendix 2.52: ^{119}Sn NMR spectroscopy for $\text{Bu}_3\text{Sn-O-SiMe}_3$



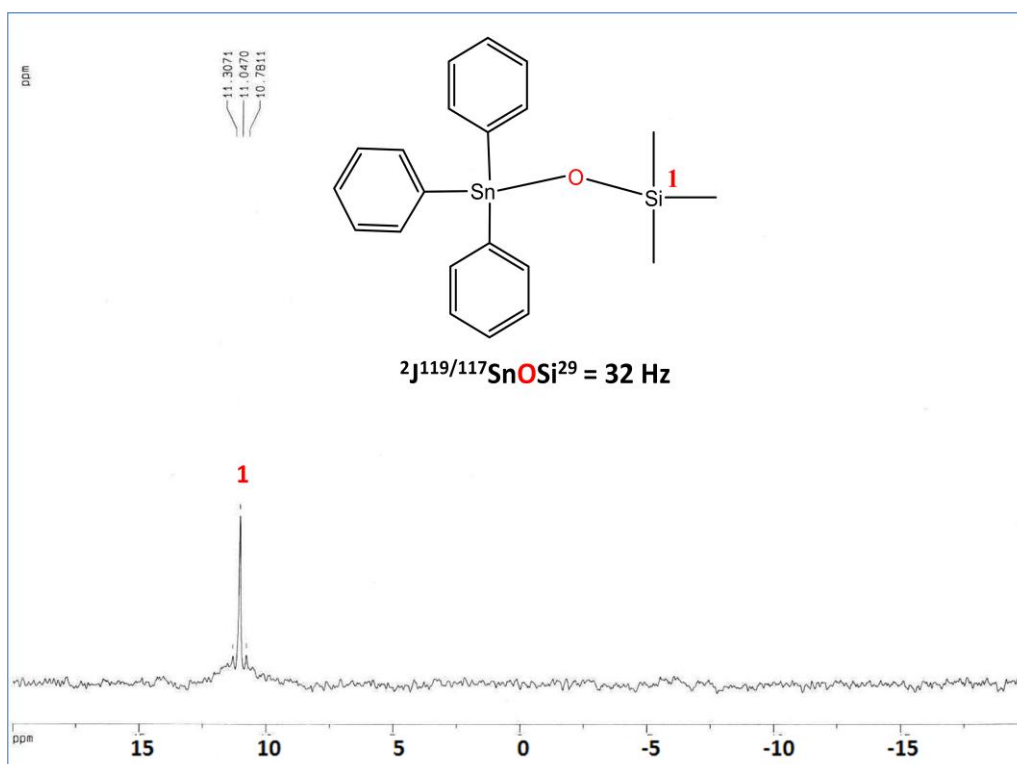
Appendix 2.53: ^1H NMR spectroscopy for $\text{Bu}_3\text{Sn-O-SiMe}_3$



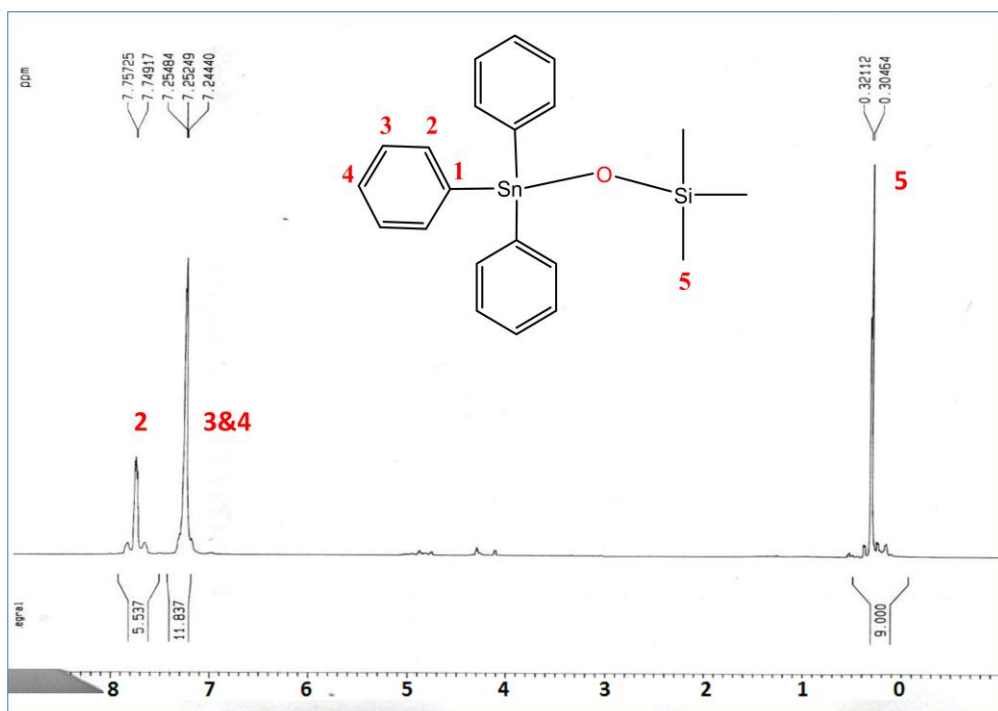
Appendix 2.54: ^{13}C NMR spectroscopy for $\text{Ph}_3\text{Sn-O-SiMe}_3$



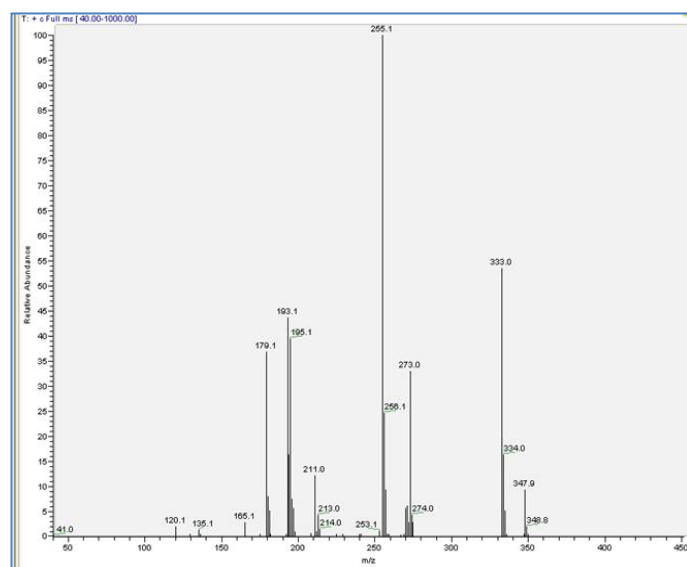
Appendix 2.55: ¹¹⁹Sn NMR spectroscopy for Ph₃Sn-O-SiMe₃



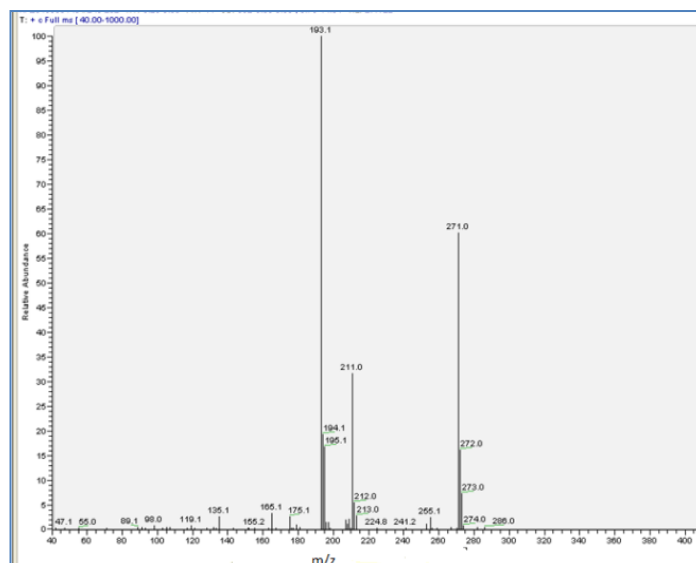
Appendix 2.56: ²⁹Si NMR spectroscopy for Ph₃Sn-O-SiMe₃



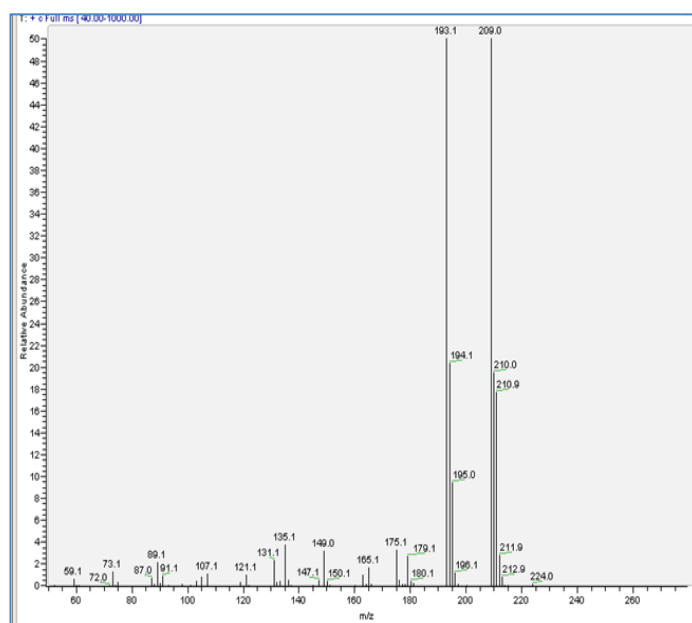
Appendix 2.57: ¹H NMR spectroscopy for Ph₃Sn-O-SiMe₃



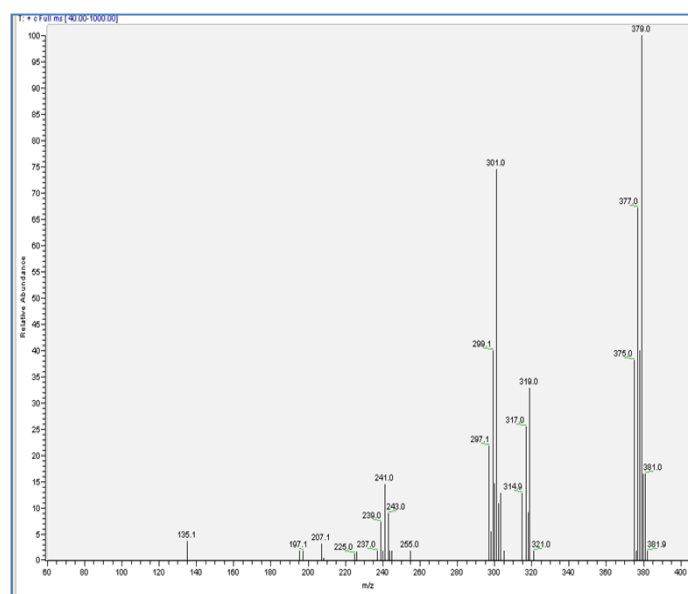
Appendix 2.58: GC-Mass spectra of Ph₃SiOSiMe₃ MW(348)



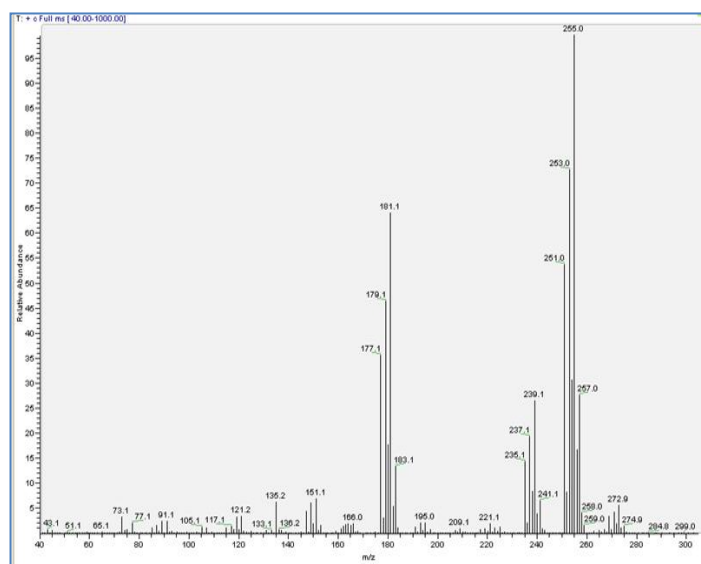
Appendix 2.59: GC-Mass spectra of $\text{Ph}_2\text{MeSiOSiMe}_3$ MW(286)



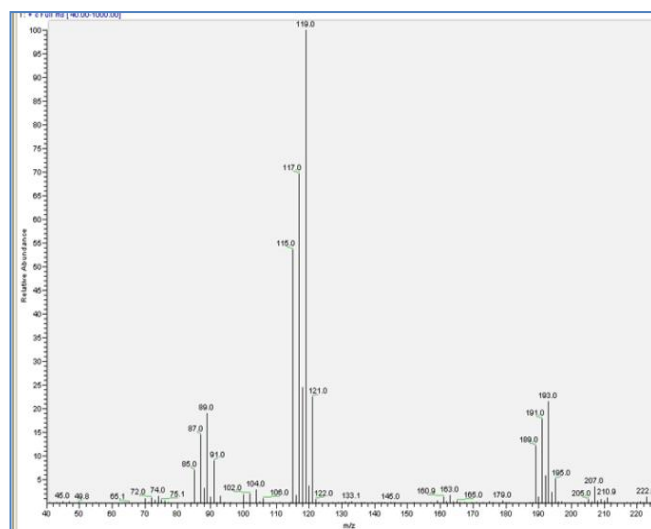
Appendix 2.60: GC-Mass spectra of $\text{PhMe}_2\text{SiOSiMe}_3$ MW(224)



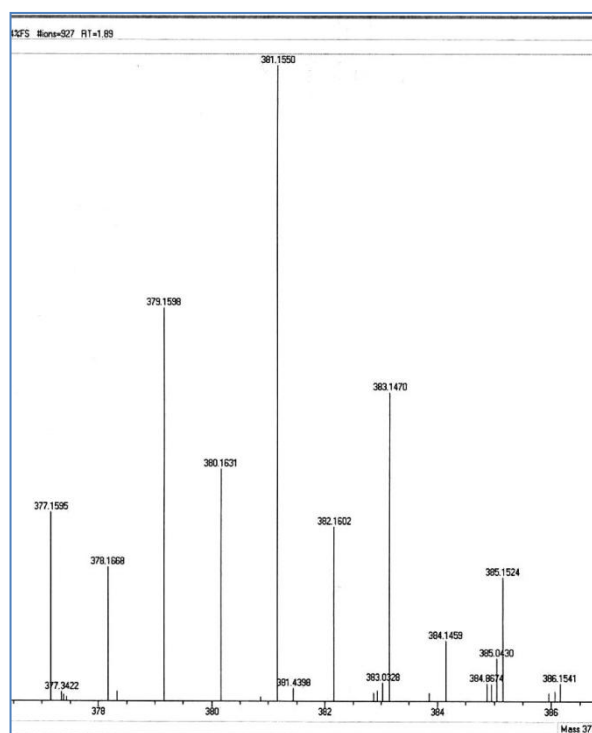
Appendix 2.61: GC-Mass spectra of $\text{Ph}_3\text{GeOSiMe}_3$ MW(394)



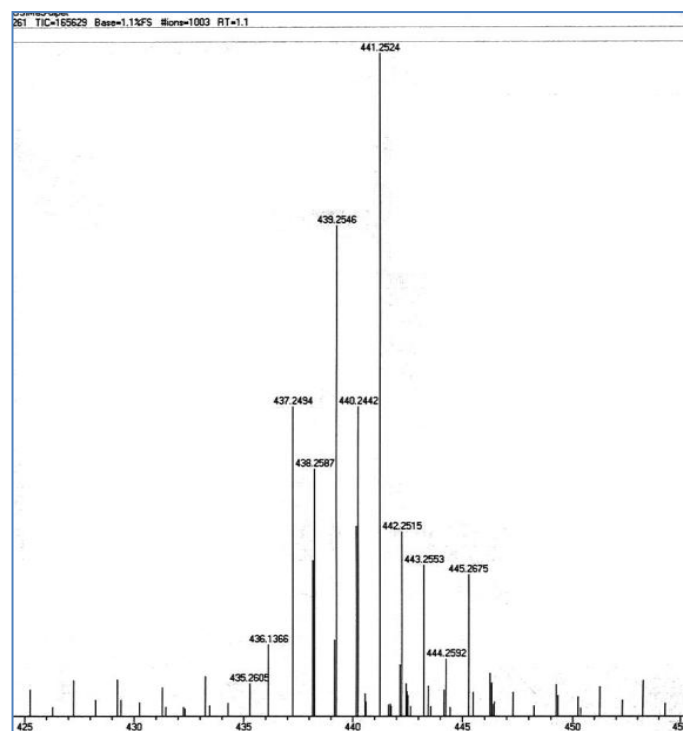
Appendix 2.62: GC-Mass spectra of $\text{PhMe}_2\text{GeOSiMe}_3$ MW(269)



Appendix 2.63: GC-Mass spectra of Me₃GeOSiMe₃ MW(207)

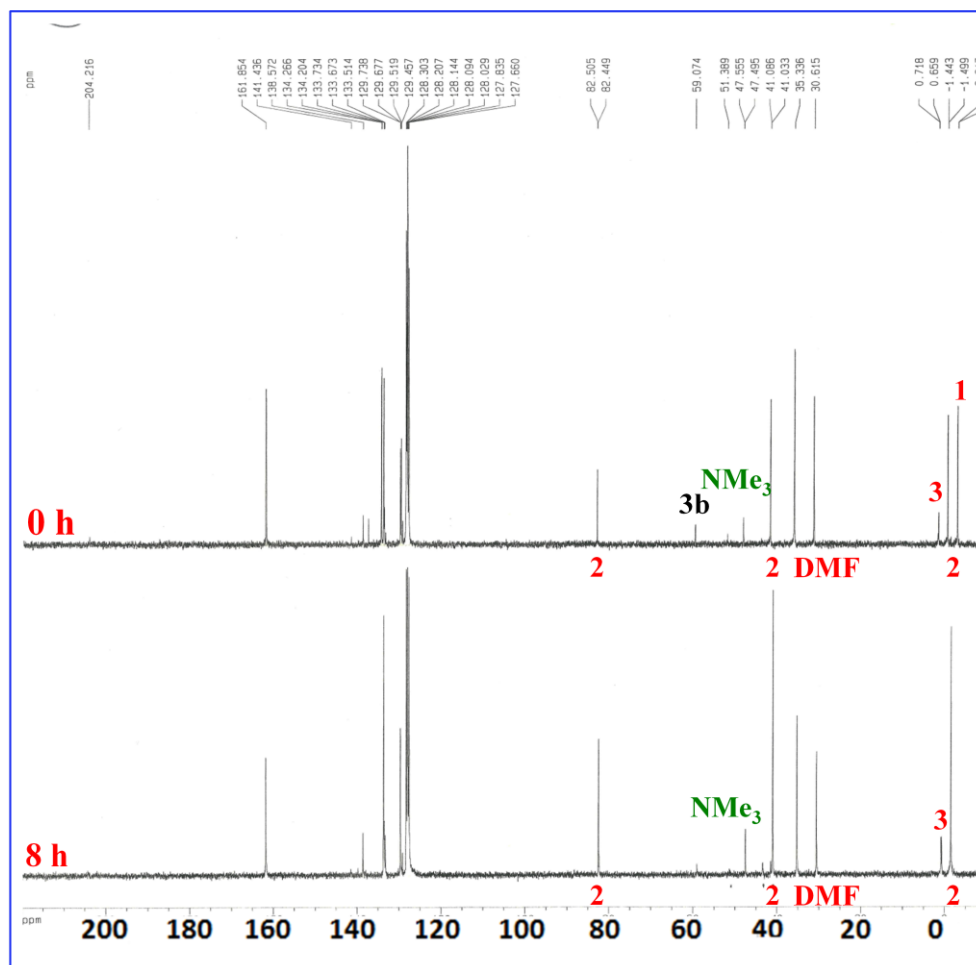


Appendix 2.64: ESI mass spectra of $\text{Bu}_3\text{SnOSiMe}_3$ MW(381)

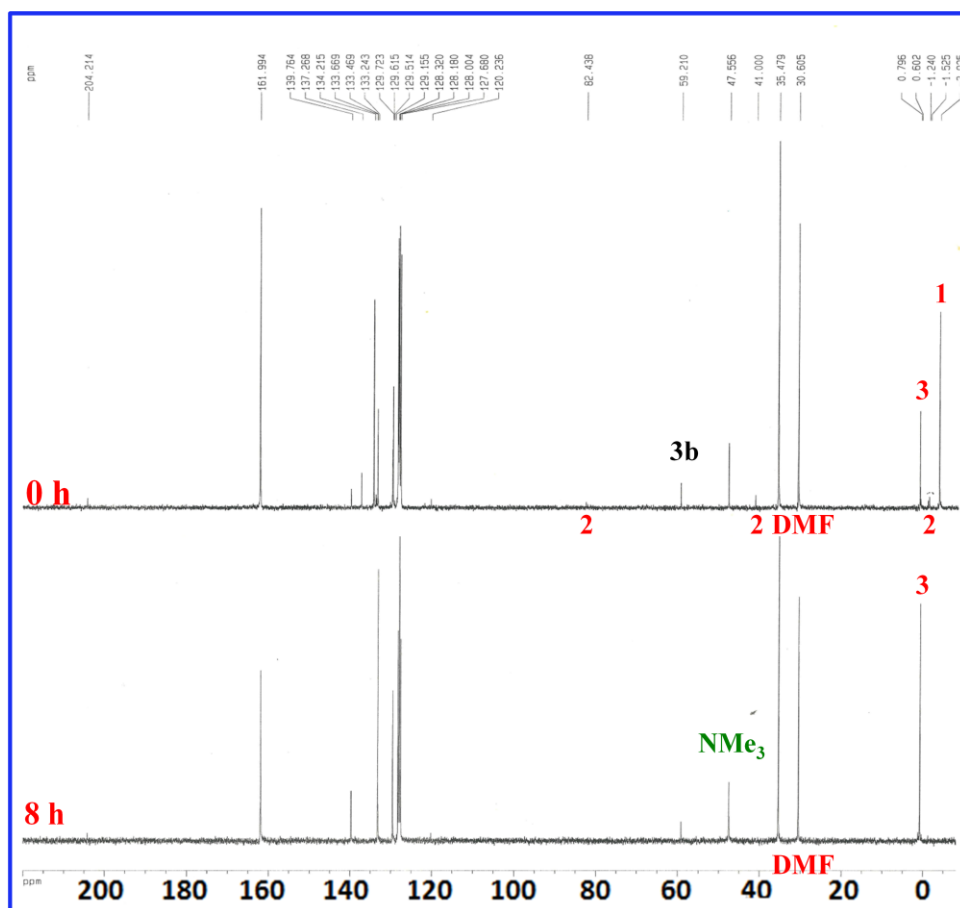


Appendix 2.65: ESI mass spectra of $\text{Ph}_3\text{SnOSiMe}_3$ MW(440)

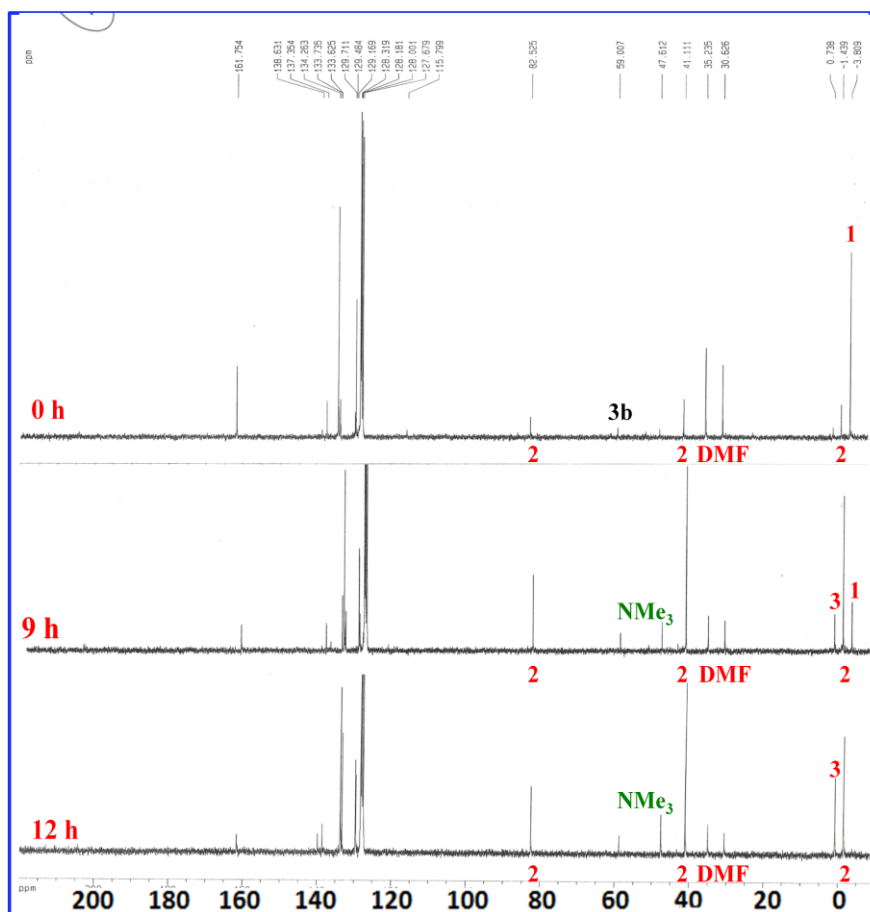
Synthesis of $R_3SiOSiR_3$ using **3b** at different concentrations



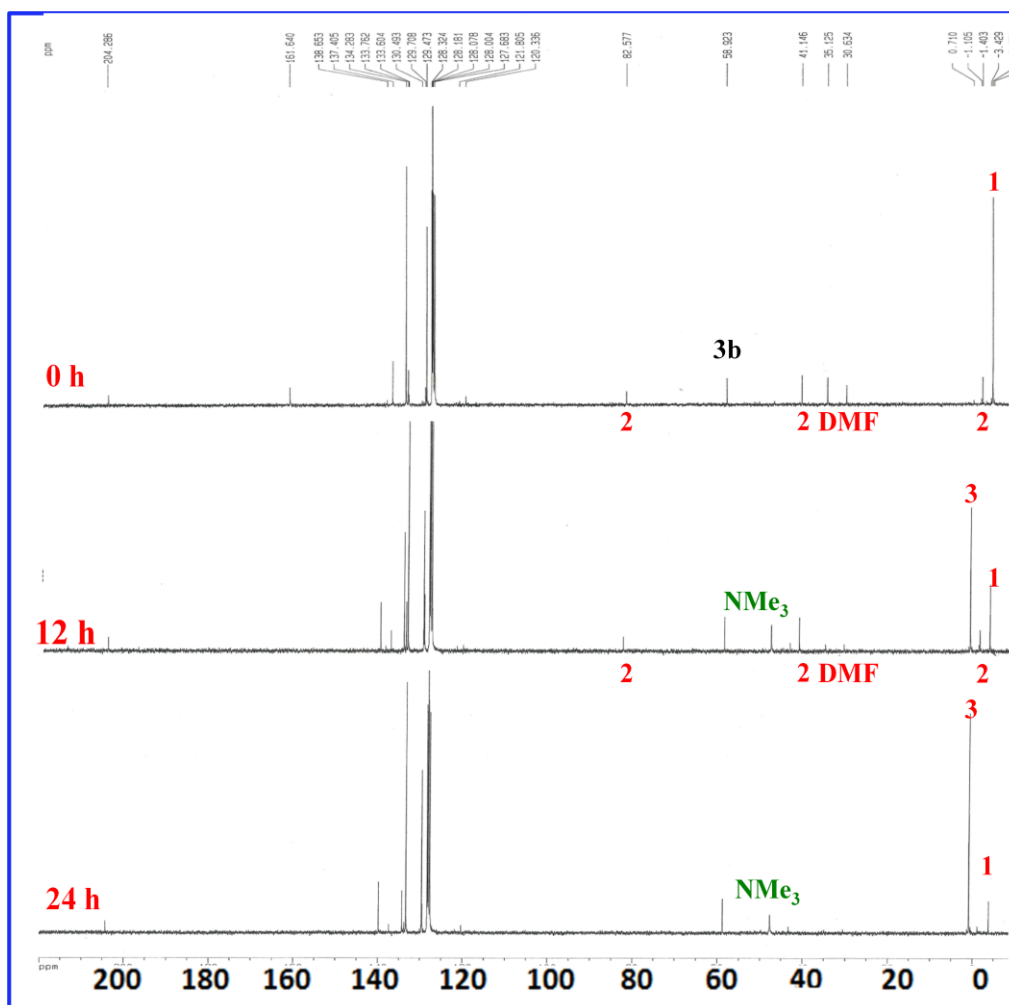
Appendix 2.66: ^{13}C NMR spectroscopy monitoring the disappearance of PhMe_2SiH (1) into $\text{PhMe}_2\text{SiOCH}_2\text{NMe}_2$ (2) and $(\text{PhMe}_2\text{Si})_2\text{O}$ (3) at RT. Ratio : (1:3) SiH-DMF with **3b**



Appendix 2.67: ^{13}C NMR spectroscopy monitoring the disappearance of PhMe₂SiH(1) into PhMe₂SiOCH₂NMe₂(2) and (PhMe₂Si)₂O(3) at RT. Ratio : (1:2) SiH-DMF with **3b**



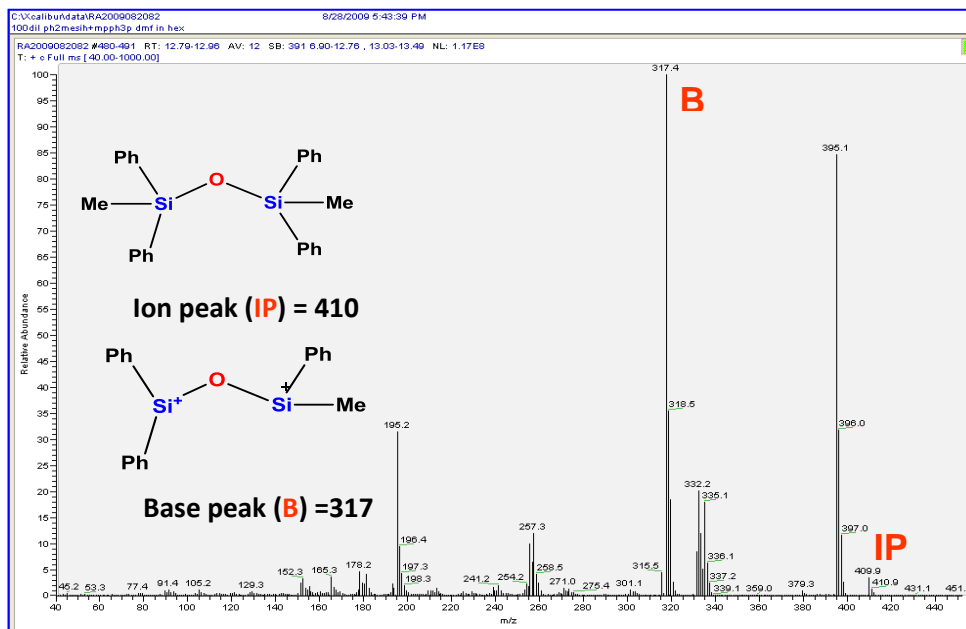
Appendix 2.68: ^{13}C NMR spectroscopy monitoring the disappearance of PhMe₂SiH(1) into PhMe₂SiOCH₂NMe₂(2) and (PhMe₂Si)₂O(3) at RT. Ratio : (1:1) SiH-DMF with **3b**



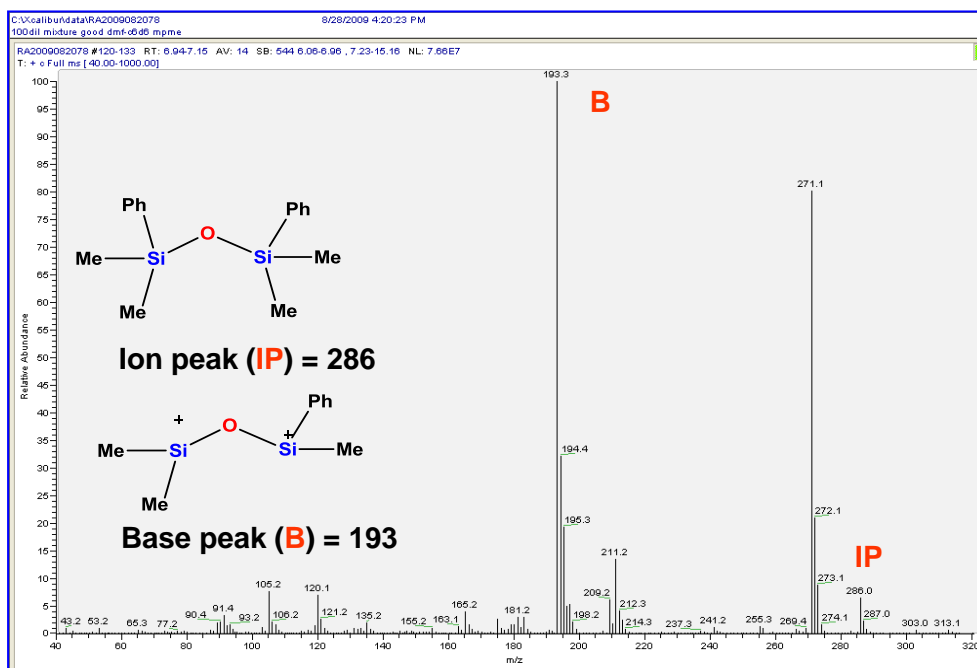
Appendix 2.69: ^{13}C NMR spectroscopy monitoring the disappearance of PhMe_2SiH (1) into $\text{PhMe}_2\text{SiOCH}_2\text{NMe}_2$ (2) and $(\text{PhMe}_2\text{Si})_2\text{O}$ (3) at RT. Ratio : (2:1) SiH-DMF with **3b**

Here we illustrate the gas chromatograph of $\text{PhMe}_2\text{SiOSiMe}_2\text{Ph}$ and $\text{Ph}_2\text{MeSiOSiMePh}_2$, where the mass spectral portion of the GC-MS analysis of the two siloxanes materials formed in our studies are illustrated. No remaining R_3SiH , nor any disilane R_3SiSiR_3 , was detected. In our hands, the use of GC to distinguish the disiloxane products resulted in retention times of 12.08 min for $\text{Ph}_2\text{MeSiOSiMePh}_2$ (a), and 7.08 min for $\text{PhMe}_2\text{SiOSiMe}_2\text{Ph}$ (b), in Hexanes solution.

(a)

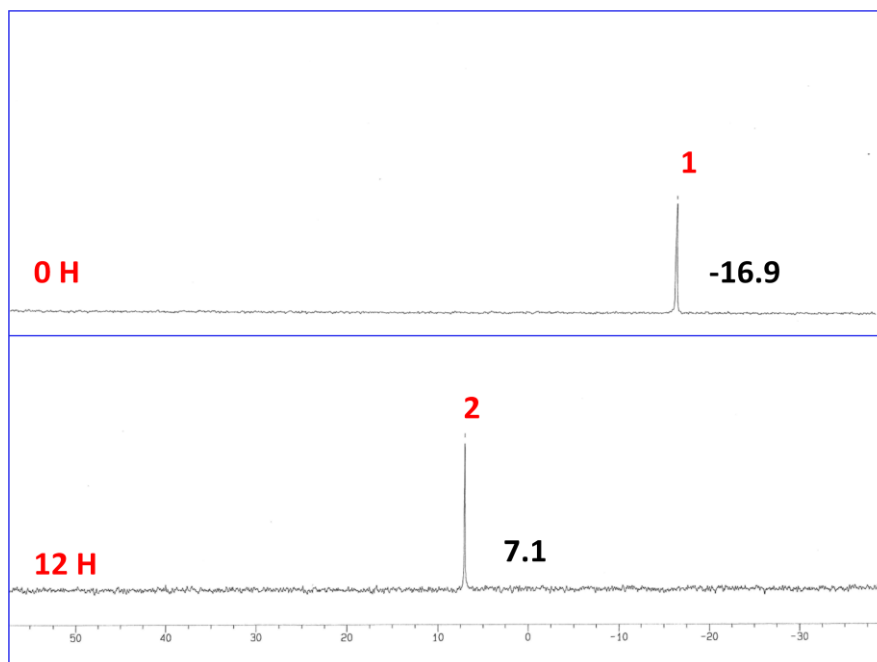


(b)

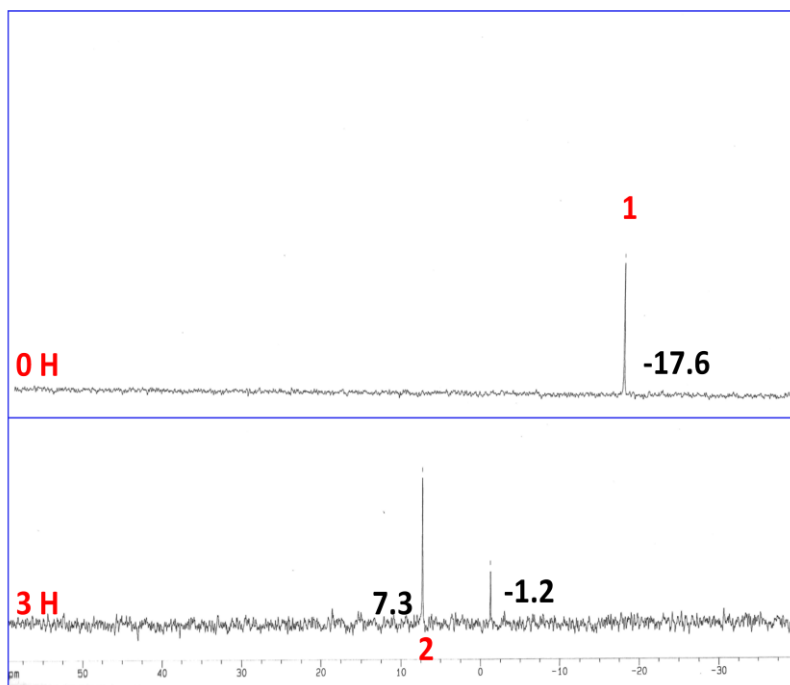


Appendix 2.70: Mass spectra of (a) $\text{Ph}_2\text{MeSiOSiMePh}_2$, (b) $\text{PhMe}_2\text{SiOSiMe}_2\text{Ph}$

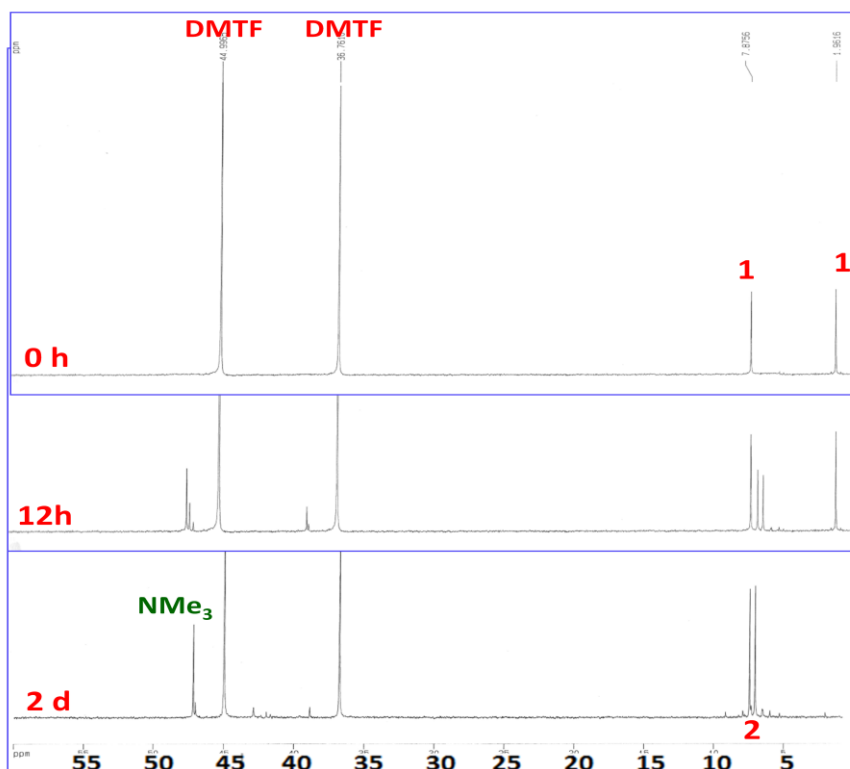
Synthesis of R_3ESiR_3 using **3a**, **3b** and **3c**



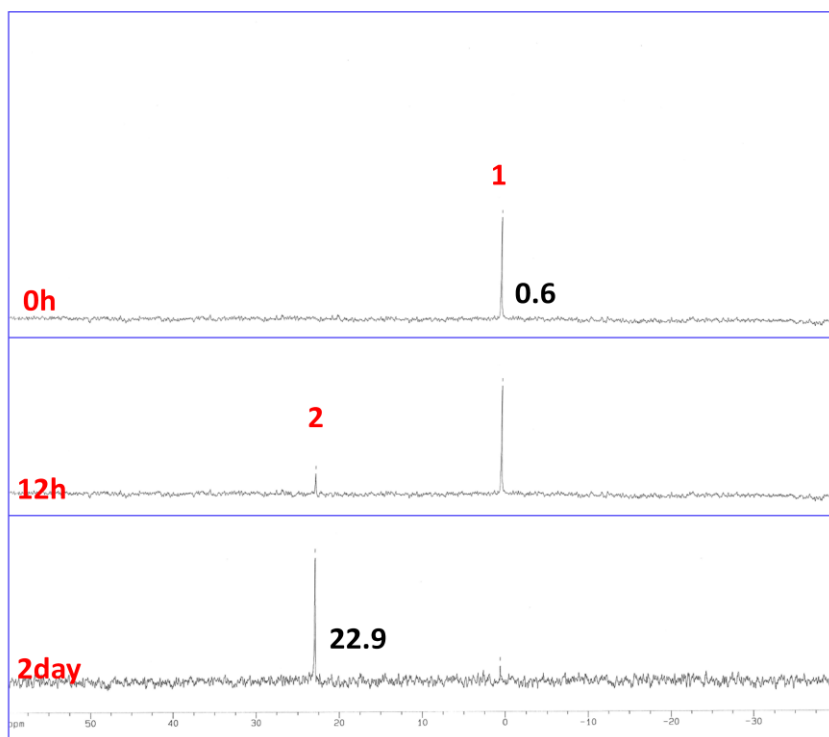
Appendix 2.71: ^{29}Si NMR spectroscopy showing the disappearance of PhMe_2SiH (1) into $\text{PhMe}_2\text{Si-S-SiPhMe}_2$ (2) with **3a** at 120°C



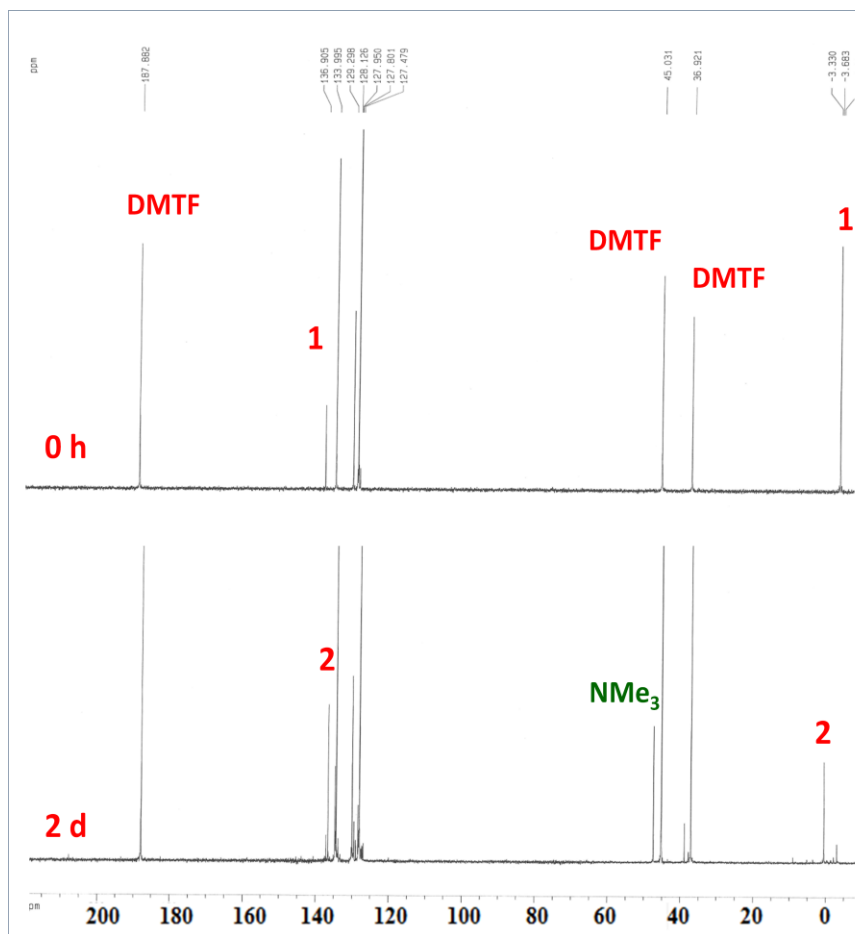
Appendix 2.72: ^{29}Si NMR spectroscopy showing the disappearance of PhMe_2SiH (1) into $\text{PhMe}_2\text{Si-S-SiPhMe}_2$ (2) with **3c** at 120°C



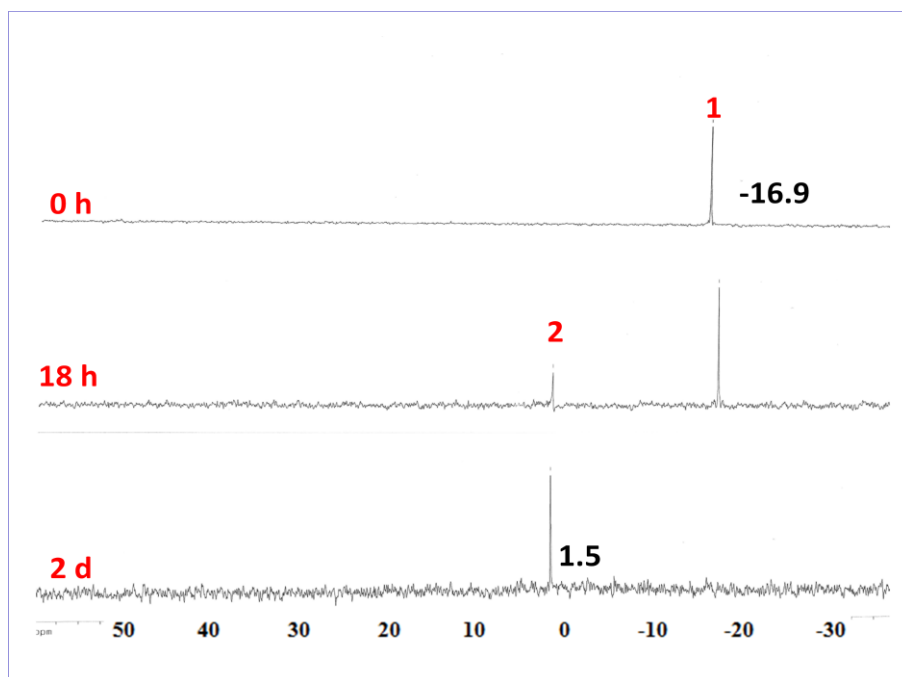
Appendix 2.73: ^{13}C NMR spectroscopy showing the disappearance of Et₃SiH (1) into Et₃Si-SiEt₃(2) with **3a** at 120°C. DMTF (HC(S)NMe₂)



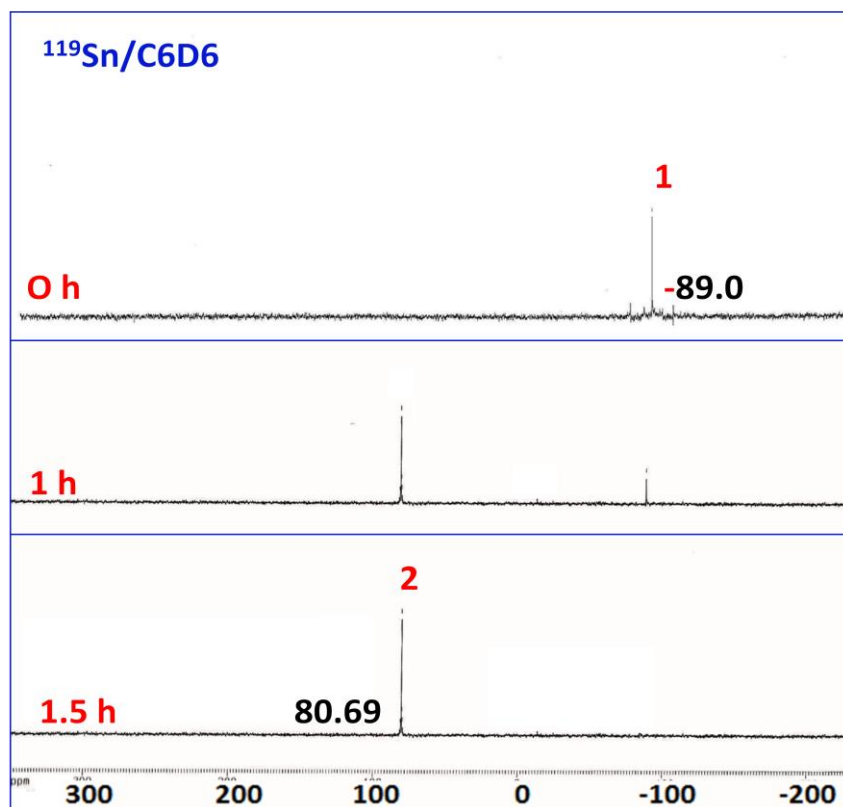
Appendix 2.74: ^{13}C NMR spectroscopy showing the disappearance of Et₃SiH (1) into Et₃Si-SiEt₃(2) with **3a** at 120°C. in the presence of DMTF (HC(S)NMe₂)



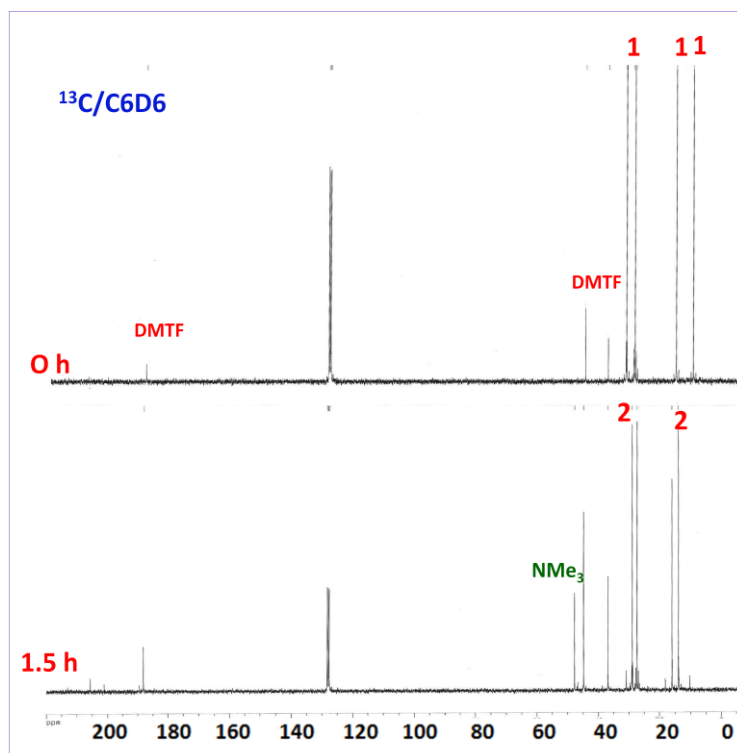
Appendix 2.75: ^{13}C NMR spectroscopy showing the disappearance of Ph_2MeSiH (1) into $\text{Ph}_2\text{MeSi-S-SiPh}_2\text{Me}$ (2) with **3a** at 120°C . in the presence of DMTF (HC(S)NMe_2)



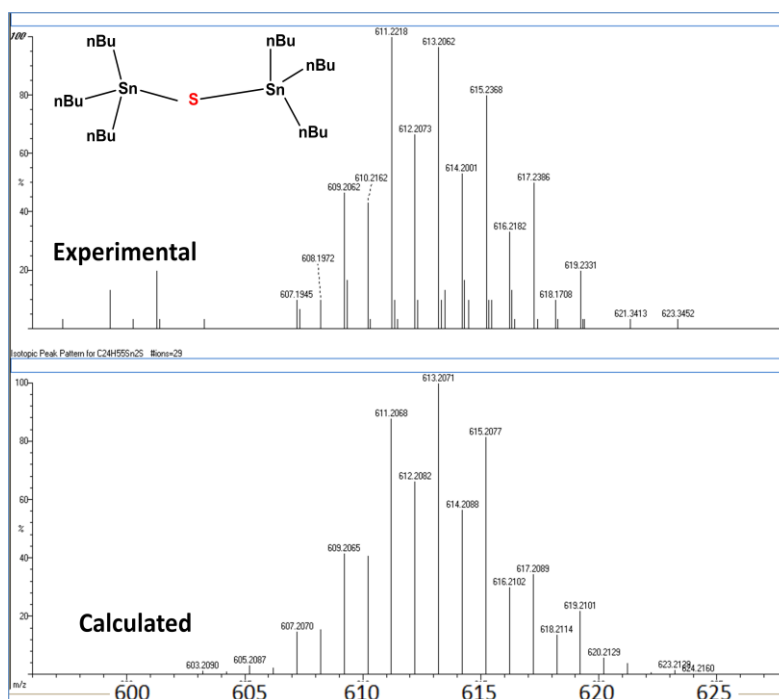
Appendix 2.76: ^{29}Si NMR spectroscopy showing the disappearance of Ph_2MeSiH (1) into $\text{Ph}_2\text{MeSi-S-SiPh}_2\text{Me}$ (2) with **3a** at 120°C . in the presence of DMTF (HC(S)NMe_2)



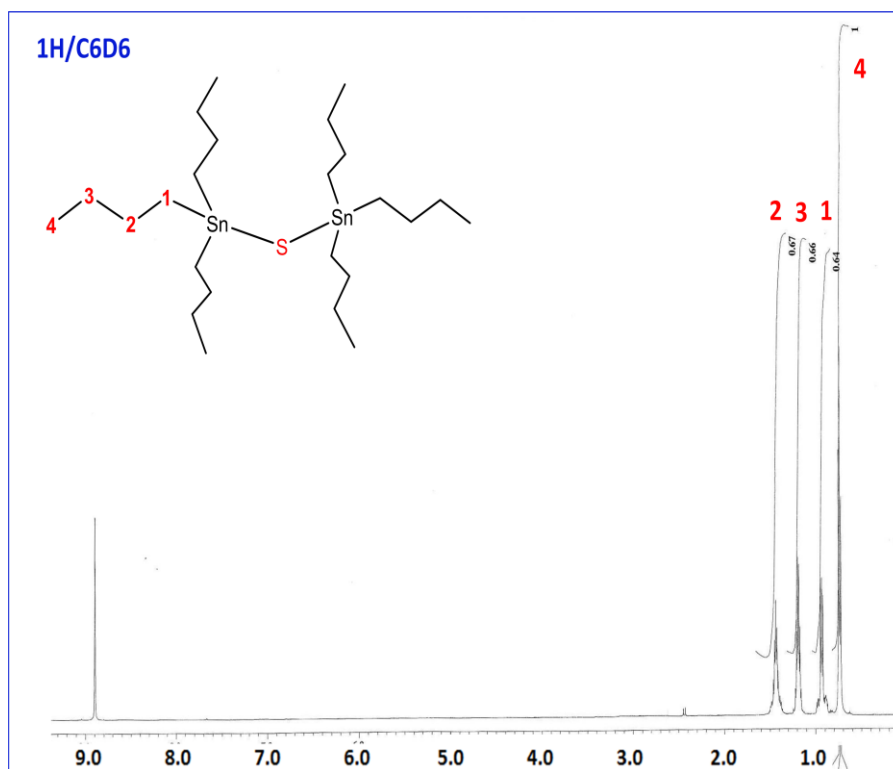
Appendix 2.77: ^{119}Sn NMR spectroscopy showing the disappearance of Bu_3SnH (1) into $\text{Bu}_3\text{Sn-S-SnBu}_3$ (2) with **3a** at 90°C . in the presence of DMTF (HC(S)NMe_2)



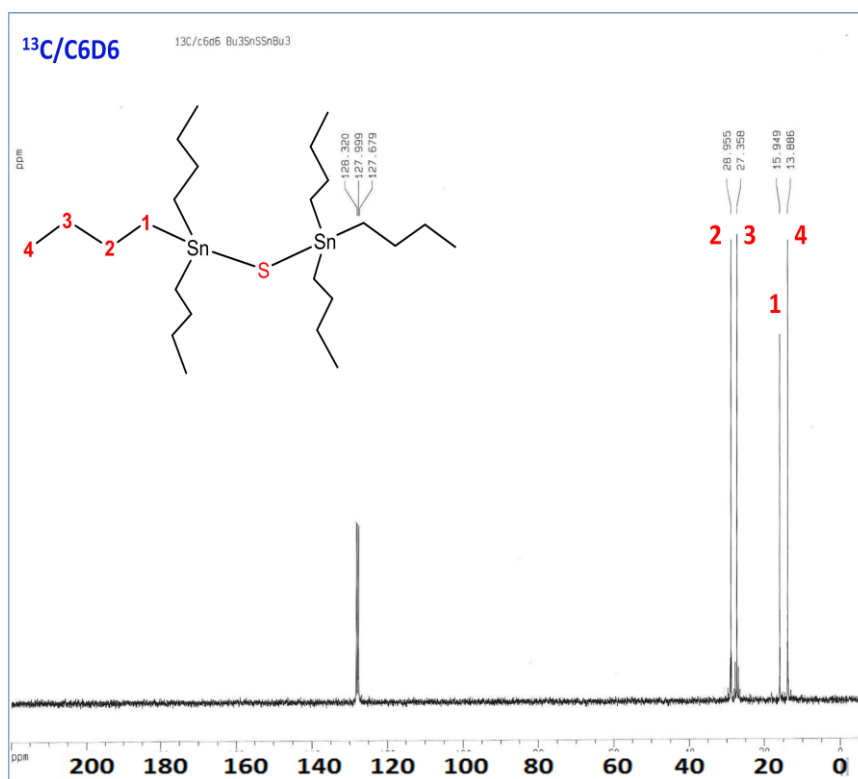
Appendix 2.78: ¹³C NMR spectroscopy showing the disappearance of Bu₃SnH (1) into Bu₃Sn-S-SnBu₃(2) with **3a** at 90°C. in the presence of DMTF (HC(S)NMe₂)



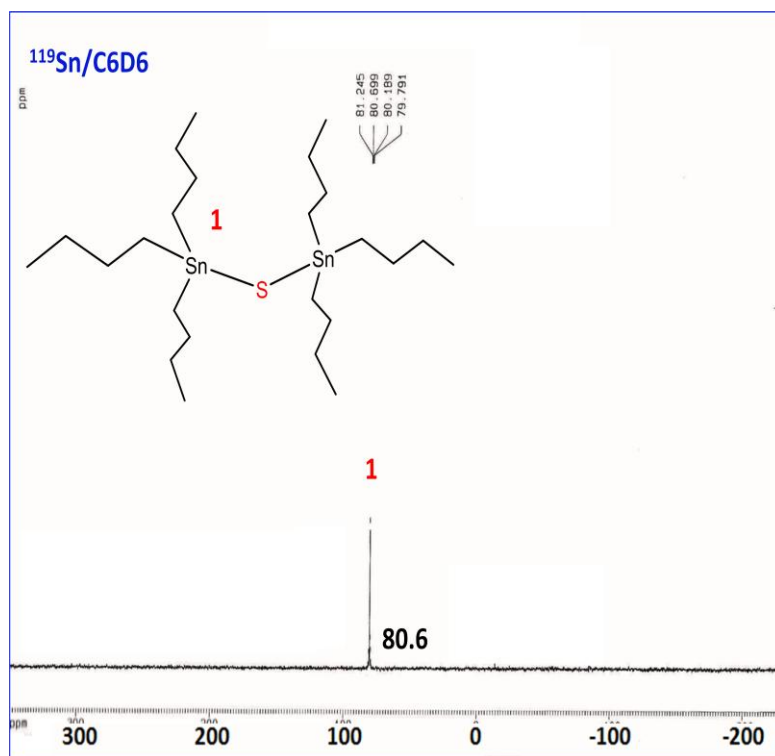
Appendix 2.79: Mass spectrum (ESI) for Bu₃Sn-S-SnBu₃



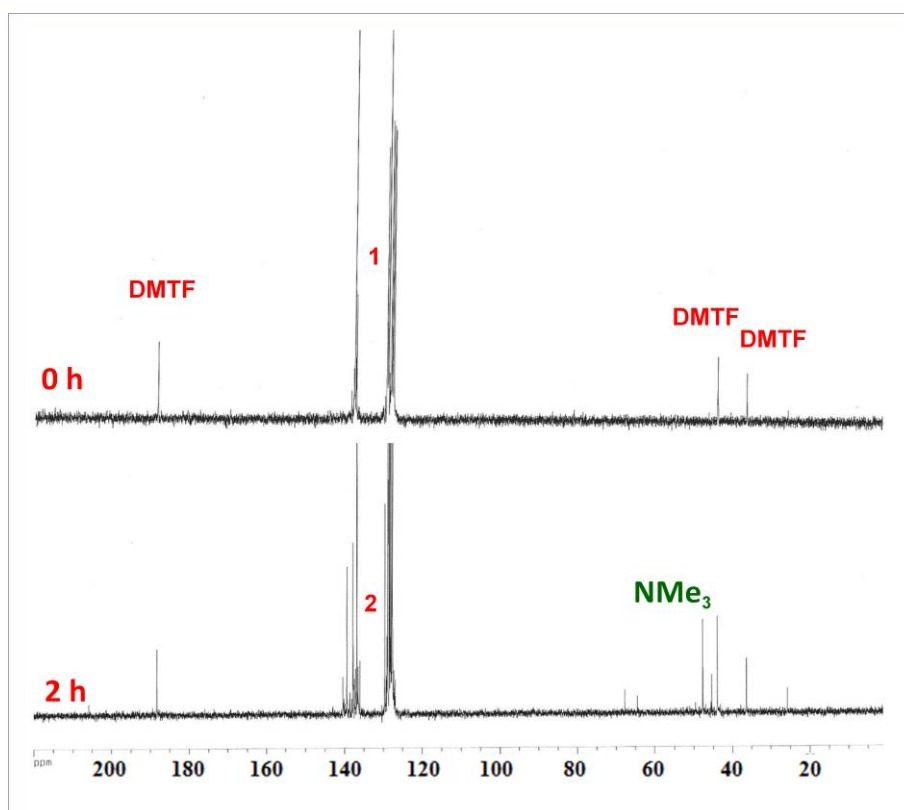
Appendix 2.80: ^{13}C NMR spectroscopy for $\text{Bu}_3\text{Sn-S-SnBu}_3$



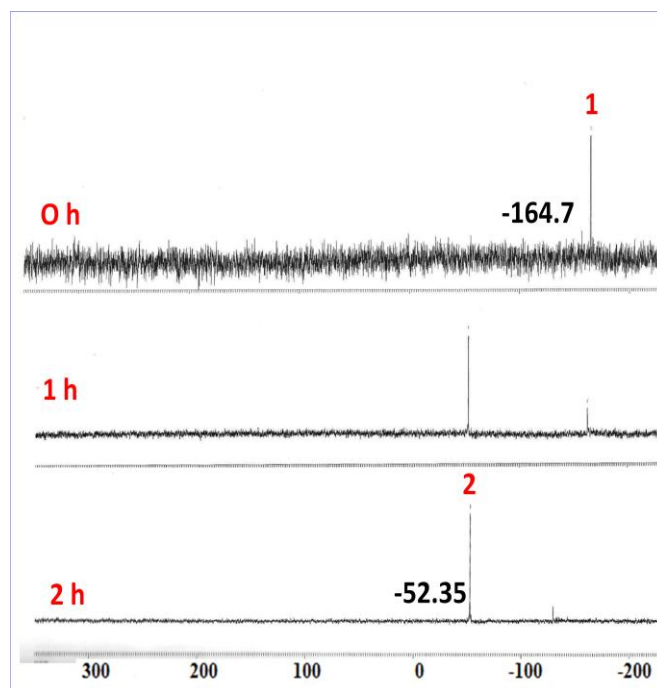
Appendix 2.81: ^{13}C NMR spectroscopy for $\text{Bu}_3\text{Sn-S-SnBu}_3$



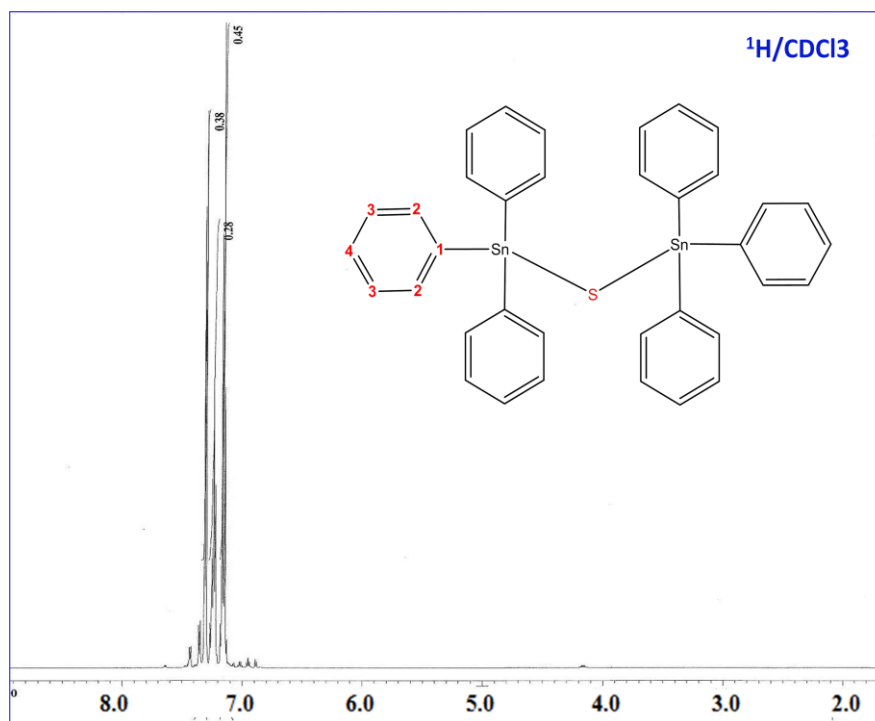
Appendix 2.82: ^{119}Sn NMR spectroscopy for $\text{Bu}_3\text{Sn-S-SnBu}_3$



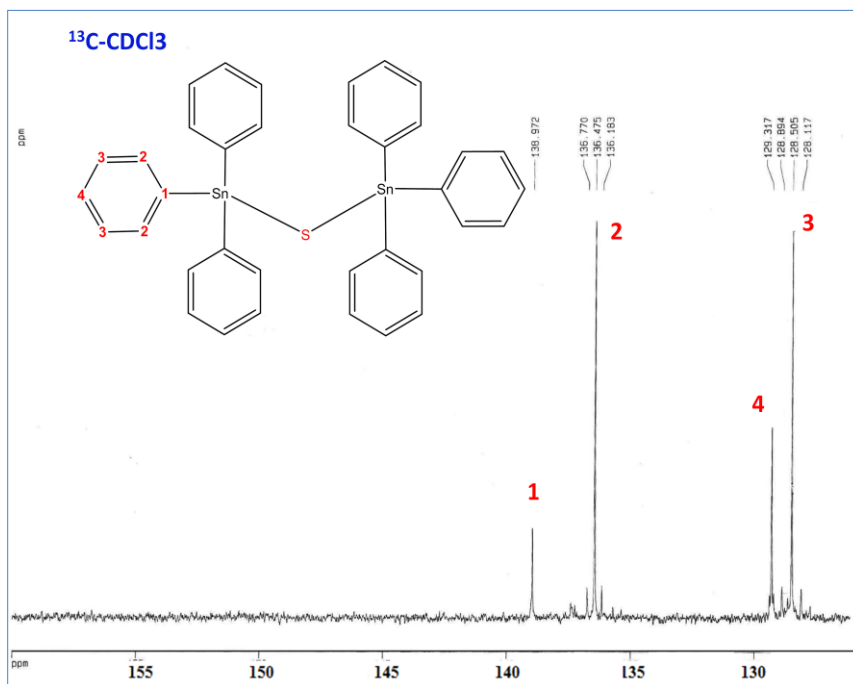
Appendix 2.83: ^{13}C NMR spectroscopy showing the disappearance of Ph_3SnH (1) into $\text{Ph}_3\text{Sn-S-SnPh}_3$ (2) with **3a** at 90°C . in the presence of DMTF (HC(S)NMe_2)



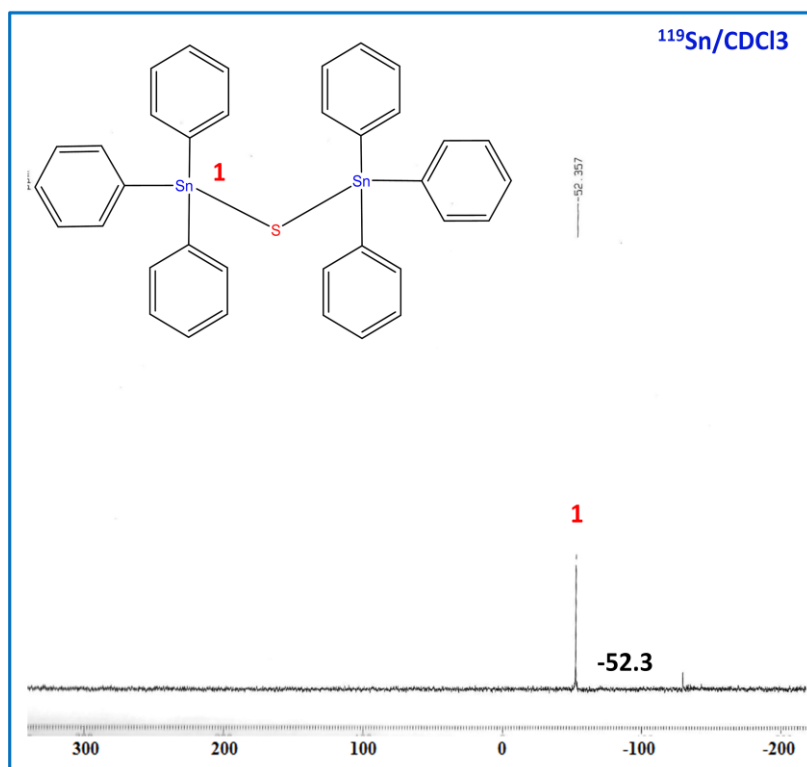
Appendix 2.84: ^{119}Sn NMR spectroscopy showing the disappearance of Ph_3SnH (1) into $\text{Ph}_3\text{Sn-S-SnPh}_3$ (2) with **3a** at 90°C . in the presence of DMTF (HC(S)NMe_2)



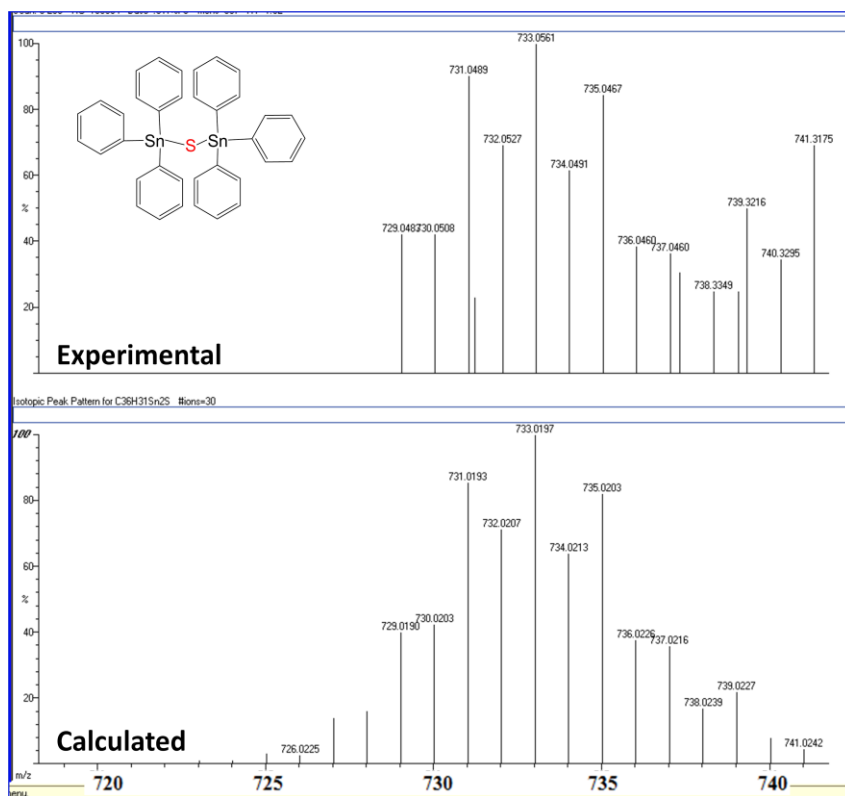
Appendix 2.85: ^1H NMR spectroscopy for $\text{Ph}_3\text{Sn-S-SnPh}_3$



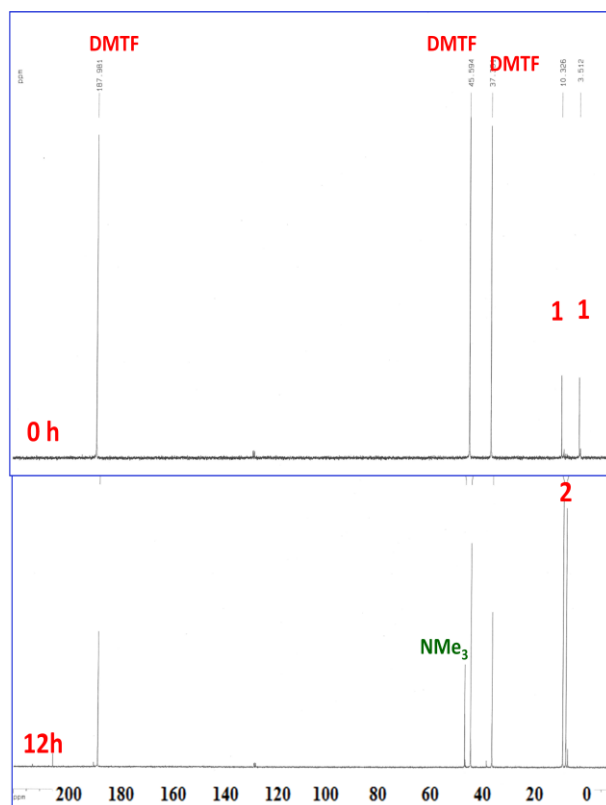
Appendix 2.86: ¹³C NMR spectroscopy for $\text{Ph}_3\text{Sn-S-SnPh}_3$



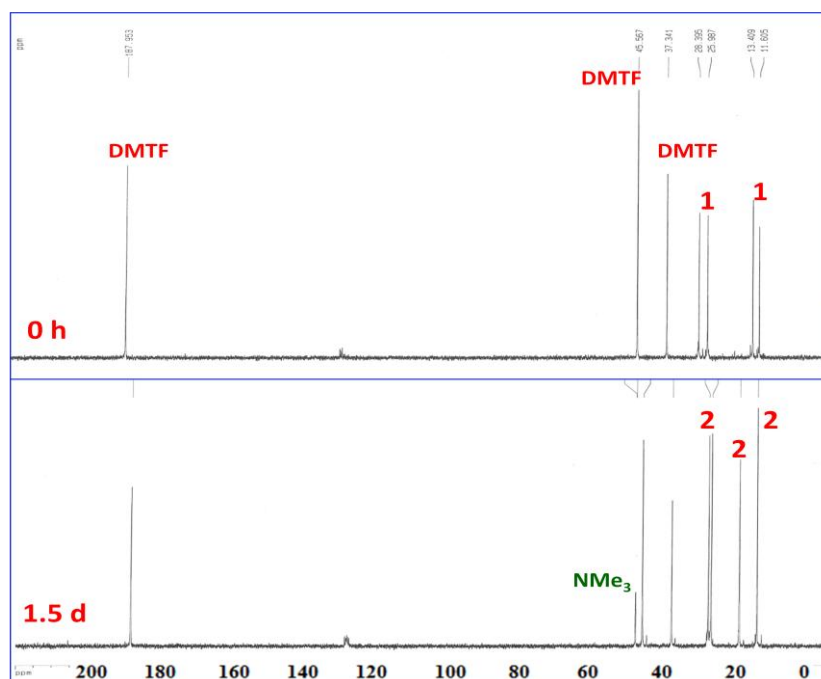
Appendix 2.87: ¹¹⁹Sn NMR spectroscopy for $\text{Ph}_3\text{Sn-S-SnPh}_3$



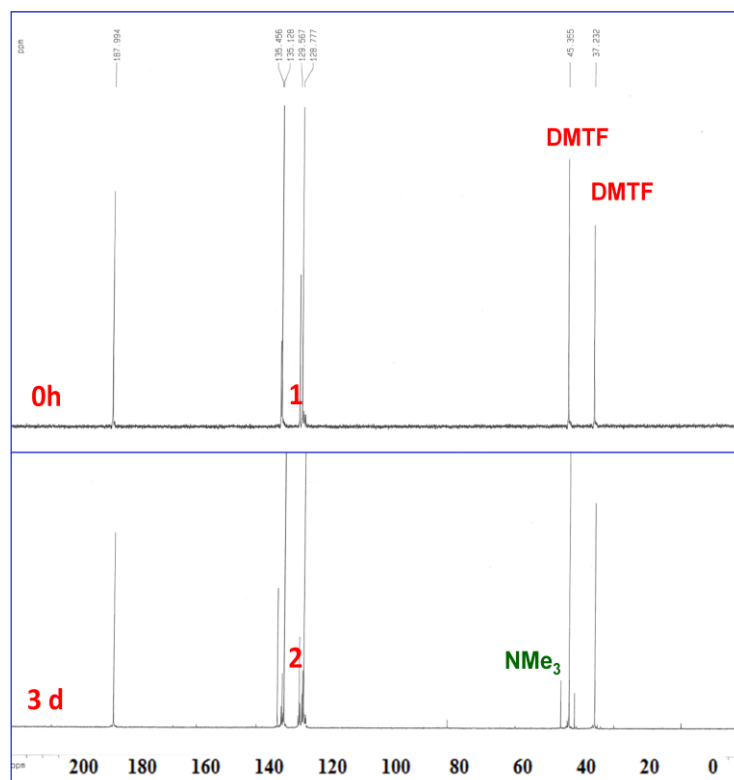
Appendix 2.88: Mass spectrum (ESI) for Ph₃Sn-S-SnPh₃



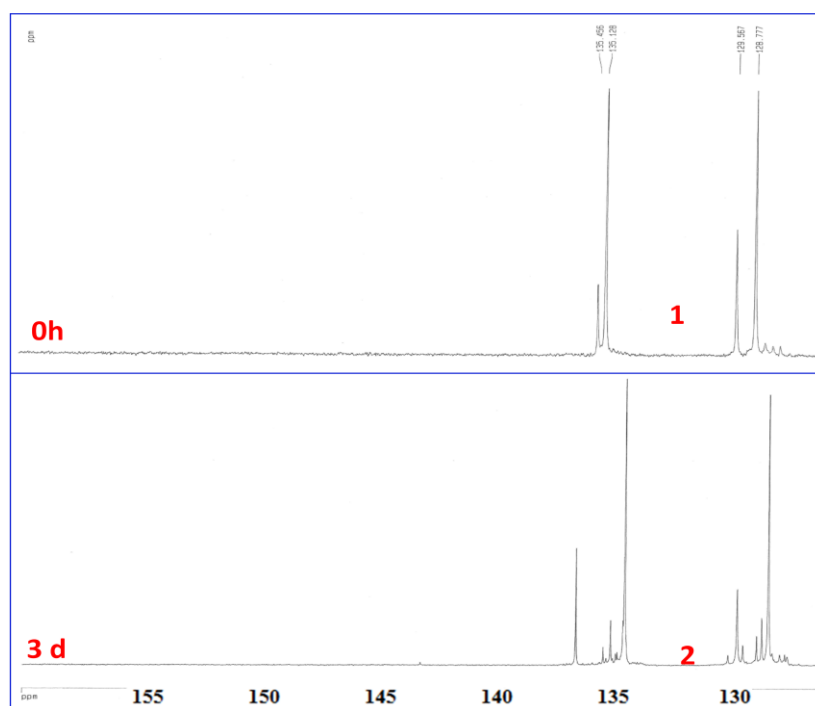
Appendix 2.89: ^{13}C NMR spectroscopy showing the disappearance of Et_3GeH (1) into $\text{Et}_3\text{Ge-S-GeEt}_3$ (2) with **3a** at 120°C . in the presence of DMTF (HC(S)NMe_2)



Appendix 2.90: ^{13}C NMR Spectroscopy showing the disappearance of Bu_3GeH (1) into $\text{Bu}_3\text{Ge-S-GeBu}_3$ (2) with **3a** at 120°C . in the presence of DMTF (HC(S)NMe_2)



Appendix 2.91: ^{13}C NMR spectroscopy showing the disappearance of Ph_3GeH (1) into $\text{Ph}_3\text{Ge-S-GePh}_3$ (2) with **3a** at 120°C . in the presence of $\text{DMTF}(\text{HC}(\text{S})\text{NMe}_2)$



Appendix 2.92: ^{13}C NMR spectroscopy showing the disappearance of Ph_3GeH (1) into $\text{Ph}_3\text{Ge-S-GePh}_3$ (2) with **3a** at 120°C . in the presence of $\text{DMTF}(\text{HC}(\text{S})\text{NMe}_2)$

Curriculum vita

Renzo N. Arias Ugarte

Chemistry/Engineering

Renzo Arias Ugarte earned his Bachelor degree in Chemical Engineering from University of San Agustin of Arequipa-Peru in 2002. Time later he decided to travel far away from his country to enrich his knowledge by joining the Master program in Chemistry in 2006, time after which his dedication and hard work take him to a higher level and by recommendation of his mentor professor Keith Pannell he joined the doctoral program in Chemistry at the University of Texas At El Paso in 2007.

Dr. Arias has not only been considered by his dedication and passion for his career but also his effort has been recognized trough numerous honors and awards such as the University Of Texas At El Paso Miner Hero nomination for outstanding research contribution in 2010.

Dr. Arias has presented his research at international conference in Austria 2010 and several other national conferences being two times awarded for best research presentation and scientific contribution in the Chicano/Latino and Native American in 2009 and 2011.

While pursuing his degree, Dr. Arias has published his work in prestigious scientific journals at *Angewandte Chemie International Edition*, 2009(1), *Chem. Commun.*, 2010(1) and recently *J. Am. Chem. Soc.* 2011 (1) and Organometallic Chemistry.(in Press)

In terms of research productivity, Dr Arias will be one of the very best to graduate from our program and indeed compares to the best of > 40 Ph.D Students that Professor Keith Pannell has mentored at the BS, MS and Ph.D levels.

Dr. Arias wants to pursue a Postdoctoral research training to enhance their skill and abilities in the Catalytic field, since part of his dreams are to contribute the design of novel and enhanced materials with potential industrial applications.

Dr. Arias' dissertation entitled, "Metal Catalyzed Activation of E-H bonds, E=Si, Ge, Sn." was supervised by Dr. Keith Pannell.

Permanent address:

J.P.V. Y Guzman II Etapa E-1, Jose L. B. Y R.
Arequipa, Peru

This dissertation was typed by the author.